A systems-level analysis of dynamic reprogramming of RNA modifications in the translational control of cellular responses

By

Tsz Yan Clement Chan

B.S. in Chemistry and Biochemistry
University of Wisconsin-Madison, WI, 2005

SUBMITTED TO THE DEPARTMENT OF CHEMISTRY
IN PARTIAL FULFILLMENT OF THE REQUIREMENTS FOR THE
DEGREE OF DOCTOR OF PHILOSOPHY
AT THE
MASSACHUSETTS INSTITUTE OF TECHNOLOGY

JUNE 2011

Signature of Author:_____

Department of Chemistry
April 25, 2011

Certified by:_____

Peter C. Dedon
Professor of Toxicology and Biological Engineering
Thesis Supervisor

Accepted by:_____

Robert W. Field
Professor of Chemistry
Chairman, Departmental Committee on Graduate Studies

This doctoral thesis has been examined by a committee of the Department of Chemistry as follows:

Chair:_____

John M. Essigmann
Professor of Chemistry and Biological Engineering

Thesis Supervisor:_____

Peter C. Dedon
Professor of Toxicology and Biological Engineering

Committee Member:_____

Steven R. Tannenbaum
Professor of Chemistry and Toxicology

A systems-level analysis of dynamic reprogramming of RNA modifications in the translational control of cellular responses

by

Tsz Yan Clement Chan

Submitted to the Department of Chemistry on May 20, 2011 in partial fulfillment of the requirements for the Degree of Doctor of Philosophy in Biological Chemistry

Abstract

In addition to the four canonical ribonucleosides (adenosine, uridine, guanosine, cytosine), transfer RNAs (tRNA) and ribosomal RNAs (rRNA) are comprised of more than 100 enzyme-catalyzed modifications, with about 20-35 found in any one organism. Many of these modifications are highly conserved in all domains of life, which suggests important biological roles for RNA modifications in cell physiology. Several recent studies have demonstrated that individual tRNA modifications and their biosynthetic pathways affect cellular stress responses. The presence of 20-35 different RNA modifications in all translationally-related non-coding RNAs suggested the possibility of systems behavior of RNA modifications in translational facets of cellular responses. The studies presented in this thesis utilize a quantitative systems-level approach to test the hypothesis that the spectrum of tRNA modifications represents a cellular program involved in modulating stress response pathways.

To initiate these studies, a novel mass spectrometric platform was developed to characterize and quantify the spectrum of modified ribonucleosides in an organism, starting with the ~25 ribonucleosides in *S. cerevisiae* tRNA. This approach was used to compare tRNA modification spectra from cells exposed to four mechanistically distinct toxicants: hydrogen peroxide, methyl methanesulfonate, arsenite, and hypochlorite. Multivariate statistical analysis revealed both dose- and agent-specific signatures in the relative quantities of tRNA modifications. Further, modifications that change significantly after exposure were shown to confer resistance to the cytotoxicity of the agent. These observations demonstrate the dynamic nature of tRNA modifications and their critical role in translational control of cellular stress responses. Also, application of the mass spectrometric method revealed several new biosynthetic pathways for tRNA modifications in yeast. These studies comprise Chapters 2 and 3.

Chapter 4 is aimed at characterizing the link between tRNA modifications and translational control of cellular responses. One of the tRNA modifications that increased

significantly following exposure of yeast to hydrogen peroxide is 5-methylcytosine (m^5C), which is located at the wobble position of the leucine tRNA for coding UUG. This suggested that it might affect translation of mRNA containing this codon. While there are 6 codons for leucine, the usage of the codon UUG for specifying leucine in the set of homologous ribosomal proteins differs widely. Using proteomics approach, it was demonstrated that m^5C regulates the levels of the homologous ribosomal protein genes *rpl22a* and *rpl22b*, with hydrogen peroxide exposure causing an increase in the proportion of ribosomes containing *rpl22a*. Further, loss of *rpl22a* conferred sensitivity to hydrogen peroxide exposure. These results suggest that the system of tRNA modifications controls cellular responses partly by determining the composition of ribosomes involved in the selective translation of critical response proteins.

As observed in Chapter 3, tRNA modifications spectrum changes specifically in responses to mechanistically distinct toxic agents; in Chapter 5, a series of studies was designed to test the hypothesis that each of these unique signatures represents a common response to different toxicant classes. To test this hypothesis, yeast cells were exposed to four different oxidizing agents (hydrogen peroxide, *tert*-butyl hydroperoxide, peroxynitrite, and gamma-radiation) and five different alkylating agents (methyl methanesulfonate, ethyl methanesulfonate, isopropyl methanesulfonate, *N*-methyl-*N'*-nitro-*N*-nitrosoguanidine, and *N*-nitroso-*N*-methylurea) at concentrations producing similar levels of cytotoxicity. The spectrum of tRNA modifications was then quantified and the results subjected to multivariate statistical analysis to identify consistent patterns. The results reveal class-specific patterns of changes, with distinct tRNA modification spectra for oxidants and alkylating agents. At a finer level of analysis, the studies revealed subclass signatures for S_N1 and S_N2 alkylating agents. The results from these experiments were used to develop a data-driven model that predicts exposures to the two classes of toxic agents accurately. Such a model may be useful for assessing ribonucleoside spectra as biomarkers of exposure.

Appendix A describes the preliminary characterization of the spectrum of modified ribonucleosides from *Mycobacterium bovis BCG* tRNA. Surveys of tRNA enzymatic hydrolysates with mass spectrometric techniques reveal the presence of modified ribonucleosides that are highly conserved among various species of organisms, as well as candidates of novel modifications.

Advisor: Peter C. Dedon

Title: Underwood-Prescott Professor of Toxicology and Biological Engineering
Singapore Research Professor of Infectious Disease
Deputy Director of MIT Center for Environmental Health Sciences
Faculty Member of Chulabhorn Graduate Research Institute

Dedicated to my parents Kwok Ping Chan and So Ngan Woo

For their counsel and support in all these years

And to my fiancée Man Yin Leung

Who keeps me full with love every day

Acknowledgements

I would like to thank my advisor, Prof. Peter C. Dedon, for giving me the opportunity to conduct my Ph.D. research in his laboratory. It is a pleasure to do science with Pete. In these years, he provided me endless patience, support and encouragement and I learned a great deal from him. I feel so honored to be a member of his group.

I am grateful to Prof. John M. Essigmann for being my thesis committee chair and Prof. Steven R. Tannenbaum for being my thesis committee member. Both of them provide a lot of insight into this research and through them, I often view my projects at different angles.

I also want to thank Prof. Thomas J. Begley in University at Albany and his group members. Tom has been working with me since the first day I join this group. He provided me a lot of advices, especially on computational statistical analysis. Thanks Prof. Sylvie Alonso in National University of Singapore and her group members for helping me to initiate my research in Singapore. They taught me everything I know in microbiology. Thanks Dr. Fugen Li for developing a data-driven model with me and leading me into the field of machine learning. Also, I am glad to work on the ABH8 project with Prof. Leona D. Samson and Dr. Dragony Fu.

Of course I cannot imagine how I can finish this thesis without all the past and present members of the Dedon group. They are always available to give me constructive suggestions and share all the ups and downs with me. In particular, I am indebted to Dr. Michael DeMott, Dr. Ramesh Indrakanti, and Dr. Megan McBee for advices on experiments and for keeping the laboratory running smoothly in all situations. I am also very grateful to the RNA group, including Dr. Kok Seong Lim, Dr. Maggie Chia-Hua Ho, Brandon Russell and especially to Dr. Joy Pang and Yok Hian Chionh, who worked closely with me on several projects. I definitely need to thank the administrative staffs, Olga Parkin and Christine Marzilli for making purchasing and many other processes much easier. Thanks Dr. Koli Taghizadeh and Dr. Peter Wishnok for teaching me mass spectrometric techniques. Also thanks Dr. Farzad Olfat for helping me to set up our lab in Singpoare.

I am inspired by several very nice people in many aspects. Thanks Dr. Pavan Vaidyanathan for all the in-depth discussions on ribosome research. Thanks Prof. Ping Li and Dr. Quamrul Hassan for sharing their experiences in career. Thanks Dr. Connie Lio and her family for all the jokes, good food, and fun we have shared.

I feel that I am indebted to everyone I know and if I continue, the acknowledgements will be likely to be longer than the rest of this thesis. At last, I want to thank my parents, Kwok Ping Chan and So Ngan Woo, for always supporting my decisions and also my fiancée, Man Yin Leung, for sharing all my feelings. Thanks God for leading me through this whole journey.

Table of Contents

List of Figures

List of Tables

Abbreviations

AA	Alkylating agents
ac^{4}C	N^4-Acetylcytidine
AsO_4^-	Arsenite
Am	2'-*O*-Methyladenosine
Ar(p)	2'-*O*-Ribosyladenosine (phosphate)
Cm	2'-*O*-Methylcytidine
CT	Control
D	Dihydrouridine
EMS	Ethyl methanesulfonate
Gm	2'-*O*-Methylguanosine
H_2O_2	Hydrogen peroxide
HC	Hierarchical clustering analysis
HPLC	High performance liquid chromatography
I	Inosine
IMS	Isopropyl methanesulfonate
i^{6}A	N^6-Isopentenyladenosine
LC	Liquid chromatography
LD	Lethal dose
m^{1}A	1-Methyladenosine
m^{1}G	1-Methylguanosine
m^{1}I	1-Methylinosine
m$^2_2$G	N^2,N^2-Dimethylguanosine
m^{2}G	N^2-Methylguanosine
m^{3}C	3-Methylcytidine
m^{5}C	5-Methylcytidine
m^{5}U	5-Methyluridine
m$^6_2$A	N^6,N^6-Dimethyladenosine
m^{7}G	7-Methylguanosine
mcm^{5}U	5-Methoxycarbonylmethyluridine
mcm^{5}s^{2}U	5-Methoxycarbonylmethyl-2-thiouridine
MMS	Methyl methanesulfonate
MNNG	*N*-Methyl-*N'*-nitro-*N*-nitrosoguanidine
MRM	Multiple reactions monitoring
MS	Mass spectrometry
ncm^{5}U	5-Carbamoylmethyluridine
ncm^{5}Um	5-Carbamoylmethyl-2'-*O*-methyluridine
NMU	*N*-Nitroso-*N*-methylurea
OCl^-	Hypochlorite
$ONOO^-$	Peroxynitrite
OX	Oxidizing agents
PCA	Principle component analysis

QQQ	Triple quadrupole mass spectrometer
QTOF	Quadrupole time-of-flight mass spectrometer
RPL	Ribosomal proteins in large subunit
RPS	Ribosomal proteins in small subunit
RT-qPCR	Real time quantitative polymerase chain reaction
t^6A	N^6-Threonylcarbamoyladenosine
TB	Tuberculosis
TBHP	*tert*-Butyl hydroperoxide
Um	2'-*O*-Methyluridine
Ψ	Pseudouridine
yW	Wybutosine
γ-rad	Gamma-radiation

Chapter 1

Background and Significance

Goals of this thesis

The goals of this thesis project are to further our understanding of the biological roles of tRNA secondary modifications in cellular response to stress and to explore the utility of changes in the spectrum of tRNA modifications as biomarker of specific physiological states. We hypothesize that changes in the levels of specific tRNA modifications are involved in regulating translation by selection of specific codons enriched in stress response proteins and by regulating other facets of the interaction of tRNA molecules with ribosomes.

Cellular responses to stress

To survive in an ever-changing environment, cells maintain biological homeostasis by balancing a wide variety of biological processes, with alterations of any of these processes affecting all others. Imbalance in these systems can be deleterious to cell survival. For instance, increasing the temperature of a cell by only several degrees can disrupt protein homeostasis by causing proteins to unfold, misfold, and aggregate (*1-4*). To survive these insults, cells have developed a large number of response pathways to adapt to environmental changes. The response begins with changes in biochemical homeostasis in a variety of metabolic pathways by changes in protein secondary modifications caused by signaling cascades (*5, 6*). At the next level of response, signaling cascades lead to changes in transcription levels of hundreds of genes (*7-14*). From here, there are numerous mechanisms controlling expression of genes, including alternative splicing of pre-mRNA, RNA interference, and protein degradation. These pathways will be considered in the following sections.

One common cellular response mechanism among all organisms involves modulating protein activity by post-translational modifications or allosteric regulation. One of the most intensively studied post-translational modifications is phosphorylation of serine and threonine amino acid residues by protein kinases and dephosphorylation by phosphatases. This modification activates or deactivates proteins for various functions, including signaling cascades, metabolism, and regulation of transcription. In signaling pathways, one kinase regulates the activity of another kinase by phosphorylation, for example in the signaling cascades mediated by mitogen-activiated protein kinases (MAPKs), MAPK kinases (MAPKK) and MAPKK kinases (*15, 16*). These pathways magnify the signal intensities when signals reach downstream of the cascades; also as each protein can be phosphorylated by more than one kinase, the diversity of signaling is promoted (*15, 16*). Some of these signaling pathways lead to activation or deactivation of enzymes directly involved in the stress response. For instance, carbamoyl phosphate synthetase II, a rate-limiting enzyme in pyrimidine nucleotide biosynthesis, is activated by phosphorylation under oxidative stress (*17*). However, the purpose of most of these signaling pathways is to regulate transcription. Using p53 as an example, during cellular exposure to a broad range of genotoxic stress, this transcription factor is subjected to several modifications, including phosphorylation, at multiple amino acid residues (*18, 19*). These modifications activate p53 to initiate the transcription of genes related to DNA repair, cell-cycle arrest, and apoptosis; p53 can potentially bind to more than 100 genes in human genome (*20*).

A second level of control of gene expression involves alteration of mRNA sequence by alternative splicing. While expression levels of proteins can be controlled at the level of transcription, it is now clear that this is not the only mechanism of regulation because the levels

of mRNA and protein for most genes are not well correlated (*21, 22*). Also, some studies have demonstrated that most genes that are up-regulated in transcription level in response to stress do not confer resistance to the stress (*23*). At the post-transcriptional level, alternative splicing of pre-mRNA plays important roles in cellular response in higher eukaryotes. Pre-mRNA splicing is catalyzed by the spliceosome that is composed of both protein and RNA, with the activities of dozens of RNA-binding proteins, regulated by expression level and post-translational modifications (*24, 25*). Depending on the cellular conditions, different parts of a DNA transcript are removed to form mature mRNA. Thus, different proteins can be expressed from the same gene to adapt changes in cellular state. For instance, heat shock induces alternative splicing in the non-coding region of HSP47 pre-mRNA, which results in a mature mRNA that is translated more efficiently under the stress (*26*). Also, the pre-mRNA of a negative regulator of p53, MDM2, is alternatively spliced following exposure to genotoxic agents, which leads to the activation of DNA damage response (*27*). Finally, cold shock causes alternative splicing in pre-mRNA of neurofibromatosis type 1 in many types of cells (*28*). In general, more than half of mammalian transcripts are spliced differently in different cells of the same organism (*29*).

Another mechanism of post-transcriptional regulation of cellular response is RNA interference (*30, 31*). mRNAs hybridize with complementing small RNA fragments (approximately 22 nucleotides in length) to form a double-stranded structure that inhibits the mRNA from being translated and, in many cases, initiates cleavage of the mRNA (*32*). These small RNA fragments include small interfering RNAs, PIWI interacting RNAs, and micro RNAs (miRNAs). miRNAs are generated from DNA transcripts that form a single-stranded stem-loop structure that is cleaved at specific position by an RNase III enzyme, such as Dicer, to form

miRNAs. It has been shown that miRNAs are involved in cellular response. For instances, translation of p53 mRNA is suppressed by miRNA miR-125b in normal conditions. The level of this miRNA decreases following DNA damage to allow a higher level of expression of p53 (*33*). A similar mechanism is employed to regulate the expression of a cationic amino acid transporter during amino acid depletion (*34*). Interestingly, individual deletion of some miRNA genes causes no changes in normal conditions (*35-37*). However, they lead to an increase in sensitivity to stress (*38-41*).

The issue of translational control of cellular stress responses will be addressed shortly, but it is important to note mechanisms for protein degradation. As cellular response to stress, asides from regulations during transcription and post-transcription, abundance levels of proteins can also be controlled by protein degradation, with considerable variation in protein half-life (*42, 43*). The rate of degradation of specific proteins changes during stress. For example, one of the pathways of degradation is initiated by post-translationally modifying the target protein with poly-ubiquitin. Under normal conditions, half-life of the transcription factor p53 is short as it is frequently poly-ubiquitinated by MDM2, while under stress, poly-ubiquitination of p53 is reduced to allow p53 to initiate the transcription of stress-response genes (*44-47*).

In the remaining portions of this chapter, I will review the mechanisms involved in protein synthesis, with a focus on the role of the family of transfer RNAs (tRNA) and their extensive system of ribonucleoside modifications. I will explore the molecular functions of

tRNA secondary modifications and how this leads to the hypothesis that tRNA secondary modifications are involved in cellular response.

Protein synthesis is a RNA-catalyzed process

As illustrated by several studies, multiple stresses induce the phosphorylation of protein eIF2 to stop translation (*48, 49*) and thus to conserve resources for the cell to express specific stress-related genes (*50*). While cellular response to stress occurs in all other steps of the lifetime of proteins, it is logical to expect regulations during the process of protein synthesis. It has been demonstrated that changing the rate of translating a mRNA can alter the function of protein products (*51*). This implies that alternating the speed of translation may gain the same benefits as gaining from alternative splicing. Also, changing in the fidelity of translation can promote cellular immune responses (*52, 53*). However, mainly due to the complexity of ribosomal machinery, mechanisms of its regulation remain eluded. Following the advances in our understandings in the mechanism of protein synthesis, evidence of regulation during protein synthesis is emerging from recent studies.

Protein synthesis in biological systems is one of the most extensively studied facets of cell and molecular biology. The process involves at least three species of RNA: messenger RNA (mRNA), transfer RNA (tRNA), and ribosomal RNA (rRNA) (*54, 55*). mRNAs carry sequence information of proteins from the genome. They convey information in a linear reading frame with 64 codons, with each codon comprising three nucleotides that represent one of the twenty amino acids or termination of synthesis. The information is read by tRNAs that interact

with the ribosome-mRNA complex to form polymers of amino acids. Each amino acid is coded by at least one tRNA, with the amino acid physically linked to the tRNA by an ester linkage at the 3'-*O* catalyzed by a specific aminoacyl-tRNA synthetase. Activated by acylation, the amino group of the amino acid carries out nucleophilic attack on the carbonyl group at the C-terminus of the growing peptide that is bound to an adjacent tRNA (peptidyl-tRNA). A new peptide bond is then formed and the peptide is elongated by one amino acid.

This whole process of protein synthesis is carried out on the ribosome, a protein-RNA complex consisting two subunits. In prokaryotes, the large subunit contains two rRNAs, 23S and 5S, so named for the sedimentation coefficient of the RNA molecule, and the small subunit contains only one rRNA, 16S rRNA. In eukaryotes, the large subunit contains three rRNAs, 28S, 5.8S, and 5S, and the small subunit contains an 18S rRNA. These two subunits play distinct roles. The formation of peptide bonds is carried out in the large subunit and the binding between mRNA and tRNA is controlled by the small subunit. Previous studies demonstrated that the two ribosomal subunits are able to perform their functions independently. Without the small subunit, the large subunit is still able to catalyze the formation of peptide bonds between analogs of peptidyl-tRNA and aminoacyl-tRNA (*56, 57*). Similarly, the small subunit, with only itself, binds mRNA; this mRNA-small subunit complex then binds specific tRNAs by hybridization of complementing codon and anticodon (*58*). The large subunit interacts with the acceptor stems of tRNAs, especially with the 3'-terminus that always ends with the sequence CCA, while the small subunit interacts with the anticodon stems. With the two subunits together in a complex, a ribosome contains three tRNA binding sites that are known as the A, P, and E. During protein synthesis, two adjacent codons in the mRNA, from 5' to 3', are localized

in the P and A sites respectively. These two codons determine which tRNAs are bound to the two sites. At the beginning of each cycle of elongation, a peptidyl-tRNA is located at the P site, a deacylated tRNA at the E site, and no tRNA at the A site. With the selection based upon the mRNA codon in the A site, a specific species of aminoacyl-tRNA is delivered to the A site by a protein complex, EF-Tu. This binding initiates the release of deacylated tRNA in the E site. tRNA in the P site is then deacylated by the formation of peptide bond between the peptide and the amino group of the aminoacyl-tRNA at the A site. With the aid of protein complex EF-G, the deacylated tRNA in the P site is then transferred to the E site and the peptidyl-tRNA in the A site to the P site. Through this process, one amino acid is added to the peptide and a new cycle of elongation can be started again. In this complex biological process, RNAs contribute to two reactions. First, they catalyze the formation of peptide bonds and second, they decode the information stored in mRNAs.

Both rRNA and tRNA play key roles in catalyzing peptide bond formation. The crystal structures of *H. marismortui* ribosomal large subunit and its complexes with tRNA analogs were determined (*59*). These structures suggest that the active site of peptide bond formation is solely composed of rRNAs; in the P site, C74 and C75 of the peptidyl-tRNA base-pair with two Gs from 23S rRNA, and, in the A site, C75 of the aminoacyl-tRNA also base-pairs with a G from 23S rRNA. These binding patterns fix the orientations of substrates so that the amino group of aminoacyl-tRNA in the A site is pointed directly to the carbonyl group of the peptide that is covalently linked to the tRNA in the P site. It was proposed that substrate orientation accounts for most of the catalytic power of ribosome (*60*). The crystal structures also suggest that the 2'-OH group of A76 from peptidyl-tRNA at P site interacts strongly with the amino group of

aminoacyl-tRNA in the A site. Replacing A76 with a 2'-deoxyA76 leads to a decrease in reaction rate of 10^2- to 10^6-fold (*61, 62*). It is proposed that the 2'- OH group catalyzes the reaction by acting as both general acid and general base (*63*). To activate the formation of peptide bond, it removes a proton from the amino group to make it a better nucleophile. To favor the break of ester bond between peptide carbonyl group and the P site tRNA, it donates the proton to 3'- O of A76 in the leaving tRNA.

tRNA and rRNA are also involved in maintaining translational fidelity. Binding of aminoacyl-tRNA to the A site is primarily determined by the base-pairing between codon and anticodon. However, forming a completely complementary codon-anticodon (cognate) complex is only slightly more energetically favorable than forming one that has one mismatch (near-cognate) in many cases. This small difference in free energy is predicted to result in one misincorporation in every ten amino acids (*64*). In reality, however, the error rate of amino acid incorporation is one in every 1000 to 100,000 (*65*), due to several factors. Several pieces of information point to enhancement of fidelity by 16S rRNA. Studies support that three nucleotides on 16S rRNA (A1492, A1493, and G530) are essential for mRNA decoding (*66, 67*). Crystal structures of the ribosome small subunit reveal that the conformation of these three nucleotides changes when cognate codon-anticodon interactions occur in the A site (*58, 68, 69*). This induces A1493 to form hydrogen bonds with the first base of the codon, and with its pairing base from the anticodon. Similarly, the base pair that consists of the second base of the codon interacts with A1492 while the conformation of A1492 is stabilized by G530. These interactions stabilize the mRNA-tRNA complex. However, the rRNA-tRNA-mRNA interactions

cannot be formed if the two bases of the pair are not complementary. Thus, the formation of cognate pairs is much more energetically favorable than the formation of non-cognate ones.

The evidence described above points to a central role for RNA in the structure and activity of the protein synthesizing machinery. Indeed, it has been hypothesized that the earliest "ribosome" is composed entirely with RNA (*70*).

Maturation of transfer RNA

Among the several species of RNA involved in protein synthesis, tRNA is particularly interesting as it is involved in both decoding the mRNA and forming the peptide bonds. To become fully functional, transcripts of pre-tRNA proceed through a series of maturation steps (*71*) that differ for the various tRNA species (*72-74*). One of the first steps involves removal of a 5'-terminal sequence from pre-tRNAs with ribonuclease P (*75, 76*). Interestingly, this enzyme is composed of both RNA and protein, with the RNA subunit of *E. coli* or *B. subtilis* capable of catalyzing this reaction *in vitro* (*77*). An additional 3'-terminal sequence is removed by any of several exoribonucleases and endoribonucleases that differ for the various species of pre-tRNA (*78*). This end is then capped with a CCA sequence in some eukaryotic tRNA species by the action of ATP(CTP):tRNA nucleotidyl transferase (*79, 80*). Some pre-tRNAs have a 14-60 nt intron located one nucleotide downstream of the anticodon (*81, 82*), with the intron removed in three reactions in nucleus. First, the intron is removed by a tRNA splicing endonuclease that is located at the nuclear membrane (*83*). A tRNA ligase then rejoins the two cleaved fragments

using GTP and ATP (*81, 84*), which leaves a 2'-phosphate at the junction of ligation. The phosphate is removed by a NAD-dependent 2'-phosphotransferase to finish the process (*85*).

RNA secondary modifications

In addition to these changes in tRNA sequence, maturation of tRNA also requires modification of the nucleobases and ribosyl moieties. Current estimates place the number of known RNA post-transcriptional or secondary modifications at approximately 100, each requiring one or more specific RNA modifying enzymes (*86*). The known set of 25 ribonucleoside modifications in *S. cerevisiae* tRNA are shown in Figure 1-1. The modifications range in complexity from simple methylations at endo- and exocyclic nitrogens of the nucleobases and the 2'-hydroxyl group, to complex and branching modifications of the nucleobase such as N^6-threonyl-carbamoyl-adenosine and wybutosine (Figure 1-1). These modifications are positioned throughout the tRNA molecules in a variety of conserved locations, but the most frequently modified site involves the anticodon loop (Table 1-1 and 1-2). Currently, about 50 genes encoding tRNA modifying enzymes have been identified in *S. cerevisiae* (Table 1-2).

While all other RNA processing steps appear to take place in the nucleus, reactions to generate the ribonucleoside secondary modifications occur in both the nucleus and cytoplasm. The modified nucleosides are derivatives of the four canonical nucleosides (adenosine, uridine, guanosine, and cytosine) and are formed at different steps during pre-tRNA processing. For example, when yeast $tRNA^{Tyr}$ was injected into nuclei of Xenopus laevis oocytes, 5 modifications

were observed to form before 5'-terminal processing occurred, 11 modifications formed after the 5' processing, and 2 modifications formed after splicing (*87*). While the size and sequence of pre-tRNAs direct the formation of modifications, these processes are also affected by several other factors.

Another example of the complexity of RNA modification involves the distinction between tRNAs generated from a single transcript and those arising as a single transcript. In some cases, several tRNA genes are transcribed as a single multimeric pre-tRNA that is cleaved to form monomeric pre-tRNAs. In a strain of *E. coli* with lack of nucleases to process pre-tRNAs, the accumulated multimeric pre-tRNAs already contained some modifications, including m^5U54, Y, and D (*88*). For the precursor of a specific leucine tRNA, the modification m^1G37 only exists in monomeric pre-tRNA but not in the multimeric form, while another modification, Gm18, is only formed on mature tRNA (*89*). However, in wild-type *E. coli*, most modifications are generated after all the cleaving and splicing steps (*90*). For example, in vitro studies on tRNA m^5U54-methyltransferase demonstrated that monomeric pre-tRNAs are preferred as substrates over multimeric pre-tRNAs (*91*). These studies suggest that tRNA modifications are determined by the abundance level of tRNAs and their precursors, and the activities of modifying enzymes.

In addition to control by substrate and enzyme concentrations, the timing and location of tRNA modifications is also affected by cellular compartmentalization of enzymes. Many enzymes for modifying tRNA at position 34 and 37 are located in cytoplasm or in mitochondria (*92*). Thus, modifications on these positions are usually the last steps of the maturation processing as they can only occur when pre-tRNAs are translocated to the cytosol (*93*).

Furthermore, the sequence of modifications may be affected by interactions between enzymes. Some tRNA modifying enzymes are a part of large multi-enzyme complexes, which may lead to specific ordering of individual processes (*94, 95*). For example, m^5C can only be formed at position 34 in pre-tRNA with an intron, though the sequence of the intron does not affect its formation (*96*). This suggests that the splicing is coupled with the formation of m^5C.

Degradation of transfer RNA

Matured tRNAs are extremely stable with half-lives in the range of days as determined by several studies (*97, 98*). Recently, Chernyakov and coworkers found that two 5'-3' exonucleases Rat1 and Xrn1 are involved in degradation of hypomodified tRNAs and this process is regulated by Met22 (*99*), suggesting the presence of a biological mechanism for tRNA quality control.

Name	Structure	Name	Structure	Name	Structure	Name	Structure
Dihydro-uridine (**D**)	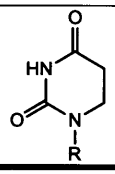	Pseudouridine (**Y**)	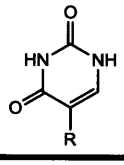	5-Carbamoyl-methyluridine (**ncm^{5}U**)	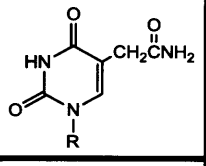	Inosine (**I**)	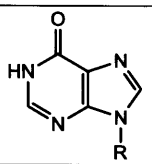
5-Carbamoyl-methyl-2'-*O*-methyluridine (**ncm^{5}Um**)	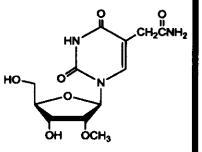	2'-*O*-Methyl-guanosine (**Gm**)	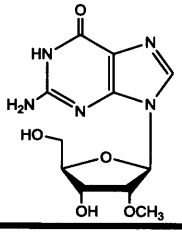	2'-*O*-Methyl-uridine (**Um**)	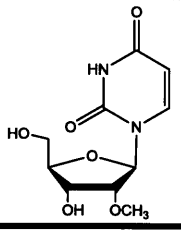	5-Methyl-cytidine (**m^{5}C**)	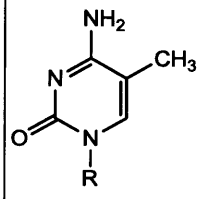
5-Methoxy-carbonyl-methyluridine (**mcm^{5}U**)	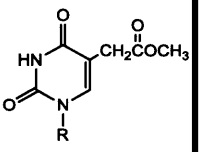	1-Methyl-guanosine (**m^{1}G**)	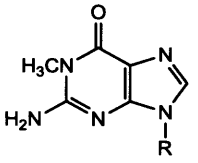	*N*^{2}-Methyl-guanosine (**m^{2}G**)	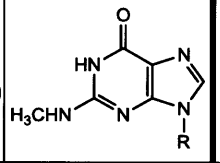	*N*^{4}-acetylcytidine (**ac^{4}C**)	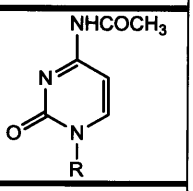
2'-O-Ribosyl-adenosine phosphate (**Ar(p)**)	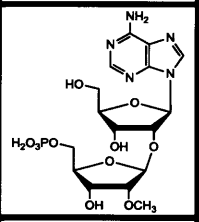	7-Methyl-guanosine (**m^{7}G**)	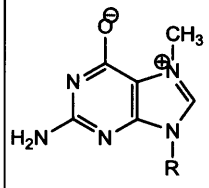	1-Methyl-inosine (**m^{1}I**)	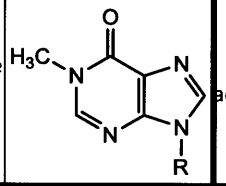	2'-*O*-Methyl-adenosine (**Am**)	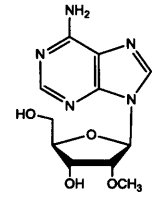
N^2,*N*^{2}-Di-methyl-guanosine (**m$^2_2$G**)	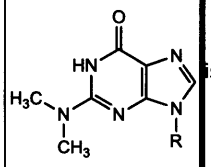	*N*^{6}-isopentenyladenosine (**i^{6}A**)	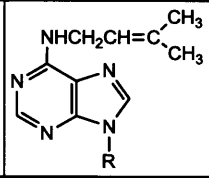	1-Methyl-adenosine (**m^{1}A**)	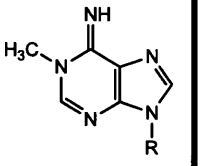	Wybutosine (**yW**)	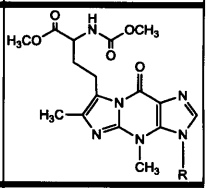
5-Methyl-uridine (**m^{5}U**)	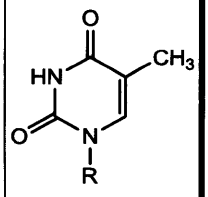	2'-*O*-Methyl-cytidine (**Cm**)	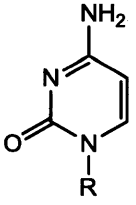	*N*^{6}-Threonyl-carbamoyl-adenosine (**t^{6}A**)	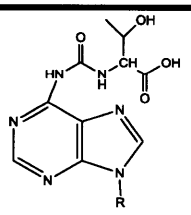	3-Methyl-cytidine (**m^{3}C**)	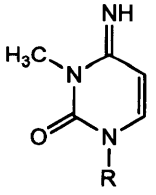
5-Methoxy-carbonyl-methyl-2-thiouridine (**mcm^{5}s^{2}U**)	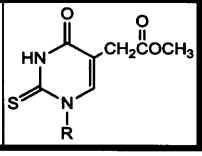						

Figure 1-1. Structures of modified nucleosides from *S. cerevisiae* tRNA. R represents ribosyl group.

	tRNA^{Lys}(CUU)	tRNA^{Lys}(mcm^{5}s^{2}UUU)	tRNA^{Met}(CUA, i)	tRNA^{Met}(CUA, m)	tRNA^{Phe}(GmAA)	tRNA^{Pro}(ncm^{5}UGG)	tRNA^{Ser}(IGA)	tRNA^{Ser}(UGA)	tRNA^{Ser}(CGA)	tRNA^{Thr}(IGU)	tRNA^{Trp}(CmCA)	tRNA^{Tyr}(GYA)	tRNA^{Val}(IAC)	tRNA^{Val}(CAC)	tRNA^{Val}(ncm^{5}UAC)
I							34			34			34		
m^{1}I															
m^{1}A	58	58	58	58	58	58				58	58	58	58	58	58
t^{6}A	37	37	37	37						37					
i^{6}A							37	37	37			37			
Ar(p)			64												
Am															
m5C	48	48, 49	48	40, 49		48	48	48	48		48	49	49	49	49
ac^{4}C						12	12	12							
m^{3}C									32						
Cm					32	4					32, 34				
m^{1}G			9			9, 37					9		9		
m^{2}G	10	10	10	10	10					10	10	10		10, 26	10
m$^2_2$G	26	26	26	26	26		26	26	26	26		26			26
Gm					34		18	18	18		18	18			
m^{7}G	46	46	46	46	46	46					46		46	46	
yW					37										
Y	27, 39, 55	1, 27, 28, 55, 67		27, 31, 39, 55	39, 55	13, 32, 38, 55	32, 39, 55	39, 55	39, 55	39, 55	26, 27, 28, 39, 55, 65	35, 39, 55	13, 27, 32, 55	13, 27, 28, 32, 55	27, 32, 55
D	16, 20	16, 17, 20, 47	16, 47	16, 47	16, 47	16, 17	16, 20	16, 20, 20A	16, 20, 20A	16, 20, 20A	16, 17, 20, 47	16, 20, 47, 20A 20B	16, 20, 47, 20A	47, 20A	16, 20, 47, 20A
m^{5}U	54	54		54	54	54	54	54	54	54	54	54	54	54	54
Um								44	44	44					
mcm^{5}U															
mcm^{5}s^{2}U		34													
ncm^{5}U						34									34
ncm^{5}Um															

	$tRNA^{Ala}(IGC)$	$tRNA^{Arg}(ICG)$	$tRNA^{Arg}(mcm^5UCU)$	$tRNA^{Asn}(GUU)$	$tRNA^{Asp}(GUC)$	$tRNA^{Cys}(GCA)$	$tRNA^{Glu}(mcm^5s^2UUC)$	$tRNA^{Gly}(GCC)$	$tRNA^{Gly}(UCC)$	$tRNA^{His}(GUG)$	$tRNA^{Ile}(IAU)$	$tRNA^{Ile}(YAY)$	$tRNA^{Leu}(m^5CAA)$	$tRNA^{Leu}(UAG)$	$tRNA^{Leu}(ncm^5UmAA)$
I	34	34									34				
m^1I	37														
m^1A		58	58	58		58					58	58		58	58
t^6A			37	37							37	37			
i^6A						37									
Ar(p)															
Am										4					
m5C		49		48	49	48	49	49		49	48	48	34, 48	48	48
ac^4C													12	12	12
m^3C															
Cm								4	4						32
m^1G	9	9	9		37			9		37	9		37	37	37
m^2G		10	10	10							10	10	10	10	10
$m^2{}_2G$	26	26	26	26									26	26	26
Gm										18			18	18	18
m^7G						46						46			
yW															
Y	38, 55	1, 27, 55	27, 39, 55	39, 55	13, 32, 55	32, 39, 55	13, 27, 55	13, 32, 38, 55	13, 55	13, 32, 39, 55	55	27, 34, 36, 55, 67	32, 39, 55	27, 32, 39, 55	39, 55
D	16, 20, 47	16, 20, 47	16, 47	16, 17, 20, 20A, 47	16, 20	16, 20, 47	20A	16, 20	16, 20, 20A	16, 20, 20A	16, 17, 20, 20A, 47	16, 20, 20A, 47	20, 20B	16, 20, 20A, 20B	16, 20, 20B
m^5U	54	54	54	54	54	54	54	54	54	54	54	54	54	54	54
Um															
mcm^5U			34												
mcm^5s^2U							34								
ncm^5U															
ncm^5Um															34

Table 1-1. Locations of modifications in *S. cerevisiae* tRNA. In this table, each column represents one species of tRNA; each row represents one species of modifications.

tRNA modification	Position of modification	Genes responsible for modification
I	34	*TAD2, TAD3*
m^1I	37	*TAD1, TRM5*
m^1A	58	*TRM6, TRM61*
t^6A	37	Unknown
i^6A	37	*MOD5*
Ar(p)	64	*RIT1*
Am	4	Unknown
m^5C	34, 40, 48, 49	*TRM4*
ac^4C	12	*TAN1*
m^3C	32	Unknown
Cm	32, 34	*TRM7*
	4	Unknown
m^1G	9	*TRM10*
	37	*TRM5*
m^2G	10	*TRM11*
	26	Unknown
$m^2{}_2G$	26	*TRM1*
Gm	18	*TRM3*
	34	*TRM7*
m^7G	46	*TRM8, TRM82*
yW	37	*TRM5*
Y	26, 27, 28, 34, 36, 65, 67	*PUS1*
	38, 39	*PUS3*
	55	*PUS4*
	31	*PUS6*
	13, 35	*PUS7*
	32	*PUS8, PUS9*
	1	Unknown
D	16, 17	*DUS1*
	20	*DUS2*
	47	*DUS3*
	20A, 20B	*DUS4*
m^5U	54	*TRM2*
Um	44	Unknown
mcm^5U	34	*TRM9, ELP1-ELP6, KTI11-KTI13*
mcm^5s^2U	34	*TRM9, NFS1, ELP1-EPL6, KTI11-KTI13*
ncm^5U	34	*ELP1-EPL6, KTI11-KTI13*
ncm^5Um	34	*ELP1-EPL6, KTI11-KTI13*

Table 1-2. Genes those are responsible for the formation of tRNA secondary modifications in *S. cerevisiae*.

Functions of tRNA secondary modifications

Modified ribonucleosides are present in all organisms that have been studied. As noted earlier, there are at least 107 RNA modifications; 92 of which are found in tRNA (*86, 100, 101*). Some modifications are common to all three phylogenetic domains of life and some are even located at the identical locations in specific tRNA species from widely differing organisms (*102*). This high degree of conservation suggests that the modified ribonucleosides have important functions in cell physiology. However, while it has been shown that individual tRNA modifications are involved in many biological processes, including aminoacylation of tRNA and decoding of codon during translation, there is surprisingly little known about the biological function of the system of modifications.

Some tRNA modifications are essential to maintain the specificity of tRNA aminoacylation. For example, unmodified yeast $tRNA^{Asp}$ has an altered tertiary structure that causes mischarging of the tRNA by arginine aminoacyl tRNA synthetase (ArgRS) (*103, 104*). Modifications at several positions are particularly important in aminoacylation. At position 10 of yeast $tRNA^{Phe}$, the modification m^2G affect the kinetics of aminoacylation (*105*). *E. coli* $tRNA^{Phe}$ has no modification at G10 and replacing G10 with m^2G10 makes this tRNA a better substrate for yeast PheRS. Interestingly, m^2G10 on the *E. coli* $tRNA^{Phe}$ diminishes the efficiency of aminoacylation by the *E. coli* PheRS. It is proposed that m^2G10 affects aminoacylation by altering tRNA structure, since this modification is not directly involved in interacting with PheRS or catalyzing the reaction. For direct interactions, tRNA recognition by aminoacyl tRNA synthase involves mainly the anticodon region. In an *E. coli* $tRNA^{Ile}$, the wobble position 34 is

modified as lysidine (k^2C) and, the absence of this modification causes mischarging by MetRS (*106, 107*). Another example involves loss of mnm^5s^2U34 in $tRNA^{Gln}$, $tRNA^{Glu}$, and $tRNA^{Lys}$ in *E. coli*, which leads to a significant decrease in the acylation activities on these tRNAs (*108-111*). The modification mannosyl-queuosine at position 34 of mammalian $tRNA^{Asp}$ has a similar effect (*112*). At position 35, the middle base of the anticodon, Y35 of $tRNA^{Tyr}$ is proposed to form hydrogen bonds with TyrRS (*113*). However, modifications surrounding the anticodon also affect aminoacylation. For example, m^1G37 of yeast $tRNA^{Asp}$ prevents misaminoacylation and t^6A37 of $tRNA^{Ile}$ promotes aminoacylation (*114*).

Besides aminoacylation, modified ribonucleosides in the anticodon region play significant roles in the efficiency of codon reading. Some modifications at the wobble position stabilize the codon-anticodon interactions. For example, a yeast leucine-inserting amber suppressor tRNA (SUP53) contains m^5C at the wobble position, with loss of the modification leading to less efficient suppression of the amber stop codon (*96*). This indicates that the modification plays a significant role in binding of the tRNA to its corresponding codon. In some situations, lacking a modified nucleoside causes misreading of codons. In *E. coli*, deletion of either *mnmE* or *gidA*, the products of which are involved in the synthesis of mnm^5s^2U34, causes a +2 frameshift when reading the sequence GAGAGA (*115*). More importantly, tRNA modifications are involved in codon recognition. Codons in some codon boxes correspond to two different amino acids (the four codons that have the same first and second bases are listed in the same codon box). Some modified nucleotides restrict wobbling to avoid misincorporation. For example, mcm^5s^2U34 in yeast $tRNA^{Glu}$ limits the tRNA to pair with A (*116*). Similarly, mnm^5s^2U at the wobble position of *E. coli* $tRNA^{Gln}$, $tRNA^{Lys}$, and $tRNA^{Glu}$ only forms a strong base pair with A, with the base pair to G

being weak (*108, 117*). Many wobble modifications with similar structures, including mcm^5U, ncm^5U, $cmnm^5U$, and $mchm^5U$, are involved in restricting codon recognition (*118*). These modifications restrict the conformation of the nucleobases to favor base pairing with A (*119-121*). Modifications on cytosine, such as Cm, ac^4C, f^5C, and k^2C, can also stabilize a conformation that promotes base pairing with A and inhibits that with other ribonucleotides (*122-125*). In contrast, some other modifications elevate the flexibility of base pairing. In some codon boxes, all four codons code for the same amino acid and so, efficiency of translation can be improved if a single species of tRNA can recognize all four codons. However, no canonical nucleobases can base pair with all four ribonucleosides. Some organisms have modified ribonucleosides at wobble position to extend the number of codons recognized by specific species of tRNA. For example, *E. coli*, $tRNA^{Val}$, $tRNA^{Ser}$, and $tRNA^{Ala}$ contain cmo^5U34 and *B. subtilis* $tRNA^{Val}$, $tRNA^{Pro}$, $tRNA^{Thr}$, and $tRNA^{Ala}$ contain mo^5U34 (*126-129*), in which these two modification allow the tRNA to interact with codons with A, U, and G at the wobble position (*126, 128, 130, 131*).

There are also other functions for modified ribonucleosides. For example, tRNA modifications may be involved in signaling for translocation of tRNA. In bean (*Phaseolus vulgaris*) and potato (*Solanum tuberosum*), a nuclear-encoded $tRNA^{Val}$ is located in both cytosol and mitochondria. While the $tRNA^{Val}$ in mitochondria has Gm18, this modification is absent in cytosolic $tRNA^{Val}$ (*132, 133*). Methyltransferase activities for formation of Gm have been identified in cytosol but not in mitochondria (*134*), which suggests that Gm18 determines the final destination of the $tRNA^{Val}$. Modified nucleotides also affect the lifetime of tRNA. In yeast, $tRNA^{Val}$(AAC) lacking m^7G and m^5C is degraded rapidly by some 5'-3' exonucleases (*99, 135*).

Degradation of $tRNA^{Ser}$(CGA) and $tRNA^{Ser}$(UGA) is also observed when these tRNAs lack ac^4C and Um (*136*). As the roles of many modified nucleotides are poorly understood, tRNA modifications are potentially involved in many other biological pathways.

Changes in levels of tRNA modifications as cellular response to stress

There are emerging evidence that tRNA modifications are involved in cellular responses to stress. From the discussion above, it is obvious that modifications in tRNA affect both the rate and fidelity of protein synthesis. There are several examples in which misincorporation of amino acids and frameshifts in codon reading frame are employed as regulatory mechanisms (*137-139*). For instance, protein synthesis of a mammalian glutathione peroxidase involves site-specific frameshift by suppressor serine tRNAs, which is necessary to incorporate a non-canonical amino acid, selenocystein, into the enzyme active site for adapting changes in physiological conditions (*140*). Modified ribonucleosides thus have the potential to regulate these pathways.

Many genes for tRNA modifying enzymes are not essential for cells growing in rich culture medium. However, deletion of these genes generates an increase in the cellular sensitivity to specific stresses. For example, the methyl transferase TRM1 is responsible for the formation of $m^2{}_2G$ in yeast tRNA. While it does not affect cell growth, loss of *trm1* leads to sensitivity to heat, benomyl, 5-florouracil, and cycloheximide (*141-143*). Similarly, the m^5C-methyltransferase TRM4 confers resistance to heat, caffeine, and rapamycin (*144, 145*), while 2'-*O*-methyltransferase TRM7 confers resistance to hydrogen peroxide, streptomycin, sulfanilamide,

and cycloheximide (*146-148*). The m^7G-methyltransferase TRM8 confers resistance to heat, cycloheximide, and 5-fluorouracil (*142, 146, 149*) and m^2G-methyltransferase TRM11 confers resistance to killer toxins and papulacandin B (*150*). These studies suggest that modified ribonucleotides in tRNA are components of cellular response pathways.

While the presence of some tRNA modifications confers resistance to specific stresses, it has also been shown that the level of individual modified nucleotide can alter in responses to physiological states. An example of this phenomenon involves starvation of different nutrients, which leads to unique changes in the level of tRNA modifications. In *Salmonella typhimurium*, ms^2io^6A37 is replaced by ms^2i^6A37 under anaerobic conditions, probably because the hydroxylation of ms^2i^6A requires molecular oxygen (*151*). Interestingly, if the hydroxylase for this reaction is absent, the cells are not able to use intermediates of the TCA cycle, including malate, fumarate, and succinate, as sources of energy (*152*). This suggests that ms^2io^6A37 plays a role in regulating metabolic pathways. While the formation of ms^2io^6A depends on the availability of its precursor, this is not always the case. Deficiency in leucine, histidine, or arginine causes under-modification at several positions in an *E. coli* phenylalanine tRNA, including decreases in the levels of acp^3U47 and Y55, as well as loss of D16 and ms^2i^6A37 (*153, 154*). The under-modification occurs even though the growth rate of the cells is not affected, which suggests that changes in the spectrum of modified ribonucleosides are not caused by lack of biosynthetic precursors (*155*).

Besides responding to changes in environment, tRNA modifications also change as a function of cell cycle. In mammalian cells, one of the leucine tRNAs, $tRNA^{Leu}(2)$, is under-

modified in some stages of the cell cyle, with the under-modified tRNA known as $tRNA^{Leu}(4)$ (*156, 157*). The level of $tRNA^{Leu}(4)$ is high during cell growth in G1 phase, while it decreases when cell enters S phase and increases again the cell is ready to go to G2 phase (*158*). For temperature-sensitive mutant that are trapped in G1 phase during heat-shock or deficiency in leucine, the level of $tRNA^{Leu}(4)$ remains low (*156*). These studies support a role for tRNA modifications in control of the cell cycle

There are a number of observations that suggest that tRNA modifications play a role in cellular responses to stress, though the mechanisms linking the RNA modification and the response are not well understood. For example, recent studies indicate that a specific modification in *S. cerevisiae* is involved in regulation of protein synthesis that somehow confers resistance to DNA damage. It is known that a tRNA methyltransferase, Trm9, modulates the toxicity of exposure to alkylating agents and ionizing radiation, with the transcription level of the *trm9* gene elevates in cells exposed to these stresses (*159-161*). Trm9 catalyzes the last step of the formation of mcm^5U and mcm^5s^2U at the anticodon wobble position of $tRNA^{Arg}(UCU)$ and $tRNA^{Glu}(CCU)$, respectively (*162, 163*). These two modifications enhance the binding of the tRNA to a specific codon: AGA for $tRNA^{Arg}(UCU)$ and GAA for $tRNA^{Glu}(UUC)$ (*164*). Several studies have demonstrated that the levels of Trm9-catalyzed tRNA modifications control the translation of genes with high usage of the AGA or GAA codons, with most AGA- and GAA-rich genes are associated with responses to DNA damage (*165*). In humans, $tRNA^{Arg}(UCU)$ also contains mcm^5U34 and its formation is catalyzed by a Trm9 homolog, ABH8 (*166*), an enzyme that possesses both a domain homologous to Trm9 and a dioxygenase domain (*166*). It has been demonstrated in vitro that ABH8 can catalyze hydroxylation of mcm^5U34 on $tRNA^{Arg}(UCU)$,

with the hydroxyl group added to the α-carbon attached to C5 of uridine to form 5-methoxycarbonylhydroxymethyluridine (mchm^{5}U) (*167*). This hydroxyl group could potentially activate the release of the side chain from C5 to form uridine (Figure 1-2). These results suggest that the level of mcm^{5}U34 is under dynamic control, and, since this modification affects the translation of specific group of genes, the dynamic control of mcm^{5}U34 level on tRNA^{Arg}(UCU) may serve to regulate protein expression to adapt to changes in environment.

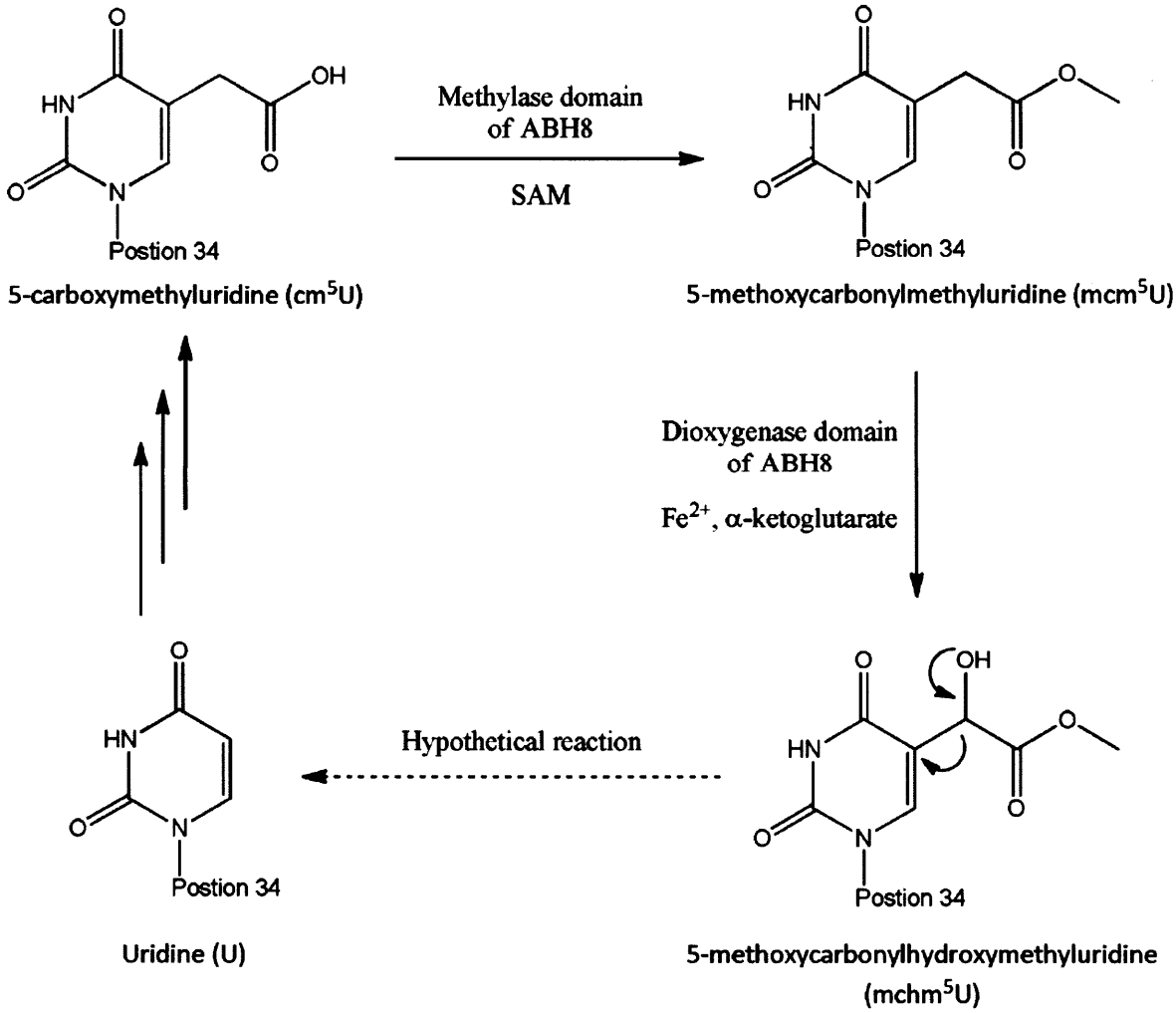

Figure 1-2. Proposed metabolic cycle of 5-methoxycarbonylmethyluridine (mcm^5U) in mammalian tRNA. U34 in $tRNA^{Arg}$(UCU) is modified to 5-carboxymethyluridine (cm^5U) in a multi-steps reaction. In *S. cerevisae*, this process involves at least 9 proteins: *ELP1-EPL6, KTI11-KTI13 (168)*. The methylase domain of ABH8 then catalyzes the methylation of cm^5U to form mcm^5U. The dioxygenase domain of ABH8 catalyzes hydroxylation of mcm^5U to form $mchm^5U$. The hydroxyl group activates the release of this side chain from C5 of uridine to from uridine again.

Studying functions of tRNA modifications with systems approach

From the studies discussed above and other studies, there is a clear role for individual RNA modifications in a variety of cellular responses to chemical exposures and other stimuli. However, given the presence of 25-35 RNA modifications in any organism, the study of individual modifications ignores possible relationships between two or more modifications functioning as a system to control translational efficiency and thus limits our understanding of how these modifications contribute to cell physiology and cell survival with toxic exposures. Further, tRNA modifications could have overlapping roles or they can function cooperatively, as illustrated by the apparent redundancy of modifications that leads to a lack of phenotypic change with the loss of a modification (*99, 135, 136, 169*). The larger biological system in which these modified nucleotides are involved is thus hidden from traditional genetic and molecular biology approaches. To understand the biological roles of tRNA modifications and those in other RNA species in cellular responses, we must study the modifications as a systems.

To this end, the research described in this dissertation aims to understand the functions of RNA modifications at a systems level, in terms of identifying interdependent patterns and behaviors of some or all of the modifications (*170*). Systems-type studies involve an initial

identification of the biological parameters, the individual RNA modifications here, followed by analysis of the behavior of the parameters under different conditions. This requires the development of a model to explain the network structures of the biological system, with the structures identified with a bottom-up or a top-down approaches. In a bottom-up approach, the system is relatively well characterized and the parameters of interest can be determined by literature search, with subsequent targeted analysis of each parameter. For instance, in studies with goals of understanding the regulatory relationships between transcription factors and transcriptional activities, the model for this biological system is that transcription factors regulate transcription; parameters to be monitored are the abundance levels of the mRNAs and the levels of the transcription factors. This approach has been used in understanding a wide range of biosystems, such as studies of embryonic developments of *Drosophila* (*171-174*). The top-down approach mainly relies on collecting large amounts of data to construct networks in a system. For instance, some studies predict the function of genes based on DNA microarray data using clustering analysis (*175-178*). The parameters monitored in systems-level studies vary widely, including lipids, metabolites, proteins, microRNA, mRNA, and carbohydrates. Data can also be generated by measurements of the frequency of biological processes, such as protein-protein interactions and assembly of organelles. Systems biology studies increasingly involve image-based spatial and time-lapse microscopic observations, including protein localization and subcellular responses (*179, 180*). In many cases, specialized tools must be developed to acquire quantifiable data for subsequent behavior analysis. Generally, the goal is to analyze the dynamic behaviors of the parameters of the system under various conditions, such as external perturbations or cell cycle phases. In addition to a systems-level understanding,

these behavior analyses may reveal targets for modulating activities in the biological system, which can also be targets of medical treatments. Also, with statistical tools and computational power, the response of biological systems to different situations can be simulated and predicted. Such simulations can provide the fundamentals for designing new biosystems or modifying existing systems for various applications.

To understand the roles of tRNA modifications in stress response, the theme of this thesis is to study modified ribonucleosides as a system of interrelated components. Based upon the examples mentioned above, we hypothesize that level of modified ribonucleosides in tRNA changes in response to specific stresses to control the translation of critical stress response proteins. To test this model, a mass spectrometry-based platform was developed to quantify modified ribonucleosides in populations of tRNA (Chapter 2). This platform was then used to assess changes in the spectrum of modified ribonucleosides in tRNA from *S. cerevisiae* exposed to toxic agents with various mechanisms of action. Statistical methods, including hierarchical clustering and principle components analysis, were employed to determine unique patterns of changes in response to different stresses (Chapter 3). We then examined the mechanism linking RNA modifications to the stress response. One of the changes noted in response to exposure to hydrogen peroxide involved *trm4*, the gene responsible for formation of m^5C in tRNA. It was observed that m^5C is mechanistically linked to expression of specific ribosomal proteins and its presence, along with the altered ribosomal proteins, confers resistance to hydrogen peroxide toxicity. These studies demonstrate a novel translational regulation pathway in response to stress (Chapter 4). Furthermore, we developed a data-driven model from changes in spectrum of *S. cerevisiae* tRNA modifications for predicting the behavior of

specific classes of toxicant exposures (Chapter 5). This work is then summarized and discussed in a larger context in Chapter 6.

References

1. Brown, J. R., and Lupas, A. N. (1998) What makes a thermophile?, *Trends Microbiol 6*, 349-350.
2. D'Amico, S., Collins, T., Marx, J. C., Feller, G., and Gerday, C. (2006) Psychrophilic microorganisms: challenges for life, *EMBO Rep 7*, 385-389.
3. Toivola, D. M., Strnad, P., Habtezion, A., and Omary, M. B. Intermediate filaments take the heat as stress proteins, *Trends Cell Biol 20*, 79-91.
4. Welch, W. J., and Suhan, J. P. (1986) Cellular and biochemical events in mammalian cells during and after recovery from physiological stress, *J Cell Biol 103*, 2035-2052.
5. Nadeau, S. I., and Landry, J. (2007) Mechanisms of activation and regulation of the heat shock-sensitive signaling pathways, *Adv Exp Med Biol 594*, 100-113.
6. Pitzschke, A., Schikora, A., and Hirt, H. (2009) MAPK cascade signalling networks in plant defence, *Curr Opin Plant Biol 12*, 421-426.
7. Eisen, M. B., Spellman, P. T., Brown, P. O., and Botstein, D. (1998) Cluster analysis and display of genome-wide expression patterns, *Proc Natl Acad Sci U S A 95*, 14863-14868.

8. Gasch, A. P., Spellman, P. T., Kao, C. M., Carmel-Harel, O., Eisen, M. B., Storz, G., Botstein, D., and Brown, P. O. (2000) Genomic expression programs in the response of yeast cells to environmental changes, *Mol Biol Cell 11*, 4241-4257.

9. GuhaThakurta, D., Palomar, L., Stormo, G. D., Tedesco, P., Johnson, T. E., Walker, D. W., Lithgow, G., Kim, S., and Link, C. D. (2002) Identification of a novel cis-regulatory element involved in the heat shock response in Caenorhabditis elegans using microarray gene expression and computational methods, *Genome Res 12*, 701-712.

10. Larkindale, J., and Vierling, E. (2008) Core genome responses involved in acclimation to high temperature, *Plant Physiol 146*, 748-761.

11. Matsuura, H., Ishibashi, Y., Shinmyo, A., Kanaya, S., and Kato, K. Genome-wide analyses of early translational responses to elevated temperature and high salinity in Arabidopsis thaliana, *Plant Cell Physiol 51*, 448-462.

12. Richmond, C. S., Glasner, J. D., Mau, R., Jin, H., and Blattner, F. R. (1999) Genome-wide expression profiling in Escherichia coli K-12, *Nucleic Acids Res 27*, 3821-3835.

13. Rohlin, L., Trent, J. D., Salmon, K., Kim, U., Gunsalus, R. P., and Liao, J. C. (2005) Heat shock response of Archaeoglobus fulgidus, *J Bacteriol 187*, 6046-6057.

14. Tabuchi, Y., Takasaki, I., Wada, S., Zhao, Q. L., Hori, T., Nomura, T., Ohtsuka, K., and Kondo, T. (2008) Genes and genetic networks responsive to mild hyperthermia in human lymphoma U937 cells, *Int J Hyperthermia 24*, 613-622.

15. Chang, L., and Karin, M. (2001) Mammalian MAP kinase signalling cascades, *Nature 410*, 37-40.

16. Martindale, J. L., and Holbrook, N. J. (2002) Cellular response to oxidative stress: signaling for suicide and survival, *J Cell Physiol 192*, 1-15.

17. Graves, L. M., Guy, H. I., Kozlowski, P., Huang, M., Lazarowski, E., Pope, R. M., Collins, M. A., Dahlstrand, E. N., Earp, H. S., 3rd, and Evans, D. R. (2000) Regulation of carbamoyl phosphate synthetase by MAP kinase, *Nature 403*, 328-332.

18. Burns, T. F., and El-Deiry, W. S. (1999) The p53 pathway and apoptosis, *J Cell Physiol 181*, 231-239.

19. Sionov, R. V., and Haupt, Y. (1999) The cellular response to p53: the decision between life and death, *Oncogene 18*, 6145-6157.

20. Riley, T., Sontag, E., Chen, P., and Levine, A. (2008) Transcriptional control of human p53-regulated genes, *Nat Rev Mol Cell Biol 9*, 402-412.

21. Futcher, B., Latter, G. I., Monardo, P., McLaughlin, C. S., and Garrels, J. I. (1999) A sampling of the yeast proteome, *Mol Cell Biol 19*, 7357-7368.

22. Gygi, S. P., Rochon, Y., Franza, B. R., and Aebersold, R. (1999) Correlation between protein and mRNA abundance in yeast, *Mol Cell Biol 19*, 1720-1730.

23. Chang, M., Bellaoui, M., Boone, C., and Brown, G. W. (2002) A genome-wide screen for methyl methanesulfonate-sensitive mutants reveals genes required for S phase progression in the presence of DNA damage, *Proc Natl Acad Sci U S A 99*, 16934-16939.

24. Luco, R. F., Allo, M., Schor, I. E., Kornblihtt, A. R., and Misteli, T. (2011) Epigenetics in alternative pre-mRNA splicing, *Cell 144*, 16-26.

25. Sharp, P. A. (2005) The discovery of split genes and RNA splicing, *Trends Biochem Sci 30*, 279-281.

26. Takechi, H., Hosokawa, N., Hirayoshi, K., and Nagata, K. (1994) Alternative 5' splice site selection induced by heat shock, *Mol Cell Biol 14*, 567-575.

27. Chandler, D. S., Singh, R. K., Caldwell, L. C., Bitler, J. L., and Lozano, G. (2006) Genotoxic stress induces coordinately regulated alternative splicing of the p53 modulators MDM2 and MDM4, *Cancer Res 66*, 9502-9508.

28. Ars, E., Serra, E., de la Luna, S., Estivill, X., and Lazaro, C. (2000) Cold shock induces the insertion of a cryptic exon in the neurofibromatosis type 1 (NF1) mRNA, *Nucleic Acids Res 28*, 1307-1312.

29. Biamonti, G., and Caceres, J. F. (2009) Cellular stress and RNA splicing, *Trends Biochem Sci 34*, 146-153.

30. Leung, A. K., and Sharp, P. A. MicroRNA functions in stress responses, *Mol Cell 40*, 205-215.

31. Leung, A. K., and Sharp, P. A. (2007) microRNAs: a safeguard against turmoil?, *Cell 130*, 581-585.

32. Siomi, H., and Siomi, M. C. (2009) On the road to reading the RNA-interference code, *Nature 457*, 396-404.

33. Junttila, M. R., and Evan, G. I. (2009) p53--a Jack of all trades but master of none, *Nat Rev Cancer 9*, 821-829.

34. Bhattacharyya, S. N., Habermacher, R., Martine, U., Closs, E. I., and Filipowicz, W. (2006) Relief of microRNA-mediated translational repression in human cells subjected to stress, *Cell 125*, 1111-1124.

35. Bushati, N., and Cohen, S. M. (2007) microRNA functions, *Annu Rev Cell Dev Biol 23*, 175-205.

36. Leaman, D., Chen, P. Y., Fak, J., Yalcin, A., Pearce, M., Unnerstall, U., Marks, D. S., Sander, C., Tuschl, T., and Gaul, U. (2005) Antisense-mediated depletion reveals essential and specific functions of microRNAs in Drosophila development, *Cell 121*, 1097-1108.

37. Miska, E. A., Alvarez-Saavedra, E., Abbott, A. L., Lau, N. C., Hellman, A. B., McGonagle, S. M., Bartel, D. P., Ambros, V. R., and Horvitz, H. R. (2007) Most Caenorhabditis elegans microRNAs are individually not essential for development or viability, *PLoS Genet 3*, e215.

38. Flynt, A. S., Thatcher, E. J., Burkewitz, K., Li, N., Liu, Y., and Patton, J. G. (2009) miR-8 microRNAs regulate the response to osmotic stress in zebrafish embryos, *J Cell Biol 185*, 115-127.

39. Li, X., Cassidy, J. J., Reinke, C. A., Fischboeck, S., and Carthew, R. W. (2009) A microRNA imparts robustness against environmental fluctuation during development, *Cell 137*, 273-282.

40. van Rooij, E., Sutherland, L. B., Qi, X., Richardson, J. A., Hill, J., and Olson, E. N. (2007) Control of stress-dependent cardiac growth and gene expression by a microRNA, *Science 316*, 575-579.

41. Xu, P., Vernooy, S. Y., Guo, M., and Hay, B. A. (2003) The Drosophila microRNA Mir-14 suppresses cell death and is required for normal fat metabolism, *Curr Biol 13*, 790-795.

42. Goldberg, A. L., and Dice, J. F. (1974) Intracellular protein degradation in mammalian and bacterial cells, *Annu Rev Biochem 43*, 835-869.

43. Goldberg, A. L., and St John, A. C. (1976) Intracellular protein degradation in mammalian and bacterial cells: Part 2, *Annu Rev Biochem 45*, 747-803.

44. Coutts, A. S., Adams, C. J., and La Thangue, N. B. (2009) p53 ubiquitination by Mdm2: a never ending tail?, *DNA Repair (Amst) 8*, 483-490.

45. Haupt, Y., Maya, R., Kazaz, A., and Oren, M. (1997) Mdm2 promotes the rapid degradation of p53, *Nature 387*, 296-299.

46. Itahana, K., Mao, H., Jin, A., Itahana, Y., Clegg, H. V., Lindstrom, M. S., Bhat, K. P., Godfrey, V. L., Evan, G. I., and Zhang, Y. (2007) Targeted inactivation of Mdm2 RING finger E3 ubiquitin ligase activity in the mouse reveals mechanistic insights into p53 regulation, *Cancer Cell 12*, 355-366.

47. Kubbutat, M. H., Jones, S. N., and Vousden, K. H. (1997) Regulation of p53 stability by Mdm2, *Nature 387*, 299-303.

48. Mathews, M., Sonenberg, N., and Hershey, J. W. B. (2007) *Translational control in biology and medicine*, [3rd ed., Cold Spring Harbor Laboratory Press, Cold Spring Harbor, N.Y.

49. Sonenberg, N., Hershey, J. W. B., and Mathews, M. (2000) *Translational control of gene expression*, 2nd ed., Cold Spring Harbor Laboratory Press, Cold Spring Harbor, NY.

50. Wek, R. C., Jiang, H. Y., and Anthony, T. G. (2006) Coping with stress: eIF2 kinases and translational control, *Biochem Soc Trans 34*, 7-11.

51. Zhang, F., Saha, S., Shabalina, S. A., and Kashina, A. Differential arginylation of actin isoforms is regulated by coding sequence-dependent degradation, *Science 329*, 1534-1537.

52. Ho, O., and Green, W. R. (2006) Alternative translational products and cryptic T cell epitopes: expecting the unexpected, *J Immunol 177*, 8283-8289.

53. Zook, M. B., Howard, M. T., Sinnathamby, G., Atkins, J. F., and Eisenlohr, L. C. (2006) Epitopes derived by incidental translational frameshifting give rise to a protective CTL response, *J Immunol 176*, 6928-6934.

54. Moore, P. B., and Steitz, T. A. The Roles of RNA in the Synthesis of Protein, *Cold Spring Harb Perspect Biol*.

55. Watson, J. D. (1963) Involvement of RNA in the synthesis of proteins, *Science 140*, 17-26.

56. Green, R., and Noller, H. F. (1997) Ribosomes and translation, *Annu Rev Biochem 66*, 679-716.

57. Monro, R. E., and Marcker, K. A. (1967) Ribosome-catalysed reaction of puromycin with a formylmethionine-containing oligonucleotide, *J Mol Biol 25*, 347-350.

58. Ogle, J. M., Brodersen, D. E., Clemons, W. M., Jr., Tarry, M. J., Carter, A. P., and Ramakrishnan, V. (2001) Recognition of cognate transfer RNA by the 30S ribosomal subunit, *Science 292*, 897-902.

59. Nissen, P., Hansen, J., Ban, N., Moore, P. B., and Steitz, T. A. (2000) The structural basis of ribosome activity in peptide bond synthesis, *Science 289*, 920-930.

60. Sievers, A., Beringer, M., Rodnina, M. V., and Wolfenden, R. (2004) The ribosome as an entropy trap, *Proc Natl Acad Sci U S A 101*, 7897-7901.

61. Hansen, J. L., Schmeing, T. M., Moore, P. B., and Steitz, T. A. (2002) Structural insights into peptide bond formation, *Proc Natl Acad Sci U S A 99*, 11670-11675.

62. Weinger, J. S., Parnell, K. M., Dorner, S., Green, R., and Strobel, S. A. (2004) Substrate-assisted catalysis of peptide bond formation by the ribosome, *Nat Struct Mol Biol 11*, 1101-1106.

63. Dorner, S., Panuschka, C., Schmid, W., and Barta, A. (2003) Mononucleotide derivatives as ribosomal P-site substrates reveal an important contribution of the 2'-OH to activity, *Nucleic Acids Res 31*, 6536-6542.

64. Xia, T., SantaLucia, J., Jr., Burkard, M. E., Kierzek, R., Schroeder, S. J., Jiao, X., Cox, C., and Turner, D. H. (1998) Thermodynamic parameters for an expanded nearest-neighbor model for formation of RNA duplexes with Watson-Crick base pairs, *Biochemistry 37*, 14719-14735.

65. Garrett, R. A. (2000) *The Ribosome : structure, function, antibiotics, and cellular interaction*, ASM Press, Washington, D.C.

66. Moazed, D., and Noller, H. F. (1990) Binding of tRNA to the ribosomal A and P sites protects two distinct sets of nucleotides in 16 S rRNA, *J Mol Biol 211*, 135-145.

67. Yoshizawa, S., Fourmy, D., and Puglisi, J. D. (1999) Recognition of the codon-anticodon helix by ribosomal RNA, *Science 285*, 1722-1725.

68. Ogle, J. M., Carter, A. P., and Ramakrishnan, V. (2003) Insights into the decoding mechanism from recent ribosome structures, *Trends Biochem Sci 28*, 259-266.

69. Ogle, J. M., and Ramakrishnan, V. (2005) Structural insights into translational fidelity, *Annu Rev Biochem 74*, 129-177.

70. Vlassov, A. V., Kazakov, S. A., Johnston, B. H., and Landweber, L. F. (2005) The RNA world on ice: a new scenario for the emergence of RNA information, *J Mol Evol 61*, 264-273.

71. Deutscher, M. P. (1995) tRNA processing nucleases, in *tRNA : structure, biosynthesis, and function* (Söll, D., and RajBhandary, U., Eds.), pp xi, 572 p., ASM Press, Washington, D.C.

72. O'Connor, J. P., and Peebles, C. L. (1991) In vivo pre-tRNA processing in Saccharomyces cerevisiae, *Mol Cell Biol 11*, 425-439.

73. Rooney, R. J., and Harding, J. D. (1986) Processing of mammalian tRNA transcripts in vitro: different pre-tRNAs are processed along alternative pathways that contain a common rate-limiting step, *Nucleic Acids Res 14*, 4849-4864.

74. van Tol, H., Stange, N., Gross, H. J., and Beier, H. (1987) A human and a plant intron-containing tRNATyr gene are both transcribed in a HeLa cell extract but spliced along different pathways, *EMBO J 6*, 35-41.

75. Hartmann, E., and Hartmann, R. K. (2003) The enigma of ribonuclease P evolution, *Trends Genet 19*, 561-569.

76. Xiao, S., Scott, F., Fierke, C. A., and Engelke, D. R. (2002) Eukaryotic ribonuclease P: a plurality of ribonucleoprotein enzymes, *Annu Rev Biochem 71*, 165-189.

77. Altman, S., Kirsebom, L., and Talbot, S. (1995) Recent studies of RNase P, in *tRNA : structure, biosynthesis, and function* (Söll, D., and RajBhandary, U., Eds.), pp xi, 572 p., ASM Press, Washington, D.C.

78. Papadimitriou, A., and Gross, H. J. (1996) Pre-tRNA 3'-processing in Saccharomyces cerevisiae. Purification and characterization of exo- and endoribonucleases, *Eur J Biochem 242*, 747-759.

79. Aebi, M., Kirchner, G., Chen, J. Y., Vijayraghavan, U., Jacobson, A., Martin, N. C., and Abelson, J. (1990) Isolation of a temperature-sensitive mutant with an altered tRNA nucleotidyltransferase and cloning of the gene encoding tRNA nucleotidyltransferase in the yeast Saccharomyces cerevisiae, *J Biol Chem 265*, 16216-16220.

80. Chen, J. Y., Kirchner, G., Aebi, M., and Martin, N. C. (1990) Purification and properties of yeast ATP (CTP):tRNA nucleotidyltransferase from wild type and overproducing cells, *J Biol Chem 265*, 16221-16224.

81. Westaway, S. K., and Abelson, J. (1995) Splicing of tRNA precursors, in *tRNA : structure, biosynthesis, and function* (Söll, D., and RajBhandary, U., Eds.), pp xi, 572 p., ASM Press, Washington, D.C.

82. Hani, J., and Feldmann, H. (1998) tRNA genes and retroelements in the yeast genome, *Nucleic Acids Res 26*, 689-696.

83. Peebles, C. L., Gegenheimer, P., and Abelson, J. (1983) Precise excision of intervening sequences from precursor tRNAs by a membrane-associated yeast endonuclease, *Cell 32*, 525-536.

84. Belford, H. G., Westaway, S. K., Abelson, J., and Greer, C. L. (1993) Multiple nucleotide cofactor use by yeast ligase in tRNA splicing. Evidence for independent ATP- and GTP-binding sites, *J Biol Chem 268*, 2444-2450.

85. McCraith, S. M., and Phizicky, E. M. (1990) A highly specific phosphatase from Saccharomyces cerevisiae implicated in tRNA splicing, *Mol Cell Biol 10*, 1049-1055.

86. Cantara, W. A., Crain, P. F., Rozenski, J., McCloskey, J. A., Harris, K. A., Zhang, X., Vendeix, F. A., Fabris, D., and Agris, P. F. (2010) The RNA Modification Database, RNAMDB: 2011 update, *Nucleic Acids Res 39*, D195-201.

87. Nishikura, K., and De Robertis, E. M. (1981) RNA processing in microinjected Xenopus oocytes. Sequential addition of base modifications in the spliced transfer RNA, *J Mol Biol 145*, 405-420.

88. Sakano, H., Shimura, Y., and Ozeki, H. (1974) Selective modification of nucleosides of tRNA precursors accumulated in a temperature sensitive mutant of Escherichia coli, *FEBS Lett 48*, 117-121.

89. Sakano, H., and Shimura, Y. (1975) Sequential processing of precursor tRNA molecules in Escherichia coli, *Proc Natl Acad Sci U S A 72*, 3369-3373.

90. Davis, A. R., and Nierlich, D. P. (1974) The methylation of transfer RNA in Escherichia coli, *Biochim Biophys Acta 374*, 23-37.

91. Schaefer, K. P., Altman, S., and Soll, D. (1973) Nucleotide modification in vitro of the precursor of transfer RNA of Escherichia coli, *Proc Natl Acad Sci U S A 70*, 3626-3630.

92. Grosjean, H., Haumont, E., Droogmans, L., Carbon, P., Fournier, M., de Henau, S., Doi, T., Keith, G., Gangloff, J., Kretz, K., and Trewyn, R. (1987) A novel approach to the biosynthesis of modified nucleosides in the anticodon loops of eukaryotic transfer RNAs, in *Biophosphates and their analogues : synthesis, structure, metabolism, and activity* (Bruzik, K. S., and Stec, W. J., Eds.), pp p. 355-378, Elsevier, Amsterdam.

93. Sharp, S. J., Schaack, J., Cooley, L., Burke, D. J., and Soll, D. (1985) Structure and transcription of eukaryotic tRNA genes, *CRC Crit Rev Biochem 19*, 107-144.

94. Agris, P. F., Playl, T., Goldman, L., Horton, E., Woolverton, D., Setzer, D., and Rodi, C. (1983) Processing of tRNA is accomplished by a high-molecular-weight enzyme complex, *Recent Results Cancer Res 84*, 237-254.

95. Harris, C. L. (1990) High-molecular-weight forms of aminoacyl-tRNA synthetases and tRNA modification enzymes in Escherichia coli, *J Bacteriol 172*, 1798-1803.

96. Strobel, M. C., and Abelson, J. (1986) Effect of intron mutations on processing and function of Saccharomyces cerevisiae SUP53 tRNA in vitro and in vivo, *Mol Cell Biol 6*, 2663-2673.

97. Hanoune, J., and Agarwal, M. K. (1970) Studies on the half life time of rat liver transfer RNA species, *FEBS Lett 11*, 78-80.

98. Miller, B. G. (1973) The biological half-lives of ribosomal and transfer RNA in the mouse uterus, *J Endocrinol 59*, 81-85.

99. Chernyakov, I., Whipple, J. M., Kotelawala, L., Grayhack, E. J., and Phizicky, E. M. (2008) Degradation of several hypomodified mature tRNA species in Saccharomyces cerevisiae is mediated by Met22 and the 5'-3' exonucleases Rat1 and Xrn1, *Genes Dev 22*, 1369-1380.

100. McCloskey, J. A., and Rozenski, J. (2005) The Small Subunit rRNA Modification Database, *Nucleic Acids Res 33*, D135-138.

101. Rozenski, J., Crain, P. F., and McCloskey, J. A. (1999) The RNA Modification Database: 1999 update, *Nucleic Acids Res 27*, 196-197.

102. Bjork, G. R., Ericson, J. U., Gustafsson, C. E., Hagervall, T. G., Jonsson, Y. H., and Wikstrom, P. M. (1987) Transfer RNA modification, *Annu Rev Biochem 56*, 263-287.

103. Perret, V., Garcia, A., Grosjean, H., Ebel, J. P., Florentz, C., and Giege, R. (1990) Relaxation of a transfer RNA specificity by removal of modified nucleotides, *Nature 344*, 787-789.

104. Perret, V., Garcia, A., Puglisi, J., Grosjean, H., Ebel, J. P., Florentz, C., and Giege, R. (1990) Conformation in solution of yeast tRNA(Asp) transcripts deprived of modified nucleotides, *Biochimie 72*, 735-743.

105. Roe, B., Michael, M., and Dudock, B. (1973) Function of N2 methylguanine in phenylalanine transfer RNA, *Nat New Biol 246*, 135-138.

106. Muramatsu, T., Miyazama, T., and Yokoyama, S. (1992) Recognition of the nucleotide in the first position of the anticodon of isoleucine tRNA by isoleucine-tRNA synthetase from *Escherichia coli*, *Nucleosides Nucleotides 11*, 719-730.

107. Muramatsu, T., Nishikawa, K., Nemoto, F., Kuchino, Y., Nishimura, S., Miyazawa, T., and Yokoyama, S. (1988) Codon and amino-acid specificities of a transfer RNA are both converted by a single post-transcriptional modification, *Nature 336*, 179-181.

108. Agris, P. F., Soll, D., and Seno, T. (1973) Biological function of 2-thiouridine in Escherichia coli glutamic acid transfer ribonucleic acid, *Biochemistry 12*, 4331-4337.

109. Kern, D., and Lapointe, J. (1979) Glutamyl transfer ribonucleic acid synthetase of Escherichia coli. Effect of alteration of the 5-(methylaminomethyl)-2-thiouridine in the anticodon of glutamic acid transfer ribonucleic acid on the catalytic mechanism, *Biochemistry 18*, 5819-5826.

110. Saneyoshi, M., and Nishimura, S. (1971) Selective inactivation of amino acid acceptor and ribosome-binding activities of Escherichia coli tRNA by modification with cyanogen bromide, *Biochim Biophys Acta 246*, 123-131.

111. Seno, T., Agris, P. F., and Soll, D. (1974) Involvement of the anticodon region of Escherichia coli tRNAGln and tRNAGlu in the specific interaction with cognate aminoacyl-tRNA synthetase. Alteration of the 2-thiouridine derivatives located in the anticodon of the tRNAs by BrCN or sulfur deprivation, *Biochim Biophys Acta 349*, 328-338.

112. Singhal, R. P., and Vakharia, V. N. (1983) The role of queuine in the aminoacylation of mammalian aspartate transfer RNAs, *Nucleic Acids Res 11*, 4257-4272.

113. Bare, L. A., and Uhlenbeck, O. C. (1986) Specific substitution into the anticodon loop of yeast tyrosine transfer RNA, *Biochemistry 25*, 5825-5830.

114. Björk, G. R. (1995) Biosynthesis and function of modified nucleosides, in *tRNA : structure, biosynthesis, and function*

(Söll, D., and RajBhandary, U., Eds.), pp 65-205, ASM Press, Washington, D.C.

115. Bregeon, D., Colot, V., Radman, M., and Taddei, F. (2001) Translational misreading: a tRNA modification counteracts a +2 ribosomal frameshift, *Genes Dev 15*, 2295-2306.

116. Sekiya, T., Takeishi, K., and Ukita, T. (1969) Specificity of yeast glutamic acid transfer RNA for codon recognition, *Biochim Biophys Acta 182*, 411-426.

117. Lustig, F., Elias, P., Axberg, T., Samuelsson, T., Tittawella, I., and Lagerkvist, U. (1981) Codon reading and translational error. Reading of the glutamine and lysine codons during protein synthesis in vitro, *J Biol Chem 256*, 2635-2643.

118. Yokoyama, S., and Nishimura, S. (1995) Modified nucleosides and codon recognition, in *tRNA : structure, biosynthesis, and function* (Söll, D., and RajBhandary, U., Eds.), pp 207-223, ASM Press, Washington, D.C.

119. Sakamoto, K., Kawai, G., Niimi, T., Satoh, T., Sekine, M., Yamaizumi, Z., Nishimura, S., Miyazawa, T., and Yokoyama, S. (1993) A modified uridine in the first position of the anticodon of a minor species of arginine tRNA, the argU gene product, from Escherichia coli, *Eur J Biochem 216*, 369-375.

120. Yokoyama, S., Watanabe, T., Murao, K., Ishikura, H., Yamaizumi, Z., Nishimura, S., and Miyazawa, T. (1985) Molecular mechanism of codon recognition by tRNA species with modified uridine in the first position of the anticodon, *Proc Natl Acad Sci U S A 82*, 4905-4909.

121. Yokoyama, S., Yamaizumi, Z., Nishimura, S., and Miyazawa, T. (1979) 1H NMR studies on the conformational characteristics of 2-thiopyrimidine nucleotides found in transfer RNAs, *Nucleic Acids Res 6*, 2611-2626.

122. Kawai, G., Hashizume, T., Miyazawa, T., McCloskey, J. A., and Yokoyama, S. (1989) Conformational characteristics of 4-acetylcytidine found in tRNA, *Nucleic Acids Symp Ser*, 61-62.

123. Kawai, G., Yamamoto, Y., Kamimura, T., Masegi, T., Sekine, M., Hata, T., Iimori, T., Watanabe, T., Miyazawa, T., and Yokoyama, S. (1992) Conformational rigidity of specific pyrimidine residues in tRNA arises from posttranscriptional modifications that enhance steric interaction between the base and the 2'-hydroxyl group, *Biochemistry 31*, 1040-1046.

124. Moriya, J., Yokogawa, T., Wakita, K., Ueda, T., Nishikawa, K., Crain, P. F., Hashizume, T., Pomerantz, S. C., McCloskey, J. A., Kawai, G., and et al. (1994) A novel modified nucleoside found at the first position of the anticodon of methionine tRNA from bovine liver mitochondria, *Biochemistry 33*, 2234-2239.

125. Muramatsu, T., Yokoyama, S., Horie, N., Matsuda, A., Ueda, T., Yamaizumi, Z., Kuchino, Y., Nishimura, S., and Miyazawa, T. (1988) A novel lysine-substituted nucleoside in the first position of the anticodon of minor isoleucine tRNA from Escherichia coli, *J Biol Chem 263*, 9261-9267.

126. Ishikura, H., Yamada, Y., and Nishimura, S. (1971) Structure of serine tRNA from Escherichia coli. I. Purification of serine tRNA's with different codon responses, *Biochim Biophys Acta 228*, 471-481.

127. Kimura, F., Harada, F., and Nishimura, S. (1971) Primary sequence of tRNA-Val-1 from Escherichia coli B. II. Isolation of large fragments by limited digestion with RNases, and overlapping of fragments to reduce the total primary sequence, *Biochemistry 10*, 3277-3283.

128. Murao, K., Hasegawa, T., and Ishikura, H. (1982) Nucleotide sequence of valine tRNA mo5UAC from bacillus subtilis, *Nucleic Acids Res 10*, 715-718.

129. Williams, R. J., Nagel, W., Roe, B., and Dudock, B. (1974) Primary structure of E. coli alanine transfer RNA: relation to the yeast phenylalanyl tRNA synthetase recognition site, *Biochem Biophys Res Commun 60*, 1215-1221.

130. Mitra, S. K., Lustig, F., Akesson, B., Axberg, T., Elias, P., and Lagerkvist, U. (1979) Relative efficiency of anticodons in reading the valine codons during protein synthesis in vitro, *J Biol Chem 254*, 6397-6401.

131. Samuelsson, T., Elias, P., Lustig, F., Axberg, T., Folsch, G., Akesson, B., and Lagerkvist, U. (1980) Aberrations of the classic codon reading scheme during protein synthesis in vitro, *J Biol Chem 255*, 4583-4588.

132. Marechal-Drouard, L., Neuburger, M., Guillemaut, P., Douce, R., Weil, J. H., and Dietrich, A. (1990) A nuclear-encoded potato (Solanum tuberosum) mitochondrial tRNA(Leu) and its cytosolic counterpart have identical nucleotide sequences, *FEBS Lett 262*, 170-172.

133. Marechal-Drouard, L., Weil, J. H., and Guillemaut, P. (1988) Import of several tRNAs from the cytoplasm into the mitochondria in bean Phaseolus vulgaris, *Nucleic Acids Res 16*, 4777-4788.

134. Cavaille, J., Chetouani, F., and Bachellerie, J. P. (1999) The yeast Saccharomyces cerevisiae YDL112w ORF encodes the putative 2'-O-ribose methyltransferase catalyzing the formation of Gm18 in tRNAs, *RNA 5*, 66-81.

135. Alexandrov, A., Chernyakov, I., Gu, W., Hiley, S. L., Hughes, T. R., Grayhack, E. J., and Phizicky, E. M. (2006) Rapid tRNA decay can result from lack of nonessential modifications, *Mol Cell 21*, 87-96.

136. Kotelawala, L., Grayhack, E. J., and Phizicky, E. M. (2008) Identification of yeast tRNA Um(44) 2'-O-methyltransferase (Trm44) and demonstration of a Trm44 role in sustaining levels of specific tRNA(Ser) species, *RNA 14*, 158-169.

137. Engelberg-Kulka, H., and Schoulaker-Schwarz, R. (1988) Stop is not the end: physiological implications of translational readthrough, *J Theor Biol 131*, 477-485.

138. Hatfield, D. L., Levin, J. G., Rein, A., and Oroszlan, S. (1992) Translational suppression in retroviral gene expression, *Adv Virus Res 41*, 193-239.

139. Hatfield, D. L., Smith, D. W., Lee, B. J., Worland, P. J., and Oroszlan, S. (1990) Structure and function of suppressor tRNAs in higher eukaryotes, *Crit Rev Biochem Mol Biol 25*, 71-96.

140. Valle, R. P., and Morch, M. D. (1988) Stop making sense: or Regulation at the level of termination in eukaryotic protein synthesis, *FEBS Lett 235*, 1-15.

141. Dudley, A. M., Janse, D. M., Tanay, A., Shamir, R., and Church, G. M. (2005) A global view of pleiotropy and phenotypically derived gene function in yeast, *Mol Syst Biol 1*, 2005 0001.

142. Gustavsson, M., and Ronne, H. (2008) Evidence that tRNA modifying enzymes are important in vivo targets for 5-fluorouracil in yeast, *RNA 14*, 666-674.

143. Sinha, H., David, L., Pascon, R. C., Clauder-Munster, S., Krishnakumar, S., Nguyen, M., Shi, G., Dean, J., Davis, R. W., Oefner, P. J., McCusker, J. H., and Steinmetz, L. M. (2008) Sequential elimination of major-effect contributors identifies additional quantitative trait loci conditioning high-temperature growth in yeast, *Genetics 180*, 1661-1670.

144. Breslow, D. K., Cameron, D. M., Collins, S. R., Schuldiner, M., Stewart-Ornstein, J., Newman, H. W., Braun, S., Madhani, H. D., Krogan, N. J., and Weissman, J. S. (2008) A comprehensive strategy enabling high-resolution functional analysis of the yeast genome, *Nat Methods 5*, 711-718.

145. Parsons, A. B., Brost, R. L., Ding, H., Li, Z., Zhang, C., Sheikh, B., Brown, G. W., Kane, P. M., Hughes, T. R., and Boone, C. (2004) Integration of chemical-genetic and genetic interaction data links bioactive compounds to cellular target pathways, *Nat Biotechnol 22*, 62-69.

146. Alamgir, M., Erukova, V., Jessulat, M., Azizi, A., and Golshani, A. Chemical-genetic profile analysis of five inhibitory compounds in yeast, *BMC Chem Biol 10*, 6.

147. Botet, J., Mateos, L., Revuelta, J. L., and Santos, M. A. (2007) A chemogenomic screening of sulfanilamide-hypersensitive Saccharomyces cerevisiae mutants uncovers ABZ2, the gene encoding a fungal aminodeoxychorismate lyase, *Eukaryot Cell 6*, 2102-2111.

148. Khoury, C. M., Yang, Z., Li, X. Y., Vignali, M., Fields, S., and Greenwood, M. T. (2008) A TSC22-like motif defines a novel antiapoptotic protein family, *FEMS Yeast Res 8*, 540-563.

149. Auesukaree, C., Damnernsawad, A., Kruatrachue, M., Pokethitiyook, P., Boonchird, C., Kaneko, Y., and Harashima, S. (2009) Genome-wide identification of genes involved in tolerance to various environmental stresses in Saccharomyces cerevisiae, *J Appl Genet 50*, 301-310.

150. de Groot, P. W., Ruiz, C., Vazquez de Aldana, C. R., Duenas, E., Cid, V. J., Del Rey, F., Rodriquez-Pena, J. M., Perez, P., Andel, A., Caubin, J., Arroyo, J., Garcia, J. C., Gil, C., Molina, M., Garcia, L. J., Nombela, C., and Klis, F. M. (2001) A genomic approach for the identification and classification of genes involved in cell wall formation and its regulation in Saccharomyces cerevisiae, *Comp Funct Genomics 2*, 124-142.

151. Buck, M., and Ames, B. N. (1984) A modified nucleotide in tRNA as a possible regulator of aerobiosis: synthesis of cis-2-methyl-thioribosylzeatin in the tRNA of Salmonella, *Cell 36*, 523-531.

152. Persson, B. C. (1993) Modification of tRNA as a regulatory device, *Mol Microbiol 8*, 1011-1016.

153. Fournier, M. J., Webb, E., and Kitchingman, G. R. (1976) General and specific effects of amino acid starvation on the formation of undermodified Escherichia coli phenylalanine tRNA, *Biochim Biophys Acta 454*, 97-113.

154. Kitchingman, G. R., and Fournier, M. J. (1977) Modification-deficient transfer ribonucleic acids from relaxed control Escherichia coli: structures of the major undermodified phenylalanine and leucine transfer RNAs produced during leucine starvation, *Biochemistry 16*, 2213-2220.

155. Thomale, J., and Nass, G. (1978) Alteration of the intracellular concentration of aminoacyl-tRNA synthetases and isoaccepting tRNAs during amino-acid limited growth in Escherichia coli, *Eur J Biochem 85*, 407-418.

156. Ortwerth, B. J., Lin, V. K., Lewis, J., and Wang, R. J. (1984) Lysine tRNA and cell division: a G1 cell cycle mutant is temperature sensitive for the modification of tRNA5Lys to tRNA4Lys, *Nucleic Acids Res 12*, 9009-9023.

157. Ortwerth, B. J., and Liu, L. P. (1973) Correlation between a specific isoaccepting lysyl transfer ribonucleic acid and cell division in mammalian tissues, *Biochemistry 12*, 3978-3984.

158. Conlon-Hollingshead, C., and Ortwerth, B. J. (1980) Lys-tRNA levels and cell division in mouse 3T3 cells, *Exp Cell Res 128*, 171-180.

159. Begley, T. J., Rosenbach, A. S., Ideker, T., and Samson, L. D. (2002) Damage recovery pathways in Saccharomyces cerevisiae revealed by genomic phenotyping and interactome mapping, *Mol Cancer Res 1*, 103-112.

160. Begley, T. J., Rosenbach, A. S., Ideker, T., and Samson, L. D. (2004) Hot spots for modulating toxicity identified by genomic phenotyping and localization mapping, *Mol Cell 16*, 117-125.

161. Bennett, C. B., Lewis, L. K., Karthikeyan, G., Lobachev, K. S., Jin, Y. H., Sterling, J. F., Snipe, J. R., and Resnick, M. A. (2001) Genes required for ionizing radiation resistance in yeast, *Nat Genet 29*, 426-434.

162. Kalhor, H. R., and Clarke, S. (2003) Novel methyltransferase for modified uridine residues at the wobble position of tRNA, *Mol Cell Biol 23*, 9283-9292.

163. Lu, J., Huang, B., Esberg, A., Johansson, M. J., and Bystrom, A. S. (2005) The Kluyveromyces lactis gamma-toxin targets tRNA anticodons, *RNA 11*, 1648-1654.

164. Weissenbach, J., and Dirheimer, G. (1978) Pairing properties of the methylester of 5-carboxymethyl uridine in the wobble position of yeast tRNA3Arg, *Biochim Biophys Acta 518*, 530-534.

165. Begley, U., Dyavaiah, M., Patil, A., Rooney, J. P., DiRenzo, D., Young, C. M., Conklin, D. S., Zitomer, R. S., and Begley, T. J. (2007) Trm9-catalyzed tRNA modifications link translation to the DNA damage response, *Mol Cell 28*, 860-870.

166. Fu, D., Brophy, J. A., Chan, C. T., Atmore, K. A., Begley, U., Paules, R. S., Dedon, P. C., Begley, T. J., and Samson, L. D. (2010) Human AlkB homolog ABH8 Is a tRNA methyltransferase required for wobble uridine modification and DNA damage survival, *Mol Cell Biol 30*, 2449-2459.

167. Fu, Y., Dai, Q., Zhang, W., Ren, J., Pan, T., and He, C. The AlkB domain of mammalian ABH8 catalyzes hydroxylation of 5-methoxycarbonylmethyluridine at the wobble position of tRNA, *Angew Chem Int Ed Engl 49*, 8885-8888.

168. Huang, B., Johansson, M. J., and Bystrom, A. S. (2005) An early step in wobble uridine tRNA modification requires the Elongator complex, *RNA 11*, 424-436.

169. Motorin, Y., and Helm, M. tRNA stabilization by modified nucleotides, *Biochemistry 49*, 4934-4944.

170. Kitano, H. (2002) Computational systems biology, *Nature 420*, 206-210.

171. Hamahashi, S., and Kitano, H. (1999) Parameter optimization in hierarchical structure, in *Advances in artificial life : 5th European Conference, ECAL'99, Lausanne, Switzerland, September 13-17, 1999 : proceedings* (Floreano, D., Nicoud, J.-D., and Mondada, F., Eds.), pp p467-471, Springer, Berlin ; New York.

172. Kitano, H. (2001) Systems biology: toward system-level understanding of biological systems, in *Foundations of systems biology* (Kitano, H., Ed.), pp p1-36, MIT Press, Cambridge, Mass.

173. Kyodo, K., and Kitano, H. (1999) A model of axis determination for the *Drosophila* wing disc, in *Advances in artificial life : 5th European Conference, ECAL'99, Lausanne,*

Switzerland, September 13-17, 1999 : proceedings (Floreano, D., Nicoud, J.-D., and Mondada, F., Eds.), pp p472-476, Springer, Berlin ; New York.

174. Reinitz, J., Mjolsness, E., and Sharp, D. H. (1995) Model for cooperative control of positional information in Drosophila by bicoid and maternal hunchback, *J Exp Zool 271*, 47-56.

175. Brown, P. O., and Botstein, D. (1999) Exploring the new world of the genome with DNA microarrays, *Nat Genet 21*, 33-37.

176. DeRisi, J. L., Iyer, V. R., and Brown, P. O. (1997) Exploring the metabolic and genetic control of gene expression on a genomic scale, *Science 278*, 680-686.

177. D'Haeseleer, P., Wen, X., Fuhrman, S., and Somogyi, R. (1999) Linear modeling of mRNA expression levels during CNS development and injury, *Pac Symp Biocomput*, 41-52.

178. Spellman, P. T., Sherlock, G., Zhang, M. Q., Iyer, V. R., Anders, K., Eisen, M. B., Brown, P. O., Botstein, D., and Futcher, B. (1998) Comprehensive identification of cell cycle-regulated genes of the yeast Saccharomyces cerevisiae by microarray hybridization, *Mol Biol Cell 9*, 3273-3297.

179. Rittscher, J. Characterization of biological processes through automated image analysis, *Annu Rev Biomed Eng 12*, 315-344.

180. Shamir, L., Delaney, J. D., Orlov, N., Eckley, D. M., and Goldberg, I. G. Pattern recognition software and techniques for biological image analysis, *PLoS Comput Biol 6*, e1000974.

Chapter 2

Development of a Platform for Characterizing and Quantifying the Spectrum of tRNA Modifications in an Organism

Part of this chapter is published as an article in

PLoS Genetics 2010, 6 (12): e1001247

Abstract

There are over 100 tRNA modifications in transfer RNA (tRNA) and ribosomal RNA (rRNA) across all organisms and many of these modifications are conserved in widely different species. However, the biological roles of RNA modifications are poorly understood. To further our understanding, we developed a quantitative systems approach to study the spectrum of tRNA modifications in any organism, beginning with *S. cerevisiae*. All species of tRNA were isolated under conditions that minimize artifacts, such as oxidation and deamination of RNA, and the tRNA rigorously quantified. The RNA was then hydrolyzed enzymatically to nucleoside level. Liquid chromatography-coupled mass spectrometric techniques (LC-MS) were then developed to characterize and quantify the spectrum of tRNA modifications in the hydrolysate. Based on high mass accuracy MS (QTOF), collision-induced dissocation fragmentation patterns, comparisons with synthetic standards, and changes in the levels of ribonucleosides in mutants lacking tRNA modifying enzymes, we identified 23 modified ribonucleosides in *S. cerevisiae* tRNA. These modifications include Y, D, m^5C, m^3C, Cm, ac^4C, Am, m^1A, t^6A, i^6A, I, m^1I, m^7G, m^1G, m^2G, $m^2{}_2G$, Gm, m^5U, Um, mcm^5U, mcm^5s^2U, ncm^5U, and yW. We then developed a liquid chromatography-coupled tandem mass spectrometry (LC/MS-MS) method to quantify the spectrum of *S. cerevisiae* tRNA modifications. These methods provide tools for comparing changes in the spectrum of RNA modifications in cells under different stress conditions ans stimulations.

Introduction

Since the first discovery of RNA modifications more than 50 years ago, over 100 modified ribonucleosides have been reported in literature (*1-3*). Many of these modifications are found in organisms from all three phylogenetic domains; some of them are even conserved at the same position in tRNA across all organims (*4*). Although this conservation strongly suggests that these modifications play important roles in cell physiology, their function of many remains undefined.

To elucidate the biological function of RNA modifications, it is essential to identify the modifications and study their changes as a function of cellular states. Classically, one of the approaches is to enzymatically hydrolyze RNA to nucleosides and post-label them with ^{32}P; the [5'-^{32}P]-NMPs are separated with 2-dimension thin-layer chromatography (TLC) and the identity of modified nucleosides is defined by migration in relation to standards (*5, 6*). This method can determine absolute quantity. However, it is not chemically specific due to co-migrations and it is not applicable to all modified nucleosides as many modification groups significantly affect the efficiency of enzymatic ^{32}P-labeling (*7*). Another approach to quantify modifications involves blocking reverse transcription by the modifications on RNA. Specific modified nucleosides can be derivatized chemically; for instance, pseudouridine can be modified by *N*-cyclohexyl-*N'*-(2-morpholinoethyl)-carbodiimid-metho-*p*-toluolsulfonate. These derivatives stop reverse transcription and thus, provide indicators of the presence of the modifications (*8*). While the modification is quantified, this approach also provides information of its location. The major

pitfall of this approach is that the quantification of each modification requires a specific chemical for derivatization and the modifications themselves alter reverse transcription.

For the purpose of characterizing the full spectrum of tRNA modifications and studying all modifications with a quantitative systems approach, we developed a liquid chromatography-coupled mass spectrometric platform (LC-MS). Previous studies demonstrated that a wide range of modified nucleosides are separable by high-performance liquid chromatography (HPLC) and in some cases, the resolved nucleosides can even be identified and quantified by comparing the UV spectrum and retention time relative to synthetic standards (*9*). With limited amounts of samples, the sensitivity of detection can be increased using mass spectrometric techniques. Also, mass spectrometry is able to structurally characterize and identify most ribonucleosides (*10*). By using these techniques, we developed a robust and sensitive method to characterize and quantify these modifications in tRNA from *S. cerevisiae*.

S. cerevisiae is one of the most studied organisms, in which at least 25 tRNA secondary modifications (*11*) and more than 50 enzymes responsible for catalyzing their formation (*12*) have been identified. For the convenience of manipulating genetic behaviors and analyzing changes in cellular compositions, we employed *S. cerevisiae* as a model to study roles of tRNA modifications in cellular responses. The spectrum of tRNA modifications was first characterized using approaches including analysis of collision-induced dissocation (CID) fragmentation patterns of modified nucleosides with tandem quadrupole (MS/MS) techniques. Nucleosides were also identified by comparison with synthetic standards. Further, we monitored changes in the levels of the modified ribonucleosides in mutants lacking the genes for tRNA modifying enzyme. With 23 tRNA modifications identified, a LC/MS-MS method was developed to

quantify them. This method provides the basis for us to compare changes in the spectrum under different physiological conditions.

Materials and Methods

Materials. All chemicals and reagents were of the highest purity available and were used without further purification. Yeast extract and peptone were purchased from Biomed Diagnostics (White City, OR). PureLink miRNA Isolation Kit was purchased from Invitrogen (Carlsbad, CA). 2′-*O*-Methyluridine (Um), pseudouridine (Y), N^1-methyladenosine (m^1A), N^2,N^2-dimethylguanosine (m^2_2G), N^6,N^6-dimethyladensoine (m^6_2A), and 2′-*O*-methylguanosine (Gm) were purchased from Berry and Associates (Dexter, MI). N^6-threonylcarbamoyladenosine (t^6A) was purchased from Biolog (Bremen, Germany). N^6-isopentenyladenosine (i^6A) was purchased from International Laboratory LLC (San Bruno, CA). 2′-*O*-Methyladenosine (Am), N^4-acetylcytidine (ac^4C), 5-methyluridine (m^5U), inosine (I), 2-methylguanosine (m^2G), N^7-methylguanosine (m^7G), 2′-*O*-methylcytidine (Cm), 3-methylcytidine (m^3C), 5-methylcytidine (m^5C), alkaline phosphatase, lyticase, RNase A, ammonium acetate, geneticine, bovine serum albumin, deferoxamine mesylate, butylated hydroxytoluene, and glucose were purchased from Sigma Chemical Co. (St. Louis, MO). Nuclease P1 was purchased from Roche Diagnostic Corp. (Indianapolis, IN). Phosphodiesterase I was purchased from USB (Cleveland, OH). HPLC-grade water, acetonitrile, and chloroform were purchased from Mallinckrodt Baker (Phillipsburg, NJ). All strains of *S. cerevisiae* BY4741 and were purchased from American Type Culture Collections (Manassas, VA).

Culturing *S. cerevisiae BY4741*. Yeast cells were grown in YPD (yeast extract, peptone, and dextrose) media. To prepare this culture media, 5 gram of yeast extract, 10 gram of peptone, and 10 gram of dextrose were dissolved in 500 mL of water. The solution was sterilized by autoclave. Cultures were incubated at 30 °C with shaking at 220 rpm until they reached mid-log phase (OD660 is in the range of 0.6 to 0.8). Cells were then collected by centrifugation at 12000x g for 10 min. Cell pellets were snap-frozen with liquid nitrogen and stored at -80 °C before use.

Isolation of tRNA from *S. cerevisiae BY4741*. Approximately 5×10^7 cells were resuspended in ~200 μL of a buffer containing 5 μg/mL coformycin, 50 μg/mL tetrahydrouridine, 0.1 mM desferrioxamine, 0.1 mM butylated hydroxytoluene, 10 mM Tris-HCl, and 1mM EDTA, pH 8.0. This solution was incubated with 10 μg of lyticase at 30°C for 10 min to digest the cell wall of yeast. Yeast cells were then recollected by centrifugation with 12000× g for 5 min. After removing the supernatant, tRNA was isolated from the pellet by using the PureLink miRNA Isolation Kit. The yield of tRNA was determined by UV absorbance at 260 nm and using Agilent bioanalyzer.

Enzymatic hydrolysis of *S. cerevisae* tRNA. An amount of 6 μg of tRNA was mixed with 50 μL of a solution at pH 6.8 that contains 30 mM of sodium acetate, 2 mM of $ZnCl_2$, 0.02 Unit/μL of nuclease P1, 0.1 Units/μL of RNase A, 5 μg/ml coformycin, 50 mg/ml tetrahydrouridine, 0.1 mM deferoxamine mesylate, and 0.1 mM butylated hydroxytoluene. The solution was

incubated at 37 °C for 3 h before adding an additional 50 μL of solution at pH 7.8 with 30 mM sodium acetate, 0.2 Units/μL of alkaline phosphatase, and 0.01 Units/μL of phosphodiesterase I. This mixture was incubated at 37 °C overnight to ensure reactions were complete. As illustrated in previous studies, artifacts of modified ribonucleosides generated during this process were neglectable (*13*). Proteins were removed from the nucleosides with a Microcon YM-10 filter.

Characterizing the modified ribonucleosides from *S. cerevisiae* tRNA by LC-QTOF. Modified nucleosides from hydrolyzed tRNA were resolved by a Thermo Scientific Hypersil GOLD aQ reverse-phase column (150×2.1 mm, 3μm particle size) on a HPLC system with 0.1% (v/v) acetic acid in water and in acetonitrile as mobile phases. The gradient of organic phase is as follow: 0-20 min, 0-1%; 20-25 min, 1%; 25-35 min, 7%; 35-50 min, 7%; 50-60 min, 100%; 60-70 min, 100%. The flow rate was 0.25 mL/min and the temperature of column was 50 °C. The HPLC column was coupled to an Agilent 6510 quadrupole time-of-flight LC/MS mass spectrometer with an electrospray ionization source. The mass spectrometer was operated in the targeted MS/MS mode with the following MS parameters: gas temperature, 350 °C; gas flow, 10 L/min; nebulizer, 35 psi; fragmentor voltage, 110; and capillary voltage 3500V. For scanning nucleosides, ions in the range of *m/z* 100 to *m/z* 1000 were monitored with an acquisition rate of 2 spectra/second. $[M+H]^+$ ions of modified nucleosides were targeted for collision-induced-dissociation. The fragmented ions were monitored with an acquisition rate of 2 spectra/second. The retention time, time period for monitoring, *m/z* of the parent ion, and collision energy for each modification are as follows: dihydrouridine (D): 2.5 min, 1.75-3.25

min, *m/z* 247.9246, 5 V; pseudouridine (Y): 2.6 min, 2-3 min, *m/z* 245.07681, 5 V; 5-caramoylmethyluridine (ncm^{5}U): 3.0 min, 2-6 min, *m/z* 302.09828, 10 V; 3-methylcytosine (m^{3}C): 3.7 min, 3-5 min, *m/z* 258.10846, 9 V; 5-methylcytosine (m^{5}C), 4.2 min, 3-5 min; *m/z* 258.10846; 9 V; 1-methyladenosine (m^{1}A): 4.2 min, 4-5 min, *m/z* 282.11968, 15V; 7-methylguanosine (m^{7}G): 6.0 min, 4-8 min, *m/z* 298.11460, 9 V; 2'-*O*-methylcytosine (Cm), 6.2 min, 6-7 min, *m/z* 258.10846, 9 V; inosine (I): 6.2 min, 5.2-7.2 min, *m/z* 269.08805, 10 V; 5-methyluridine (m^{5}U): 7.0 min, 6-10 min, *m/z* 259.09246, 7 V; 2'-*O*-methyluridine (Um), 8.7 min, 6-10 min, *m/z* 259.09246, 7 V; 1-methylguanosine (m^{1}G): 12.3 min, 11.5-16.5 min, *m/z* 298.11460, 9 V; 1-methylinosine (m^{1}I): 12.4 min, 11-14 min, *m/z* 283.10370, 10 V; 5-methoxycarbonylmethyluridine (mcm^{5}U): 12.7 min, 11.8-13.8 min, *m/z* 317.09794, 7 V; 2'-*O*-methylguanosine (Gm): 13.0 min, 11.5-16.5 min, *m/z* 298.11460, 9 V; 4-acetylcytosine (ac^{4}C): 14.5 min, 13.5-15.5 min, m/z 286.10336, 6V; N^2-methylguanosine (m^{2}G): 15.0 min, 11.5-16.5 min, *m/z* 298.11460, 9 V; 2'-O-methyladenosine (Am): 17.6 min, 17-19 min, *m/z* 282.11968, 15 V; N^2, N^2-dimethylguanosine (m$^2_2$G): 26.0 min, 24.7-26.7 min, *m/z* 312.13025, 8 V; 5-methoxycarbonylmethyl-2-thiouridine (mcm^{5}s^{2}U): 26.2 min, 25.5-27.5 min, *m/z* 333.07510, 7 V; N^6-threonylcarbamoyladenosine (t^{6}A): 41.4 min, 40-42 min, *m/z* 413.14154, 8 V; wybutosine (yW): 57.4 min, 56.5-58.5 min, *m/z* 509.19905, 10 V; and N^6-isopentenyladenosine (i^{6}A): 58.1 min, 57-59 min, *m/z* 336.16663, 15 V.

Developing an LC-MS/MS method to quantify the spectrum of *S. cerevisiae* tRNA modifications. Samples of ribonucleosides were resolved with a Thermo Scientific Hypersil GOLD aQ reverse-phase column (150×2.1 mm, 3 μm particle size) eluted with the following

gradient of acetonitrile in 8 mM ammonium acetate at a flow rate of 0.3 mL/min and 36°C: 0–18 min, 1–2%; 18–23 min, 2%; 23–28 min, 2–7%; 28–30 min, 7%; 30–31 min, 7–100%; 31–41 min, 100%. The HPLC column was coupled to an Agilent 6410 triple quadrupole mass spectrometer with an electrospray ionization source where it was operated in positive ion mode with the following parameters for voltages and source gas: gas temperature, 350°C; gas flow, 10 L/min; nebulizer, 20 psi; and capillary voltage, 3500 V. The first and third quadrupoles (Q1 and Q3) were fixed to unit resolution and the modifications were quantified by pre-determined molecular transitions. Q1 was set to transmit the parent ribonucleoside ions and Q3 was set to monitor the deglycosylated product ions, except for Y for which the stable C-C glycosidic bond led to fragmentation of the ribose ring; we used the *m/z* 125 ion for quantification. The dwell time for each ribonucleoside was 200 ms. The retention time, *m/z* of the transmitted parent ion, *m/z* of the monitored product ion, fragmentor voltage, and collision energy of each modified nucleoside and ^{15}N-labeled internal standard are as follow: D, 1.9 min, *m/z* 247→115, 80 V, 5 V; Y, 2.5 min, *m/z* 245→125, 80 V, 10 V; m^{5}C, 3.3 min, *m/z* 258→126, 80 V, 8 V; Cm, 3.6 min, *m/z* 258→112, 80 V, 8 V; m^{5}U, 4.2 min, *m/z* 259→127, 80 V, 7 V; ncm^{5}U, 4.3 min, *m/z* 302→170, 90 V, 7 V; ac^{4}C, 4.4 min, *m/z* 286→154, 80 V, 6 V; m^{3}C, 4.4 min, *m/z* 258→126, 80 V, 8 V; ncm^{5}Um, 5.5 min, *m/z* 316→170, 90 V, 7 V; Um, 5.1 min, *m/z* 259→113, 80 V, 7 V; m^{7}G, 5.1 min, *m/z* 298→166, 90 V, 10 V; m^{1}A, 5.7 min, *m/z* 282→150, 100 V, 16 V; mcm^{5}U, 6.4 min, *m/z* 317→185, 90 V, 7 V; m^{1}I, 7.3 min, *m/z* 283→151, 80 V, 10 V; Gm, 8.0 min, *m/z* 298→152, 80 V, 7 V; m^{1}G, 8.3 min, *m/z* 298→166, 90 V, 10 V; m^{2}G, 9.4 min, *m/z* 298→166, 90 V, 10 V; I, 10.9 min, *m/z* 269→137, 80 V, 10 V; mcm^{5}s^{2}U, 14.2 min, *m/z* 333→201, 90 V, 7 V; [^{15}N]$_5$-dA, 14.4 min, *m/z* 257→141, 90 V, 10 V; m$^2{}_2$G, 15.9 min, *m/z* 312→180, 100 V, 8 V; t^{6}A,

17.2 min, *m/z* 413→281, 100 V, 8 V; Am, 19 min, *m/z* 282→136, 100 V, 15 V; yW, 34.2 min, *m/z* 509→377, 80 V, 5 V, and i^6A, 34.4 min, *m/z* 336→204, 100 V, 17 V. The mass spectrometer monitored ions with the molecular transitions of D, Y, m^5C, and Cm from 1 to 4 min; molecular transitions of m^5U, ncm^5U, ac^4C, m^3C, ncm^5Um, Um, m^7G, m^1A, and mcm^5U from 4 to 7 min; molecular transitions of m^1I, Gm, m^1G, and m^2G from 7 to 10 min; molecular transitions of I, mcm^5s^2U, $[^{15}N]_5$-dA, $m^2{}_2G$, t^6A, and Am from 10 to 30 min; molecular transitions of yW and i^6A from 30 to 40 min.

Results

Isolation of tRNA. Obtaining tRNA samples of high quality is one of the key features of rigorous quantitative comparison of changes in levels of tRNA modifications. Each organism contains various species of RNA, including tRNA, rRNA, and mRNA, which makes purification of tRNA a challenging task. As the size of tRNA is about 70 nucleotides and most other species of RNA are much larger, we decided to purify tRNA with a commercial kit that can isolate RNA below 200 nucleotides. While most species of RNA in this range of size are tRNA, there is also a small amount of other species of RNA, including microRNA (~21 nt) and 5S rRNA (~120 nt) (*14*). To assess the purity of each sample, we used an Agilent Bioanalyzer (microfluidics-based sizing and quantification against an internal standard) for quantification of total tRNA species, which amounted to 85±5% (N = 39) in the mixture of small RNA. Based upon the quantification, an internal standard ($[^{15}N_5]$-2′-deoxyriboadenosine) was added before enzymatic hydrolysis to minimize variation in the levels of the individual ribonucleosides.

Characterization of the spectrum of *S. cerevisiae* tRNA modifications by LC-QTOF mass spectrometry. In *S. cerevisiae*, 25 modified ribonucleosides in tRNA are reported in the literature (*11*). To identify these modified ribonucleosides in the hydrolyzed tRNA samples, we used an LC-QTOF system to obtain high mass accuracy (error < 10 ppm) characterization of the ionized ribonucleosides. Ions with expected mass were selected for collision-induced dissociation (CID) to determine the fragmentation patterns of the ribonucleosides. These fragmentation patterns further confirm the identities of these molecules; they were compared with the fragmentation patterns of commercially available nucleosides (Y, I, m^5U, Gm, Um, m^5C, m^3C, Cm, m^2G, ac^4C, t^6A, m^7G, Am, $m^2{}_2G$, i^6A, and m^1A). For those modified nucleosides with no available standards (D, ncm^5U, mcm^5U, m^1G, mcm^5s^2U, m^1I, and yW), they were compared to the fragmentations reported in the literature (*10, 15, 16*). Two of the 25 known *S. cerevisiae* modifications were not detected (ncm^5Um and Ar(p)). The mass spectra of CID fragmentation for the other 23 modified nucleosides are shown in figure 2-1.

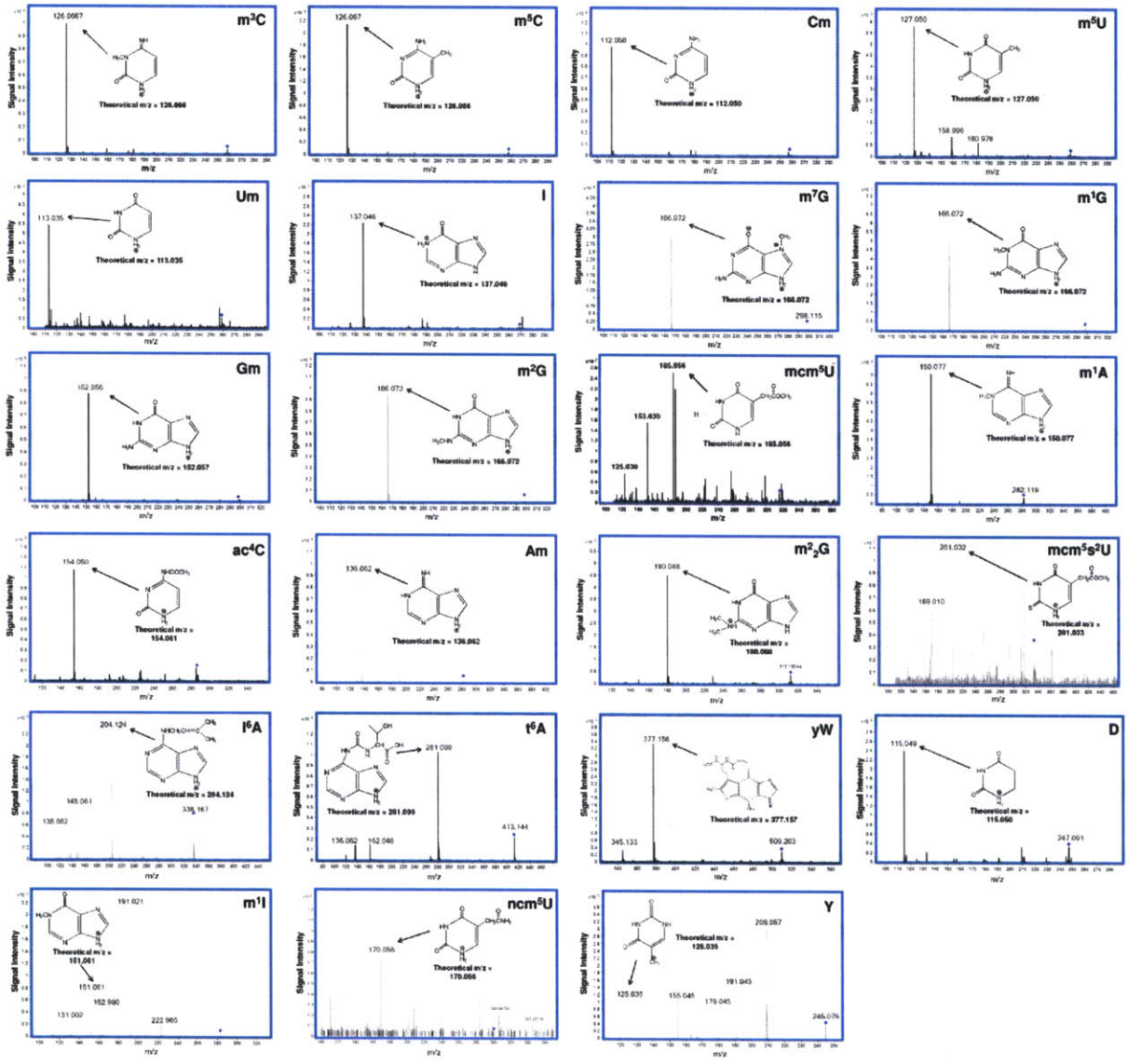

Figure 2-1. Mass spectra of fragmentized nucleosides by collision-induced dissocation. These characterizations were performed with LC/QTOF as described in the Materals and Methods. A total of 23 modifications were analyzed, including m^3C, m^5C, Cm, m^5U Um, I, m^7G, m^1G, Gm, m^2G, mcm^5U, m^1A, ac^4C, Am, $m^2{}_2G$, mcm^5s^2U, i^6A, t^6A, yW, D, m1I, ncm^5U, and Y.

LC-MS/MS-based quantification of the spectrum of modified nucleosides in *S. cerevisiae* tRNA. An LC-MS/MS method was developed to quantify *S. cerevisiae* tRNA modifications. Based upon the fragmentation of nucleosides in high mass-accuracy mass spectrometry, the modifications were quantified by pre-determined molecular transitions during CID. The transitions monitored for all nucleosides are the dissociation of ribosyl group from the base, except for pseudouridine that the base is linked to the ribose via a C-C bond. CID of pseudouridine leads to the formation of a fragment, consisting of the base and the 1'-CH_2^+ from ribose, which we chose as product ion for quantification (*17*). Even though the ncm^5Um was not observed with quadrupole time-of-flight mass spectrometer (QTOF), an ion with the expected molecular transition for this nucleoside was detected by triple quadrupole mass spectrometer (QQQ). This could be because the sensitivity of QQQ is higher than QTOF. A chromatogram of nucleosides quantified by this method is shown in Figure 2-2. By analyzing a series of samples with different quantity of hydrolyzed tRNA (0 μg, 0.05 μg, 0.1 μg, 0.2 μg, 0.4 μg, 0.8 μg, 1.2 μg, 1.6 μg, and 2.0 μg), we determined that the signal intensities of all modified nucleosides are linear to the amount of samples in the range of 0.05 μg to 0.8 μg (Figure 2-3).

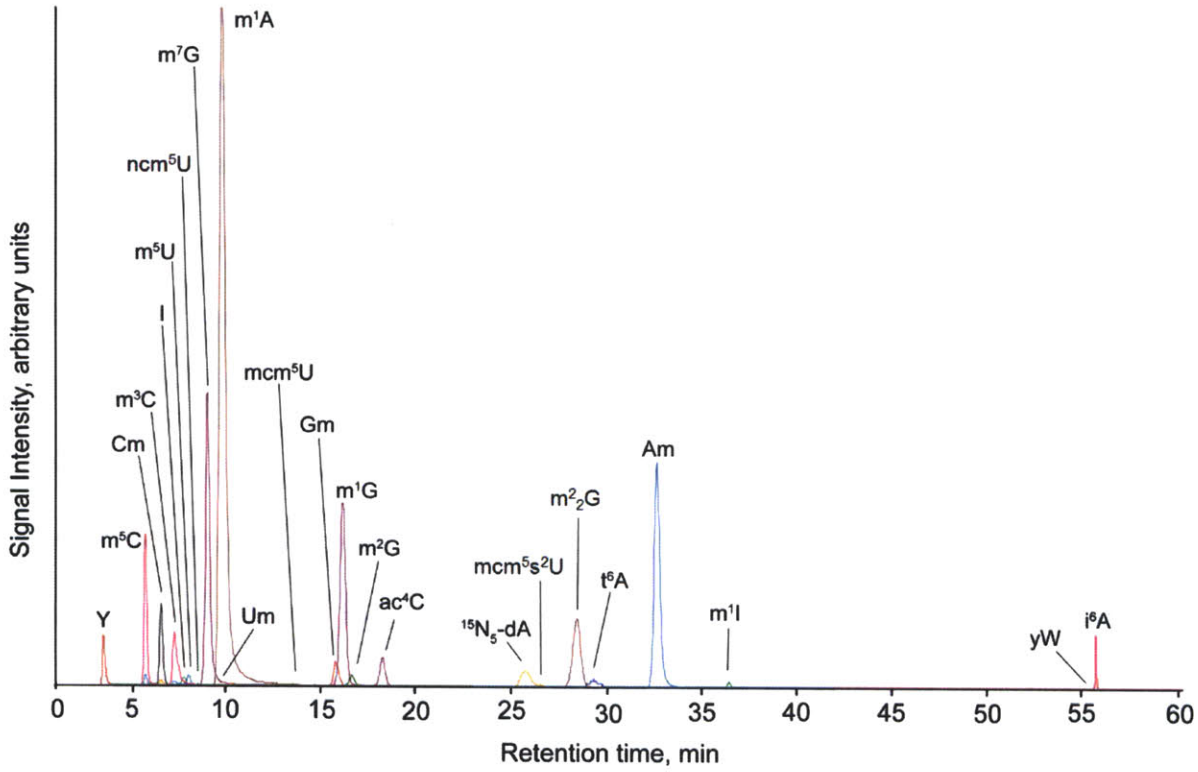

Figure 2-2. Total ion chromatogram of *S. cerevisiae* tRNA modified ribonucleosides from LC-MS/MS analysis. A total of 23 ribonucleosides were monitored.

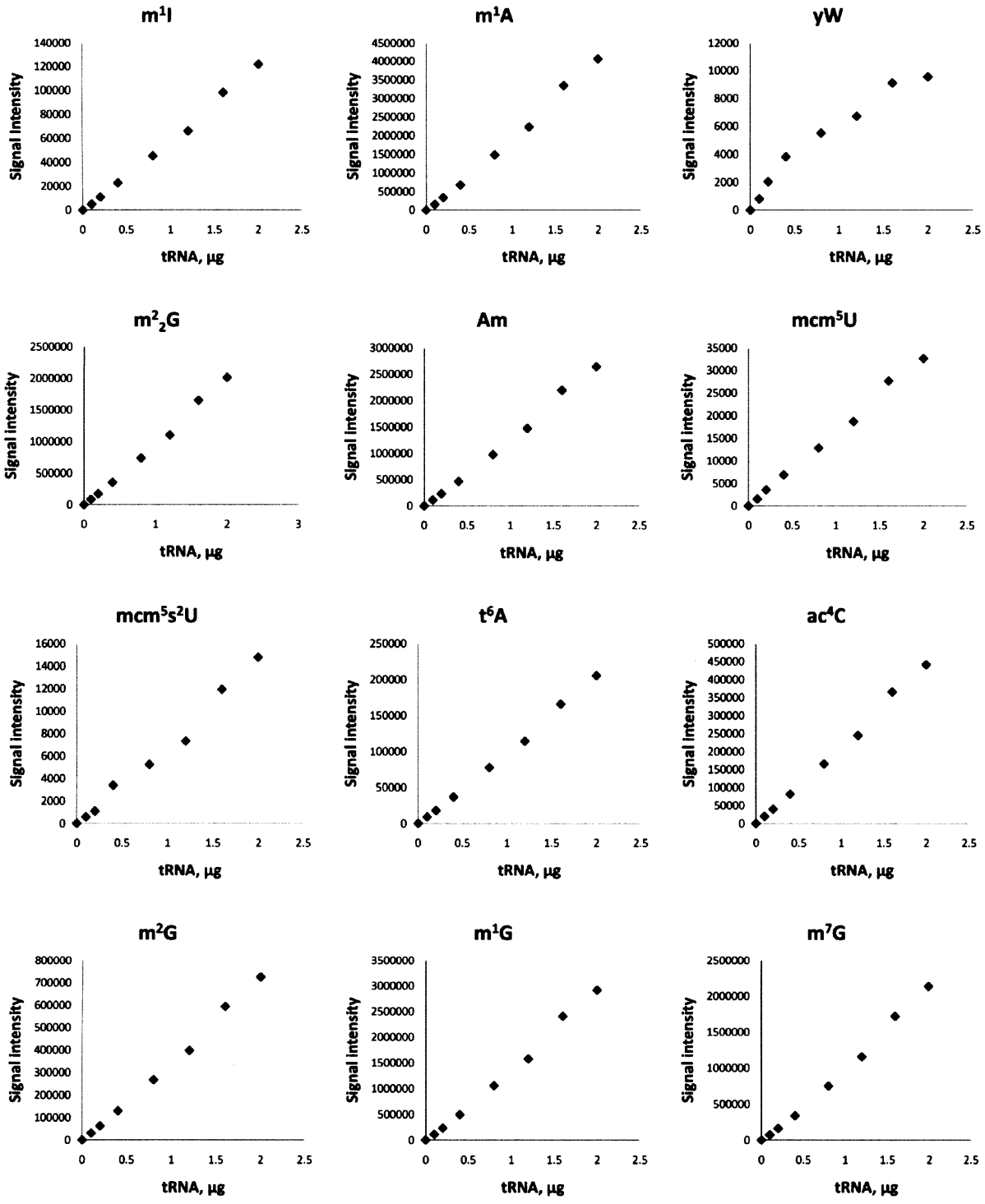
m1I
Signal Intensity
tRNA, µg
m1A
Signal Intensity
tRNA, µg
yW
Signal Intensity
tRNA, µg
m22G
Signal Intensity
tRNA, µg
Am
Signal Intensity
tRNA, µg
mcm5U
Signal Intensity
tRNA, µg
mcm5s2U
Signal Intensity
tRNA, µg
t6A
Signal Intensity
tRNA, µg
ac4C
Signal Intensity
tRNA, µg
m2G
Signal Intensity
tRNA, µg
m1G
Signal Intensity
tRNA, µg
m7G
Signal Intensity
tRNA, µg

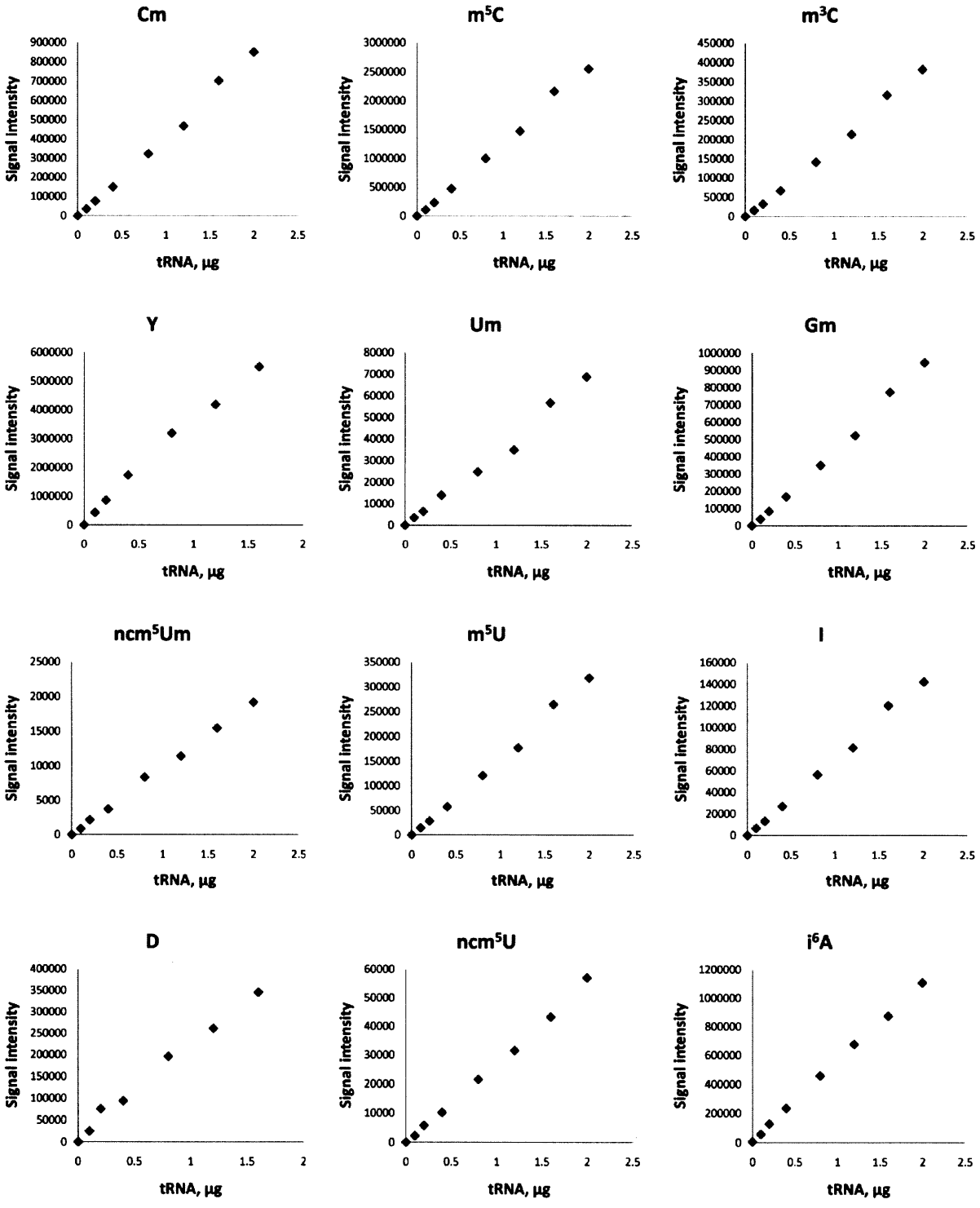
Cm
Signal intensity
tRNA, µg
m5C
Signal intensity
tRNA, µg
m3C
Signal intensity
tRNA, µg
Y
Signal intensity
tRNA, µg
Um
Signal intensity
tRNA, µg
Gm
Signal intensity
tRNA, µg
ncm5Um
Signal intensity
tRNA, µg
m5U
Signal intensity
tRNA, µg
I
Signal intensity
tRNA, µg
D
Signal intensity
tRNA, µg
ncm5U
Signal intensity
tRNA, µg
i6A
Signal intensity
tRNA, µg

Figure 2-3. Mass spectrometer signal intensities for tRNA ribonucleoside modifications. Small RNA isolates containing tRNA were enzymatically hydrolyzed and quantities ranging from 0.1 to 2 μg were analyzed by LC-MS/MS. Mass spectrometric signal intensities were determined for 23 of 25 modified ribonucleosides from yeast tRNA and plotted against total tRNA. Data represent mean ± SD for three analyses of the same sample.

Monitoring levels of modified nucleosides in yeast mutants. With the quantitative method developed, we further confirmed the identity of modified ribonucleosides by comparing the levels of specific modifications in a wild-type strain to those in mutant strains each lacking a corresponding tRNA modifying enzyme. If the identity of the modification is correct, a decrease in MS signal intensity is expected with loss of its biosynthetic pathway. As shown in Table 2-1, we used 17 mutants to confirm 15 modifications. Deletion of some tRNA modifying enzyme genes led to their corresponding modifications to drop below detection limit; these include *trm1Δ* for $m^2{}_2G$, *trm2Δ* for m^5U, *trm9Δ* for mcm^5U and mcm^5s^2U, *trm11Δ* for m^2G, *trm12Δ* fro yW, and *tad1Δ* for m^1I. As formation of some modifications is catalyzed independently by multiple enzymes, modifications in corresponding mutants did not disappear completely; these overlaps in gene function include *trm3* and *trm7* for catalyzing Gm, *trm5* and *tad1* for m^1I, *trm5* and *trm10* for m^1G, and, *trm7* and *trm13* for Cm. However, for m^5C, m^7G, Um, i^6A, and ac^4C, even though only one biosynthetic pathway was discovered for each of these modifications, these modified nucleosides were still observed in the corresponding mutants. These observations suggest that the formation of these modified nucleosides involves more than one pathway, or the modified nucleosides were from other speices of RNA, such as 5S rRNA.

Genes deleted in mutants	Modified nucleoside(s) from the gene	Modified MS signal intensity in wild-type (Avg ± SD)	Modified MS signal intensity in mutant (Avg ± SD)	Fold-change (mutant:wild-type)
trm1	m^2_2G	52029 ± 1233	nd	0
trm2	m^5U	1419 ± 15	nd	0
trm3	Gm	25736 ± 1145	24948 ±1261	0.97
trm4	m^5C	52457 ± 1254	3883 ± 159	0.07
trm5	m^1I	5775 ± 420	3687 ± 149	0.64
	yW	153 ± 21	43 ± 9	0.28
	m^1G	148698 ± 13388	90329 ± 6727	0.61
trm7	Cm	34402 ± 614	16373 ± 500	0.48
	Gm	25736 ± 1145	19694 ± 6660	0.77
trm8	m^7G	66810 ± 8171	7642 ± 160	0.11
trm9	mcm^5U	457 ± 42	nd	0
	mcm^5s^2U	638 ± 67	nd	0
trm10	m^1G	105441 ± 7738	31437 ± 1898	0.30
trm11	m^2G	19552 ± 835	nd	0
trm12	yW	71 ± 28	nd	0
trm13	Cm	37912 ± 4121	25946 ± 568	0.68
trm44	Um	1569 ± 413	331 ± 31	0.21
trm82	m^7G	66810 ± 8171	8509 ± 184	0.13
tad1	m^1I	3941 ± 622	nd	0
mod5	i^6A	3115 ± 39	39 ± 6	0.01
tan1	ac^4C	14277 ± 2248	4419 ± 237	0.31

Table 2-1. Quantitative assessments of changes in modified nucleosides in mutants with loss of corresponding enzymes. "nd" indicates the modification was not detectable in that mutant.

Discussion

Mass spectrometry-based methods for quantifying spectrum of tRNA modifications in *S. cerevisiae*. We developed an LC-MS/MS method capable of quantifying 23 of the 25 known ribonucleoside modifications in cytoplasmic tRNA in *S. cerevisiae*. This method begins with

isolation of small RNA species below 200 nt and quantification of the tRNA content with bianalyzer and UV-vis spectrophotometer. Individual ribonucleosides in enzymatic hydrolysates of tRNA were resolved by HPLC and determined by their characteristic fragmentation pattern using mass spectrometry.

As modifications in *S. cerevisiae* are well-studied, we identified them using high mass-accuracy mass spectrometry to compare fragmentation patterns with chemical standards and literature in a highly targeted manner. Each ribonucleoside was subsequently quantified by pre-determined molecular transitions during CID in the LC-MS/MS system. We were able to identify and quantify 23 of the 25 tRNA modifications in yeast, with 2'-*O*-ribosyladenosine phosphate (Ar(p)) not detected in positive ion mode (*18, 19*), possibly due to the negatively charged phosphate, and only tentative identification of ncm^5Um by CID due to weak signal intensities.

A critical feature of our approach is quantitative rigor given the need for highly precise measurement of even small changes in the relative quantities of ribonucleosides. To this end, we used an Agilent Bioanalyzer (microfluidics-based sizing and quantification against an internal standard) for quantification of total tRNA species in the mixture of small RNA and an internal standard ($[^{15}N_5]$-2'-deoxyriboadenosine) to minimize variation in the levels of the individual ribonucleosides.

We monitored specific modified ribonucleosides in mutants with deletion of corresponding tRNA modifying enzyme genes. As shown in Table 2-1, the abundance of modifications decreased when the responsible gene was lost. The formation of some modifications is catalyzed by multiple genes independently, including Gm, m^1I, m^1G, and Cm,

and these modifications were not completely lost in the mutants. However, for some modifications (m^5C, m^7G, Um, i^6A, and ac^4C) that only one biosynthetic pathway is characterized, they were still detectable in their corresponding mutants. It is possible that these modifications were formed via alternative pathways. For instance, m^1A and m^7G are common adducts that can be formed chemically (*20, 21*). One caveat here is low-level contamination (a few percent) with 5S rRNA that also contains ribonucleoside modifications. We were able to obtain highly reproducible data for the signal intensity associated with each ribonucleoside (see Figure 2-3 for linearity of signal intensity for the 23 ribonucleosides). Multiple reaction monitoring (MRM) mode yielded no detectable background signal in the absence of tRNA hydrolysates except for i^6A (9 ± 2%). Analysis of tRNA from wild type cells revealed a three-log range of signal intensity, with I and ac^4C producing the highest intensity and ncm^5Um the lowest (Figure 2-2 and Table 2-2). In general, modifications can be categorized in high (I, ac^4C, m^1A, $m^2{}_2G$, Am, Y), medium (Cm, m^5C, Gm, m^1G, t^6A, m^7G, m^2G, m^3C, i^6A) and low signal intensities (m^1I, D, m^5U, ncm^5Um, mcm^5U, mcm^5s^2U, Um, yW, ncm^5U), with signal intensity reflecting both the abundance and mass spectrometric sensitivity for each ribonucleoside. This MS quantification method is used to study the changes in the spectrum of *S. cerevisiae* tRNA modifications in response to exposure to different type of toxic agents (Chapter 3).

	0.4 µg of hydrolyzed tRNA				
	Expt. 1	Expt. 2	Expt. 3	Average	Std. Dev.
D	424088.4	423640.7	427548.5	425092.5	2138.689
Y	2600599	2388005	2463198	2483934	107803.5
ncm^5U	10587.98	9967.097	10180.51	10245.2	315.4535
I	41189.76	39247.89	39772.93	40070.19	1004.483
m^5U	102418.4	100054.1	100503.1	100991.9	1255.656
ncm^5Um	4582.739	4674.049	4448.249	4568.345	113.5859
Gm	223923.7	210210.5	212587.9	215574	7328.098
Um	18719.91	16800.13	17000.06	17506.7	1055.413
m^3C	45560.77	42904.79	40723.55	43063.04	2422.486
m^5C	424830.2	400425.2	408744.8	411333.4	12406.74
Cm	122686.3	117802.3	114972.7	118487.1	3902.139
mcm^5U	9778.705	9686.143	9617.348	9694.065	80.9694
m^7G	306670.2	287031.1	295568.3	296423.2	9847.455
m^1G	397554.9	379427.3	384249.4	387077.2	9388.839
m^2G	178295.5	166431.3	174566	173097.6	6066.884
ac^4C	77889.31	71419.34	71098.4	73469.01	3831.446
t^6A	79569.02	74730.69	77152.04	77150.58	2419.163
mcm^5s^2U	4356.895	4381.075	4653.992	4463.987	164.9921
m^1I	17948.28	16791.12	17414.55	17384.65	579.1582
Am	307639.5	288643.2	290306.1	295529.6	10520.39
$m^2{}_2G$	350220.4	325874.8	338643.6	338246.2	12177.65
i^6A	244157.1	227802.4	230786.3	234248.6	8709.734
m^1A	535454.3	517797.7	513667.6	522306.5	11572.01

Table 2-2. MS Signal intensities of modified nucleosides from *S. cerevisiae* tRNA. An amount of 1 pmol of [$^{15}N_5$]-2'-deoxyadenosine was added per µg of tRNA as internal standard. After enzymatic hydrolysis, 0.4 µg of nucleosides were analyzed with LC/MS-MS. Quantity of signal for each nucleoside in the three experiments was normalized by the signal intensity of the internal standard.

References

1. Czerwoniec, A., Dunin-Horkawicz, S., Purta, E., Kaminska, K. H., Kasprzak, J. M., Bujnicki, J. M., Grosjean, H., and Rother, K. (2009) MODOMICS: a database of RNA modification pathways. 2008 update, *Nucleic Acids Res 37*, D118-121.
2. McCloskey, J. A., and Rozenski, J. (2005) The Small Subunit rRNA Modification Database, *Nucleic Acids Res 33*, D135-138.
3. Grosjean, H., and Benne, R. (1998) *Modification and editing of RNA*, ASM Press, Washington, DC.
4. Björk, G. R. (1986) Transfer RNA modifications of different organisms, in *Molecular evolution of life : proceedings of a conference held at Södergarn, Lidingö, Sweden, 8-12 September 1985* (Baltscheffsky, H., Jörnvall, H., and Rigler, R., Eds.), pp 91-95, Cambridge University Press, Cambridge ; New York.
5. Keith, G. (1995) Mobilities of modified ribonucleotides on two-dimensional cellulose thin-layer chromatography, *Biochimie 77*, 142-144.
6. Silberklang, M., Gillum, A. M., and RajBhandary, U. L. (1979) Use of in vitro 32P labeling in the sequence analysis of nonradioactive tRNAs, *Methods Enzymol 59*, 58-109.
7. Xue, H., Glasser, A. L., Desgres, J., and Grosjean, H. (1993) Modified nucleotides in Bacillus subtilis tRNA(Trp) hyperexpressed in Escherichia coli, *Nucleic Acids Res 21*, 2479-2486.
8. Bakin, A. V., and Ofengand, J. (1998) Mapping of pseudouridine residues in RNA to nucleotide resolution, *Methods Mol Biol 77*, 297-309.

9. Buck, M., Connick, M., and Ames, B. N. (1983) Complete analysis of tRNA-modified nucleosides by high-performance liquid chromatography: the 29 modified nucleosides of Salmonella typhimurium and Escherichia coli tRNA, *Anal Biochem 129*, 1-13.

10. Pomerantz, S. C., and McCloskey, J. A. (1990) Analysis of RNA hydrolyzates by liquid chromatography-mass spectrometry, *Methods Enzymol 193*, 796-824.

11. Johansson, M. J. O., and Byström, A. S. (2005) *Transfer RNA modifications and modifying enzymes in Saccaromyces cerevisiae*, Springer-Verlag, Heidelberg, Germany.

12. Christie, K. R., Weng, S., Balakrishnan, R., Costanzo, M. C., Dolinski, K., Dwight, S. S., Engel, S. R., Feierbach, B., Fisk, D. G., Hirschman, J. E., Hong, E. L., Issel-Tarver, L., Nash, R., Sethuraman, A., Starr, B., Theesfeld, C. L., Andrada, R., Binkley, G., Dong, Q., Lane, C., Schroeder, M., Botstein, D., and Cherry, J. M. (2004) Saccharomyces Genome Database (SGD) provides tools to identify and analyze sequences from Saccharomyces cerevisiae and related sequences from other organisms, *Nucleic Acids Res 32*, D311-314.

13. Taghizadeh, K., McFaline, J. L., Pang, B., Sullivan, M., Dong, M., Plummer, E., and Dedon, P. C. (2008) Quantification of DNA damage products resulting from deamination, oxidation and reaction with products of lipid peroxidation by liquid chromatography isotope dilution tandem mass spectrometry, *Nat Protoc 3*, 1287-1298.

14. Szymanski, M., Barciszewska, M. Z., Erdmann, V. A., and Barciszewski, J. (2002) 5S Ribosomal RNA Database, *Nucleic Acids Res 30*, 176-178.

15. Bullinger, D., Neubauer, H., Fehm, T., Laufer, S., Gleiter, C. H., and Kammerer, B. (2007) Metabolic signature of breast cancer cell line MCF-7: profiling of modified nucleosides via LC-IT MS coupling, *BMC Biochem 8*, 25.

16. Kalhor, H. R., and Clarke, S. (2003) Novel methyltransferase for modified uridine residues at the wobble position of tRNA, *Mol Cell Biol 23*, 9283-9292.

17. Dudley, E., Tuytten, R., Bond, A., Lemiere, F., Brenton, A. G., Esmans, E. L., and Newton, R. P. (2005) Study of the mass spectrometric fragmentation of pseudouridine: comparison of fragmentation data obtained by matrix-assisted laser desorption/ionisation post-source decay, electrospray ion trap multistage mass spectrometry, and by a method utilising electrospray quadrupole time-of-flight tandem mass spectrometry and in-source fragmentation, *Rapid Commun Mass Spectrom 19*, 3075-3085.

18. Desgres, J., Keith, G., Kuo, K. C., and Gehrke, C. W. (1989) Presence of phosphorylated O-ribosyl-adenosine in T-psi-stem of yeast methionine initiator tRNA, *Nucleic Acids Res 17*, 865-882.

19. Keith, G., Glasser, A. L., Desgres, J., Kuo, K. C., and Gehrke, C. W. (1990) Identification and structural characterization of O-beta-ribosyl-(1"----2')-adenosine-5"-phosphate in yeast methionine initiator tRNA, *Nucleic Acids Res 18*, 5989-5993.

20. Pfeifer, G. P., You, Y. H., and Besaratinia, A. (2005) Mutations induced by ultraviolet light, *Mutat Res 571*, 19-31.

21. Zhao, C., Tyndyk, M., Eide, I., and Hemminki, K. (1999) Endogenous and background DNA adducts by methylating and 2-hydroxyethylating agents, *Mutat Res 424*, 117-125.

Chapter 3

A Quantitative systems approach reveals dynamic control of tRNA modifications during cellular stress

Part of this chapter is published as an article in

PLoS Genetics 2010, 6 (12): e1001247

Abstract

Decades of study have revealed more than 100 ribonucleoside structures incorporated as post-transcriptional modifications mainly in tRNA and rRNA, yet the functional dynamics of this conserved system are unclear. To this end, we used a highly precise mass spectrometric method to quantify tRNA modifications in *Saccharomyces cerevisiae*. Our approach revealed several novel biosynthetic pathways for RNA modifications and led to the discovery of signature changes in the spectrum of tRNA modifications in the damage response to mechanistically different toxicants. This is illustrated with the RNA modifications Cm, m^5C, and $m^2{}_2G$, which increase following hydrogen peroxide exposure but decrease or are unaffected by exposure to methylmethane sulfonate, arsenite, and hypochlorite. Cytotoxic hypersensitivity to hydrogen peroxide is conferred by loss of enzymes catalyzing the formation of Cm, m^5C, and $m^2{}_2G$, which demonstrates that tRNA modifications are critical features of the cellular stress response. The results of our study support a general model of dynamic control of tRNA modifications in cellular response pathways and add to the growing repertoire of mechanisms controlling translational responses in cells.

Introduction

The complexity of the transfer RNA (tRNA) system confers great potential for its use in cellular regulatory programs. There are hundreds of tRNA-encoding genes in *S. cerevisiae* and human genomes, with extensive post-transcriptional processing that includes enzyme-

mediated ribonucleoside modifications (*1*). Considering both tRNA and ribosomal RNA (rRNA), there are more than 100 known ribonucleoside modifications across all organisms in addition to the canonical adenosine, guanosine, cytidine and uridine (*2, 3*). In general, tRNA modifications enhance ribosome binding affinity, reduce misreading and modulate frame-shifting, all of which affect the rate and fidelity of translation (*4-7*). However, information about the higher-level biological function of ribonucleoside modifications has only recently begun to emerge. We have approached this problem with a systems-level analysis of changes in the spectrum of ribonucleosides in tRNA as a function of cell stress, which has revealed novel insights into the biosynthesis of tRNA modifications and their role in cellular responses.

Emerging evidence points to a critical role for tRNA and rRNA modifications in cellular responses to stimuli, with evidence for a role in tRNA stability, cellular stress responses, and cell growth (*8-13*). We recently used high-throughput screens and targeted studies to show that the tRNA methyltransferase 9 (Trm9) modulates the toxicity of methylmethanesulfonate (MMS) in *S. cerevisiae (11, 14)*. This is similar to the observed role of Trm9 in modulating the toxicity of ionizing radiation and of Trm4 in promoting viability after methylation damage (*15, 16*). Trm9 catalyzes the methyl esterification of the uracil-based cm^5U and cm^5s^2U to mcm^5U and mcm^5s^2U, respectively, at the wobble bases of $tRNA^{UCU}$-ARG and $tRNA^{CCU}$-GLU, among others (*17*). These wobble base modifications in the tRNA enhance binding of the anticodon with specific codons in mixed codon boxes (*18*). Codon-specific reporter assays and genome-wide searches revealed that Trm9-catalyzed tRNA modifications enhanced the translation of AGA- and GAA-rich transcripts that functionally mapped to processes associated with protein synthesis, metabolism and stress signaling (*11*). The resulting model proposes that specific

codons will be more efficiently translated by anticodons containing the Trm9-modified nucleoside and that tRNA modifications can dynamically change in response to stress.

To assess the dynamic nature of tRNA modifications proposed by this model, we quantified the full set of tRNA modifications in *S. cerevisiae* with a systems-oriented approach using liquid chromatography-coupled, tandem quadrupole mass spectrometry (LC-MS/MS) as described in Chapter 2. Mass spectrometry-based methods have recently emerged as powerful tools for identifying and quantifying RNA modifications (*19, 20*). We applied such an approach to quantify changes in the spectrum of tRNA modifications in yeast exposed to four toxicants: hydrogen peroxide (H_2O_2), sodium hypochlorite (NaOCl), sodium arsenite ($NaAsO_2$), and methyl methanesulfonate (MMS). H_2O_2 is an oxidizing agent that can form hydroxyl radical by reacting with reduced transition metal ions (Fenton reactions) (*21*). Hydroxyl radical leads to DNA damages via various mechanisms (*22-24*). While NaOCl also induces oxidative stress and forms hydroxyl radical at low pH, it can also from singlet oxygen, molecular chlorine, and chloramines that are all cytotoxic (*24*). Arsenite is a carcinogen, as indicated by studies with animal models; even though its mechanism of action is not understood, evidences suggest that it generates oxidative stress and leads to adduction in both proteins and DNA (*25*). MMS is an alkylating agent that methylates nucleophiles, such as amines, in a wide range of biological macromolecules (*26*). These four reagents generate stress with dissimilar mechanisms.

Multivariate statistical analysis of the data reveals dynamic shifts in the population of RNA modifications as part of the response to damage, with signature changes for each agent and dose. Further, analysis of yeast mutants lacking specific modification enzymes revealed novel biosynthetic pathways and compensatory or cooperative shifts in the population of RNA

modifications as part of the response to damage, with signature changes for each agent and dose. Further, analysis of yeast mutants lacking specific modification enzymes revealed novel biosynthetic pathways and compensatory or cooperative shifts in the levels of other modifications.

Materials and Methods

Materials. All chemicals and reagents were of the highest purity available and were used without further purification. 2′-*O*-Methyluridine (Um), pseudouridine (Y), N^1-methyladenosine (m^1A), N^2,N^2-dimethylguanosine ($m^2{}_2G$), and 2′-*O*-methylguanosine (Gm) were purchased from Berry and Associates (Dexter, MI). N^6-Threonylcarbamoyladenosine (t^6A) was purchased from Biolog (Bremen, Germany). N^6-Isopentenyladenosine (i^6A) was purchased from International Laboratory LLC (San Bruno, CA). 2′-*O*-Methyladenosine (Am), N^4-acetylcytidine (ac^4C), 5-methyluridine (m^5U), inosine (I), 2-methylguanosine (m^2G), N^7-methylguanosine (m^7G), 2′-*O*-methylcytidine (Cm), 3-methylcytidine (m^3C), 5-methylcytidine (m^5C), alkaline phosphatase, lyticase, RNase A, ammonium acetate, geneticine and desferrioxamine were purchased from Sigma Chemical Co. (St. Louis, MO). Nuclease P1 was purchased from Roche Diagnostic Corp. (Indianapolis, IN). Phosphodiesterase I was purchased from USB (Cleveland, OH). PureLink miRNA Isolation Kits were purchased from Invitrogen (Carlsbad, CA). Acetonitrile and HPLC-grade water were purchased from Mallinckrodt Baker (Phillipsburg, NJ). All strains of *S. cerevisiae* BY4741 were purchased from American Type Culture Collections (Manassas, VA).

Sensitivity assay of S. cerevisiae to toxic agents. All strains of *S. cerevisiae* BY4741 were cultured in YPD (yeast extract-peptone-dextrose) media with 200 μg/mL of geneticine at 30 °C with shaking at 220 rpm. Cultures were grown to mid-log phase (OD660 ~ 0.6 to 0.8) followed by addition of water, to serve as untreated control, or toxic agents, including hydrogen peroxide (H_2O_2), methyl methanesulfonate (MMS), sodium hypochlorite (NaOCl), or sodium arsenite ($NaAsO_2$). After 1 hour, these cultures were diluted 10^4- to 10^6-fold with YPD media and then plated to YPD agar plates. Survival rates of exposed cells were determined by comparing the number of colonies formed from untreated culture with that from each exposed culture after two days.

Exposure of S. cerevisiae. Cultures of *S. cerevisiae* BY4741 were grown to mid-log phase followed by addition of toxicants to the noted final concentrations (cytotoxicity of ~20%, 50% and 80%): H_2O_2, 2, 5 or 12 mM; MMS, 6, 12 or 24 mM; $NaAsO_2$, 20, 40 or 60 mM; NaOCl, 3.2, 4.0 or 4.8 mM. The sensitivity of the following mutant strains to toxicant exposure was also determined (doses producing ~80% cytotoxicity in wild-type: 12 mM H_2O_2, 24 mM MMS, 60 mM $NaAsO_2$, or 4.8 mM NaOCl): *trm1*, *trm2*, *trm3*, *trm4*, *trm7*, *trm8*, *trm9*, *trm10*, *trm11*, *trm12*, *trm13*, *trm44*, *trm82*, *tad1*, *mod5*, and *tan1*. Since *trm5* is essential, a diploid strain (*GBY1*) lacking one copy of *trm5* was used. After a 1 h, cells were collected and viability determined by plating.

tRNA isolation and quantification of cytoplasmic tRNA modifications. tRNA isolation and quantification of modified nucleosides are described in details in Chapter 2. This process involves lyzing cells with lyticase, extracting tRNA from cell lysate by using Invitrogen PureLink small RNA isolation kit, enzymatically hydrolyzing tRNA to nucleosides, resolving these nucleosides by HPLC, and monitoring each species based on pre-determined molecular transitions by mass spectrometer (MS^2).

Quantification of m^7G in control and MMS-treated yeast. To assess the direct and indirect effects of MMS on levels of methylated ribonucleosides, the absolute levels of m^7G were quantified in small RNA hydrolysates isolated from MMS-exposed and unexposed mutant and wild type strains of yeast by the LC-MS/MS method described above. Calibration curves were generated by mixing variable amounts of m^7G (final concentrations of 0, 5, 50, 300, 600, 1000, and 2000 nM) with a fixed concentration of $[^{15}N]_5$-dA (40 nM). A volume of 10 µl of each solution was analyzed with the LC-MS/MS system described earlier.

Statistical analysis of changes in the levels of tRNA modifications. Differences in the levels of ribonucleosides in exposed *versus* unexposed and in mutant *versus* wild-type yeast were analyzed by Student's t-test. Hierarchical clustering analyses were performed using Cluster 3.0. Data were transformed to $\log_2$ ratios of modification levels in treated cells relative to unexposed controls. Clustering was carried out using the centroid linkage algorithm based on the distance between each dataset measured using the Pearson correlation, with heat map representations produced using Java Treeview. Principal component analysis was performed

using XLStat (Addinsoft SARL, Paris, France), with a Pearson correlation matrix consisting of data that were mean-centered and normalized to the standard deviation. Correlation analysis was used to assess the degree of covariance among the various sets of fold-change values for each mutant , with correlation coefficients calculated using Excel (Microsoft).

Results

Cytotoxicity dose-response studies with *S. cerevisiae* exposed to various toxic agents. To test the hypothesis that the changes in spectrum of tRNA modifications are unique to different stress, we decided to expose cells to four different toxic reagents with doses that cause the same survival rate. The doses for exposures were determined by assessing the sensitivity of cells to a serial concentration of H_2O_2 (1, 2, 5, 7, 9, 11, 12, 13, and 15 mM), MMS (0, 1.2, 6, 12, 24, 36, and 48 mM), NaOCl (0, 0.16, 0.8, 1.6, 3.2, 4, 4.8, 8, and 16 mM), and $NaAsO_2$ (0, 10, 20, 40, 60, 80, and 100 mM). Based on these assays (Figure 3-1), we decided to quantify spectra of tRNA modifications in cells exposed to 2, 5, and 12 mM of H2O2, 6, 12, and 24 mM of MMS, 20, 40, and 60 mM of NaAsO2, and 3.2, 4.0, and 4.8 mM of NaOCl. The three doses of each reagent led to cytotoxicity of approximately 20%, 50%, and 80%.

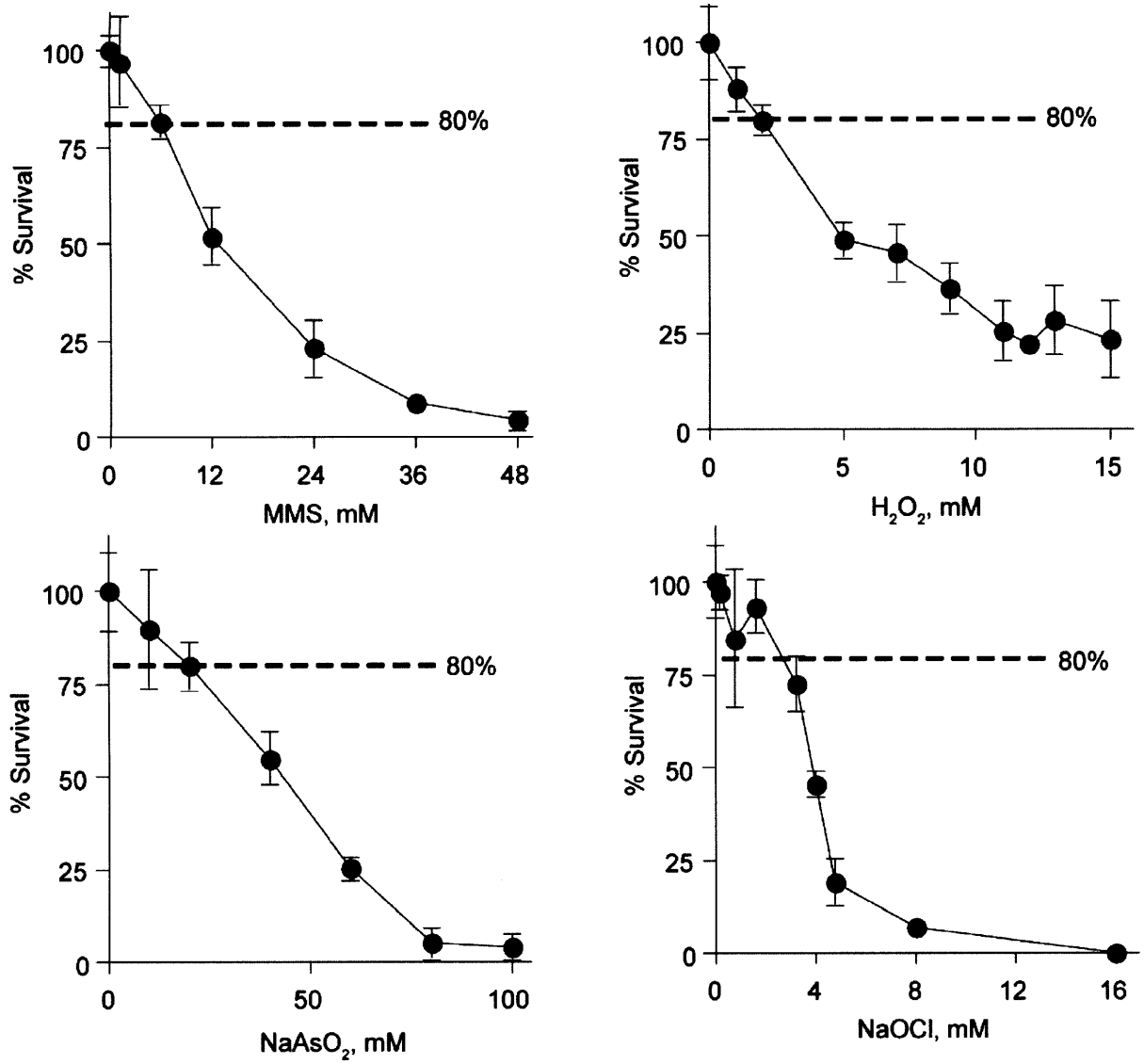

Figure 3-1. Cytotoxicity dose-response studies with S. cerevisiae exposed to H_2O_2, MMS, NaAsO4, and NaOCl. Data represent mean ± SD for three biological replicates. The dotted line marks the 80% survival level.

Changes in spectrum of tRNA modifications in response to stress. By using the LC/MS-MS method described in Chapter 2, we compared the spectrum of tRNA modifications from cells exposed to the three doses of each of the four reagents as described above. Each exposure condition was carried out in biological triplicates. Signal intensities from all nucleosides were normalized by that from the internal standard, [$^{15}N_5$]-labeled 2'-deoxyadenosine, so that the relative quantity of each modification can be compared across samples; average of normalized signal intensities was calculated (Table 3-1). Changes in the spectrum were expressed as fold-change of the levels of nucleosides in treated cells relative to in untreated cells; statistical significance of these changes were determined by Student's t-test (Table 3-2). The results demonstrated that levels of m^5C, Cm, and $m^2{}_2G$ increased, and level of yW and m^1G decreased statistically significantly ($p<0.1$) after exposed to all three doses of H_2O_2. For MMS-exposed cells, levels of I, Gm, Cm, t^6A, Am, $m^2{}_2G$, and yW decreased and that of m^7G and m^3C increased. Exposures of $NaAsO_2$ led to a general decreases in the level of all modifications. Cells treated with NaOCl had a decrease in the level of m^1I and an increase in the levels of Um and Am. Hierarchical clustering analysis and principle components analysis on this set of fold-change data demonstrate that the spectrum of tRNA modifications changed specifically in response to each toxic agent (Figure 3-2 and 3-3).

	Control		2mM H_2O_2			5mM H_2O_2			12mM H_2O_2			6mM MMS			12mM MMS			24mM MMS		
	Average	SD	Average	SD	Ttest	Average	SD	Ttest	Average	SD	Ttest	Average	SD	Ttest	Average	SD	Ttest	Average	SD	Ttest
D	1686	13	1986	281	0.14	1842	79	0.03	2254	171	0.00	1700	70	0.76	1985	221	0.08	1921	391	0.36
ncm^5U	1664	135	1916	277	0.23	1759	214	0.55	1821	281	0.43	1769	179	0.46	1841	199	0.27	1941	135	0.07
I	250480	1392	257046	12547	0.42	241875	17587	0.45	250050	20166	0.97	223885	12822	0.02	210225	16080	0.01	220102	8971	0.00
m^5U	1675	88	1537	155	0.25	1430	221	0.15	1395	177	0.07	1619	133	0.58	1695	109	0.82	1518	128	0.16
Gm	45474	1577	49022	2453	0.10	41391	3670	0.15	42649	2117	0.14	39611	2775	0.03	38677	2047	0.01	36970	3531	0.02
Um	279	24	413	75	0.04	264	49	0.67	304	32	0.34	233	33	0.12	254	14	0.20	249	57	0.44
m^5C	39253	16194	75290	4063	0.02	84353	32490	0.10	77521	23005	0.08	33226	7583	0.59	33177	18704	0.69	28240	11893	0.40
m^3C	10889	703	10921	793	0.96	11637	4111	0.77	9960	230	0.10	13262	563	0.01	15328	412	0.00	13048	3166	0.31
Y	6753	999	6454	2178	0.84	7541	3623	0.74	4871	479	0.04	7480	784	0.38	6190	581	0.45	6043	703	0.37
Cm	25418	1842	38600	2591	0.00	39780	4380	0.01	38679	951	0.00	21883	1804	0.08	19956	2916	0.05	19031	1456	0.01
mcm^5U	245	22	213	26	0.17	207	65	0.39	207	21	0.09	248	11	0.89	284	33	0.17	265	32	0.43
m^7G	65612	9718	59284	7193	0.42	77334	45788	0.69	50903	1049	0.06	106987	6999	0.00	143214	7346	0.00	116659	49765	0.16
m^1G	59822	2872	51537	3469	0.03	48143	7020	0.06	45700	5714	0.02	55953	3142	0.19	57718	1657	0.33	51272	4363	0.05
m^2G	67775	3772	57313	6617	0.08	53298	11990	0.12	52085	12215	0.10	61161	7695	0.25	58984	3730	0.05	53313	5269	0.02
ac^4C	178172	8545	189350	12934	0.28	183742	5507	0.40	191576	16123	0.27	178450	7044	0.97	167917	18329	0.43	166783	15679	0.33
t^6A	60740	1623	53669	3863	0.04	49925	4521	0.02	123421	8103	0.00	55981	3326	0.09	55864	1870	0.03	51368	2652	0.01
mcm^5s^2U	513	65	458	54	0.32	382	13	0.03	367	35	0.03	448	16	0.17	444	50	0.22	376	35	0.03
m^1I	3128	317	2966	44	0.43	2702	417	0.23	2594	295	0.10	3054	41	0.71	3002	211	0.60	2675	348	0.17
Am	82676	2070	94388	5736	0.03	73858	12598	0.30	81631	5185	0.76	64714	6106	0.01	63191	2913	0.00	65214	12956	0.08
m^2_2G	133248	4375	257373	2009	0.00	280206	29780	0.00	309183	13971	0.00	122876	7381	0.10	125986	1482	0.05	112355	6407	0.01
I^6A	12673	3141	9592	1197	0.19	9094	1656	0.16	8926	1585	0.14	10061	849	0.24	9117	394	0.12	8627	433	0.09
yW	254	14	204	18	0.02	173	21	0.00	186	20	0.01	217	7	0.01	201	40	0.09	180	35	0.03
m^1A	141199	6656	123987	8584	0.05	125365	34747	0.48	111213	15492	0.04	155570	8122	0.08	166538	910	0.00	144187	24864	0.85

	Control		20mM $NaAsO_2$			40mM $NaAsO_2$			60mM $NaAsO_2$			3.2mM NaOCl			4.0mM NaOCl			4.8mM NaOCl		
	Average	SD	Average	SD	Ttest	Average	SD	Ttest	Average	SD	Ttest	Average	SD	Ttest	Average	SD	Ttest	Average	SD	Ttest
D	698	281	646	129	0.79	780	152	0.68	643	153	0.78	821	165	0.55	986	90	0.17	954	168	0.25
ncm^5U	1061	178	1012	191	0.76	1242	278	0.39	1096	302	0.87	1177	325	0.62	1339	175	0.13	1467	295	0.11
I	220448	18428	203800	9591	0.24	209163	8493	0.39	217528	15976	0.85	252051	19311	0.11	260166	6120	0.02	237714	13057	0.26
m^5U	2210	90	2513	461	0.33	2087	234	0.44	1827	302	0.10	2153	65	0.42	1885	109	0.02	1948	296	0.22
Gm	95582	7170	87325	11710	0.36	85861	5299	0.13	87900	7364	0.27	118264	16693	0.10	118582	3773	0.01	101952	9384	0.40
Um	263	16	226	29	0.13	249	50	0.68	252	50	0.75	376	54	0.03	386	19	0.00	317	35	0.07
m^5C	52030	12069	48771	9709	0.73	44164	17102	0.55	24144	14414	0.06	27036	18513	0.12	28589	6125	0.04	38245	14717	0.28
m^3C	10211	1405	10785	1185	0.62	9524	1143	0.55	8215	677	0.09	10249	1516	0.98	9390	1575	0.54	9648	1818	0.69
Y	6753	999	6161	479	0.41	5696	1476	0.36	5033	777	0.08	5578	1801	0.38	3363	327	0.01	4338	314	0.02
Cm	28112	4393	24804	4325	0.41	23893	4033	0.29	18889	7032	0.13	23094	11411	0.52	25705	3299	0.49	26144	5728	0.66
mcm^5U	259	18	225	15	0.07	239	37	0.44	189	12	0.00	289	72	0.53	511	464	0.40	258	59	0.97
m^7G	90563	8069	93100	11042	0.76	86918	8329	0.62	71430	3273	0.02	92691	5347	0.72	88108	4016	0.66	81446	9267	0.27
m^1G	143507	12855	154839	21460	0.48	146691	14931	0.79	117558	9635	0.05	130656	16219	0.34	132287	3785	0.22	126490	14136	0.20
m^2G	124734	14061	129941	21137	0.74	126325	13108	0.89	104067	7433	0.09	117919	11146	0.55	116662	2554	0.38	110416	12166	0.25
ac^4C	22052	1665	21142	2459	0.62	20440	1549	0.29	18978	1223	0.06	23781	3119	0.44	23964	775	0.15	21640	2214	0.81
t^6A	66785	5932	59705	5138	0.19	57821	6389	0.15	49945	3083	0.01	65494	6507	0.81	63792	4870	0.54	61653	8554	0.44
mcm^5s^2U	528	80	522	69	0.93	487	69	0.55	374	32	0.04	492	40	0.53	478	58	0.43	447	65	0.25
m^1I	4172	146	4285	979	0.85	3672	587	0.23	3316	836	0.16	3018	326	0.01	3178	615	0.05	3186	242	0.00
Am	83039	4757	62376	8050	0.02	67489	1734	0.01	84669	5938	0.73	127864	8201	0.00	120941	1250	0.00	97826	7735	0.05
m^2_2G	162682	10475	164928	23674	0.89	155837	15424	0.56	135192	4577	0.01	156039	8431	0.44	150193	3051	0.12	140531	14810	0.10
I^6A	16188	2844	13327	2307	0.25	14062	2288	0.37	11717	1381	0.07	14069	604	0.28	14363	19	0.33	13277	1252	0.18
yW	289	23	242	39	0.15	235	31	0.07	182	11	0.00	280	16	0.63	259	3	0.09	250	45	0.25
m^1A	165385	11810	176791	24022	0.50	164125	15479	0.92	138153	4467	0.02	171485	8437	0.51	164512	5825	0.91	148475	14172	0.19

Table 3-1. Normalized MS signal intensities for tRNA modifications in *S. cerevisiae* treated with four toxicants. Data represent mean ± SD for N = 3, with Student's t-test relative to control values.

	H_2O_2, mM			MMS, mM			$NaAsO_2$, mM			NaOCl, mM		
	2	5	12	6	12	24	20	40	60	3.2	4	4.8
D	1.17762	1.092246	1.336312	1.008073	1.177209	1.138843	0.925642	1.117973	0.921993	1.176083	1.413422	1.367941
Y	1.048207	1.011943	0.906502	0.942232	0.852851	0.891963	0.86479	0.856079	0.783348	1.113707	1.024734	0.996259
ncm^5U	1.151324	1.056956	1.094415	1.063012	1.106319	1.166317	0.954578	1.171254	1.033215	1.109587	1.262151	1.383549
I	1.026212	0.965643	0.998282	0.893823	0.839287	0.878721	0.924478	0.948808	0.986754	1.143359	1.180168	1.078319
m^5U	0.917486	0.853888	0.832692	0.966747	1.011623	0.906295	1.137101	0.944218	0.826607	0.974009	0.852679	0.881178
Gm	1.078032	0.910225	0.93788	0.871084	0.85053	0.81299	0.913613	0.898294	0.919625	1.237301	1.240635	1.066641
Um	1.480943	0.947464	1.090912	0.833669	0.91136	0.891144	0.860356	0.949127	0.959982	1.429083	1.470347	1.204729
m^5C	1.918083	2.148977	1.97494	0.846477	0.845219	0.719437	0.937362	0.848824	0.464038	0.519621	0.549473	0.735072
m^3C	1.00289	1.068647	0.914668	1.217897	1.407598	1.198253	1.056243	0.932754	0.804495	1.003756	0.919617	0.944877
Cm	1.518601	1.565037	1.521726	0.86092	0.78512	0.748736	0.882314	0.849917	0.671907	0.821497	0.914356	0.929981
mcm^5U	0.866434	0.842557	0.842458	1.008793	1.155832	1.080345	0.868517	0.921413	0.728908	1.11455	1.967932	0.993679
m^7G	0.903554	1.178655	0.775828	1.630612	2.182745	1.778017	1.028016	0.959749	0.788733	1.0235	0.97289	0.899333
m^1G	0.861505	0.804767	0.763929	0.935312	0.964822	0.857064	1.078963	1.022186	0.819179	0.910449	0.921813	0.881423
m^2G	0.845636	0.7864	0.768506	0.902425	0.870305	0.78662	1.041745	1.012757	0.834309	0.945365	0.935283	0.885212
ac^4C	1.062737	1.031264	1.075229	1.00156	0.942444	0.93608	0.958734	0.926895	0.860621	1.07839	1.086729	0.981309
t^6A	0.883575	0.821947	2.031944	0.921653	0.919712	0.845696	0.893989	0.86578	0.74785	0.980664	0.955176	0.923151
mcm^5s^2U	0.892611	0.744478	0.714488	0.873775	0.865399	0.732333	0.989633	0.923494	0.708597	0.932034	0.904726	0.847081
m^1I	0.948333	0.863812	0.829329	0.976277	0.959663	0.855285	1.027179	0.880136	0.794772	0.723356	0.761645	0.763554
Am	1.141667	0.893342	0.987364	0.78274	0.764325	0.78879	0.751164	0.812745	1.019632	1.539809	1.456433	1.178079
m^2_2G	1.931529	2.102891	2.320356	0.922161	0.945495	0.843199	1.013808	0.957922	0.831018	0.959165	0.923232	0.863837
i^6A	0.756877	0.717579	0.704337	0.793874	0.71939	0.680728	0.823242	0.868636	0.723785	0.869071	0.887255	0.820137
yW	0.801611	0.680539	0.732286	0.853446	0.789282	0.709106	0.837658	0.815594	0.629701	0.971463	0.896387	0.864683
m^1A	0.878101	0.887864	0.787636	1.101781	1.179458	1.021162	1.068969	0.99238	0.835342	1.036885	0.994723	0.897756

Table 3-2. Fold-change values for *S. cerevisiae* tRNA modifications in treated cells relative to untreated controls. Shading color indicates significant difference from control by Student's t-test: blue, $p<0.05$; yellow, $p<0.1$.

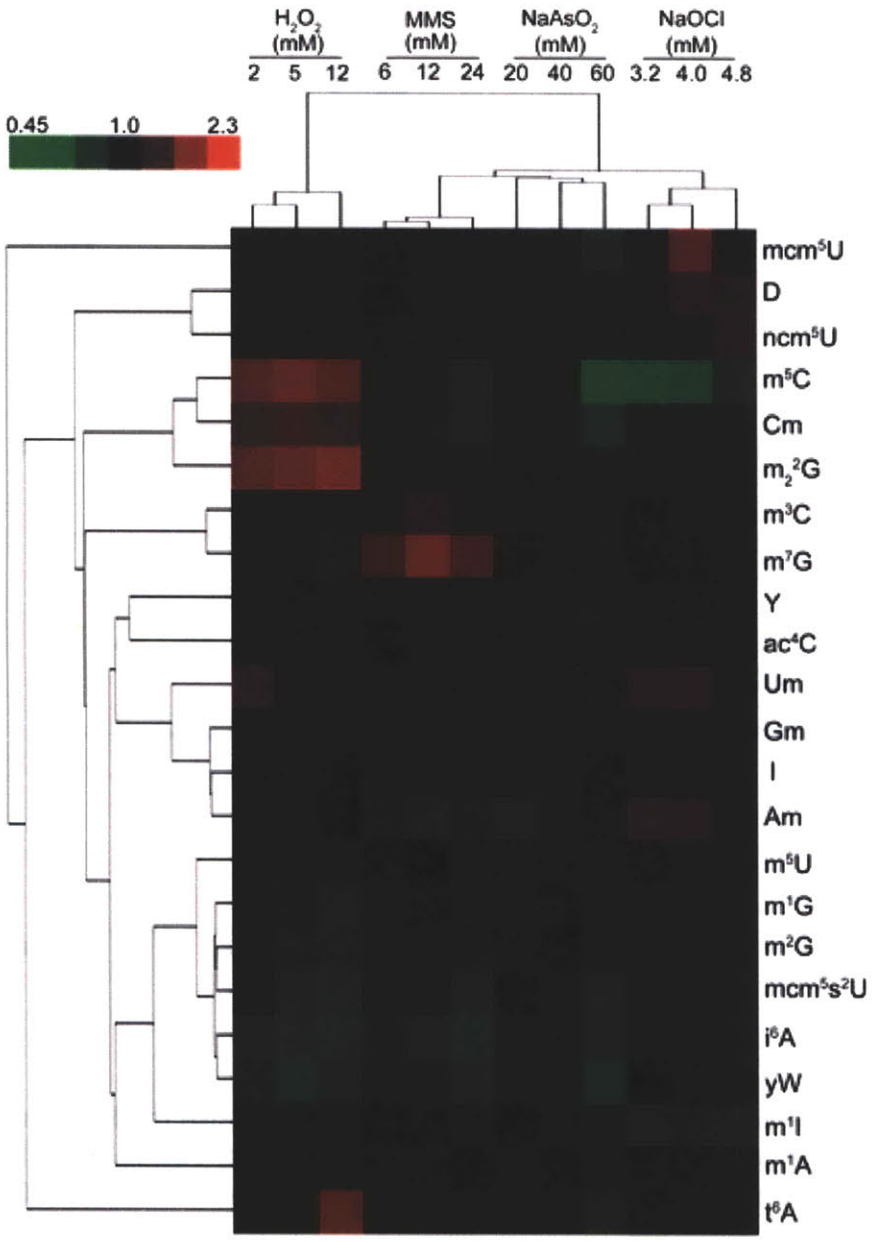

Figure 3-2. Hierarchical cluster analysis of toxicant-induced changes in tRNA modification spectra in wild-type yeast exposed to concentrations of MMS, H_2O_2, NaOCl, and $NaAsO_2$ producing 20%, 50%, and 80% cytotoxicity. Scale of fold-changes is indicated by the color bar on the top-left of this figure.

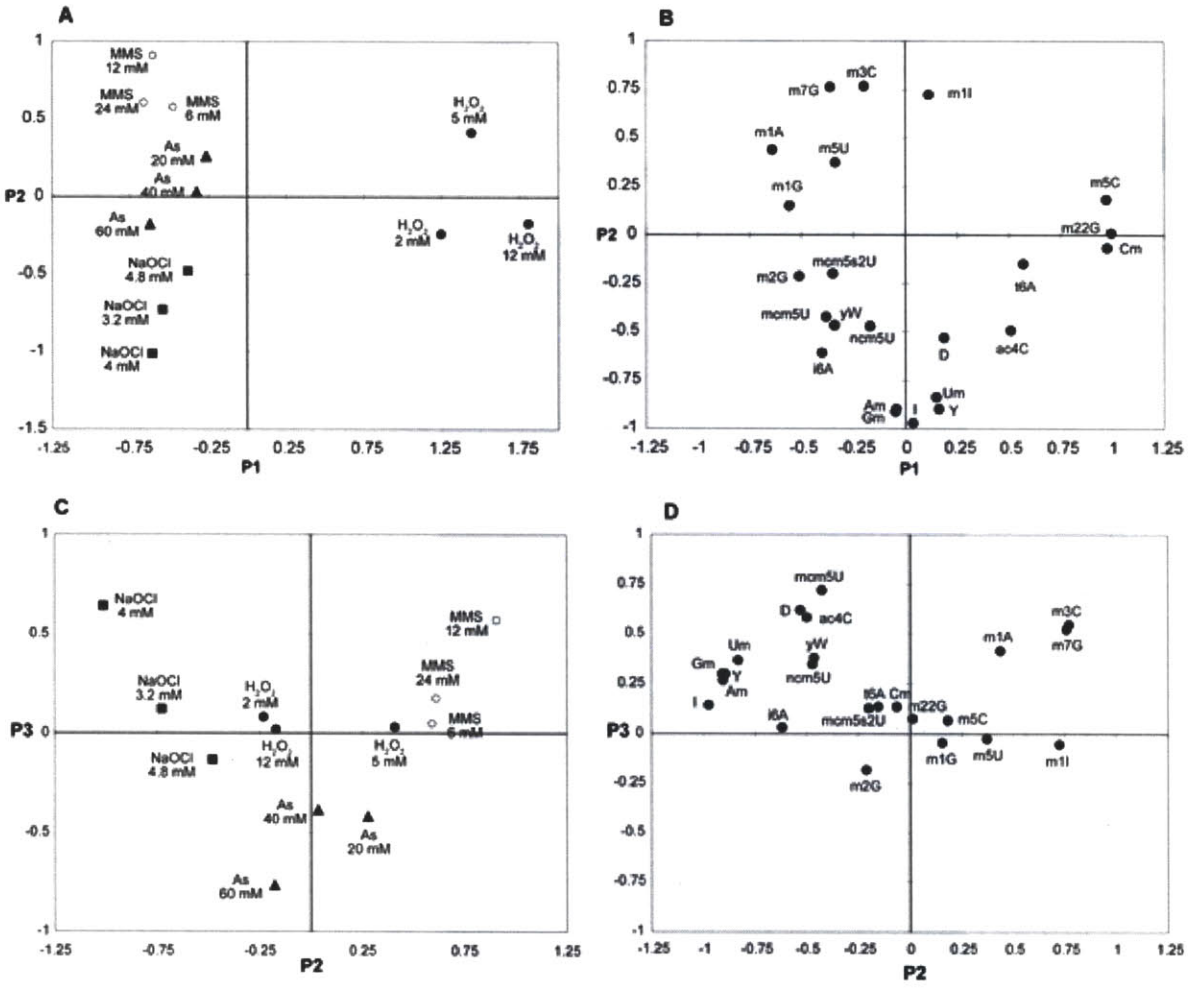

Figure 3-3. Principal component analysis (PCA) of changes in the levels of tRNA modifications caused by exposure to MMS, H_2O_2, NaOCl, and $NaAsO_2$. **(A)** Scoring plot of PC1 vs. PC2; **(B)** Loading plot of PC1 vs. PC2; **(C)** Scoring plot of PC2 vs. PC3; and **(D)** Loading plot of PC2 vs. PC3.

Sensitivity of tRNA modifying enzyme-deficient mutants to various stresses. To determine the importance of modified nucleosides in stress responses, we assessed sensitivity of tRNA modifying enzyme-deficient mutants of *S. cerevisiae* to the four toxic agents. Each

mutant had a knock-out of one of the following genes: *trm1*, *trm2*, *trm3*, *trm4*, *trm5*, *trm7*, *trm8*, *trm9*, *trm10*, *trm11*, *trm12*, *trm13*, *trm44*, *trm82*, *tad1*, *mod5*, and *tan1*. As *trm5* is an essential gene, we used a diploid strain of yeast (*S. cerevisiae GBY1*) with deletion of one of the copies of trm5. Besides that, all mutants were originated from the haploid strain *S. cerevisiae BY4741*. As shown in figure 3-4, cells were increased in sensitivity to H_2O_2 in the absence of *trm4* or *trm7*; also, the genes *trm1*, *trm4*, *trm7*, *trm9*, and *trm44* conferred resistance to MMS; *trm1*, *trm4*, and *trm9* conferred resistance to $NaAsO_2$; at last, *trm4Δ* mutant was sensitivity to NaOCl.

Changes in spectrum of modified nucleosides in tRNA as a function of deficiency in tRNA modifying enzymes. Spectra of tRNA modifications from those tRNA modifying enzyme-deficient mutants of *S. cerevisiae* were compared to that of wild-type cells. The results shown in Table 3-3 illustrated that knockout of each tRNA modifying enzyme led to the loss of its corresponding modification(s): *trm1Δ* mutant lost $m^2{}_2G$; *trm2Δ* lost m^5U; *trm10Δ* lost m^1G; *tad1Δ* lost m^1I; *trm4Δ* lost m^5C; *trm8Δ* and *trm82Δ* lost m^7G; *mod5Δ* lost i^6A; *tan1Δ* lost ac^4C; *trm5Δ* and *trm12Δ* lost yW; *trm11Δ* lost m^2G; and *trm9Δ* lost mcm^5U and mcm^5s^2U. However, as the formations of some modifications are catalyzed by several enzymes, loss of one of these enzymes did not lead to complete depletion of the modified nucleoside. For instance, both TRM3 and TRM7 catalyze the formation of Gm; TRM7 and TRM12 catalyze the formation of Cm.

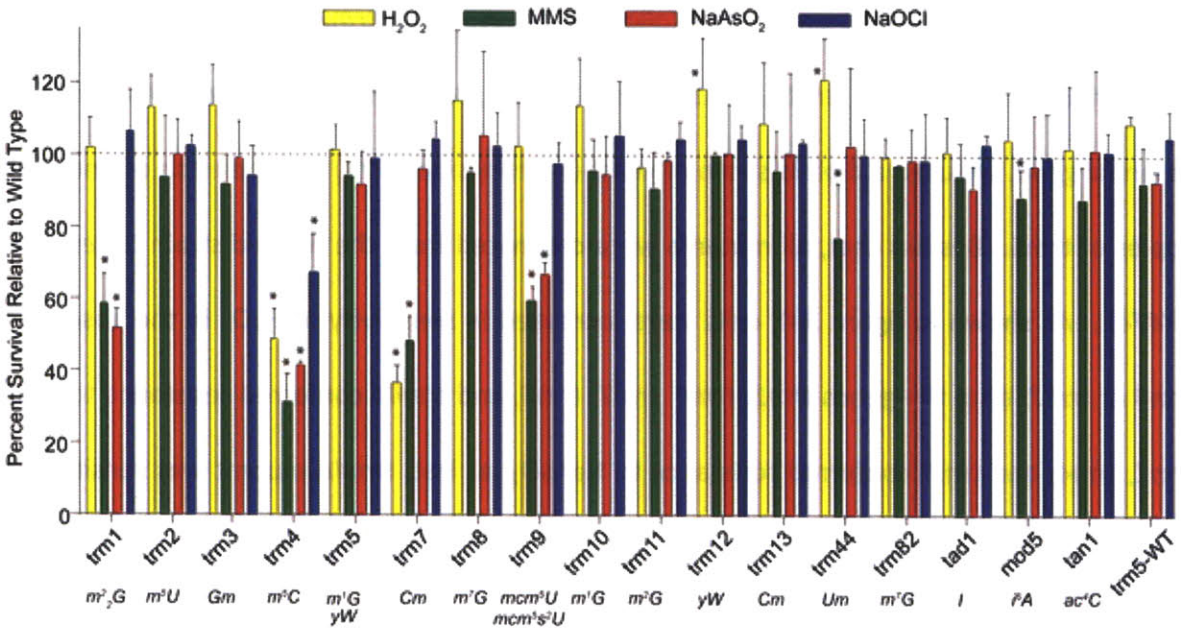

Figure 3-4. Phenotypic analysis of cytotoxicity induced by H_2O_2, MMS, NaOCl, and $NaAsO_2$ in *S. cerevisiae* mutants lacking tRNA methyltransferase and other modification genes. The mutants were exposed to 12 mM H_2O_2, 24 mM MMS, 60 mM NaAsO2, or 4.8 mM NaOCl, which generated ~80% cytotoxicity. Data represent mean ± SD for three biological replicates. Asterisks denote values statistically different from unexposed controls by Student's t-test, $p<0.05$. Associated RNA modifications are listed below each enzyme.

	trm1	trm2	trm3	trm4	trm7	trm8	trm82	tad1	mod5	tan1	trm9	trm10	trm11	trm12	trm13	trm44	trm5
D	0.713842	0.6843	0.799161	0.828137	0.899072	0.825256	0.796538	0.544586	0.514717	0.583542	0.687507	0.706263	0.695729	0.630171	0.753443	0.793753	1.224693
I	1.026083	0.947245	1.184603	0.916817	0.796736	0.960603	1.223109	1.015979	0.624147	1.207896	1.164556	1.0172	0.892598	0.877719	0.909553	0.959943	0.948123
m5U	0.987038	0.00001	1.127997	0.971096	0.853232	0.945465	1.114468	0.879221	0.785055	1.037878	1.211402	0.972925	0.824946	0.893913	0.857149	0.95087	0.689327
ncm5Um	1.115053	1.442154	1.557688	1.00714	0.00001	0.99317	1.240788	1.010364	0.714159	0.97679	1.332745	1.804322	1.088102	1.150931	1.045787	1.204891	0.935474
Gm	0.892365	0.917907	0.969365	1.057554	0.765217	1.150425	1.355311	1.001871	0.743076	1.143667	0.95433	0.797357	0.907308	0.892193	1.034241	1.032041	1.583792
Um	0.707096	0.799301	0.772762	0.721069	0.498528	1.063909	1.225548	0.888201	0.582978	1.000561	0.68786	0.580268	0.696481	0.72486	0.755065	0.934333	1.798396
m3C	1.009635	1.007132	1.117877	0.925553	0.818491	1.274988	1.640635	1.30592	0.720901	1.674109	0.984104	0.964265	0.804095	0.805582	0.83824	0.931621	0.754647
m5C	1.082153	1.039257	1.226132	0.074026	0.805458	1.312151	1.443209	1.315717	0.838067	1.44199	1.210642	1.057321	0.965305	0.979524	0.993751	1.10052	0.791606
Cm	0.989427	0.929491	0.725017	0.870177	0.47598	1.201562	1.43464	1.120126	0.756758	1.305789	0.949605	0.709137	0.830921	0.832116	0.68439	0.911343	1.403351
mcm5U	1.00257	1.233468	1.156333	1.043397	0.945752	1.286914	1.639825	1.240346	0.788122	1.465071	0.00001	1.302712	1.20087	1.265654	1.309793	1.449138	0.627248
m7G	1.127881	1.013837	1.152332	0.947088	0.828513	0.114377	0.122159	1.4128	0.876977	1.677075	1.266986	1.018026	0.977665	1.02766	1.04834	1.173779	0.721473
m1G	1.307866	1.100389	1.156634	1.111559	1.055314	1.341812	1.757386	1.416961	0.904092	1.658933	1.260681	0.798146	0.960458	0.977426	0.974135	1.157466	0.607465
m2G	1.057559	1.092171	1.173847	0.951106	0.844212	1.358752	1.765857	1.316199	0.825633	1.522788	1.308046	1.058935	0.00001	0.973728	1.02583	1.12363	0.635986
ac4C	0.923116	0.957369	1.082035	0.909021	0.752637	1.061283	1.293255	0.939698	0.65876	0.30954	1.004896	0.874492	0.885059	0.891602	0.961265	0.965705	1.118684
t6A	1.097099	0.993229	1.106762	0.956773	0.90882	1.185038	1.532206	1.279125	0.756742	1.425328	1.187497	1.067276	0.906737	0.930285	0.953587	1.069266	0.63846
mcm5s2U	1.130653	1.127265	1.287195	0.953813	0.949808	1.187338	1.546039	1.277672	0.724113	1.400445	0.00001	1.311106	1.038589	1.041001	1.130092	1.255393	0.561531
m1I	1.171277	1.210978	1.043962	1.044721	0.919583	1.33084	1.680196	0.00001	0.83825	1.598951	1.354337	1.076146	1.040276	1.079506	1.073863	1.212763	0.638423
Am	0.783387	0.792853	0.772943	0.800324	0.545612	1.015545	1.15388	0.828891	0.699742	0.945327	1.320257	1.188623	1.097077	1.13754	1.156384	1.295224	1.959901
m22G	0.00001	1.042508	1.149887	0.978005	0.833386	1.252354	1.649986	1.292432	0.800677	1.693383	1.22816	1.073447	0.940472	0.978967	0.992541	1.112964	1.963598
i6A	1.00373	1.013344	1.249815	1.071445	0.904218	0.954777	1.281665	1.203227	0.012504	1.26141	1.182784	1.178433	0.903244	0.929682	0.95893	0.933019	0.681736
yW	1.408351	1.147706	1.406329	0.826683	0.00001	0.488963	0.559251	0.48456	0.424868	0.512475	1.127805	1.206756	0.473142	0.00001	0.935482	0.944868	0.279563
m1A	1.099058	0.944103	1.112871	0.944254	0.838408	1.289652	1.379047	1.389095	0.883242	1.571972	1.17681	0.963162	0.88898	0.921767	0.937037	1.049542	0.767246
ncm5U	0.708553	0.640167	0.724605	0.711749	0.810952	0.993275	0.805267	0.606002	0.822832	0.743067	0.847963	0.886971	0.718471	0.762053	0.930234	0.869326	0.91634

Table 3-3. Fold-changes of levels of tRNA modifications in mutant strains relative to in wild type *S. cerevisiae*. Underlined: Mutant was determined to be significantly different from wild type by Student's t-test with $P<0.05$; Yellow: ratios <0.02 (values of 0.00001 indicate undetectable ribonucleosides in the mutant strains); Green: ratios <0.6; Red: ratios >1.5.

Discussion

Yeast exposure parameters. To quantify the dynamics of tRNA modifications in cellular responses, we selected four well studied chemicals that possess distinct mechanisms of toxicity: MMS, hydrogen peroxide (H_2O_2), sodium arsenite ($NaAsO_2$), and sodium hypochlorite (NaOCl, pK_a 7.5 (*27*)). The behavior of yeast upon exposure to MMS, $NaAsO_2$ and H_2O_2 has been extensively studied in terms of transcriptional response and cytotoxicity phenotyping (*11, 12, 28*). We also chose NaOCl since it produces an oxidative stress distinct from that of H_2O_2 and could thus affect the tRNA modification spectrum differently. We then performed cytotoxicity dose-response studies in *S. cerevisiae* exposed to agents (Figure 3-1), choosing concentrations that produced ~20%, 50% and 80% cytotoxicity to ensure a common phenotypic endpoint for comparison.

One important issue with the methylating agent, MMS, was the possibility that changes in methyl-based modifications in tRNA could be due to both enzymatic methylation and direct chemical methylation. Literature precedent indicates that MMS reacts with DNA to form adducts mainly at guanine N^7 (68%), adenine N^1 (18%) and cytosine N^3 (10%) (*29, 30*). To address the extent of direct methylation of RNA by MMS, control studies were performed and

revealed that direct alkylation by MMS contributes <25% to the cellular burden of m^7G in small RNA, with the bulk of m^7G arising by enzymatic methylation of tRNA (Figure 3-5). No other agent affected tRNA modifications in this manner, with changes in the relative quantities of the modifications resulting from alterations in biosynthesis, tRNA gene transcription or tRNA degradation.

A

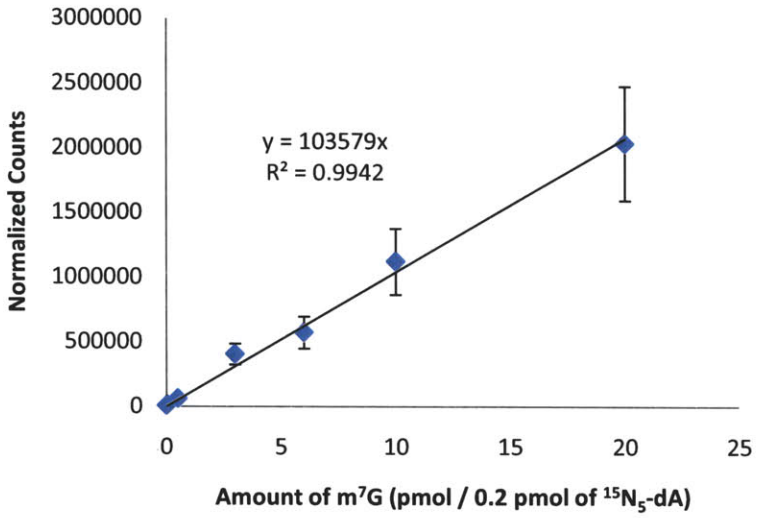

B

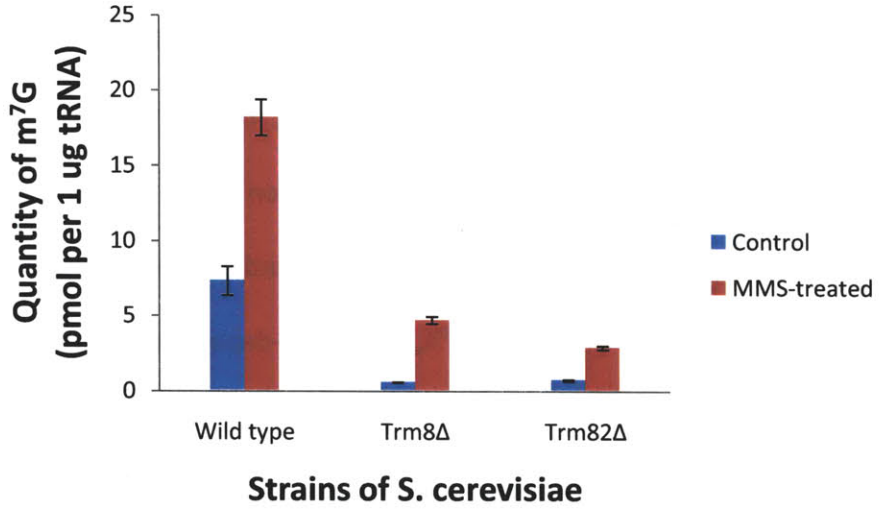

Figure 3-5. Quantification of absolute level of m^7G in different strains of yeast with or without MMS-exposure. (**A**) External calibration curve for m7G. (**B**) Absolute quantities of m^7G. Data represent mean ± SD for three biological replicates.

Reprogramming tRNA modifications during the stress response. With exposure and analytical parameters established, we tested the hypothesis that the spectrum of tRNA modifications would dynamically change as a function of the *S. cerevisiae* stress response. In addition, we predicted that these changes would serve as biomarkers of each exposure. Cells were exposed to three concentrations of each chemical and 23 tRNA modifications were quantified by LC-MS/MS, with the results shown in Tables 3-1 and 3-2, the latter as the ratio of treated to control signal intensities. A crude analysis of the data shows fold-changes ranging from 0.2 to 4, with 25% and 36% of the exposure data significantly different from control values by Student's t-test at $p<0.05$ and $p<0.1$, respectively (Table 3-2). These results point to the non-random and regulated nature of the exposure-induced changes in the levels of the tRNA modifications.

Multivariate statistical analyses revealed important patterns or signatures in the toxicant-induced changes in tRNA modifications. As shown in Figure 3-2, hierarchical clustering distinguished both agent- and dose-specific changes in the modification spectra, with unique patterns of increase and decrease apparent in all cases. H_2O_2 consistently increased the levels of m^5C, Cm and $m^2{}_2G$ and, at the highest concentration, t^6A, with dose-dependent decreases in m^5U, m^1G, m^2G, mcm^5s^2U, i^6A, yW and m^1A. MMS consistently increased the level of m^7G, and decreased Am, m^5C, Cm, mcm^5s^2U, i^6A, and yW. $NaAsO_2$ caused only decreases in modification levels at the highest concentration, most notably for mcm^5U, m^3C, m^7G, mcm^5s^2U, i^6A, yW, m^5C, and Cm. Interestingly, the dose-response for NaOCl showed an inverse correlation between concentration and increased levels of Am and Um and decreased levels of m^5C. Given the

reproducibility of the data, the changes in tRNA modification spectra can be considered signature biomarkers of exposure for these four classes of chemical stressor.

Principal component analysis (PCA) creates a model that reduces the complexity of a data set by identifying hidden correlations (the principal components) comprised of weighted, linear combinations of the original variables, with the first principal component (P1) accounting for the largest portion of the variation of the data and so on. The results of PCA of the dataset of nucleoside fold-change values (Table 3-2) are shown in Figure 3-3. With 88% of the variability expressed in the first 3 principal components (56%, 22% and 10%, respectively), individual agents contributed variance to each as shown in Table 3-4, with H_2O_2 contributing 74% in P1, MMS and NaOCl each contributing >40% in P2 and $NaAsO_2$ contributing 53% in P3. The scores plots (Figure 3-3) clearly distinguish the four agents, with H_2O_2-induced changes as the major determinant of P1 and with MMS, NaOCl and $NaAsO_2$ distinguished best in P2. While H_2O_2 and NaOCl are negatively correlated in P1, they are more closely grouped in P2 and P3, which suggests that the changes in tRNA modifications reflect both common and unique facets of the toxic mechanism of each agent. For example, H_2O_2 and NaOCl are both oxidizing agents, but H_2O_2 generates hydroxyl radicals by Fenton chemistry while the protonated form of NaOCl yields hydroxyl radicals, chloramines and singlet oxygen (*24, 31-33*). Similarly, MMS and $NaAsO_2$ are negatively correlated in P3 and more positively correlated in P2, with the latter consistent with recent evidence for alkylation-like adduction of arsenic to DNA and proteins following its metabolism (*25, 34*). This would also explain the negative correlation of $NaAsO_2$ and H_2O_2 in P1, while the recognized oxidative stress caused by arsenite is consistent with a positive correlation between $NaAsO_2$ and H_2O_2 in P2 (*35*).

	PC1	PC2	PC3
H_2O_2	74%	6.9%	0.45%
MMS	11%	42%	21%
$NaAsO_2$	6.2%	2.8%	53%
NaOCl	8.7%	49%	26%

Table 3-4. Contribution of each agent to variance in principal component analysis.

Both PCA (Figure 3-3) and cluster analysis (Figure 3-2) revealed that m^5C, m_2^2G, Cm and t^6A are major features of the H_2O_2 response, while m^1A, m^3C and m^7G were associated with MMS. Increases in Gm, Um, I and Am were responsible for the variance induced by NaOCl, which is consistent with the inversely related doses and levels for Am and Um observed in cluster analysis. $NaAsO_2$ was poorly distinguished in P2, with only m^2G accounting for variance only at the highest concentrations (Figure 3-2).

tRNA modification biosynthetic pathways are critical to the stress response. The observation of toxicant- and dose-dependent changes in the levels of the 23 tRNA modifications is consistent with a model in which cells respond to toxicant exposure by modifying tRNA structure to enhance the synthesis of proteins critical to cell survival, as has been proposed in previous studies with yeast exposure to MMS (*11*). In these studies, the conversion of cm^5U to mcm^5U by Trm9 was found to be critical for surviving MMS exposure. To define the roles of

specific tRNA modifications in the toxicant response, cytotoxicity phenotypic analyses were performed with yeast mutants lacking each of 13 *trm* tRNA methyltransferase genes and 3 other types of RNA modification biosynthetic genes. As shown in Figure 4, heightened sensitivity to H_2O_2 was observed in mutants lacking Trm4 and Trm7, which catalyze formation of two modifications elevated by H_2O_2 exposure: m^5C and Cm, respectively (*36, 37*). The simple explanation is that the increase in a specific tRNA modification is needed to promote an efficient stress response. However, $m^2{}_2G$ was also elevated by H_2O_2 (Figure 3-2), yet loss of an enzyme involved in its biosynthesis, Trm1, did not confer H_2O_2 sensitivity, as shown in Figure 3-4 (*38, 39*). This behavior draws a comparison to mRNA, as it has been reported that many of the transcripts induced in response to a stress are not essential for viability during a challenge from that stress (*40, 41*). MMS sensitivity was identified in *trm1*, *trm4* and *trm9* mutants, whose corresponding proteins synthesize $m^2{}_2G$, m^5C and mcm^5U/mcm^5s^2U, respectively. However, these modifications were not strongly associated with MMS exposure in PCA (Figure 3-3). Somewhat surprisingly, loss of Trm1, Trm4, Trm7 and Trm9 conferred $NaAsO_2$ sensitivity. These methyltransferases are responsible for forming $m^2{}_2G$, m^5C, m^1G and mcm^5U/mcm^5s^2U, respectively, of which only m^2G was found to vary significantly in PCA (Figure 3-3). For NaOCl, only *trm4* was sensitive to exposure and the m^5C product of Trm4 was not associated with NaOCl exposure (Figure 3-3). Again, this behavior parallels that of mRNA transcripts the levels of which do not change after exposure but that encode proteins important for viability after exposure (*40, 41*).

Potential mechanisms linking tRNA modifications and the stress response. These results reveal a complex and dynamic control of tRNA modifications in cellular survival responses and suggest models for homeostasis of the modifications. One example involves modifications for which the biosynthetic mutant is sensitive to exposure but the modification level does not change in wild type cells following exposure (*e.g.*, MMS exposure and *trm1*/$m^2{}_2G$, *trm4*/m^5C, *trm9*/mcm^5U or mcm^5s^2U). The simplest explanation here is that the modification change occurs in a single tRNA species and the change is masked by an inverse change in the level of the modification in the larger population of tRNA molecules; it is known that both m^2G and m5C occurs in mutiple tRNAs (*2-4*). A second explanation parallels the idea of both pre-existing mRNA and stressor-induced transcription during a stress response. We have observed stress-induced increases in the levels of several modifications required for the survival response. However, other modifications may already exist on tRNA molecules involved in selective translation of stress response messages. In both cases, the modifications are absolutely required for survival, but some are already present in unstressed cells and others are induced. Finally, it is possible that a modification, though its level may not change, is required for the subsequent synthesis of other modifications that are critical to the survival response. Such "cooperativity" is suggested by data from *mod5*-deficient cells, in which i^6A decreases by ~75-fold while D is reduced by ~2-fold. The presence of i^6A may signal downstream biosynthetic events, with deficiencies promoting a general reprogramming of tRNA. Similarly, cells deficient in Trm82, a subunit of m^7G methyltransferase, had a ~7-fold reduction in m^7G and a >1.5-fold increase in m^3C, mcm^5U, m^1G, m^2G, t^6A, mcm^5s^2U and $m_2{}^2G$ (Table 3-3), which raises the possibility that Trm82 itself or m^7G inhibits other tRNA modifying enzymes. With the caveat of

possible increases in tRNA copy number, the ~50% increase in these modifications suggests a pool of unmodified tRNA molecules, an observation supported by increases in m^3C after exposure to MMS, mcm^5U after exposure to NaOCl, and both t^6A and m^2_2G after exposure to H_2O_2 (Figure 3-2).

Cooperativity could also explain the case in which the level of a modification changes significantly following exposure yet the mutant strain is not sensitive to the exposure. For example, loss of *trm1* did not confer sensitivity to H_2O_2 but its product, m^2_2G, rose significantly with H_2O_2 exposure (Figure 3-2 and Figure 3-4). The stress-induced change in m^2_2G may be a response to a change occurring with another modification for which the mutant strain might be sensitive to the exposure. In support of this argument, m^5C modifications increase along with m^2_2G after H_2O_2 exposure and deficiencies in the m^5C-producing methyltransferase Trm4 confer sensitivity to H_2O_2. Some other studies have also demonstrated such cooperativity among RNA modifications in the observation of the negative regulation of wobble position C-to-U editing by thiolation of a U at position 33 outside the anticodon in *T. brucei (42)*.

Finally, there is the case in which a modification decreases with exposure to a stressor and a deficiency in the enzyme responsible for that modification confers sensitivity, as in the case of m^5C, *trm4* and NaOCl (Figure 3-2 and Figure 3-4). The population level of m^5C may decrease with NaOCl exposure in spite of a protective increase in the level of m^5C at some critical tRNA location. This may reflect a decrease in the transcription of tRNA substrates of Trm4 or the targeted degradation of specific tRNA species. It is important to note that biosynthetic redundancy, as in the case of Gm with Trm3 and Trm7, could mask any major changes in tRNA modification levels that are associated with mutational loss of one enzyme (Table 3-3), yet loss

of one of the redundant enzymes can induce sensitivity, such as the case of H_2O_2 and *trm7*. These observations lead to many questions that obviously require more mechanistic study to define the precise role of tRNA modifications in cellular responses to stress.

One consistent feature that arose from our studies of modifications affected by or protecting against toxicant exposure was the frequent involvement of the wobble position, 34 (Table 1-2 in Chapter 1 and Table 3-2). The correlation between the wobble modification and the importance of a corresponding enzyme after toxicant exposure is not surprising in light of recent observations of the critical role played by these modifications and anticodon loop ribonucleosides in translational fidelity and efficiency (*4*). Controlled alteration of ribonucleoside structure at position 34, and that at the conserved purine at position 37, is proposed to allow reading of degenerate codons by modulating the structure of the anticodon domain to facilitate correct codon binding. As the most frequently modified ribonucleosides, positions 34 and 37 also have the largest variety of modifications, so it is reasonable that they would be extensively involved in translational control of the survival response (*43, 44*). This is also consistent with previous studies that mcm^5U at the wobble position was critical to the translation of a specific group of genes related to DNA damage response (*11*).

Perhaps more interesting is a potential role for putative non-anticodon loop ribonucleoside modifications in the survival response. For example, Trm44 is the 2′-*O*-methyltransferase in yeast responsible for formation of 2′-*O*-methyl-U (Um), which occurs only at position 44 in yeast tRNA (*45, 46*). Loss of Trm44 conferred sensitivity to $NaAsO_2$ exposure. This observation suggests three possibilities: (1) that Trm44 synthesizes or influences the synthesis of modifications at other positions in tRNA; (2) that Um occurs in positions other than

44 (*e.g.*, anticodon loop); or (3) that Um(44) plays a role in modulating translation in response to $NaAsO_2$ exposure. Another example involves Trm1 and $m^2{}_2G$ at position 26. Current evidence suggests that $m^2{}_2G$ occurs only at position 26 in yeast tRNA and that Trm1 is the methyltransferase responsible for its formation (*39, 45*). The fact that loss of Trm1 conferred sensitivity to MMS and $NaAsO_2$ exposure and that H_2O_2 exposure increased the level of $m^2{}_2G$ again suggest the three possibilities analogous to those for Trm44 and Um. Similar arguments can be made for Trm3 and Gm at position 18 with NaOCl exposure, for Trm11 and m^2G at position 10 with NaOCl and $NaAsO_2$ exposure, and for Trm8/82 and m^7G at position 46 with MMS exposure.

All of these observations point to participation of wobble and non-wobble RNA modifications in a complex and dynamic network of translational mechanisms in cellular responses. This expands the repertoire of translational control mechanisms, which includes recent discoveries about the effect of ribonucleoside modifications on tRNA stability (*8, 9*). In this model, cell stress leads to rapid degradation of specific tRNAs and subsequent effects on translational efficiency. Another similar stress response involves cleavage of cytoplasmic transfer RNAs by ribonucleases released during the stress [10]. One consequence of these degradation pathways would be to decrease the amount of modified ribonucleoside detected in our assay, which may explain some of our observations with the toxicant stresses. Our approach to quantifying tRNA modifications provides information only about population-level changes, so the observed changes could result from modification of existing tRNA molecules or changes in the number of tRNA copies. Of particular importance here is the observation by Phizicky and coworkers that loss of m^7G at position 46 leads to degradation of specific tRNAs [9],

which suggests that our observation of changes in the levels of RNA modifications could be amplified by both reduction in the activity of modifying enzymes and by tRNA degradation. On the other hand, one argument against large increases in tRNA copy number arises from recent observations of repressed tRNA transcription during S-phase and, of direct relevance to the present studies, during replication stress induced by MMS, hydroxyurea and likely other toxicants (*47*). Finally, our findings may also parallel recent work on tRNA charging. Reactive oxygen species have been implicated as a methionine misacylation trigger and modification status could help promote these programmed changes to the genetic code (*12*). As we are beginning to appreciate the precision and coordinated nature by which cells mount a regulated stress-response, it is most likely the observed changes in tRNA modification levels promote multiple biological responses.

Novel biosynthetic pathways for tRNA modifications. As recognized by several groups, the LC-MS/MS platform facilitates definition of biosynthetic pathways for RNA modifications (*19, 20*). This is illustrated in Table 3-3, which contains ratios of the basal levels of tRNA modifications in yeast mutants lacking various tRNA modification enzymes compared to wild type yeast. These data corroborate known substrate/enzyme pairs and further demonstrate the highly quantitative nature of our approach (*45*). For example, the level of m^1I drops to nearly undetectable levels with loss of Tad1, the adenosine deaminase producing the inosine precursor to m^1I (*48*). That a diploid heterozygous mutant of *trm5*, the product of which catalyzes *N*-methylation of I [47], caused a ~40% reduction in total m^1I attests to the accuracy of our assay and demonstrate that gene dosage effects alter the level of tRNA modification (*49*).

A similar ~50% reduction in yW occurred in the *trm5* mutant due to the absence of the m^1G37 precursor to yW, while complete loss of Trm12, which methylates the 4-demethylwyosine precursor of yW, made yW undetectable. Other pathways critical to yW are apparent in the smaller decreases in yW (0.3– to 0.5-fold) occurred in cells deficient in other enzymes (Trm8, Trm82, Tad1, Mod5, Tan1, Trm11, Trm5).

The data in Table 3-3 also reveal several novel observations. It has been observed that Trm7 catalyzes 2′-*O*-methylation of G and C nucleosides at positions 32 and 34, but they could not detect the ncm^5Um product of 2′-*O*-methylation of ncm^5U (*37*). While we could only tentatively identify ncm^5Um, we observed a quantifiable signal for a species with the correct molecular transition for ncm^5Um and observed that loss of Trm7 led to a lowering of putative ncm^5Um to undetectable levels. This supports their prediction that Trm7 catalyzes formation of ncm^5Um in yeast.

Another example involves the formation of Um. While Trm44 catalyzes synthesis of Um at position 44 in tRNA(ser) (*46*), analysis of *trm* mutants as shown in Table 3-3 suggests a redundancy in methyltransferase activity capable of 2′-*O*-methylation of U(44), including Trm7, which methylates U at positions 32 and 34 (*37*), and Trm13 methylation of C and A at position 4 in several yeast tRNAs. Cells lacking Trm44, Trm7 or Trm13 have 53%, 50% and 76% of wild type levels of Um, respectively.

In summary, a quantitative bioanalytical approach to the study of tRNA modifications has revealed several novel biosynthetic pathways for RNA modifications and has led to the discovery of signature changes in the spectrum of tRNA modifications in the damage response to different toxicant exposures. The results support a general model of dynamic control of

tRNA modifications in cellular response pathways and add to the growing repertoire of mechanisms controlling translational responses in cells (*9, 10, 13, 50*). Further, these cellular response mechanisms almost certainly involve parallel changes in spectrum of ribonucleoside modifications in rRNA and perhaps other RNA species.

References

1. Alberts, B. (2008) *Molecular biology of the cell*, 5th ed., Garland Science, New York.
2. Rozenski, J., Crain, P. F., and McCloskey, J. A. (1999) The RNA Modification Database: 1999 update, *Nucleic Acids Res 27*, 196-197.
3. Czerwoniec, A., Dunin-Horkawicz, S., Purta, E., Kaminska, K. H., Kasprzak, J. M., Bujnicki, J. M., Grosjean, H., and Rother, K. (2009) MODOMICS: a database of RNA modification pathways. 2008 update, *Nucleic Acids Res 37*, D118-121.
4. Agris, P. F., Vendeix, F. A., and Graham, W. D. (2007) tRNA's wobble decoding of the genome: 40 years of modification, *J Mol Biol 366*, 1-13.
5. Yarian, C., Townsend, H., Czestkowski, W., Sochacka, E., Malkiewicz, A. J., Guenther, R., Miskiewicz, A., and Agris, P. F. (2002) Accurate translation of the genetic code depends on tRNA modified nucleosides, *J Biol Chem 277*, 16391-16395.
6. Urbonavicius, J., Qian, Q., Durand, J. M., Hagervall, T. G., and Bjork, G. R. (2001) Improvement of reading frame maintenance is a common function for several tRNA modifications, *EMBO J 20*, 4863-4873.

7. Bjork, G. R., Durand, J. M., Hagervall, T. G., Leipuviene, R., Lundgren, H. K., Nilsson, K., Chen, P., Qian, Q., and Urbonavicius, J. (1999) Transfer RNA modification: influence on translational frameshifting and metabolism, *FEBS Lett 452*, 47-51.

8. Motorin, Y., and Helm, M. tRNA stabilization by modified nucleotides, *Biochemistry 49*, 4934-4944.

9. Alexandrov, A., Chernyakov, I., Gu, W., Hiley, S. L., Hughes, T. R., Grayhack, E. J., and Phizicky, E. M. (2006) Rapid tRNA decay can result from lack of nonessential modifications, *Mol Cell 21*, 87-96.

10. Thompson, D. M., and Parker, R. (2009) Stressing out over tRNA cleavage, *Cell 138*, 215-219.

11. Begley, U., Dyavaiah, M., Patil, A., Rooney, J. P., DiRenzo, D., Young, C. M., Conklin, D. S., Zitomer, R. S., and Begley, T. J. (2007) Trm9-catalyzed tRNA modifications link translation to the DNA damage response, *Mol Cell 28*, 860-870.

12. Netzer, N., Goodenbour, J. M., David, A., Dittmar, K. A., Jones, R. B., Schneider, J. R., Boone, D., Eves, E. M., Rosner, M. R., Gibbs, J. S., Embry, A., Dolan, B., Das, S., Hickman, H. D., Berglund, P., Bennink, J. R., Yewdell, J. W., and Pan, T. (2009) Innate immune and chemically triggered oxidative stress modifies translational fidelity, *Nature 462*, 522-526.

13. Emilsson, V., Naslund, A. K., and Kurland, C. G. (1992) Thiolation of transfer RNA in Escherichia coli varies with growth rate, *Nucleic Acids Res 20*, 4499-4505.

14. Begley, T. J., Rosenbach, A. S., Ideker, T., and Samson, L. D. (2004) Hot spots for modulating toxicity identified by genomic phenotyping and localization mapping, *Mol Cell 16*, 117-125.

15. Bennett, C. B., Lewis, L. K., Karthikeyan, G., Lobachev, K. S., Jin, Y. H., Sterling, J. F., Snipe, J. R., and Resnick, M. A. (2001) Genes required for ionizing radiation resistance in yeast, *Nat Genet 29*, 426-434.

16. Rooney, J. P., George, A. D., Patil, A., Begley, U., Bessette, E., Zappala, M. R., Huang, X., Conklin, D. S., Cunningham, R. P., and Begley, T. J. (2009) Systems based mapping demonstrates that recovery from alkylation damage requires DNA repair, RNA processing, and translation associated networks, *Genomics 93*, 42-51.

17. Kalhor, H. R., and Clarke, S. (2003) Novel methyltransferase for modified uridine residues at the wobble position of tRNA, *Mol Cell Biol 23*, 9283-9292.

18. Weissenbach, J., and Dirheimer, G. (1978) Pairing properties of the methylester of 5-carboxymethyl uridine in the wobble position of yeast tRNA3Arg, *Biochim Biophys Acta 518*, 530-534.

19. Meng, Z., and Limbach, P. A. (2006) Mass spectrometry of RNA: linking the genome to the proteome, *Brief Funct Genomic Proteomic 5*, 87-95.

20. Suzuki, T., Ikeuchi, Y., Noma, A., and Sakaguchi, Y. (2007) Mass spectrometric identification and characterization of RNA-modifying enzymes, *Methods Enzymol 425*, 211-229.

21. Wardman, P., and Candeias, L. P. (1996) Fenton chemistry: an introduction, *Radiat Res 145*, 523-531.

22. Dizdaroglu, M. (1994) Chemical determination of oxidative DNA damage by gas chromatography-mass spectrometry, *Methods Enzymol 234*, 3-16.

23. Imlay, J. A., Chin, S. M., and Linn, S. (1988) Toxic DNA damage by hydrogen peroxide through the Fenton reaction in vivo and in vitro, *Science 240*, 640-642.

24. Ohshima, H., Tatemichi, M., and Sawa, T. (2003) Chemical basis of inflammation-induced carcinogenesis, *Arch Biochem Biophys 417*, 3-11.

25. Kitchin, K. T. (2001) Recent advances in arsenic carcinogenesis: modes of action, animal model systems, and methylated arsenic metabolites, *Toxicol Appl Pharmacol 172*, 249-261.

26. Beranek, D. T. (1990) Distribution of methyl and ethyl adducts following alkylation with monofunctional alkylating agents, *Mutat Res 231*, 11-30.

27. Morris, J. C. (1966) The acid ionization constant of HOCl from 5 to 35°, *J Phys Chem 70*, 3798-3805.

28. Fry, R. C., Begley, T. J., and Samson, L. D. (2005) Genome-wide responses to DNA-damaging agents, *Annu Rev Microbiol 59*, 357-377.

29. Loechler, E. L. (1994) A violation of the Swain-Scott principle, and not SN1 versus SN2 reaction mechanisms, explains why carcinogenic alkylating agents can form different proportions of adducts at oxygen versus nitrogen in DNA, *Chem Res Toxicol 7*, 277-280.

30. Singer, B., and Grunberger, D. (1983) *Molecular biology of mutagens and carcinogens*, Plenum Press, New York.

31. Hampton, M. B., Kettle, A. J., and Winterbourn, C. C. (1998) Inside the neutrophil phagosome: oxidants, myeloperoxidase, and bacterial killing, *Blood 92*, 3007-3017.

32. Suzuki, T., Masuda, M., Friesen, M. D., Fenet, B., and Ohshima, H. (2002) Novel products generated from 2'-deoxyguanosine by hypochlorous acid or a myeloperoxidase-H2O2-

Cl- system: identification of diimino-imidazole and amino-imidazolone nucleosides, *Nucleic Acids Res 30*, 2555-2564.

33. Winterbourn, C. C., and Kettle, A. J. (2000) Biomarkers of myeloperoxidase-derived hypochlorous acid, *Free Radic Biol Med 29*, 403-409.

34. Higashikawa, Y., Kazui, Y., Suzuki, S., and Ohtsuru, O. (2008) Arsenic speciation of arsine-exposed blood samples by high-performance liquid chromatography-inductively coupled plasma mass spectrometry and as-adduct, a possible indicator of AsH3 exposure, *J Anal Toxicol 32*, 344-348.

35. Hei, T. K., and Filipic, M. (2004) Role of oxidative damage in the genotoxicity of arsenic, *Free Radic Biol Med 37*, 574-581.

36. Motorin, Y., and Grosjean, H. (1999) Multisite-specific tRNA:m5C-methyltransferase (Trm4) in yeast Saccharomyces cerevisiae: identification of the gene and substrate specificity of the enzyme, *RNA 5*, 1105-1118.

37. Pintard, L., Lecointe, F., Bujnicki, J. M., Bonnerot, C., Grosjean, H., and Lapeyre, B. (2002) Trm7p catalyses the formation of two 2'-O-methylriboses in yeast tRNA anticodon loop, *EMBO J 21*, 1811-1820.

38. El Yacoubi, B., Lyons, B., Cruz, Y., Reddy, R., Nordin, B., Agnelli, F., Williamson, J. R., Schimmel, P., Swairjo, M. A., and de Crecy-Lagard, V. (2009) The universal YrdC/Sua5 family is required for the formation of threonylcarbamoyladenosine in tRNA, *Nucleic Acids Res 37*, 2894-2909.

39. Ellis, S. R., Morales, M. J., Li, J. M., Hopper, A. K., and Martin, N. C. (1986) Isolation and characterization of the TRM1 locus, a gene essential for the N2,N2-dimethylguanosine

modification of both mitochondrial and cytoplasmic tRNA in Saccharomyces cerevisiae, *J Biol Chem 261*, 9703-9709.

40. Begley, T. J., Rosenbach, A. S., Ideker, T., and Samson, L. D. (2002) Damage recovery pathways in Saccharomyces cerevisiae revealed by genomic phenotyping and interactome mapping, *Mol Cancer Res 1*, 103-112.

41. Birrell, G. W., Brown, J. A., Wu, H. I., Giaever, G., Chu, A. M., Davis, R. W., and Brown, J. M. (2002) Transcriptional response of Saccharomyces cerevisiae to DNA-damaging agents does not identify the genes that protect against these agents, *Proc Natl Acad Sci U S A 99*, 8778-8783.

42. Wohlgamuth-Benedum, J. M., Rubio, M. A., Paris, Z., Long, S., Poliak, P., Lukes, J., and Alfonzo, J. D. (2009) Thiolation controls cytoplasmic tRNA stability and acts as a negative determinant for tRNA editing in mitochondria, *J Biol Chem 284*, 23947-23953.

43. Agris, P. F. (1996) The importance of being modified: roles of modified nucleosides and Mg2+ in RNA structure and function, *Prog Nucleic Acid Res Mol Biol 53*, 79-129.

44. Sprinzl, M., and Vassilenko, K. S. (2005) Compilation of tRNA sequences and sequences of tRNA genes, *Nucleic Acids Res 33*, D139-140.

45. Johansson, M. J. O., and Byström, A. S. (2005) Transfer RNA modifications and modifying enzymes in Saccaromyces cerevisiae, in *Fine-tuning of RNA functions by modifications and editing.* (Grosjean, H., Ed.), pp 87-120, Springer-Verlag, Heidelberg, Germany.

46. Kotelawala, L., Grayhack, E. J., and Phizicky, E. M. (2008) Identification of yeast tRNA Um(44) 2'-O-methyltransferase (Trm44) and demonstration of a Trm44 role in sustaining levels of specific tRNA(Ser) species, *RNA 14*, 158-169.

47. Nguyen, V. C., Clelland, B. W., Hockman, D. J., Kujat-Choy, S. L., Mewhort, H. E., and Schultz, M. C. (2010) Replication stress checkpoint signaling controls tRNA gene transcription, *Nat Struct Mol Biol 17*, 976-981.

48. Gerber, A., Grosjean, H., Melcher, T., and Keller, W. (1998) Tad1p, a yeast tRNA-specific adenosine deaminase, is related to the mammalian pre-mRNA editing enzymes ADAR1 and ADAR2, *EMBO J 17*, 4780-4789.

49. Bjork, G. R., Jacobsson, K., Nilsson, K., Johansson, M. J., Bystrom, A. S., and Persson, O. P. (2001) A primordial tRNA modification required for the evolution of life?, *EMBO J 20*, 231-239.

50. Motorin, Y., and Helm, M. (2010) tRNA stabilization by modified nucleotides, *Biochemistry 49*, 4934-4944.

Chapter 4

Changes in composition of ribosome caused by *trm4*-deletion and by exposure to hydrogen peroxide

Abstract

As noted in Chapter 3, the relative level of 5-methylcytosine (m^5C) in the yeast *S. cerevisiae* tRNA increases after the cells are exposed to hydrogen peroxide and loss of tRNA m^5C-methyltransferase Trm4 reduces the survivability of cells under this stress. While m^5C is found in many species of tRNA, only a leucine tRNA for coding the codon UUG comprises this modification at the wobble position which may affect the translation efficiency of UUG. Intriguingly, *S. cerevisiae* contains many duplicated ribosomal genes with significant difference in usage of UUG. Through quantitative studies of homologous ribosomal proteins with liquid chromatogarpahy-coupled time-of-flight mass spectrometiry (LC-QTOF), we demonstrate that in relative to its homologue, the protein expression of a UUG-enriched gene *rpl22a* decreases in the absence of Trm4 and increases in H_2O_2-exposed cells. Moreover, exposing H_2O_2 to *trm4Δ* mutant does not lead to changes in relative level of Rpl22a. Also, only the gene *rpl22a* confers resistance to H_2O_2 but not *rpl22b*. These results support a model of which Trm4 and m^5C are involved in regulating the expression of homologous ribosomal proteins by modulating the translation efficiency of UUG.

Introduction

Modifications in tRNA are known to confer resistance to specific stresses but the underlying mechanisms are not well-studied (*1, 2*). Recently, Begley and coworkers have shown that a *S. cerevisiae* tRNA methyltransferase Trm9 confers resistance to DNA damage by

promoting the translation of a specific set of genes (*3*). The enzyme Trm9 catalyzes the last step of the formation of mcm^5U and mcm^5s^2U at the wobble position of $tRNA^{Arg}(mcm^5UCU)$ and $tRNA^{Glu}(mcm^5s^2UUC)$ respectively (*4, 5*). These two modifications modulate the efficiency of these two species of tRNA in translating their corresponding codon, AGA for $tRNA^{Arg}(mcm^5UCU)$ and GAA for $tRNA^{Glu}(mcm^5s^2UUC)$ (*6*). Through this mechanism, Trm9-catalyzed modifications on tRNA control the translation level of genes with high usage of AGA or GAA while many of them are associated with DNA damage responses (*3*). The studies suggest that modifications at wobble position of tRNA can affect the efficiency of translating specific codons and thus, they can be used as mechanisms of translational regulation in response to stress.

In chapter 3, differential patterns of changes in the spectrum of tRNA modifications are observed in the yeast *S. cerevisiae* exposed to four mechanistically distinct toxic agents, hydrogen peroxide, methyl methanesulfonate, sodium hypochlorite, and sodium arsenite, which suggests that responses to different stress involve different subsets of modifications. After exposing to H_2O_2, the levels of several modifications, including 5-methylcytosine (m^5C), increase and also, tRNA m^5C-methyltransferse Trm4 protects cells against this toxic agent; these observations strongly suggest that m^5C is involved in stress response to H_2O_2. In addition, this modification may be involved in a broad range of cellular responses as *trm4Δ* mutant is also sensitive to heat-shock, killer toxins, and various chemicals (*7-10*).

The modification m^5C is reported in at least 34 different species of tRNA and is located at position 34, 40, 48, and 49 (*11*). However, only a leucine tRNA for translating UUG on mRNA contains m^5C at the wobble position. As m^5C at wobble position has previously been demonstrated to promote the efficiency of translation (*12*), we then hypothesized that Trm4

modulates the translation of UUG by regulating the level of m^5C. To test this, we searched for DNA transcripts enriched in this specific codon, UUG, and found that many of them are encoding for ribosomal proteins while the others are mostly related to energy metabolism (Table 1).

Yeast ribosomes comprise 78 proteins in which 59 of them have two duplicated genomic copies. Even though the amino acid sequences of homologous ribosomal proteins are very similar, UUG codon usage patterns of the two proteins can be significantly different (Table 4-2). Homologous ribosomal genes were arose from a whole genome duplication; while most duplicated genes were eliminated as they were redundant, some of them were retained by evolving to new functions (*13*). Indeed, evidence supports that ribosomal homologues play specific biological roles; for instances, the lack of specific ribosomal homologue leads to defects in ribosomal assembly (*14*), sporulation (*15*), actin organization (*16*), and bud-site selection (*17*). Komili and coworkers have provided insights in mechanistic roles of ribosomal homologous proteins by demonstrating that a specific subset of ribosomal homologues is necessary for the translation of localized ASH1 mRNA during bud tip formation (*18*). These observations led us to hypothesize that Trm4 regulates the protein composition of ribosome for adapting changes in cellular conditions.

Systematic Name	#UUG	Freq. of UUG	Protein Functions
YLR029C	13	1	Protein component of the large (60S) ribosomal subunit
YGL103W	9	1	Ribosomal protein of the large (60S) ribosomal subunit
YJL189W	2	1	Protein component of the large (60S) ribosomal subunit
YMR230W	9	1	Protein component of the small (40S) ribosomal subunit
YLR110C	9	1	Cell wall mannoprotein
YLR061W	7	1	Protein component of the large (60S) ribosomal subunit
YPR043W	3	1	Protein component of the large (60S) ribosomal subunit
YDR500C	2	1	Protein component of the large (60S) ribosomal subunit
YLR185W	2	1	Protein component of the large (60S) ribosomal subunit
YEL034W	11	1	Translation elongation factor eIF-5A
YOL040C	9	1	Protein component of the small (40S) ribosomal subunit
YPL249C-A	6	1	Protein component of the large (60S) ribosomal subunit
YHR072W-A	5	1	Constituent of small nucleolar ribonucleoprotein particles
YER131W	4	1	Protein component of the small (40S) ribosomal subunit
YFL014W	3	1	Plasma membrane localized protein
YGR192C	20	0.95	Glyceraldehyde-3-phosphate dehydrogenase, isozyme 3
YJR009C	20	0.95	Glyceraldehyde-3-phosphate dehydrogenase, isozyme 2
YJL052W	19	0.95	Glyceraldehyde-3-phosphate dehydrogenase, isozyme 1
YHL033C	19	0.95	Ribosomal protein L4 of the large (60S) ribosomal subunit
YBR181C	19	0.95	Protein component of the small (40S) ribosomal subunit
YPL090C	19	0.95	Protein component of the small (40S) ribosomal subunit
YLR075W	16	0.94	Protein component of the large (60S) ribosomal subunit
YBR031W	26	0.93	Protein component of the large (60S) ribosomal subunit
YDR012W	26	0.93	Protein component of the large (60S) ribosomal subunit
YDR064W	13	0.93	Protein component of the small (40S) ribosomal subunit
YJR123W	13	0.93	Protein component of the small (40S) ribosomal subunit
YHR174W	35	0.92	Enolase II
YJR047C	11	0.92	Translation elongation factor eIF-5A
YAL038W	32	0.91	Pyruvate kinase
YDR418W	10	0.91	Protein component of the large (60S) ribosomal subunit
YLR044C	49	0.91	Major of three pyruvate decarboxylase isozymes
YGL123W	19	0.90	Protein component of the small (40S) subunit
YLL045C	19	0.90	Ribosomal protein L4 of the large (60S) ribosomal subunit
YGR254W	36	0.90	Enolase I
YKL180W	9	0.90	Protein component of the large (60S) ribosomal subunit
YJL177W	9	0.90	Protein component of the large (60S) ribosomal subunit
YBR189W	18	0.90	Protein component of the small (40S) ribosomal subunit
YGL147C	9	0.90	Protein component of the large (60S) ribosomal subunit

Table 4-1. List of *S. cerevisiae* genes with transcripts with highest usage frequency of UUG. This table includes the systematic name, the number of UUG, the UUG usage frequency, and a description of the function of gene product. UUG usage frequency is the number of UUG codon in a transript divided by the total number of leucine that its protein is comprised of. Only genes with UUG usage frequency above 0.9 are listed.

A

Gene Name	#TTG	TTG frequency	Different in #TTG	Difference in TTG frequency	Gene Name	#TTG	TTG frequency	Different in #TTG	Difference in TTG frequency
RPL1A	22	0.88	0	0.00	RPL23A	5	0.56	1	0.11
RPL1B	22	0.88			RPL23B	4	0.44		
RPL2A	13	0.81	3	0.19	RPL24A	6	0.86	0	0.00
RPL2B	10	0.63			RPL24B	6	0.86		
RPL3	18	0.86	--	--	RPL25	9	0.82	--	--
RPL4A	26	0.93	0	0.00	RPL26A	9	0.64	0	0.00
RPL4B	26	0.93			RPL26B	9	0.64		
RPL5	17	0.74	--	--	RPL27A	5	0.71	0	0.12
RPL6A	13	0.68	2	0.07	RPL27B	5	0.83		
RPL6B	15	0.75			RPL28	9	1.00	--	--
RPL7A	17	0.85	0	0.00	RPL29	2	0.67	--	--
RPL7B	17	0.85			RPL30	11	0.85	--	--
RPL8A	19	0.95	0	0.05	RPL31A	6	0.55	0	0.00
RPL8B	19	0.90			RPL31B	6	0.55		
RPL9A	9	0.90	1	0.01	RPL32	7	0.78	--	--
RPL9B	8	0.89			RPL33A	5	0.83	1	0.17
RPL10	16	0.94	--	--	RPL33B	4	0.67		
RPL11A	8	0.73	1	0.09	RPL34A	4	0.80	0	0.00
RPL11B	7	0.64			RPL34B	4	0.80		
RPL12A	6	0.55	4	0.36	RPL35A	11	0.85	1	0.08
RPL12B	10	0.91			RPL35B	10	0.77		
RPL13A	5	0.45	4	0.36	RPL36A	4	0.67	2	0.33
RPL13B	9	0.82			RPL36B	6	1.00		
RPL14A	7	0.64	0	0.00	RPL37A	2	1.00	0	0.00
RPL14B	7	0.64			RPL37B	2	1.00		
RPL15A	13	1.00	5	0.38	RPL38	8	0.89	--	--
RPL15B	8	0.62			RPL39	2	1.00	--	--
RPL16A	9	0.50	5	0.32	RPL40A	12	0.86	2	0.14
RPL16B	14	0.82			RPL40B	10	0.71		
RPL17A	9	0.90	0	0.00	RPL41A	0	0.00	0	0.00
RPL17B	9	0.90			RPL41B	0	0.00		
RPL18A	11	0.73	1	0.07	RPL42A	7	1.00	1	0.14
RPL18B	10	0.67			RPL42B	6	0.86		
RPL19A	9	0.56	1	0.06	RPL43A	3	1.00	2	0.67
RPL19B	10	0.63			RPL43B	1	0.33		
RPL20A	8	0.89	2	0.29	RPP0	21	0.84	--	--
RPL20B	6	0.60			RPP1A	9	0.82	5	0.32
RPL21A	4	0.50	2	0.36	RPP1B	4	0.50		
RPL21B	6	0.86			RPP2A	5	0.50	0	0.06
RPL22A	7	1.00	4	0.63	RPP2B	5	0.56		
RPL22B	3	0.38							

B

Gene Name	#TTG	TTG frequency	Different in #TTG	Difference in TTG frequency	Gene Name	#TTG	TTG frequency	Different in #TTG	Difference in TTG frequency
RPS0A	9	0.47	5	0.23	RPS17A	13	0.87	0	0.00
RPS0B	14	0.70			RPS17B	13	0.87		
RPS1A	16	0.73	3	0.10	RPS18A	11	0.73	1	0.07
RPS1B	19	0.83			RPS18B	10	0.67		
RPS2	19	0.90	--	--	RPS19A	6	0.75	1	0.13
RPS3	12	0.63	--	--	RPS19B	7	0.88		
RPS4A	16	0.64	2	0.08	RPS20	5	0.83	--	--
RPS4B	18	0.72			RPS21A	4	0.57	1	0.14
RPS5	13	0.93	--	--	RPS21B	5	0.71		
RPS6A	19	0.95	0	0.00	RPS22A	8	0.80	2	0.25
RPS6B	19	0.95			RPS22B	6	0.55		
RPS7A	18	0.86	4	0.19	RPS23A	10	0.77	0	0.00
RPS7B	14	0.67			RPS23B	10	0.77		
RPS8A	5	0.50	0	0.00	RPS24A	3	0.18	3	0.49
RPS8B	5	0.50			RPS24B	6	0.67		
RPS9A	12	0.60	6	0.30	RPS25A	4	0.44	2	0.22
RPS9B	18	0.90			RPS25B	6	0.67		
RPS10A	7	0.78	2	0.22	RPS26A	2	0.50	2	0.50
RPS10B	9	1.00			RPS26B	4	1.00		
RPS11A	3	0.60	0	0.00	RPS27A	3	0.33	2	0.22
RPS11B	3	0.60			RPS27B	5	0.56		
RPS12	11	0.73	--	--	RPS28A	3	0.50	1	0.17
RPS13	13	0.93	--	--	RPS28B	4	0.67		
RPS14A	4	0.67	0	0.10	RPS29A	1	0.50	0	0.00
RPS14B	4	0.57			RPS29B	1	0.50		
RPS15	9	1.00	--	--	RPS30A	2	0.50	0	0.00
RPS16A	7	0.64	1	0.09	RPS30B	2	0.50		
RPS16B	8	0.73			RPS31	11	0.79	--	--

Table 4-2. Usage of TTG of *S. cerevisiae* ribosomal protein genes for proteins in **(A)** large subunit and in **(B)** small subunit. The number of TTG used for coding leucine (#TTG) and the proportion of leucine coded by TTG (TTG frequency) are included in this table. For the genes having a homologue, the differences in #TTG and in TTG frequency are also listed.

In the following studies, we sought to determine whether Trm4 is involved in regulating the levels of homologous proteins in ribosomes. We showed that the translation level of ribosomal protein Rpl22a decreases relative to its homologue Rpl22b in the *trm4* knockout, the *rpl22a* gene has a higher usage frequency of TTG. Also, *rpl22a* confers resistance to hydrogen peroxide toxicity but *rpl22b* does not. Further, we showed that the relative level of Rpl22a protein to Rpl22b protein increases after cellular exposure to hydrogen peroxide only when Trm4 is present. These results are consistent with the hypothesis that Trm4 confers resistance to stress by regulating the translation of homologous ribosomal proteins, which is a novel pathway of stress response.

Materials and Methods

Materials. All chemicals and reagents were of the highest purity available and were used without further purification. Hydrogen peroxide, trypsin, ammonium chloride, magnesium chloride, potassium chloride, magnesium acetate, ammonium acetate, dithiothreitol, and glucose were purchased from Sigma Chemical Co. (St. Louis, MO). Yeast extract and peptone were purchased from Biomed Diagnostics, Inc. (White City, OR). Tris-acetate was purchased from USB Corp. (Cleveland, OH). HEPES was purchased from EM Science (Darmstadt, Germany). Micron YM10 filters were purchased from PALL Corp. (Port Washington, NY). HPLC-grade water and acetonitrile were purchased from Mallinckrodt Baker (Phillipsburg, NJ). Biorad Protein Assay was purchased from Biorad laboratories (Hercules, CA). All strains of *S. cerevisiae* BY4741 were purchased from American Type Culture Collections (Manassas, VA).

Exposure of *S. cerevisiae*. Cultures of wild-type, *rpl16aΔ*, *rpl16bΔ*, *rpl22aΔ*, and *rpl22bΔ* strains of *S. cerevisiae* BY4741 were grown to mid-log phase. A final concentration of 2 mM hydrogen peroxide was then added into each culture and cells were harvested after 3 hours by centrifugation at 8000× g for 15 minutes. The H_2O_2 sensitivity of these strains of yeast was also assessed by exposing each mid-log phase culture to 5 mM of hydrogen peroxide; after 1 hr, cells were plated on YPD agar plate to determine the viability.

Isolation of ribosome. Approximately 10^{10} cells were resuspended in 10 mL of the lysis buffer with 50 mM Tris-acetate, 50 mM ammonium chloride, 12 mM magnesium chloride, and 1 mM dithiothreitol, pH 7.0. Cells were then lyzed mechanically by bead-beating. Lysate was centrifuged at 10000x g for 10 minutes and the supernatant was collected to repeat the centrifugation two more times to remove all particulates. The supernatant was layered over 2.5 mL of a solution with 1 M sucrose, 20 mM HEPES, 500 mM KCl, 2.5 mM magnesium acetate, and 2 mM dithiothreitol, pH 7.4 and centrifuged for 110 minutes at 60000 rpm in a Beckman 70 Ti rotor. Supernatant was removed and the pellet of ribosomes was resuspended in 1.5 mL of a digestion buffer with 100 mM ammonium acetate, pH 8.5. The samples were concentrated by centrifuging on a YM10 filter and re-diluted with the digestion buffer for 5 times to remove the remaining salts. Approximately 300 μg of ribosome was obtained based on the results of Biorad Protein Assay.

Identification of ribosomal proteins. An amount of 1 μg of proteomics-grade trypsin was added into 50 μg of ribosome in 200 μL of the digestion buffer (100 mM ammonium acetate

solution, pH 8.5). Samples were incubated at 37 °C for 12 hours before dried by lyophilization and resuspended in 100 µL of a 0.1% formic acid solution. Roughly 2.5 µg (5 µL) of peptide products from tryptic digestion were resolved with an Agilent ZORBAX 300SB-C18 column (100 × 0.3 mm, 3µ particle size) eluted with the following gradient of acetonitrile in 0.1% formic acid at a flow rate of 20 µL/min and 45 °C: 0-25 min, 1-30%; 25-30 min, 30-60%; 30-31 min, 60-95%; 31-36 min, 95%. The HPLC column was coupled to an Agilent 6510 QTOF LC/MS Mass spectrometer with an electrospray ionization source. The mass spectrometer was operated in positive ion mode to scan for ions within the range of m/z 100 to m/z 1700 at an acquisition rate of 1.4 spectrum/second with the following parameters for voltages and source gas: fragmentor voltage, 110 V; gas temperature: 300 °C; gas flow: 5 L/min; nebulizer: 20 psi; and capillary voltage: 3500 V. Compounds detected by the mass spectrometer were identified using the molecular feature extraction function in the Agilent MassHunter Workstation Software with the following filter parameters: minimum peak height: 300 counts; and maximum charge state: 2. The lists of compounds were then analyzed with the Agilent Spectrum Mill mass spectrometric data analysis software to identify proteins based upon peptide mass fingerprints. A search was performed against the NCBInr protein database for *Sacchromyces cerevisiae* with no protein modifications and missed cleavage considered. The search parameters were set with a mass tolerance of 20 ppm and protein coverage of at least 25%.

Identification of peptides. Samples of tryptic-digested peptides were resolved with the same HPLC method as described in the above section. The HPLC column was coupled to the same mass spectrometer that was operating in positive ion, targeted MS/MS mode with a

constant collision energy of 15 V to monitor ions within the range of m/z 100 to m/z 3000; the acquisition rates for MS scan and MS/MS scan were both 1.4 spectrum/second and all the parameters for voltages and source gas are the same as in the LC/MS analysis for characterizing ribosomal proteins. The peptides monitored in MS/MS analysis are described in Figure 4-5.

Transcription level assay. Total RNA was isolated from *S. cerevisiae* BY4741 using the Qiagen RNeasy Mini kit. An amount of 100 ng of total RNA was used to perform real-time quantitative PCR with Applied Biosystems Power SYBR Green RNA-to-C_T kit and an Applied Biosystems 7900HT Fast Real-Time PCR System to determine the relative transcription levels of ribosomal protein genes *rpl16a*, *rpl16b*, *rpl22a*, and *rpl22b* with *act1* chosen as a housekeeping gene for normalization. Primer sequences are listed in Table 4-3. The $\Delta\Delta C_T$ method was used to compare the transcription levels in different samples (*19*).

Gene	Forward (5' to 3')	Reverse (5' to 3')
act1	GAAAAGATCTGGCATCATACCTTC	AAAACGGCTTGGATGGAAAC
rpl16a	AGGTCGTTTAGCTTCCGTTGTTGCT	GCGGCCTTACCACGAGCAGT
rpl16b	GTTGGGTCGTTTGGCCTCCACTA	GCCTTACCACGGGCGGTCTT
rpl22a	AGATTGCCAAGACCTTTACCGTCGA	CCATCTTCAGTGACAGTGACAGCGT
rpl22b	AAACGGAGTCTTCGATCCGGCTT	GTCAGCATCTTCAGGGGTGACTTGA

Table 4-3. Sequence of primers for RT-qPCR.

Results

Identification of ribosomal proteins. As the mass of ribosomal complex is significantly larger than any other biological macromolecules, ultracentrifugation can isolate ribosomes from cell lysate to high purity (*20*). Ribosomes were digested by trypsin to peptide fragments before analyzed with a liquid chromatographic-mass spectrometric approach. Compounds detected by high mass accuracy mass spectrometry were compared to theoretical tryptic fragments from proteins in the yeast protein database. From this analysis, a total of 39 proteins were identified consistently in three biological replicates (Table 4-4). Either because the two homologous proteins have identical amino acid sequence or the detected tryptic peptides did not cover the regions with difference, we could not distinguish the proteins from 9 pairs of homologous genes. These proteins include Rpl9a/b, Rpl11a/b, Rpl22a/b, Rps1a/b, Rps4a/b, Rps9a/b, Rps17a/b, Rps25a/b, and Rps28a/b. Also, we were able to identify Rpl2b, Rpl15a, Rpl18b, Rpl19b, Rpl20a, Rpl23a, Rpl27a, Rpl35a, Rps19b, Rps24a, and Rps26b but not their homologues. Some ribosomal proteins with no homologues were also identified, including Rpl32, Rps2, Rps3, and Rps13. For proteins that both homologues were identified, there were Rpl6a and Rpl6b, Rpl7a and Rpl7b, Rpl16a and Rpl16b, Rpl22a and Rpl22b, Rpl33a and Rpl33b, Rpl36a and Rpl36b, and Rps7a and Rps7b. These 7 pairs of homologous ribosomal proteins served as the basis for studying the changes in ratios of homologues.

	Protein Coverage (%)			Mass Error Mean (Std. Dev.) (ppm)		
Proteins	**Expt. 1**	**Expt. 2**	**Expt. 3**	**Expt. 1**	**Expt. 2**	**Expt. 3**
RPL2B	46	38	40	-5.5 (5.8)	-5.3 (6.4)	-6.1 (6.3)
RPL6A	37	40	32	1.2 (6.1)	-3.3 (6.6)	-2.7 (7.3)
RPL6B	48	44	36	-5.9 (5.9)	-3.1 (4.7)	-2.1 (7.0)
RPL7A	40	35	40	1.1 (6.5)	-1.8 (4.5)	-2.5 (7.0)
RPL7B	40	35	40	0.8 (6.6)	-2.0 (4.6)	-2.8 (7.1)
RPL9A/B	50	41	41	-2.1 (8.2)	-3.3 (8.3)	-3.1 (10.7)
RPL11A/B	28	31	25	1.5 (3.2)	-0.9 (4.4)	-1.8 (2.6)
RPL15A	31	33	33	0.3 (2.3)	2.3 (6.5)	-0.3 (8.6)
RPL16A	44	37	44	-2.6 (8.7)	-2.5 (8.4)	-2.1 (7.6)
RPL16B	45	42	39	-1.8 (8.5)	-3.9 (8.3)	-3.8 (8.6)
RPL18B	41	38	46	-1.3 (8.2)	-2.5 (8.3)	-2.4 (7.0)
RPL19B	29	32	63	-4.3 (6.3)	-2.7 (9.3)	-4.4 (7.3)
RPL20A	51	47	48	1.8 (7.3)	1.9 (7.3)	-0.6 (5.1)
RPL21A/B	46	46	46	-3.7 (4.8)	-3.2 (6.1)	-2.4 (5.5)
RPL22A	35	68	54	1.7 (12.3)	0.2 (6.6)	3.3 (9.4)
RPL22B	49	50	50	0.2 (5.8)	1.1 (6.2)	1.8 (10.8)
RPL23A	55	48	55	-0.4 (6.6)	-0.5 (9.4)	-1.1 (8.0)
RPL27A	46	46	43	-0.4 (9.4)	-2.6 (8.7)	-4.4 (6.5)
RPL32	46	56	53	0.1 (4.2)	0.5 (6.2)	-1.2 (1.2)
RPL33A	49	44	49	0.7 (8.8)	-5.3 (10.2)	-0.8 (8.5)
RPL33B	49	44	49	0.7 (8.8)	-5.3 (10.2)	-0.8 (8.5)
RPL35A	30	37	37	-0.3 (6.2)	-4.8 (5.0)	-4.2 (5.5)
RPL36A	52	52	39	-5.3 (5.7)	-2.4 (8.3)	-0.1 (1.9)
RPL36B	52	52	52	-4.8 (6.1)	-2.0 (8.4)	-4.8 (6.1)
RPS1A/B	45	36	36	1.4 (7.5)	-4.0 (5.6)	-0.9 (5.9)
RPS2	38	38	36	-0.4 (10)	-4.7 (4.5)	-1.6 (8.7)
RPS3	48	56	56	-2.7 (4.7)	-3.5 (4.8)	-4.0 (4.5)
RPS4A/B	59	57	63	-1.5 (8.3)	-2.1 (8.2)	-3.7 (9.3)
RPS7A	64	64	66	-0.5 (5.8)	-1.5 (7.0)	-2.5 (7.1)
RPS7B	68	64	66	-2.3 (6.6)	-5.1 (6.6)	-5.6 (6.6)
RPS9A/B	54	54	54	-0.5 (7.5)	-1.4 (7.2)	-1.8 (6.9)
RPS13	68	62	58	-2.1 (4.0)	-2.8 (5.8)	-3.5 (3.7)
RPS17A/B	62	52	52	-0.6 (10.3)	-2.3 (7.4)	-5.5 (8.6)
RPS19B	59	67	63	-4.2 (6.9)	-3.8 (6.9)	-4.4 (7.3)
RPS20	52	52	52	-0.6 (7.1)	-3.5 (4.3)	-2.0 (5.4)
RPS24A	36	36	36	0.4 (1.4)	-0.8 (1.6)	-1.2 (1.4)
RPS25A/B	52	52	52	-1.0 (5.0)	-1.1 (6.4)	-1.3 (7.3)
RPS26A	49	42	50	2.3 (5.9)	-1.8 (7.3)	-4.6 (5.1)
RPS28A/B	70	58	64	-2.3 (11.7)	-3.6 (7.6)	-3.4 (5.6)

Table 4-4. List of ribosomal proteins identified from LC/MS analysis of tryptic peptides. Data was obtained from three biological replicates. The table contains the percent of amino acid residues covered by the detected peptides and the average mass difference between the MS detections and theoretical values for all detected peptides of each protein.

Characterization of unique peptides from ribosomal proteins. Amino acid sequences of homologous ribosomal proteins are nearly identical. Thus, most tryptic fragments from the two ribosomal homologues are the same. Therefore, instead of monitoring all peptides from each ribosomal protein, the quantification of each ribosomal protein was based on mass spectrometric signal intensities from a unique peptide. These peptides are listed in Table 4-5. Even though the mass values detected by mass spectrometer were highly accurate (error < 10 ppm), identity of peptides can still be mis-assigned as peptides with different amino acid sequence and even different amino acid composition can have the same mass. For confirmation, these unique peptides were subjected to targeted MS-MS analysis to determine their amino acid sequence based upon the detection of b- and y- ions formed in collision-induced dissociation (CID). CID mass spectra of the 14 unique peptides, each from one protein of the 7 pairs of ribosomal homologues, are shown in Figure 4-1.

Frequency of UUG	# UUG	Protein	Sequence (location of the peptide)	Theoretical m/z of $[M+2H]^{2+}$ ion
0.68	13	RPL6A	EANLFPEQQNK (118 to 128)	659.3198
0.75	15	RPL6B	EANLFPEQQTK (118 to 128)	652.8223
0.85	17	RPL7A	TAEQVAAER (22 to 30)	487.7433
0.85	17	RPL7B	TAEQIAAER (22 to 30)	494.7513
0.50	9	RPL16A	VASANATAAESDVAK (178 to 192)	702.8463
0.82	14	RPL16B	VSSASAAASESDVAK (177 to 191)	690.3303
1.00	7	RPL22A	LAFYQVTPEEDEEEDEE (105 to 121)	1036.4233
0.38	3	RPL22B	LVFYQVTPEDADEEEDDE (105 to 121)	1071.9418
0.83	5	RPL33A	IEGVATPQDAQFYLGK (32 to 47)	868.9408
0.67	4	RPL33B	IEGVATPQEAQFYLGK (32 to 47)	875.9488
0.67	4	RPL36A	VTSMTPARK (17 to 25)	466.2443
1.00	6	RPL36B	VTQMTPARK (17 to 25)	486.7573
0.86	18	RPS7A	ILEDLVFPTEIVGK (125 to 138)	786.9423
0.67	14	RPS7B	VLEDMVFPTEIVGK (125 to 138)	788.9128

Table 4-5. The list of peptides selected for quantification. This table contains the UUG usage frequency of each gene transcript, the number of UUG, the name of protein that each peptide is originated, the sequence of the peptides, the position of the peptide, and the m/z value of the ion of these peptides.

A

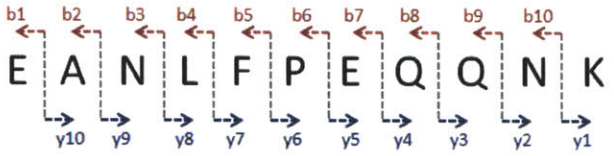

	RPL6A			
	b-ions		y-ions	
	Expected mass	Detected mass	Expected mass	Detected mass
1	--		147.1128	--
2	201.0870	201.0902	261.1557	--
3	315.1299	315.1233	372.1878 ($y3-NH_3$)	372.1846
4	428.2140	428.1977	517.2729	517.2711
5	575.2824	575.2824	646.3155	--
6	672.3352	--	743.3682	743.3624
7	801.3777	--	890.4357	890.4251
8	929.4363	--	1003.521	--
9	1057.495	--	1117.564	--
10	1171.538	--	1188.601	--
11	--	--	--	--

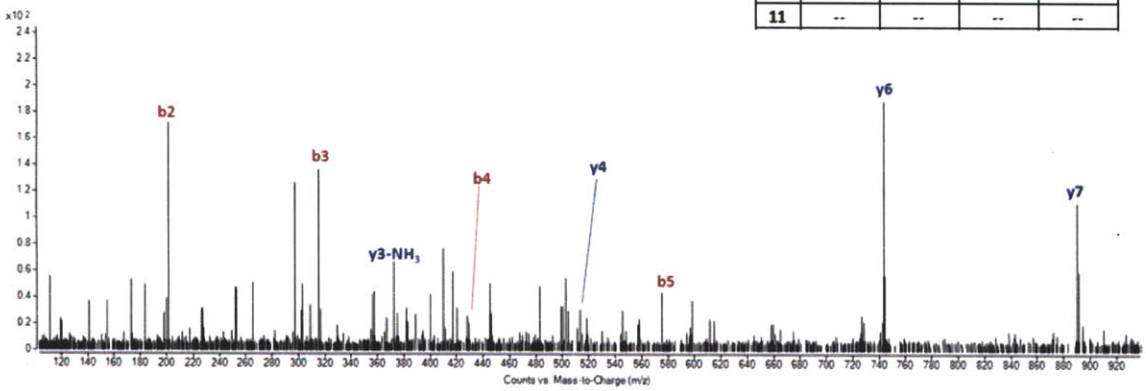

B

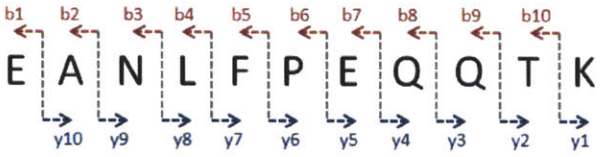

	RPL6B			
	b-ions		y-ions	
	Expected mass	Detected mass	Expected mass	Detected mass
1	--	--	147.1128	--
2	201.0870	201.0818	248.1605	248.1659
3	315.1299	315.1357	376.2191	376.2193
4	428.2140	428.2057	504.2776	504.2426
5	575.2824	575.2701	633.3202	633.3251
6	672.3352	--	730.3730	730.3743
7	801.3777	--	877.4414	877.4486
8	929.4363	--	990.5255	--
9	1057.495	--	1104.568	1104.575
10	1158.543	--	1175.606	--
11	--	--	--	--

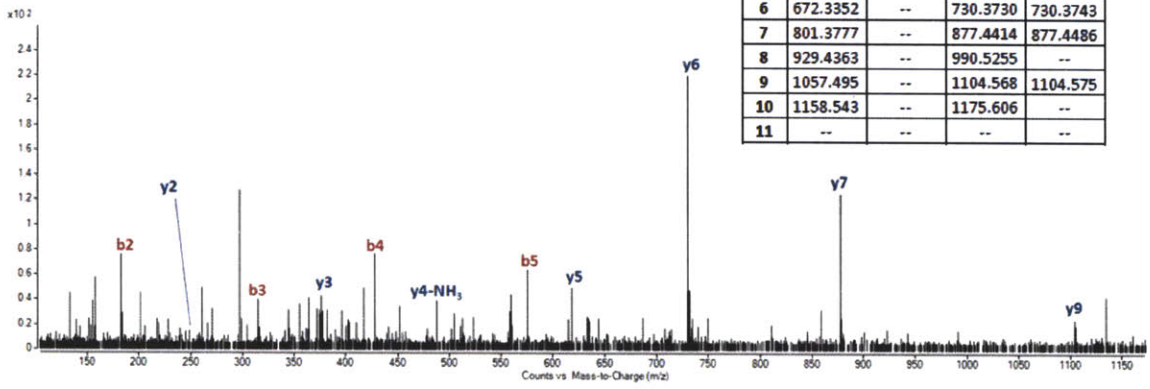

C

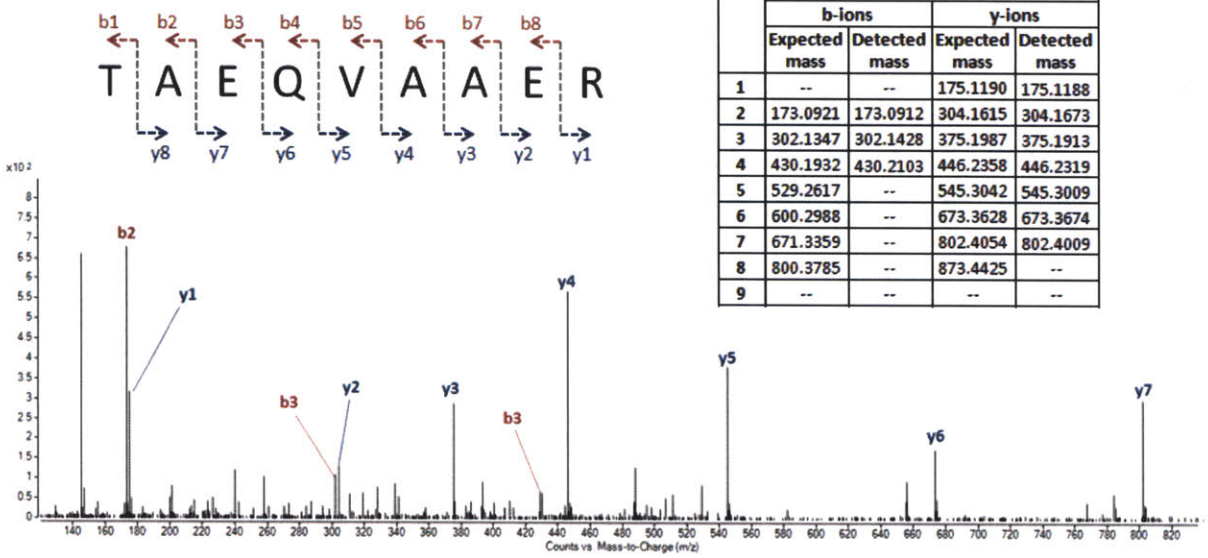

	RPL7A			
	b-ions		y-ions	
	Expected mass	Detected mass	Expected mass	Detected mass
1	--	--	175.1190	175.1188
2	173.0921	173.0912	304.1615	304.1673
3	302.1347	302.1428	375.1987	375.1913
4	430.1932	430.2103	446.2358	446.2319
5	529.2617	--	545.3042	545.3009
6	600.2988	--	673.3628	673.3674
7	671.3359	--	802.4054	802.4009
8	800.3785	--	873.4425	--
9	--	--	--	--

D

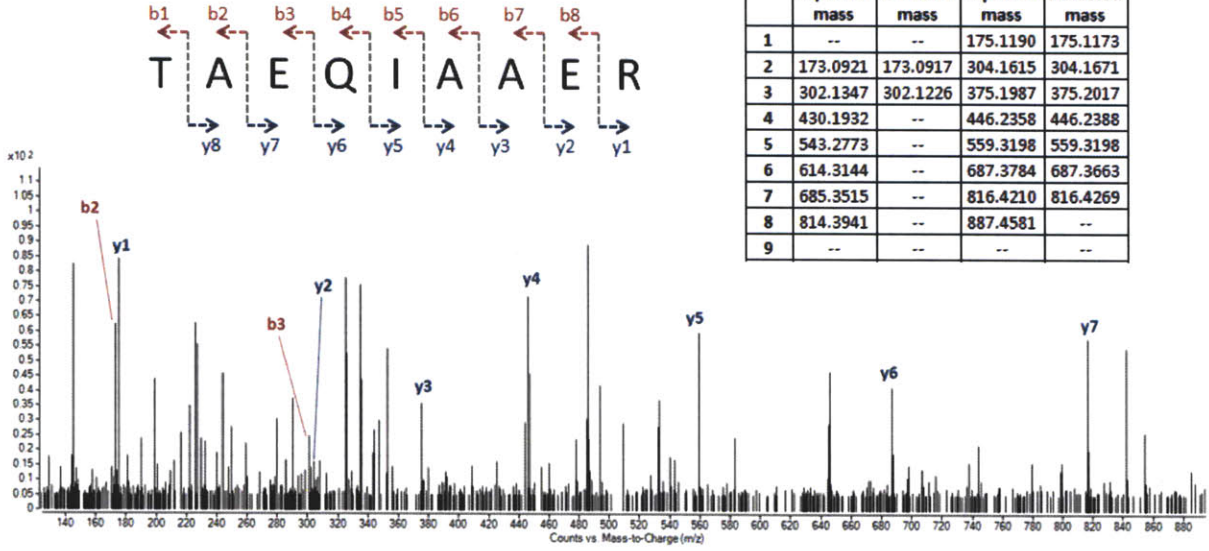

	RPL7B			
	b-ions		y-ions	
	Expected mass	Detected mass	Expected mass	Detected mass
1	--	--	175.1190	175.1173
2	173.0921	173.0917	304.1615	304.1671
3	302.1347	302.1226	375.1987	375.2017
4	430.1932	--	446.2358	446.2388
5	543.2773	--	559.3198	559.3198
6	614.3144	--	687.3784	687.3663
7	685.3515	--	816.4210	816.4269
8	814.3941	--	887.4581	--
9	--	--	--	--

E

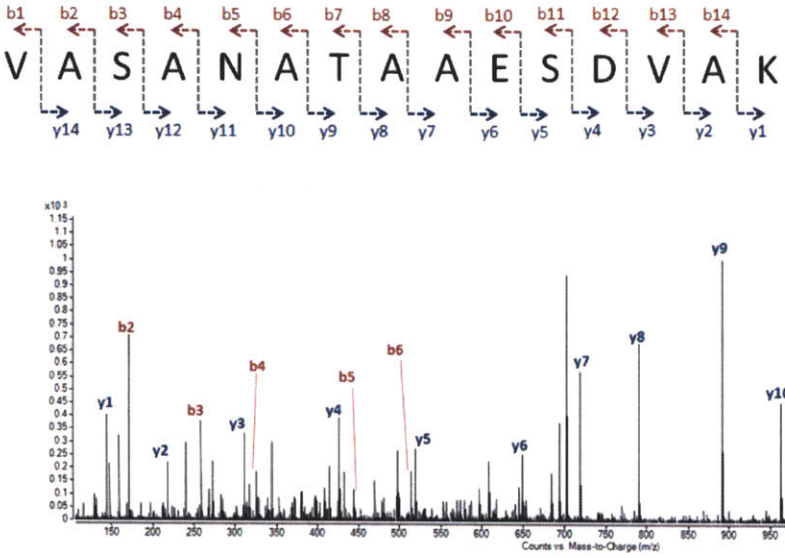

	RPL16A			
	b-ions		y-ions	
	Expected mass	Detected mass	Expected mass	Detected mass
1	--	--	147.1128	147.1103
2	171.1128	171.1102	218.1499	218.1502
3	258.1448	258.1402	317.2183	317.2167
4	329.1819	329.1748	432.2453	432.2375
5	443.2249	443.2135	519.2773	519.2664
6	514.2620	514.2597	648.3199	648.3131
7	615.3097	--	719.3570	719.3486
8	686.3468	--	790.3941	790.3827
9	757.3839	--	891.4418	891.4268
10	886.4265	--	962.4789	962.4716
11	973.4585	--	1076.522	1076.412
12	1088.486	--	1147.559	1147.557
13	1187.554	--	1234.591	--
14	1258.5910	--	1305.628	--
15	--	--	--	--

F

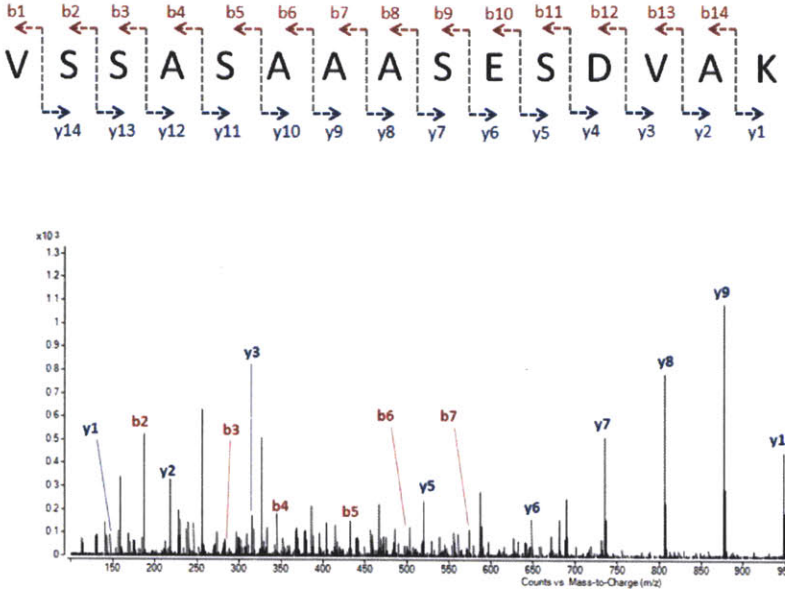

	RPL16B			
	b-ions		y-ions	
	Expected mass	Detected mass	Expected mass	Detected mass
1	--	--	147.1128	147.1074
2	187.1077	187.1054	218.1499	218.1457
3	274.1397	274.1341	317.2183	317.2075
4	345.1769	345.172	432.2453	--
5	432.2089	432.2041	519.2773	519.2682
6	503.2460	503.2423	648.3199	648.3192
7	574.2831	574.2731	735.3519	735.3468
8	645.3202	--	806.3890	806.3727
9	732.3523	--	877.4262	877.4169
10	861.3949	--	948.4633	948.4472
11	948.4269	--	1035.495	1035.476
12	1063.454	--	1106.532	1106.517
13	1162.522	--	1193.564	1193.561
14	1233.559	--	1280.597	1280.629
15	--	--	--	--

G

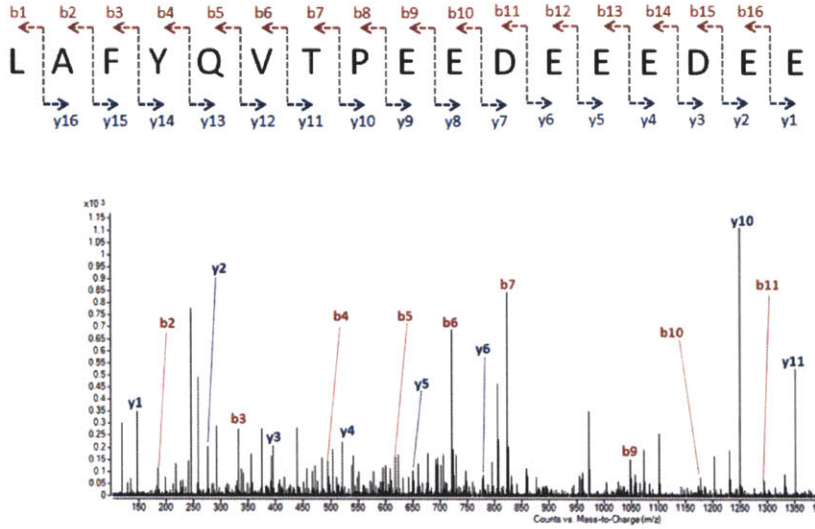

	RPL22A			
	b-ions		y-ions	
	Expected mass	Detected mass	Expected mass	Detected mass
1	--	--	148.0604	148.0576
2	185.1285	185.1251	277.1030	277.0992
3	332.1969	332.1974	392.1300	392.1257
4	495.2602	495.2576	521.1726	521.1600
5	623.3188	623.3119	650.2152	650.2152
6	722.3872	722.3821	779.2577	779.2301
7	823.4349	823.4325	894.2874	--
8	920.4876	--	1023.327	--
9	1049.530	1049.528	1152.370	--
10	1178.573	1178.583	1249.423	1249.415
11	1293.600	1293.584	1350.470	1350.466
12	1422.642	1422.601	1449.539	--
13	1551.685	1551.671	1577.597	--
14	1680.728	1680.718	1740.661	--
15	1795.755	1795.767	1887.729	--
16	1924.797	--	1958.766	--
17	--	--	--	--

H

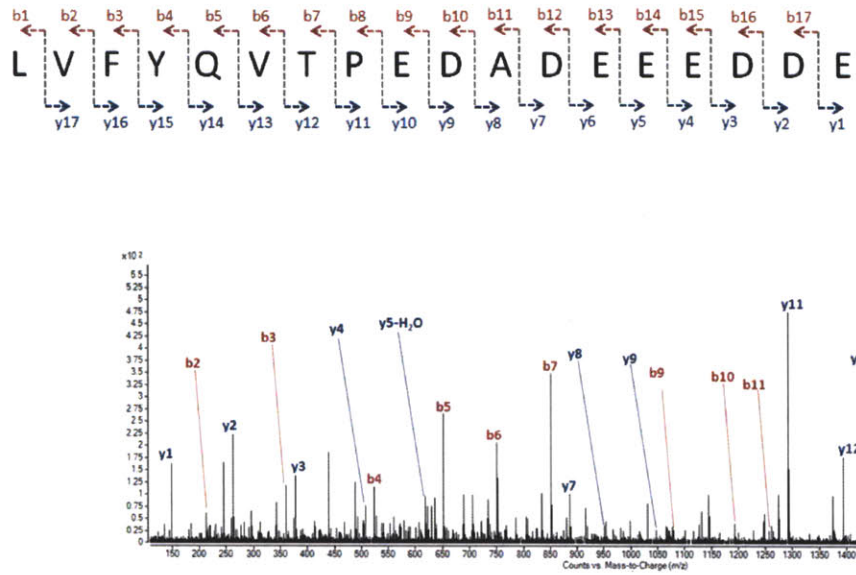

	RPL22B			
	b-ions		y-ions	
	Expected mass	Detected mass	Expected mass	Detected mass
1	--	--	148.0604	148.0661
2	213.1598	213.1677	263.0874	263.0825
3	360.2282	360.2146	378.1143	378.124
4	523.2915	523.2985	507.1569	507.1633
5	651.3501	651.358	618.1889 (y5-H_2O)	618.1894
6	750.4185	750.4256	765.2421	--
7	851.4662	851.4692	880.2690	880.2449
8	948.5189		951.3062	951.3154
9	1077.562	1077.576	1066.333	1066.341
10	1192.589	1192.59	1195.376	--
11	1263.626	--	1292.429	--
12	1378.653	--	1393.476	--
13	1507.695	--	1492.545	--
14	1636.738	1636.738	1620.603	--
15	1765.780	1765.831	1783.667	--
16	1880.807	--	1930.735	--
17	1995.834	--	2029.803	--
18	--	--	--	--

I

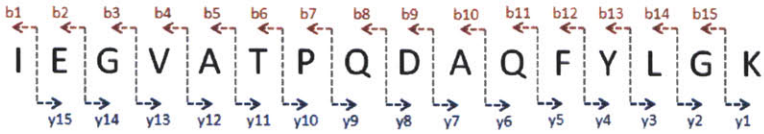

	RPL33A			
	b-ions		y-ions	
	Expected mass	Detected mass	Expected mass	Detected mass
1	--	--	147.1128	--
2	243.1339	243.1356	204.1343	204.1336
3	300.1554	300.1547	317.2183	317.2199
4	399.2238	399.2216	480.2817	480.2965
5	470.2609	470.2603	627.3501	627.3487
6	571.3086	571.3072	755.4087	755.4039
7	668.3614	--	826.4458	826.4454
8	796.4199	--	941.4727	941.4765
9	911.4469	--	1069.531	--
10	982.4840	--	1166.584	1166.585
11	1110.543	--	1267.632	1267.630
12	1257.611	--	1338.669	1338.669
13	1420.674	--	1437.737	--
14	1533.758	--	1494.759	--
15	1590.780	--	1623.801	--
16	--	--	--	--

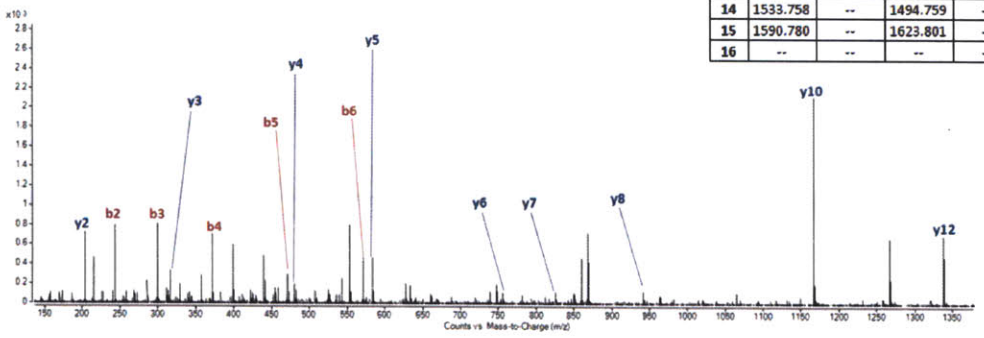

J

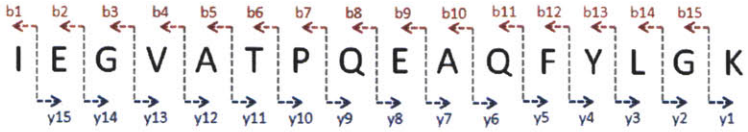

	RPL33B			
	b-ions		y-ions	
	Expected mass	Detected mass	Expected mass	Detected mass
1	--	--	147.1128	--
2	243.1339	243.1369	204.1343	204.1328
3	300.1554	300.1513	317.2183	317.2187
4	399.2238	399.2188	480.2817	480.2843
5	470.2609	470.2501	627.3501	627.3490
6	571.3086	571.3026	755.4087	755.4096
7	668.3614	--	826.4458	826.4491
8	796.4199	--	955.4884	--
9	925.4625	--	1083.547	1083.51
10	996.4997	--	1180.600	1180.597
11	1124.558	--	1281.647	--
12	1271.627	--	1352.685	--
13	1434.690	--	1451.753	--
14	1547.774	--	1508.774	--
15	1604.796	--	1637.817	--
16	--	--	--	--

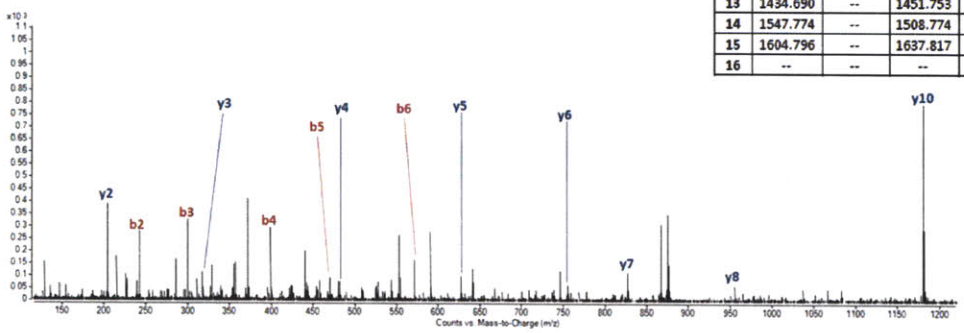

K

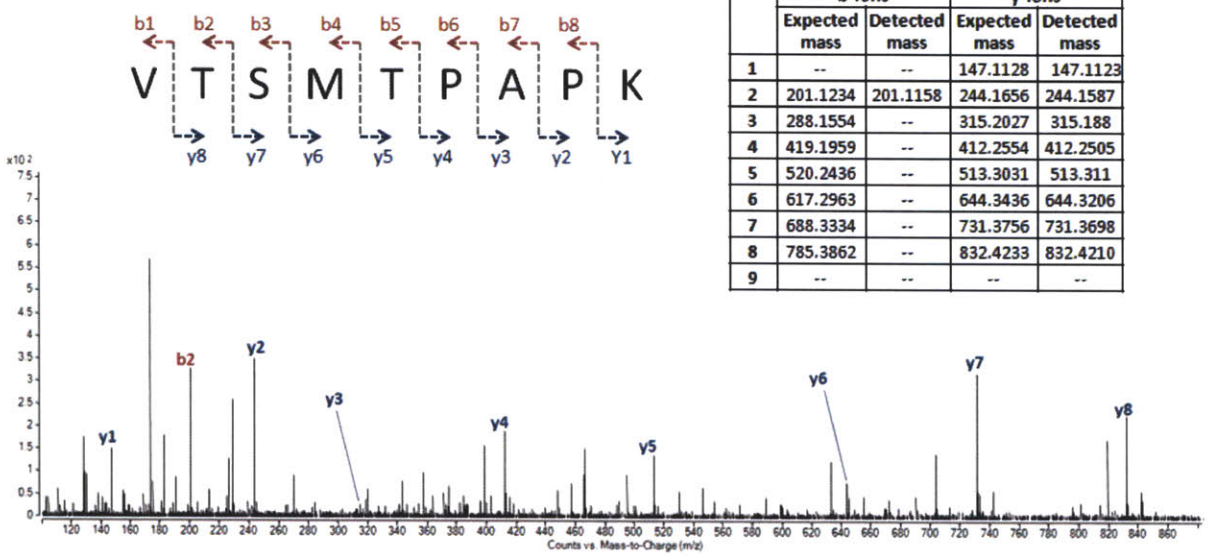

	RPL36A			
	b-ions		y-ions	
	Expected mass	Detected mass	Expected mass	Detected mass
1	--	--	147.1128	147.1123
2	201.1234	201.1158	244.1656	244.1587
3	288.1554	--	315.2027	315.188
4	419.1959	--	412.2554	412.2505
5	520.2436	--	513.3031	513.311
6	617.2963	--	644.3436	644.3206
7	688.3334	--	731.3756	731.3698
8	785.3862	--	832.4233	832.4210
9	--	--	--	--

L

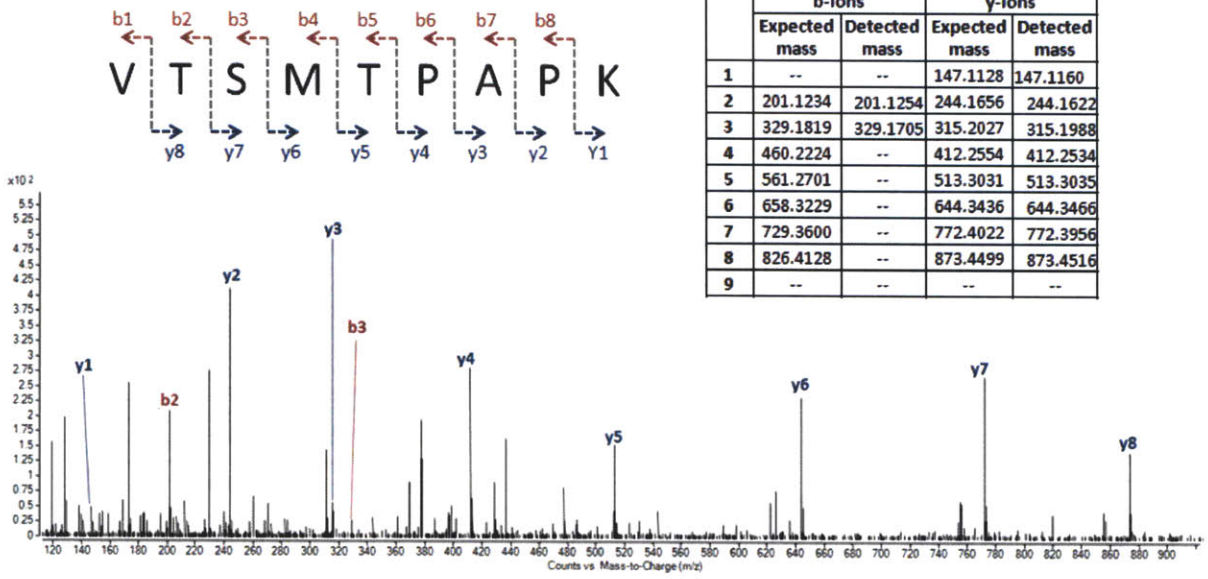

	RPL36B			
	b-ions		y-ions	
	Expected mass	Detected mass	Expected mass	Detected mass
1	--	--	147.1128	147.1160
2	201.1234	201.1254	244.1656	244.1622
3	329.1819	329.1705	315.2027	315.1988
4	460.2224	--	412.2554	412.2534
5	561.2701	--	513.3031	513.3035
6	658.3229	--	644.3436	644.3466
7	729.3600	--	772.4022	772.3956
8	826.4128	--	873.4499	873.4516
9	--	--	--	--

M

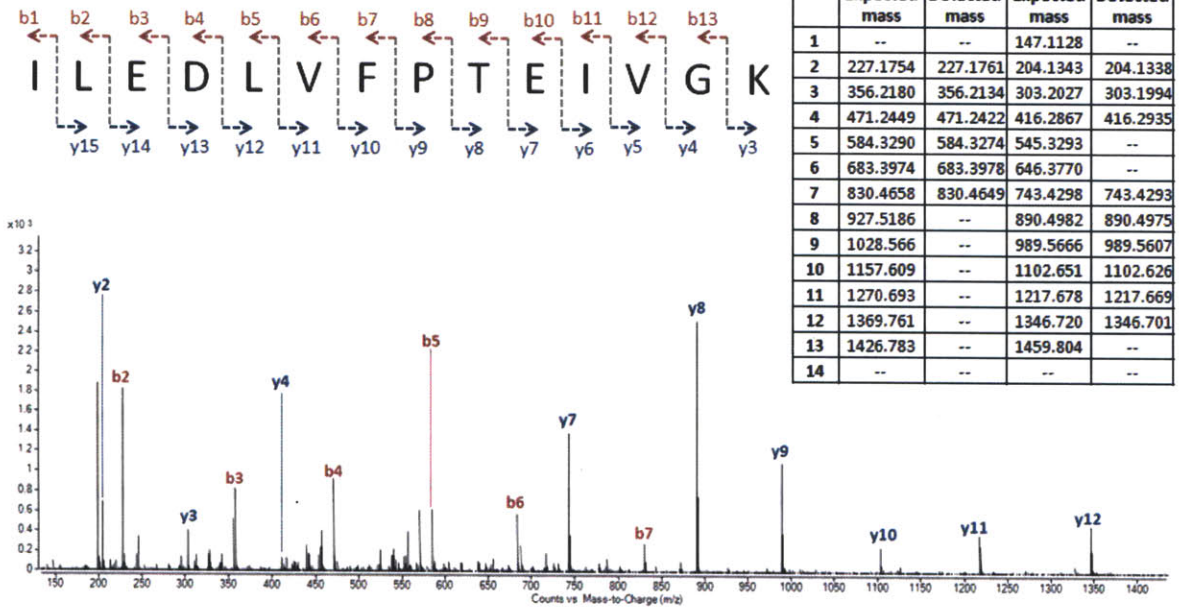

	RPS7A			
	b-ions		y-ions	
	Expected mass	Detected mass	Expected mass	Detected mass
1	--	--	147.1128	--
2	227.1754	227.1761	204.1343	204.1338
3	356.2180	356.2134	303.2027	303.1994
4	471.2449	471.2422	416.2867	416.2935
5	584.3290	584.3274	545.3293	--
6	683.3974	683.3978	646.3770	--
7	830.4658	830.4649	743.4298	743.4293
8	927.5186	--	890.4982	890.4975
9	1028.566	--	989.5666	989.5607
10	1157.609	--	1102.651	1102.626
11	1270.693	--	1217.678	1217.669
12	1369.761	--	1346.720	1346.701
13	1426.783	--	1459.804	--
14	--	--	--	--

N

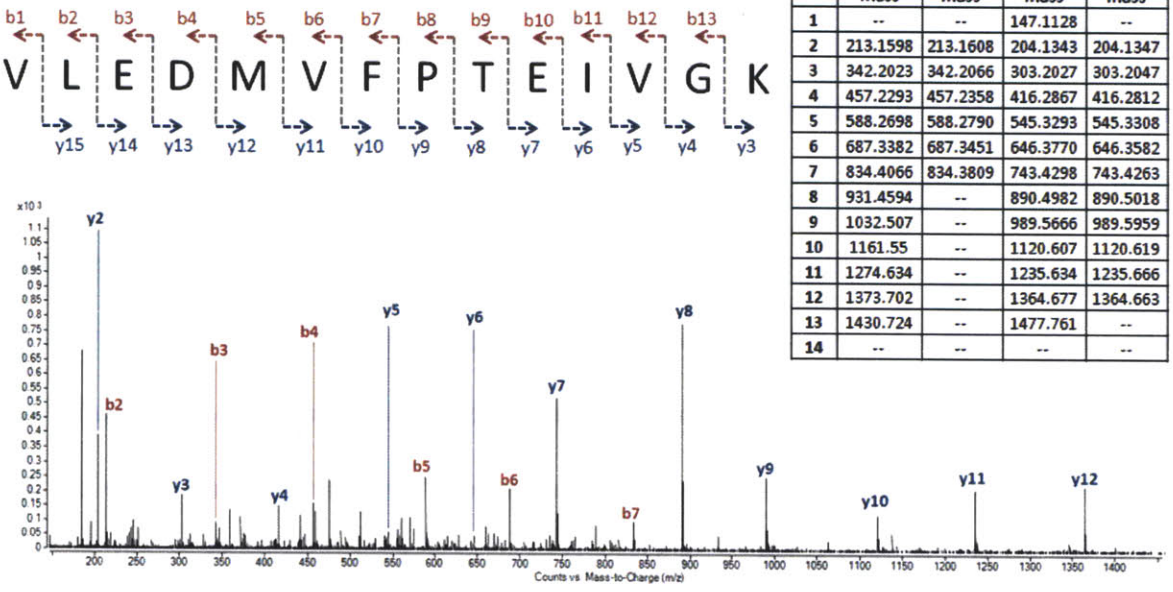

	RPS7B			
	b-ions		y-ions	
	Expected mass	Detected mass	Expected mass	Detected mass
1	--	--	147.1128	--
2	213.1598	213.1608	204.1343	204.1347
3	342.2023	342.2066	303.2027	303.2047
4	457.2293	457.2358	416.2867	416.2812
5	588.2698	588.2790	545.3293	545.3308
6	687.3382	687.3451	646.3770	646.3582
7	834.4066	834.3809	743.4298	743.4263
8	931.4594	--	890.4982	890.5018
9	1032.507	--	989.5666	989.5959
10	1161.55	--	1120.607	1120.619
11	1274.634	--	1235.634	1235.666
12	1373.702	--	1364.677	1364.663
13	1430.724	--	1477.761	--
14	--	--	--	--

Figure 4-1. Collision-induced dissociation mass spectra of peptides. Each peptide is unique to one of the 14 proteins in the 7 pairs of homologues: (A) Rpl6a; (B) Rpl6b; (C) Rpl7a; (D) Rpl7b; (E) Rpl16a; (F) Rpl16b; (G) Rpl22a; (H) Rpl22b; (I) Rpl33a; (J) Rpl33b; (K) Rpl36a; (L) Rpl36b; (M) Rps7a; and (N) Rps7b. The table in each figure lists the m/z values of expected b- and y-ions and the m/z values of detected ions.

Changes in composition of ribosome at various cellular conditions. With the seven pairs of ribosomal homologues identified, we first determined the relative level of each pair of homologues in wild-type and *trm4Δ* strains of cells (Table 4-6 and 4-7); relative level was defined as ratio of the level of homologue with high usage of UUG to that with low usage. As shown in Table 4-5, the difference of UUG codon usage frequency between the two genes, *rpl22a* and *rpl22b* is about 0.6, which is the largest within the 7 pairs of homologous proteins. Absence of Trm4 caused a statistically significant decrease in the relative level of Rpl22a to Rpl22b; the relative level decreased 40% in *trm4Δ* mutant with $p < 0.01$ in student's t-test. Similarly, as the pair of homologues with the second largest difference in UUG usage frequency (the difference is about 0.3), relative level of Rpl16a to Rpl16b also decreased in *trm4Δ* mutant by 10% ($p < 0.05$). Relative levels of the other 5 pairs of homologues had no statistically significant changes in *trm4Δ* mutant.

We then assessed changes in relative levels of these 7 pairs of homologues in response to H_2O_2-exposure (Table 4-5 and 4-6). In wild-type cells, exposure of H_2O_2 led to a 30%-increase in the relative level of Rpl22a and Rpl22b. However, in the absence of Trm4, the relative level between these two homologous ribosomal proteins did not change in response to H_2O_2. Changes in relative level of Rpl16a to Rpl16b also followed the same trend but with a smaller

amplitude. Relative levels of the other 5 pairs of homologues were not affected by H_2O_2 in either wild-type or *trm4Δ* cells.

	Untreated wild type			H_2O_2-exposed wild type			Untreated *trm4 Δ*			H_2O_2-exposed *trm4 Δ*		
	Expt. 1	Expt. 2	Expt. 3	Expt. 1	Expt. 2	Expt. 3	Expt. 1	Expt. 2	Expt. 3	Expt. 1	Expt. 2	Expt. 3
RPL6A (Low TTG)	37202	34838	32168	29167	35729	36437	34839	33189	45467	34448	37473	36774
RPL6B (High TTG)	37772	34787	35296	32688	37779	42100	35890	31606	45913	35444	35900	38462
Ratio (High TTG:Low TTG)	1.02	1.00	1.10	1.12	1.06	1.16	1.03	0.95	1.01	1.03	0.96	1.05
RPL7A (High TTG)	52125	58358	63886	74369	82757	83302	62527	54725	68598	57060	44969	48997
RPL7B (Low TTG)	17710	19592	17632	23190	27501	25342	16287	12382	22589	12710	15531	14762
Ratio (High TTG:Low TTG)	2.94	2.98	3.62	3.21	3.01	3.29	3.84	4.42	3.04	4.49	2.90	3.32
RPL16A (Low TTG)	26441	25322	26059	30370	32684	32427	24239	21581	29295	23720	22763	25216
RPL16B (High TTG)	47808	48619	45449	61319	65143	64909	40599	34275	49250	35821	37258	41661
Ratio (High TTG:Low TTG)	1.81	1.92	1.74	2.02	1.99	2.00	1.67	1.59	1.68	1.51	1.64	1.65
RPL22A (High TTG)	82104	78812	79959	100923	113122	104331	68494	62884	91551	65753	72045	75433
RPL22B (Low TTG)	5135	4540	4855	5003	5433	4238	6567	5868	7976	6229	7390	6490
Ratio (High TTG:Low TTG)	15.99	17.36	16.47	20.17	20.82	24.62	10.43	10.72	11.48	10.56	9.75	11.62
RPL36A (Low TTG)	19685	21034	20425	24329	25429	23785	22614	15387	23366	22005	18688	18690
RPL36B (High TTG)	66330	64554	59024	71843	80215	78331	56138	51568	68440	49292	52990	58109
Ratio (High TTG:Low TTG)	3.37	3.07	2.89	2.95	3.15	3.29	2.48	3.35	2.93	2.24	2.84	3.11
RPL33A (High TTG)	98668	93021	100545	118034	139000	129200	92192	81121	113781	85621	91965	100247
RPL33B (Low TTG)	38656	36228	38861	41246	53358	46685	37164	31947	41556	32080	37467	36725
Ratio (High TTG:Low TTG)	2.55	2.57	2.59	2.86	2.61	2.77	2.48	2.54	2.74	2.67	2.45	2.73
RPS7A (High TTG)	114436	112016	117772	134724	165935	149546	99232	96376	149868	118242	132693	131115
RPS7B (Low TTG)	33420	33119	32254	38212	46501	40892	30173	26912	45140	36514	38219	38574
Ratio (High TTG:Low TTG)	3.42	3.38	3.65	3.53	3.57	3.66	3.29	3.58	3.32	3.24	3.47	3.40

Table 4-6. Relative quantification of ribosomal homologues in *S. cerevisiae* under various cellular conditions. Ribosomes were isolated from three biological replicates of untreated wild-type cells, H_2O_2-exposed wild-type cells, untreated *trm4Δ* mutant cells, and H_2O_2-exposed *trm4Δ* mutant cells and were digested to peptide fragments as described in Materials and Method section. Numerical values unshaded: MS signals detected from the unique peptide of each ribosomal homologue; numerical values shaded in grey: ratio of MS signals from the homologue with high TTG usage to that from the homologue with low TTG usage.

	H_2O_2-exposed WT:untreated WT		*trm4 Δ* mutant: WT		H_2O_2-treated *trm4 Δ* :untreated *trm4Δ*	
	Fold change	t-Test	Fold change	t-Test	Fold change	t-Test
Ratio (RPL6A:RPL6B)	1.07	0.15	0.96	0.36	1.01	0.72
Ratio (RPL7A:RPL7B)	1.00	0.96	1.18	0.27	0.95	0.77
Ratio (RPL16B:RPL16A)	1.10	0.03	0.90	0.04	0.97	0.42
Ratio (RPL22A:RPL22B)	1.32	0.02	0.65	0.00	0.98	0.73
Ratio (RPL36B:RPL36A)	1.01	0.89	0.94	0.55	0.93	0.62
Ratio (RPL33A:RPL33B)	1.07	0.08	1.01	0.84	1.01	0.79
Ratio (RPL7A:RPL7B)	1.03	0.35	0.97	0.51	0.99	0.83

Table 4-7. Fold-change of relative levels of ribosomal proteins in various cellular conditions. Results in this table were based on calculation on data in Table 4-6. These include changes in H_2O_2-exposed wild-type cells relative to unexposed wild-type cells, changes in unexposed *trm4Δ* mutant relative to in unexposed wild-type, and changes in H_2O_2-exposed *trm4Δ* mutant relative to unexposed *trm4Δ* mutant. Statistically significant changes ($p < 0.05$) are highlighted in red.

Sensitivity of mutants lacking ribosomal protein genes to hydrogen peroxide toxicity. As described above, hydrogen peroxide treatment led to increases in the protein levels of RPL16B and RPL22A relative to their homologues. To assess the importance of these changes in stress responses, we assayed the H2O2 sensitivity of *rpl16aΔ*, *rpl16bΔ*, *rpl22aΔ*, and *rpl22bΔ* mutants. As shown in Figure 4-2, *rpl22aΔ* mutant was more sensitive to H_2O_2 than the wild-type strain. However, the loss of any other ribosomal proteins (Rpl16a, Rpl16b, and Rpl22b) did not result in changes in phenotype toward H_2O_2.

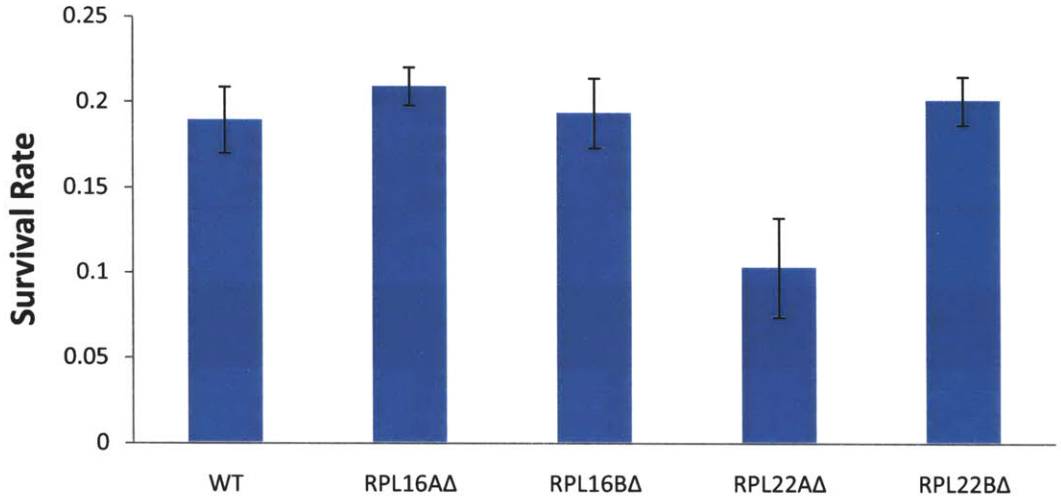

Figure 4-2. Sensitivity of ribosomal protein-deleted mutants to hydrogen peroxide toxicity. The cytotoxicity assay was performed as described in the Materials and Methods section. Survival rate for each strain of cells was represented by the ratio of number of colonies formed from the H_2O_2-exposed culture to that from the unexposed culture.

Transcription levels of ribosomal protein genes. To understand the underlying mechanism of regulation of ribosomal homologous proteins expressions, we compare the transcript levels of *rpl16a*, *rpl16b*, *rpl22a*, and *rpl22b* as a function of Trm4 availability and of H_2O_2-exposure by using RT-qPCR. Results as shown in Table 4-8 illustrates that expressions of mRNA for these four genes were statistically the same in all conditions.

A

	RPL16A Average $C_T \pm SD$	*ACT1* Average $C_T \pm SD$	$\Delta C_T \pm SD$	$\Delta\Delta C_T \pm SD$	*RPL16A* fold change relative to *ACT1*
Untreated WT	13.03 ± 0.68	12.99 ± 0.23	0.04 ± 0.72	0 ± 0.72	1 (0.6-1.7)
WT with H_2O_2	13.05 ± 0.24	13.12 ± 0.26	-0.08 ± 0.35	-0.11 ± 0.35	1.1 (0.8-1.4)
Untreated *trm4Δ*	12.63 ± 0.28	13.27 ± 0.24	-0.64 ± 0.37	-0.68 ± 0.37	1.6 (1.2-2.1)
Trm4Δ with H_2O_2	12.58 ± 0.55	13.09 ± 0.14	-0.51 ± 0.57	-0.55 ± 0.57	1.5 (1.0-2.2)

B

	RPL16B Average $C_T \pm SD$	*ACT1* Average $C_T \pm SD$	$\Delta C_T \pm SD$	$\Delta\Delta C_T \pm SD$	*RPL16B* fold change relative to *ACT1*
Untreated WT	13.43 ± 0.60	12.99 ± 0.23	0.44 ± 0.64	0 ± 0.64	1 (0.6-1.6)
WT with H_2O_2	13.36 ± 0.20	13.12 ± 0.26	0.23 ± 0.33	-0.21 ± 0.33	1.2 (0.9-1.5)
Untreated *trm4Δ*	13.24 ± 0.38	13.27 ± 0.24	-0.02 ± 0.45	-0.46 ± 0.45	1.4 (1.0-1.9)
Trm4Δ with H_2O_2	12.76 ± 0.17	13.09 ± 0.14	-0.33 ± 0.22	-0.77 ± 0.14	1.7 (1.4-2.0)

C

	RPL22A Average $C_T \pm SD$	*ACT1* Average $C_T \pm SD$	$\Delta C_T \pm SD$	$\Delta\Delta C_T \pm SD$	*RPL22A* fold change relative to *ACT1*
Untreated WT	14.20 ± 0.26	12.99 ± 0.23	1.21 ± 0.35	0 ± 0.35	1 (0.8-1.3)
WT with H_2O_2	14.57 ± 0.67	13.12 ± 0.26	1.44 ± 0.72	0.24 ± 0.72	0.8 (0.5-1.4)
Untreated *trm4Δ*	14.18 ± 0.11	13.27 ± 0.24	0.92 ± 0.27	-0.29 ± 0.27	1.2 (1-1.5)
Trm4Δ with H_2O_2	14.22 ± 0.65	13.09 ± 0.14	1.13 ± 0.67	-0.09 ± 0.67	1.1 (0.7-1.7)

D

	RPL22B Average $C_T \pm SD$	*ACT1* Average $C_T \pm SD$	$\Delta C_T \pm SD$	$\Delta\Delta C_T \pm SD$	*RPL22B* fold change relative to *ACT1*
Untreated WT	16.65 ± 0.32	12.99 ± 0.23	3.66 ± 0.40	0 ± 0.40	1 (0.8-1.3)
WT with H_2O_2	16.83 ± 0.16	13.12 ± 0.26	3.70 ± 0.30	0.04 ± 0.30	1 (0.8-1.2)
Untreated *trm4Δ*	16.54 ± 0.15	13.27 ± 0.24	3.28 ± 0.28	-0.39 ± 0.28	1.3 (1.1-1.6)
Trm4Δ with H_2O_2	16.44 ± 0.22	13.09 ± 0.14	3.35 ± 0.26	-0.31 ± 0.26	1.2 (1.0-1.5)

Table 4-8. Relative transcript levels of ribosomal protein genes in cells under various cellular conditions. These genes include: (**A**) *rpl16a*; (**B**) *rpl16b*; (**C**) *rpl22a*; and (**D**) *rpl22b*. Experiments and analyses were performed as described in Materials and Methods section.

Discussion

Characterization of ribosomal proteins. Our goal of characterizing ribosomal proteins is to define a sample set for testing the hypothesis that tRNA m^5C-methyltransferase Trm4 regulates the selection of homologous proteins for ribosome assembly based upon the difference in UUG codon usage frequency between the two homologues. Thus, we aimed to identify homologous pairs with a coverage of a wide range of difference in UUG codon usage frequency. A proteomics approach was used to serve this purpose which involves isolation of ribosomes from cell lysate by ultracentrifugation, cleavage of proteins to peptide fragments with trypsin, resolution of peptides with HPLC, and monitoring of these peptides by mass spectrometric techniques. By comparing the mass of peptides determined by mass spectrometry with the peptide mass fingerprints of proteins in *S. cerevisae* database, we identified 39 ribosomal proteins reproducibly in three biological replicates (Table 4-4). These proteins include 7 pairs of ribosomal homologues, Rpl6a and Rpl6b, Rpl7a and Rpl7b, Rpl16a and Rpl16b, Rpl22a and Rpl22b, Rpl33a and Rpl33b, Rpl36a and Rpl36b, and Rps7a and Rpl7b; the difference in UUG codon usage frequency between the two homologues of these pairs cover the range from 0 to 0.62 (Table 4-5). The transcripts of *rpl22a* and *rpl22b*, with a value of 0.62, have the largest difference in UUG codon usage frequency among all ribosomal homologue pairs in *S. cerevisiae*. These 7 pairs cover the whole range of difference in UUG codon usage frequency and thus, are adequate to serve as the testing targets for our studies.

As the sequences of the two homologues of each ribosomal protein pair are only different by a few amino acids, most tryptic fragments from the two proteins are identical. Thus, instead

of including all peptides from each protein for quantification, we only selected one specific peptide (Table 4-3) which is unique in the whole *S. cerevisiae* protein database. To avoid mistakes in assigning peptides, as peptides with different amino acid sequences or different amino acid compositions can have the same mass, each peptide was analyzed with MS-MS studies to determine its amino aicd sequece based on b- and y-ions formed in collision-induced dissociation (Figure 4-1).

In *S. cerevisiae*, each ribosome is composed by 78 proteins with 59 of them preserve two homologues in the genome, while the homologues of 22 of these proteins are identical (these identical proteins include RPS4A/B, RPS6A/B, RPS8A/B, RPS11A/B, RPS16A/B, RPS17A/B, RPS18A/B, RPS23A/B, RPS24A/B, RPS30A/B, RPL2A/B, RPL1A/B, RPL12A/B, RPL18A/B, RPL20A/B, RPL19A/B, RPL23A/B, RPL35A/B, RPL42A/B, RPL43A/B, RPL40A/B, and RPL41A/B) (*21*). Thus, *S. cerevisiae* ribosomes potentially comprise 115 sequence-specific proteins. While we only identified 39 of them, the detection can be improved with at least two ways. First, the sensitivity of detection can be improved by purifying each protein before MS analysis. Carroll and coworkers studied ribosomal proteins in *Arabidopsis* by resolving each protein with SDS-PAGE gels before enzymatic digestions and LC/MS analysis (*22*). With this approach, they were able to identified 87 ribosomal proteins. Second, coverage of peptides identified can be improved by including peptides with modifications in database search. In protein identification, we only considered peptide with no post-translational modifications. Even though no post-translation modifications are found on the 14 peptides that we have identified, it has been shown that a number of modifications are present in ribosomal proteins, including phosphorylation, lysine *N*-methylation, *N*-terminal acetylation, and N-terminal methylation (*22,*

23). Including these modifications in database search and validating these modified peptides with MS-MS analyses may increase the number of proteins identified.

As a conclusion on this method, it is sufficient for understanding the correlations between expression level of proteins with different UUG codon usage and level of m^5C on tRNA. However, the method can be improved to include a larger number of proteins for quantification.

tRNA m^5C-methyltransferase Trm4 regulates the relative level of Rpl22a and Rpl22b in ribosome. The 7 pairs of ribosomal homologues identified in proteomics analysis were used to investigate the relationship between UUG usages and protein expression levels as a function of activities of tRNA m^5C-methyltransferase Trm4. Strobel and Abelson found that an amber suppressor tRNA, $tRNA^{SUP53}$, comprises an m^5C at the wobble position, in which the lack of this modification reduces the efficiency of suppressor activity (*12*). This study has demonstrated that m^5C at wobble position of tRNA can affect translation of the corresponding codon. In *S. cerevisaie*, m^5C is located at the wobble position of a leucine tRNA for coding the codon UUG in mRNA. Thus, the translation of UUG may be regulated by the activity of tRNA m^5C-methyltransferase.

To test this hypothesis, we quantified the relative protein levels of the 7 pairs of ribosomal homologues in wild-type and *trm4*-deleted strains of cells. These homologous pairs are an ideal system for testing the hypothesis because amino acid sequences between the two homologues in each pair are very similar but the UUG usage frequency varies from 0 to 0.62. As shown in Table 4-6 and 4-7, the relative level of RPL22A/B and RPL16A/B are affected, in which the absence of *trm4* led to decreases in protein levels of the genes with high usage of UUG

relative to that of their homologous gene with low usage of UUG in both cases. Differences in the usage frequency of UUG and in the number of UUG between *rpl22a* and *rpl22b* are 0.62 and 4 respectively; the relative protein level of RPL22A decreased 1.5-fold in *trm4Δ* mutant ($p < 0.01$ from Student's t-test). Those between *rpl16a* and *rpl16b* are 0.32 (UUG usage frequency) and 5 (number of UUG) and the relative level of RRPL16B decreased only 1.1-fold in the absence of Trm4 ($p < 0.05$). For *rpl36a* and *rpl36b*, while the difference in UUG frequency is 0.33, the difference in number of UUG is only 2, the lack of Trm4 did not affect the relative protein expression level of this homologous pair. These observations suggest that the activity of Trm4 affect the protein expression levels based upon both the UUG codon usage frequency and the number of UUG codon.

Changes in the relative protein level between Rpl22a and Rpl22b in response to hydrogen peroxide. As described in Chapter 3, level of m^5C in *S. cerevisiae* tRNA increases after exposing to hydrogen peroxide and Trm4 confers resistance to this toxic agent which indicates that m^5C and Trm4 are important for stress responses. To investigate the cellular response pathways that Trm4 is involved, we compared the relative levels of ribosomal homologous pairs in H_2O_2-exposed and unexposed cells. For the proteins Rpl22a and Rpl22b in wild-type cells, relative level of homologue with high usage of UUG in H_2O_2-exposed cells increases 1.3 folds compared to that in unexposed cells. However, exposure of H_2O_2 to *trm4Δ* mutant does not cause any statistically significant changes in the relative expression level of this pair of homologues. Similarly, the relative level of Rpl16a and Rpl16b increases 1.1 folds in wild-type

cells exposed to H_2O_2 but that in *trm4Δ* mutant does not change after the same treatment. These results suggest that Trm4 is involved in regulating the composition of ribosome.

Rpl22a and Rpl22b may perform different biological roles. The changes in ribosome composition in response to hydrogen peroxide exposure led us to the question that whether these changes contribute to improvement in survival rate under the stressful condition. We assessed the sensitivity of *S. cerevisiae* mutants with *rpl16aΔ*, *rpl16bΔ*, *rpl22aΔ*, or *rpl22bΔ* to hydrogen peroxide relative to wild-type strain of cells and determined that only Rpl22a confers resistance to H_2O_2 within these four genes. Prior studies have suggested that ribosomal homologue-specific defects are simply due to differences between expression levels of the two homologues (*24-28*). Indeed, based on the C_T values from RT-qPCR (Table 4-7) and MS signal intensities (Table 4-6), expression of Rpl22a was significantly higher than that of Rpl22b in both transcription level and translation level. However, Komili and coworkers have illustrated that translation of ASH1 requires a specific subset of ribosomal homologues, which suggests that ribosome composed by different homologues are specialized for differential cellular functions (*18*). Applying this model to our case, ribosome with Rpl22a may responsible for the translation of genes that are important for responding to H_2O_2.

Correlations between H_2O_2-sensitivity of *trm4Δ* and *rpl22aΔ* strains. In chapter 3, we have observed that H_2O_2 cytotoxicity increased in cells lacking Trm4. As described above, the lack of Trm4 leads to a decrease in the relative level of ribosomal protein Rpl22a to Rpl22b, in which Rpl22a also confers resistance to hydrogen peroxide. The ribosomal protein expression

level pattern in *trm4* knockout and the role of Rpl22a can then be correlated to the fact that Trm4 also confers resistance to H_2O_2 toxicity. However, this may not be the only related pathway that Trm4 is involved. As illustrated in Table 4-1, genes encoding many ribosomal proteins and metabolic enzymes are also enriched in UUG which may also participate in critical processes for stress responses.

tRNA modifying enzymes as components of translational regulation pathways. Our data is consistent with a model in which Trm4 modulates the translation of UUG by catalyzing the formation of m^5C at wobble position of the tRNA for coding UUG and this leads to selection in protein expression between UUG-enriched genes and UUG-depleted genes. In 66 species of *S. cerevisiae* tRNA that were completely sequenced, 28 of them have modifications in the anticodon region, including Y, Gm, Cm, I, m^5C, ncm^5U, ncm^5Um, mcm^5U, and mcm^5s^2U (*11*), and these modifications have high potential to be utilized in regulating translation of genes enriched in different codons. Indeed, as described above, Trm9, which is responsible for the formation of mcm^5U, modulates the translation of a group of AGA-enriched genes (*3*).

Our studies have specifically demonstrated that the relative level of two ribosomal homologues is modulated by Trm4 to improve survivability during H_2O_2 exposure. This level of regulation may be extendable to other homologous protein pairs. Kellis and coworkers proposed that whole genome duplication occurred in an ancestor of *S. cerevisiae* and about 90% of these redundant copies were lost during evolution while the last 10% of duplicated genes retained because they have evolved to serve new functions (*13*). Interestingly, codon usage patterns of some duplicated genes diverged significantly; one example is the two

pyruvate kinase genes, *cdc19* and *pyk2*, which *pyk2* is expressed preferentially during conditions of low glycolytic flux (*29*). In *cdc19*, 32 of 35 leucines are coded by UUG (frequency = 0.91) while in *pyk2*, only 15 of 45 leucines are coded by UUG (frequency = 0.33). Thus, Trm4 may also involve in translational regulation of these two genes.

In conclusion, our studies support the hypothesis that Trm4 is involved in translational regulation by selectively affecting translation of genes enriched in UUG. As a specific example, we demonstrated that Trm4 promotes the relative level of Rpl22a comparing to it homologue Rpl22b in response to H_2O_2-exposure, for which Rpl22a confers resistance to H_2O_2. Similar pathways may be applied generally to genes with high usage of UUG, which provide a new level of regulation in gene expression.

Reference

1. Johansson, M. J. O., and Byström, A. S. (2005) *Transfer RNA modifications and modifying enzymes in Saccaromyces cerevisiae*, Springer-Verlag, Heidelberg, Germany.
2. Björk, G. R. (1995) *Biosynthesis and Function of Modified Nucleosides*, ASM Press, Washington, D.C.
3. Begley, U., Dyavaiah, M., Patil, A., Rooney, J. P., DiRenzo, D., Young, C. M., Conklin, D. S., Zitomer, R. S., and Begley, T. J. (2007) Trm9-catalyzed tRNA modifications link translation to the DNA damage response, *Mol Cell 28*, 860-870.
4. Kalhor, H. R., and Clarke, S. (2003) Novel methyltransferase for modified uridine residues at the wobble position of tRNA, *Mol Cell Biol 23*, 9283-9292.

5. Lu, J., Huang, B., Esberg, A., Johansson, M. J., and Bystrom, A. S. (2005) The Kluyveromyces lactis gamma-toxin targets tRNA anticodons, *RNA 11*, 1648-1654.

6. Weissenbach, J., and Dirheimer, G. (1978) Pairing properties of the methylester of 5-carboxymethyl uridine in the wobble position of yeast tRNA3Arg, *Biochim Biophys Acta 518*, 530-534.

7. de Groot, P. W., Ruiz, C., Vazquez de Aldana, C. R., Duenas, E., Cid, V. J., Del Rey, F., Rodriquez-Pena, J. M., Perez, P., Andel, A., Caubin, J., Arroyo, J., Garcia, J. C., Gil, C., Molina, M., Garcia, L. J., Nombela, C., and Klis, F. M. (2001) A genomic approach for the identification and classification of genes involved in cell wall formation and its regulation in Saccharomyces cerevisiae, *Comp Funct Genomics 2*, 124-142.

8. Li, Z., Lee, I., Moradi, E., Hung, N. J., Johnson, A. W., and Marcotte, E. M. (2009) Rational extension of the ribosome biogenesis pathway using network-guided genetics, *PLoS Biol 7*, e1000213.

9. Pan, X., Reissman, S., Douglas, N. R., Huang, Z., Yuan, D. S., Wang, X., McCaffery, J. M., Frydman, J., and Boeke, J. D. (2010) Trivalent arsenic inhibits the functions of chaperonin complex, *Genetics 186*, 725-734.

10. Teixeira, M. C., Raposo, L. R., Mira, N. P., Lourenco, A. B., and Sa-Correia, I. (2009) Genome-wide identification of Saccharomyces cerevisiae genes required for maximal tolerance to ethanol, *Appl Environ Microbiol 75*, 5761-5772.

11. Czerwoniec, A., Dunin-Horkawicz, S., Purta, E., Kaminska, K. H., Kasprzak, J. M., Bujnicki, J. M., Grosjean, H., and Rother, K. (2009) MODOMICS: a database of RNA modification pathways. 2008 update, *Nucleic Acids Res 37*, D118-121.

12. Strobel, M. C., and Abelson, J. (1986) Effect of intron mutations on processing and function of Saccharomyces cerevisiae SUP53 tRNA in vitro and in vivo, *Mol Cell Biol 6*, 2663-2673.

13. Kellis, M., Birren, B. W., and Lander, E. S. (2004) Proof and evolutionary analysis of ancient genome duplication in the yeast Saccharomyces cerevisiae, *Nature 428*, 617-624.

14. Baudin-Baillieu, A., Tollervey, D., Cullin, C., and Lacroute, F. (1997) Functional analysis of Rrp7p, an essential yeast protein involved in pre-rRNA processing and ribosome assembly, *Mol Cell Biol 17*, 5023-5032.

15. Enyenihi, A. H., and Saunders, W. S. (2003) Large-scale functional genomic analysis of sporulation and meiosis in Saccharomyces cerevisiae, *Genetics 163*, 47-54.

16. Haarer, B., Viggiano, S., Hibbs, M. A., Troyanskaya, O. G., and Amberg, D. C. (2007) Modeling complex genetic interactions in a simple eukaryotic genome: actin displays a rich spectrum of complex haploinsufficiencies, *Genes Dev 21*, 148-159.

17. Ni, L., and Snyder, M. (2001) A genomic study of the bipolar bud site selection pattern in Saccharomyces cerevisiae, *Mol Biol Cell 12*, 2147-2170.

18. Komili, S., Farny, N. G., Roth, F. P., and Silver, P. A. (2007) Functional specificity among ribosomal proteins regulates gene expression, *Cell 131*, 557-571.

19. Livak, K. J., and Schmittgen, T. D. (2001) Analysis of relative gene expression data using real-time quantitative PCR and the 2(-Delta Delta C(T)) Method, *Methods 25*, 402-408.

20. Zinker, S., and Warner, J. R. (1976) The ribosomal proteins of Saccharomyces cerevisiae. Phosphorylated and exchangeable proteins, *J Biol Chem 251*, 1799-1807.

21. Nakao, A., Yoshihama, M., and Kenmochi, N. (2004) RPG: the Ribosomal Protein Gene database, *Nucleic Acids Res 32*, D168-170.

22. Carroll, A. J., Heazlewood, J. L., Ito, J., and Millar, A. H. (2008) Analysis of the Arabidopsis cytosolic ribosome proteome provides detailed insights into its components and their post-translational modification, *Mol Cell Proteomics 7*, 347-369.

23. Chang, I. F., Szick-Miranda, K., Pan, S., and Bailey-Serres, J. (2005) Proteomic characterization of evolutionarily conserved and variable proteins of Arabidopsis cytosolic ribosomes, *Plant Physiol 137*, 848-862.

24. Abovich, N., and Rosbash, M. (1984) Two genes for ribosomal protein 51 of Saccharomyces cerevisiae complement and contribute to the ribosomes, *Mol Cell Biol 4*, 1871-1879.

25. Herruer, M. H., Mager, W. H., Woudt, L. P., Nieuwint, R. T., Wassenaar, G. M., Groeneveld, P., and Planta, R. J. (1987) Transcriptional control of yeast ribosomal protein synthesis during carbon-source upshift, *Nucleic Acids Res 15*, 10133-10144.

26. Leer, R. J., van Raamsdonk-Duin, M. M., Molenaar, C. M., Witsenboer, H. M., Mager, W. H., and Planta, R. J. (1985) Yeast contains two functional genes coding for ribosomal protein S10, *Nucleic Acids Res 13*, 5027-5039.

27. Lucioli, A., Presutti, C., Ciafre, S., Caffarelli, E., Fragapane, P., and Bozzoni, I. (1988) Gene dosage alteration of L2 ribosomal protein genes in Saccharomyces cerevisiae: effects on ribosome synthesis, *Mol Cell Biol 8*, 4792-4798.

28. Rotenberg, M. O., Moritz, M., and Woolford, J. L., Jr. (1988) Depletion of Saccharomyces cerevisiae ribosomal protein L16 causes a decrease in 60S ribosomal subunits and formation of half-mer polyribosomes, *Genes Dev 2*, 160-172.

29. Boles, E., Schulte, F., Miosga, T., Freidel, K., Schluter, E., Zimmermann, F. K., Hollenberg, C. P., and Heinisch, J. J. (1997) Characterization of a glucose-repressed pyruvate kinase (Pyk2p) in Saccharomyces cerevisiae that is catalytically insensitive to fructose-1,6-bisphosphate, *J Bacteriol 179*, 2987-2993.

Chapter 5

Spectrum of tRNA modifications as a source of biomarkers

Abstract

In previous studies, we observed unique patterns in the spectrum of tRNA modifications from cells exposed to mechanistically distinct toxicants, which lead us to hypothesize that the spectrum can serve as index of cellular conditions. To test this hypothesis, we characterized changes in the spectrum from cells exposed to four oxidizing agents, hydrogen peroxide, *tert*-butyl hydroperoxide, peroxynitrite, and gamma-radiation, and five alkylating agents, methyl methanesulfonate, ethyl methanesulfonate, isopropyl methanesulfonate, *N*-methyl-*N'*-nitro-*N*-nitrosoguanidine, and *N*-nitroso-*N*-methylurea. Multivariate statistical analysis on these data indicates class-specific features for both oxidizing agents and alkylating agents, involving 14 modifications, Am, m^2G, mcm^5U, mcm^5s^2U, m^3C, m^7G, yW, Gm, m^5C, ncm^5U, $m^2{}_2G$, i^6A, and Cm. These features were used to develop a data-driven model that can accurately predict the class of toxic agents. These results demonstrate that spectrum of tRNA modifications is a potential source of biomarkers, which may be abe to provide a new level of information for development of diagnostic and prognostic tools.

Introduction

Each organism is a complex biological system that comprises proteins, DNA, RNA, lipids, and various types of metabolites. In such complex systems, the expressions of all components are correlated and so, small deviations in physiological conditions may lead to significant changes in different parts of the system and vice versa, changes in a specific set of biological,

biochemical, or chemical features or characteristics can be used as index of health, disease, or response to a therapeutic intervention. Indeed, with advances in DNA sequencing, microarray technologies, mass spectrometry and many other quantitative techniques in recent years, many biomarker signatures of exposures and diseases were determined. For instance, C-reactive protein is identified as a biomarker of health risk and inflammation, as this protein increases several orders of magnitude during states of systemic inflammation and is directly and positively correlated with the risk of cardiovascular diseases (*1-3*). Another well-studied biomarker is a DNA adduct, aflatoxin-B1-N7-guanine, which is used to indicate food poisoning as it is found in urine from patients ingested the fungal toxin, aflatoxin (*4, 5*). In the systems level, signature patterns for exposure to toxicants and for disease states were discovered in profiles of transcripts, proteins, and metabolites (*6, 7*).

tRNA secondary modifications are also a part of complex biological systems. Using *S. cerevisiae* for illustration, there are more than 50 genes encoding tRNA modifying enzymes, 280 genes encoding tRNA, and at least 25 tRNA modifications (*8, 9*). A combination of changes from so many factors can potentially serve as highly specific biomarkers with a large dynamic range. In chapter 3, we have shown that the spectrum of tRNA modifications changes specifically when cells are exposed to 4 mechanistically distinct toxic agents, which implies that the patterns of changes can reflect cellular conditions of the cells. Expanding along this line, in this study we tested whether toxic agents with similar mechanisms of action can lead to common features in the spectrum of tRNA modifications.

By using a liquid chromatography-triple quadrupole mass spectrometric method, we characterized the changes in spectra from cells exposed to oxidizing agents and alkylating

agents relative to spectrum of unexposed cells. Multivariate statistical analysis on the data revealed that spectra from cells exposed to the same class of toxicants share common features that are unique from the other class. Based upon these class-specific features, we developed a data-driven model that can identify alkylating agent-exposed cells, oxidizing agent-exposed cells, and unexposed cells with high accuracy.

Materials and Methods

Materials. All chemicals and reagents were of the highest purity available and were used without further purification. Methyl methanesulfonate, ethyl methane sulfonate, *N*-nitroso-*N*-methylurea, hydrogen peroxide, RNase A, alkaline phosphatase, and *tert*-butyl hydroperoxide were purchased from Sigma Chemical Co. (St. Louis, MO). Isopropyl methanesulfonate was purchased from Pfaltz & Bauer, Inc. (Waterbury, CT). *N*-methyl-*N'*-nitro-*N*-nitrosoguanidine was purchased from TCI America (Portland, OR). Sodium peroxynitrite was purchased from Cayman Chemical Co. (Ann Arbor, MI). Nuclease P1 was purchased from Roche Diagnostic Corp. (Indianapolis, IN). Phosphodiesterase I was purchased from USB (Cleveland, OH). Yeast extract and peptone were purchased from Biomed Diagnostics, Inc. (White City, OR). Micron YM10 filters were purchased from PALL Corp. (Port Washington, NY). HPLC-grade water and acetonitrile were purchased from Mallinckrodt Baker (Phillipsburg, NJ). *S. cerevisiae* BY4741 cells were purchased from American Type Culture Collections (Manassas, VA).

Sensitivity assay of *S. cerevisiae* to toxic agents. *S. cerevisiae* BY4741 was cultured in YPD (yeast extract-peptone-dextrose) media with 200 μg/mL of geneticine at 30 °C with shaking at 220 rpm. Each culture was grown to mid-log phase (OD660 ~ 0.6 to 0.8) followed by exposing to one of the following chemical in one of the dosages: hydrogen peroxide (H_2O_2; 0, 2, 3.5, 5, 10, 15, and 20 mM); *tert*-butyl hydroperoxide (TBHP; 0, 0.7, 2, 4, 7, 14, 22, 25, and 29 mM); sodium peroxynitrite ($ONOO^-$; 0, 0.3, 0.5, 0.8, 1.0, 1.5, and 2.0 mM); γ-radiation (0, 21.3, 168, 327, 513, and 606 G); methyl methanesulfonate (MMS; 0, 1.2, 6, 12, 24, 36, and 48 mM), ethyl methanesulfonate (EMS; 0, 0.19, 0.29, 0.39, 0.49, and 0.58 M); isopropyl methanesulfonate (IMS; 0, 8, 17, 33, 50, and 66 mM); *N*-methyl-*N'*-nitro-*N*-nitrosoguanidine (MNNG; 0, 41, 61, 82, 102, and 136 mM); and *N*-nitro-*N*-methylurea (NMU; 0, 1.3, 2.3, 3.2, and 4.2 mM). After 1 hour, these cultures were diluted 10^4 folds with YPD culture media and 50 μL of the diluted culture was plated to YPD agar plates. Survival rates of exposed cells were determined by comparing the number of colonies formed from untreated culture with that from each exposed culture after two days.

Exposure of *S. cerevisiae*. Cultures of *S. cerevisiae* at mid-log phase (OD660 ~0.6) was exposed to 5 mM H_2O_2, 25 mM TBHP, 0.8 mM $ONOO^-$, 500 G γ-radiation, 24 mM MMS, 190 mM EMS, 50 mM IMS, 82 mM MNNG, or 3.2 mM NMU for 1 h, in which each of these exposures produced approximately 80% cytotoxicity (Figure 1). Three unexposed cultures were also prepared to serve as control. Approximately 2×10^7 cells from each culture were then pelleted by centrifugation. The whole set of experiments was replicated five times.

Isolation of tRNA from *S. cerevisiae*. Pellets of cells were resuspended in TRIZOL reagent with the addition of antioxidants (0.1 mM desferrioxamine and 0.1 mM butylated hydroxytoluene) and deaminase inhibitors (5 μg/mL coformycin and 50 μg/mL tetrahydrouridine). Cells in this solution were lyzed by mechanical disruption. The solution was mixed with chloroform and this mixture was centrifuged to separate the aqueous phase and the organic phase. The aqueous phase, which contained all species of RNA, was collected and tRNA in this solution was isolated by using PureLink miRNA Isolation Kit, following manufacturer's instructions. Approximately 6 μg of tRNA was isolated from 2×10^7 cells based on quantification with UV-vis spectrophotometer and bioanalyzer.

Enzymatic hydrolysis of *S. cerevisiae* tRNA. The procedure has already been described in Chapter 2. An amount of 6 μg of tRNA was mixed with 50 μL of a solution at pH 6.8 that contains 30 mM of sodium acetate, 2 mM of $ZnCl_2$, 0.02 Unit/μL of nuclease P1, 0.1 Units/μL of RNase A, 5 μg/ml coformycin, 50 mg/ml tetrahydrouridine, 0.1 mM deferoxamine mesylate, and 0.1 mM butylated hydroxytoluene. Also, 6 pmol of $[^{15}N]_5$-labeled 2'-deoxyadenosine ($[^{15}N]_5$-dA) was added to serve as internal standard. The solution was incubated at 37 °C for 3 hours before adding an additional 50 μL of solution at pH 7.8 with 30 mM sodium acetate, 0.2 Units/μL of alkaline phosphatase, and 0.01 Units/μL of phosphodiesterase I. This mixture was incubated at 37 °C overnight to ensure reactions were completed. Proteins were removed from the nucleosides with a Microcon YM-10 filter.

Method to quantify spectrum of *S. cerevisiae* tRNA modifications with LC/QQQ. An amount of 0.4 μg of ribnucleosides were resolved with a Thermo Scientific Hypersil GOLD aQ reverse-phase column (150×2.1 mm, 3 μm particle size) eluted with the following gradient of acetonitrile in 8 mM ammonium acetate at a flow rate of 0.3 mL/min and 36°C: 0–18 min, 0%; 18–23 min, 0-1%; 23–28 min, 1–6%; 28–30 min, 6%; 30–40 min, 6–100%; 40–50 min, 100%. The HPLC column was coupled to an Agilent 6410 Triple Quadrupole LC/MS mass spectrometer with an electrospray ionization source where it was operated in positive ion mode with the following parameters for voltages and source gas: gas temperature, 350°C; gas flow, 10 L/min; nebulizer, 20 psi; and capillary voltage, 3500 V. The first and third quadrupoles (Q1 and Q3) were fixed to unit resolution and the modifications were quantified by pre-determined molecular transitions. Q1 was set to transmit the parent ribonucleoside ions and Q3 was set to monitor the deglycosylated product ions, except for Y for which the stable C-C glycosidic bond led to fragmentation of the ribose ring; we used the *m/z* 125 ion for quantification. The dwell time for each ribonucleoside was 200 ms. The retention time, *m/z* of the transmitted parent ion, *m/z* of the monitored product ion, fragmentor voltage, and collision energy of each modified nucleoside and ^{15}N-labeled internal standard are as follow: D, 2.2 min, *m/z* 247→115, 80 V, 5 V; Y, 2.3 min, *m/z* 245→125, 80 V, 10 V; m^{5}C, 5.4 min, *m/z* 258→126, 80 V, 8 V; Cm, 6.4 min, *m/z* 258→112, 80 V, 8 V; m^{5}U, 7.9 min, *m/z* 259→127, 90 V, 7 V; ncm^{5}U, 8.7 min, *m/z* 302→170, 90 V, 7 V; ac^{4}C, 19.7 min, *m/z* 286→154, 80 V, 6 V; m^{3}C, 5.0 min, *m/z* 258→126, 80 V, 8 V; Um, 10.7 min, *m/z* 259→113, 90 V, 7 V; m^{7}G, 8.5 min, *m/z* 298→166, 90 V, 10 V; m^{1}A, 6.9 min, *m/z* 282→150, 100 V, 16 V; mcm^{5}U, 15.5 min, *m/z* 317→185, 90 V, 7 V; m^{1}I, 16.9 min, *m/z* 283→151, 80 V, 10 V; Gm, 18.2 min, *m/z* 298→152, 80 V, 7 V; m^{1}G, 18.8 min, *m/z* 298→166, 90 V, 10 V;

m^2G, 22.2 min, *m/z* 298→166, 90 V, 10 V; I, 7.8 min, *m/z* 269→137, 80 V, 10 V; mcm^5s^2U, 31.3 min, *m/z* 333→201, 90 V, 7 V; $[^{15}N]_5$-dA, 31.0 min, *m/z* 257→141, 90 V, 10 V; $m^2{}_2G$, 31.7 min, *m/z* 312→180, 100 V, 8 V; t^6A, 32.8 min, *m/z* 413→281, 100 V, 8 V; Am, 33.1 min, *m/z* 282→136, 100 V, 15 V; yW, 37.1 min, *m/z* 509→377, 120 V, 10 V, and i^6A, 37.9 min, *m/z* 336→204, 120 V, 17 V. The mass spectrometer monitored ions with the molecular transitions of D, Y, m^3C and m^5C from 1 to 4.4 min; molecular transitions of mcm^5U, ncm^5U, m7G, m^1I, m^1A, I, m^5U, m^3C, m^5C, and Cm from 4.4 to 6.5 min; molecular transitions of mcm^5U, ncm^5U, m^1G, Gm, ac^4C, m^1I, m^1A, I, m^5U, Um m^5C, and Cm from 6.5 to 9 min; molecular transitions of mcm^5U, ncm^5U, m^2G, Gm, ac^4C, m^1I, m^1A, I, m^5U, Um, and $[^{15}N]_5$-dA from 9 to 13 min; molecular transitions of t^6A, mcm^5s^2U, mcm^5U, $m^2{}_2G$, m^2G, Gm, ac^4C, m^1I, Am, m^5U, Um, and $[^{15}N]_5$-dA from 13 to 24 min. The signals from each modified nucleoside were normalized with the signals from $[^{15}N]_5$-dA for the purpose of comparison between samples.

Hierarchical clustering analysis. To eliminate batch-to-batch variations between the five sets of replicates, the MS signal intensity of each ribonucleoside in each sample was divided by the averaged MS signal intensity of the same nucleoside in three controls (unexposed cells) in the same batch. This ratio is considered as the fold-change in the level of modification in response to the exposure. These fold-change data were transformed to $\log_2$ ratios before being used to perform hierarchical clustering analysis with the centroid linkage algorithm in the software Cluster 3.0, based on the distance between each dataset measured using the Pearson correlation, with heat map representations produced using Java Treeview.

Classification of toxic agents associated with tRNA modifications. All data from five batches are combined together with exposure labels. There were three classes of exposures: CT (unexposed), AA (alkylating agent-exposed) and OX (oxidizing agent-exposed). K-nearest neighbor (KNN) classification method was used to establish the classification model; from each class of exposures, changes of each ribonucleoside were compared to those in the other classes by using multiple t-test with bonferroni correction and those with p values < 0.01 were assigned as unique features of that exposure group. All these unique features were set as parameters to construct a data-driven model by using the programming software R, in which all data were randomly assigned into 2 groups; one group was used as a training set to build the model and the other group was used as a testing set to evaluate the prediction accuracy of this model. For this evaluation, the confusion matrix method was used to determine prediction sensitivity and prediction specificity with one of these matrices shown in Table 5-1 for illustration. These experiments were performed in collaboration with Dr. Fugen Li.

		Predicted classes			
		AA	CT	OX	Total
actual classes	AA	8	0	0	8
	CT	0	6	1	7
	OX	2	0	7	9
	Total	10	6	8	24

Table 5-1. Confusion matrix for evaluation of prediction accuracy. Our model is to predict the classes of samples: alkylating agent-exposed (AA), unexposed (CT), and oxidizing agent-exposed (OX). In this matrix, each column represents a predicted class and each row represents an actual class. This exercise used 8 samples of AA, 7 samples of CT, and 9 samples of OX, as shown on the last column and the number of samples predicted as each of the classes is shown

on the last row. For AA, all 8 samples in this actual class were predicted correctly and thus the prediction sensitivity was 100% (8 out of 8). However, two other samples actually from OX were also classified into the AA predicted class and so, the prediction specificity was only 80% (8 out of 10). Similarly, for CT, prediction sensitivity was 86% (6 out of 7) and prediction specificity was 100% (6 out of 6), and for OX, prediction sensitivity was 78% (7 out of 9) and prediction specificity was 86% (7 out of 8). The exercise was repeated 20 times with randomly selected samples.

Results

Cytotoxicity dose-response studies of *S. cerevisiae* to various toxic agents. The dosage of toxic agents may affect which cellular response pathways to be activated. We thus decided to expose cells to nine toxic agents in which each with a dosage that causes a cytotoxicity of 80%. These nine toxic agents includes five alkylating agents: methyl methanesulfonate (MMS), ethyl methanesulfonate (EMS), isopropyl methanesulfonate (IMS), *N*-methyl-*N'*-nitro-*N*-nitrosoguanidine (MNNG), and *N*-nitro-*N*-methylurea (NMU), and four oxidizing agents: hydrogen peroxide (H_2O_2), *tert*-butyl hydroperoxide (TBHP), gamma-radiation (γ-radiation), and sodium peroxynitrite ($ONOO^-$). To determine the LD80 of these reagents, we assessed the sensitivity of cells to a serial concentration of each of the reagents. As shown in Figure 5-1, the survival rates of *S. cerevisiae* to different dosages of these nine reagents were determined and based upon these results, we exposed cells to 5 mM H_2O_2, 25 mM TBHP, 0.8 mM $ONOO^-$, 510 G γ-radiation, 24 mM MMS, 190 mM EMS, 50 mM IMS, 82 mM MNNG, and 3 mM NMU.

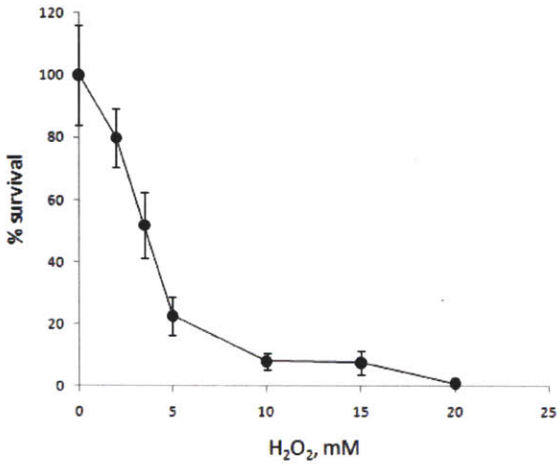
% survival
120
100
80
60
40
20
0
0
5
10
15
20
25
H_2O_2, mM

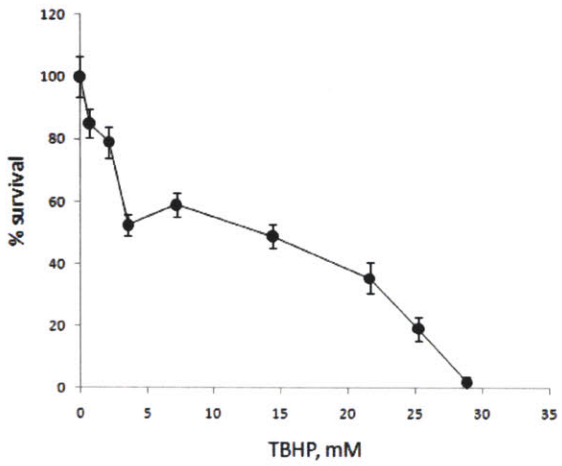
% survival
120
100
80
60
40
20
0
0
5
10
15
20
25
30
35
TBHP, mM

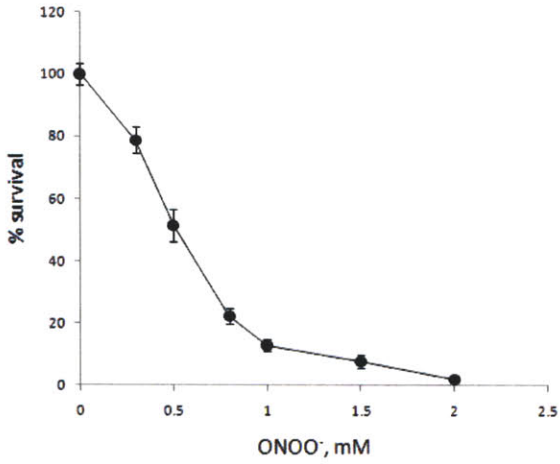
% survival
120
100
80
60
40
20
0
0
0.5
1
1.5
2
2.5
$ONOO^-$, mM

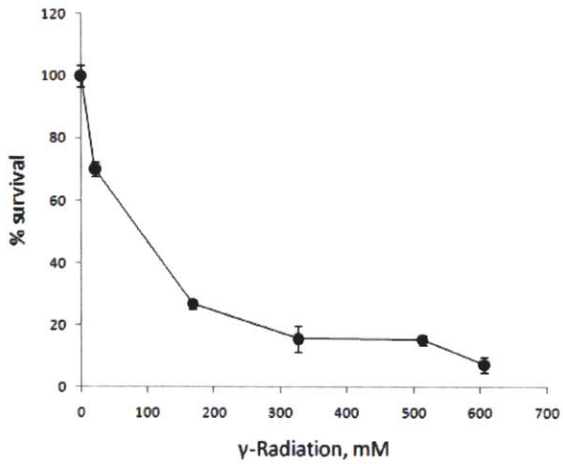
% survival
120
100
80
60
40
20
0
0
100
200
300
400
500
600
700
γ-Radiation, mM

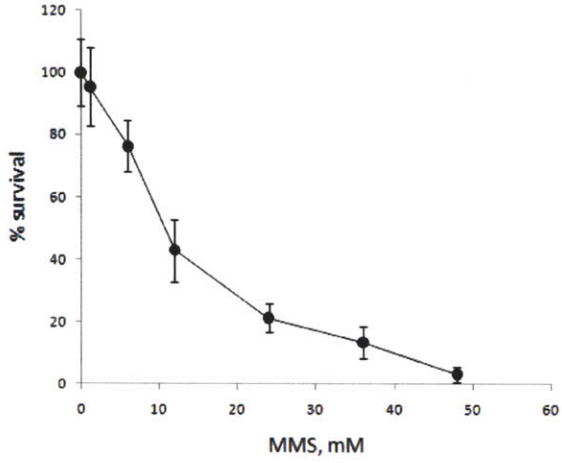
% survival
120
100
80
60
40
20
0
0
10
20
30
40
50
60
MMS, mM

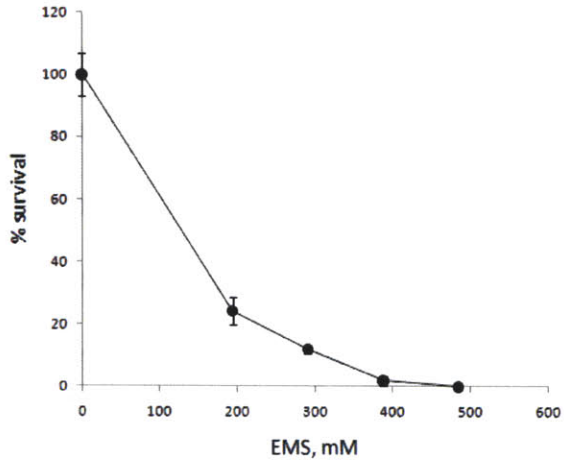
% survival
120
100
80
60
40
20
0
0
100
200
300
400
500
600
EMS, mM

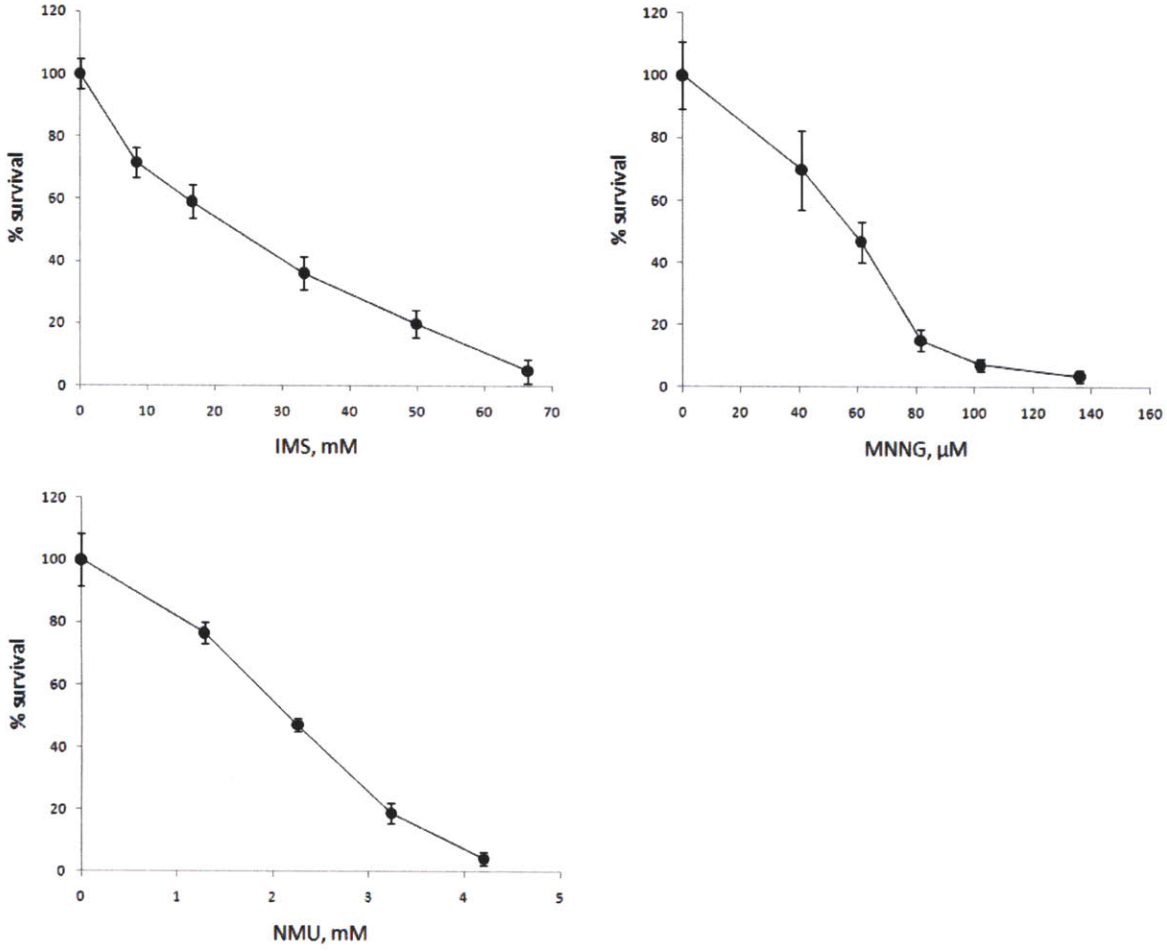

Figure 5-1. Cytotoxicity dose-response studies with *S. cerevisiae* exposed to H_2O_2, TBHP, $ONOO^-$, γ-radiation, MMS, EMS, IMS, MNNG, and NMU. Data represents mean ± SD for three biological replicates.

Characterization of changes in the spectrum of tRNA modifications in response to different toxic agents. With the exposure conditions determined, a liquid chromatography-triple quadrupole mass spectrometric (LC/QQQ) method was used to relatively quantify the

spectrum of 23 tRNA modifications from cells exposed to each of the toxic agent. Identification of modified nucleosides and validation of this LC/QQQ method was described in Chapter 2. The method was used to characterize nine samples from cells exposed to different toxic agents (5 mM H_2O_2, 25 mM TBHP, 0.8 mM $ONOO^-$, 510 G γ-radiation, 24 mM MMS, 190 mM EMS, 50 mM IMS, 82 mM MNNG, and 3 mM NMU) and three samples from unexposed cells (a total of 12 samples). From the three samples of unexposed cells, mass spectrometric signal intensities of each modification were averaged and this average was used as the basal level to determine the fold-change of modification levels in each of the 12 samples. This set of experiments was replicated 5 times to increase statistical power for distinguishing differences between spectra (Table 5-2) and the results reveal that in overall, about 40% of modified nucleosides changed statistically significantly (p values are less than 0.05 in Student's t-test) in response to these nine toxic agents. The mean values of data points from these 5 sets of data and the nucleosides with significant changes are shown in Table 5-3.

Set 1												
Nucleosides	Ctrl1_1	Ctrl1_2	Ctrl1_3	EMS_1	γ-rad_1	H_2O_2_1	IMS_1	MMS_1	MNNG_1	NMU_1	ONOO_1	TBHP_1
D	1.023	1.003	0.973	1.298	1.098	1.048	1.103	0.996	1.030	1.071	1.073	1.092
Y	1.011	1.001	0.988	1.225	1.092	1.035	1.079	0.972	1.024	1.054	1.085	1.082
ncm^5U	1.034	1.055	0.911	1.354	1.557	1.412	1.018	0.927	1.075	0.987	1.365	1.481
I	1.042	0.942	1.015	0.842	1.018	0.965	1.091	0.985	1.012	1.074	1.002	1.022
m^5U	1.054	0.959	0.988	1.158	1.043	1.007	1.078	0.989	1.029	1.028	1.040	1.032
Gm	0.964	1.000	1.036	0.803	1.031	1.009	1.556	1.136	1.285	1.120	1.026	1.055
Um	1.012	0.977	1.011	1.278	1.025	0.891	1.262	0.977	1.104	1.188	1.604	1.257
m^5C	1.034	0.971	0.995	1.112	1.243	1.282	1.094	1.021	1.045	1.055	1.313	1.294
m^3C	1.019	1.004	0.976	1.703	1.105	1.043	1.190	1.515	1.088	1.157	1.074	1.083
Cm	1.028	0.950	1.022	0.828	1.048	1.207	1.099	0.993	0.996	1.063	1.073	1.319
mcm^5U	1.026	0.968	1.006	1.125	1.068	1.083	1.158	1.052	1.074	1.164	1.043	1.128
m^1G	0.974	1.008	1.018	0.853	1.059	1.020	1.095	1.074	0.969	1.040	1.041	1.075
m^2G	0.962	0.992	1.046	0.718	1.035	1.012	1.183	1.098	1.074	1.159	0.994	1.044
ac^4C	1.022	0.991	0.988	1.312	1.085	1.024	1.061	0.956	0.973	0.969	1.113	1.086
t^6A	0.970	1.016	1.014	0.929	1.044	1.171	1.164	1.056	1.075	1.138	1.000	1.064
mcm^5s^2U	1.008	1.005	0.987	1.053	1.045	1.043	1.054	1.031	1.051	1.043	1.014	1.094
m^7G	1.065	0.985	0.949	1.214	1.105	1.034	1.098	1.433	0.900	1.289	1.106	1.087
m^1I	0.958	1.003	1.039	0.670	1.065	0.791	0.988	0.902	0.838	0.882	1.027	1.075
Am	1.008	0.991	1.001	0.989	1.063	0.972	1.666	0.982	1.526	1.604	1.619	1.065
$m^2{}_2G$	0.961	1.003	1.035	0.708	1.349	1.440	1.159	1.005	1.047	1.126	0.997	1.042
I6A	1.044	0.991	0.966	1.429	1.125	1.059	1.122	1.012	1.010	1.053	1.130	1.145
yW	1.456	0.712	0.832	1.005	0.743	0.715	1.313	0.612	1.429	1.244	1.624	0.720
m^1A	1.013	1.007	0.979	1.106	1.086	1.046	1.103	1.002	0.998	1.072	1.071	1.082

Set 2												
Nucleosides	Ctrl2_1	Ctrl2_2	Ctrl2_3	EMS_2	γ-rad_2	H_2O_2_2	IMS_2	MMS_2	MNNG_2	NMU_2	ONOO_2	TBHP_2
D	1.016	1.065	0.918	1.065	1.128	1.093	1.249	1.131	1.023	1.031	1.016	1.011
Y	1.098	1.006	0.895	0.941	1.074	1.082	1.133	1.083	0.953	0.953	1.063	0.987
ncm^5U	0.982	0.897	1.121	0.765	1.071	1.274	0.990	0.949	0.836	1.057	1.250	1.112
I	1.111	0.972	0.917	0.994	1.034	1.002	1.186	1.052	0.899	0.947	1.006	0.932
m^5U	1.089	0.997	0.914	1.049	1.129	1.072	1.241	1.097	0.995	1.041	1.052	1.099
Gm	0.945	1.063	0.992	1.184	1.037	1.062	1.768	1.149	1.250	1.029	0.922	0.981
Um	1.089	0.988	0.924	0.814	0.704	1.129	0.985	0.823	0.868	0.997	1.142	0.834
m^5C	1.029	1.033	0.937	0.933	1.319	1.366	1.121	0.958	0.870	0.942	1.226	1.224
m^3C	0.993	1.052	0.954	1.608	1.028	1.056	1.375	1.763	1.141	1.194	0.962	1.015
Cm	1.052	1.028	0.920	0.915	1.015	1.218	1.182	1.027	0.850	0.894	0.910	1.227
mcm^5U	0.969	1.051	0.979	1.207	1.113	1.043	0.986	1.103	0.973	1.320	0.985	0.960
m^1G	0.971	1.079	0.950	1.045	1.084	1.067	1.206	1.092	0.958	0.995	0.972	1.014
m^2G	0.960	1.063	0.977	1.081	1.085	1.070	1.347	1.211	1.063	1.107	0.914	1.017
ac^4C	1.013	1.050	0.936	1.000	1.068	1.040	1.160	1.059	0.929	0.988	0.984	0.979
t^6A	0.996	1.036	0.968	1.132	1.040	1.910	1.296	1.215	1.001	1.129	0.955	1.031
mcm^5s^2U	0.986	1.079	0.935	1.102	1.005	1.448	1.701	1.259	0.946	1.053	1.175	1.166
m^7G	1.004	1.050	0.946	1.487	1.073	1.076	1.285	1.802	0.999	1.461	0.979	1.021
m^1I	0.958	1.151	0.891	0.787	0.988	0.676	0.949	1.022	0.717	0.934	0.916	0.827
Am	0.934	1.076	0.990	1.056	1.045	1.036	1.526	1.157	1.618	1.611	1.530	0.980
$m^2{}_2G$	0.960	1.052	0.988	1.114	1.581	1.757	1.294	1.157	1.044	1.085	0.948	1.035
I6A	0.914	1.104	0.982	1.157	1.067	1.250	1.349	1.151	1.036	1.155	1.008	1.029
yW	1.037	0.988	0.975	0.802	1.026	1.170	0.738	0.378	0.627	0.674	1.214	0.929
m^1A	0.984	1.084	0.931	1.084	1.096	1.092	1.318	1.163	1.010	1.070	0.986	1.022

Set 3												
Nucleosides	Ctrl3_1	Ctrl3_2	Ctrl3_3	EMS_3	γ-rad_3	H_2O_2_3	IMS_3	MMS_3	MNNG_3	NMU_3	ONOO_3	TBHP_3
D	1.069	0.975	0.956	1.026	0.898	0.963	1.084	0.998	1.072	1.040	0.841	0.875
Y	1.084	0.943	0.974	1.044	0.892	0.930	1.069	0.976	1.134	1.012	0.888	0.880
ncm^5U	0.982	1.112	0.905	1.165	1.086	0.951	1.095	1.014	1.118	1.138	0.817	1.035
I	1.062	0.940	0.998	0.989	0.877	0.971	0.996	0.925	1.034	0.941	0.885	0.802
m^5U	0.989	1.015	0.996	1.007	0.935	0.976	1.154	1.058	1.125	0.999	0.994	0.994
Gm	0.965	1.043	0.991	1.268	0.991	0.994	1.681	0.950	1.307	1.039	0.955	0.960
Um	1.085	0.816	1.100	0.675	1.494	0.642	1.288	0.812	1.110	1.114	1.524	1.097
m^5C	0.982	1.029	0.989	1.069	1.257	1.310	1.095	1.064	1.122	1.038	1.268	1.229
m^3C	0.962	1.041	0.997	1.752	0.970	0.984	1.300	1.493	1.218	1.142	0.948	0.963
Cm	1.011	0.986	1.003	0.967	0.933	1.103	1.009	0.923	0.992	0.944	0.883	1.138
mcm^5U	0.798	1.164	1.038	1.529	1.211	1.348	1.408	1.284	1.480	1.241	1.188	1.247
m^1G	1.000	1.028	0.972	0.988	0.957	0.952	1.033	0.962	1.045	0.972	0.874	0.908
m^2G	1.001	1.011	0.988	1.179	0.992	0.991	1.176	1.064	1.209	1.141	0.961	0.974
ac^4C	1.069	1.025	0.906	1.066	0.961	0.946	1.071	0.970	1.043	1.016	1.016	0.888
t^6A	0.956	1.029	1.015	1.180	0.998	1.586	1.165	1.115	1.164	1.113	1.022	0.990
mcm^5s^2U	0.840	1.059	1.100	1.267	1.209	1.341	1.392	1.462	1.550	1.065	1.249	1.155
m^7G	1.006	1.011	0.983	1.454	0.909	0.940	1.116	1.812	1.190	1.505	0.872	0.893
m^1I	1.103	0.972	0.925	0.885	0.861	0.813	0.764	0.679	0.852	0.777	0.879	0.669
Am	0.992	1.025	0.983	1.103	0.995	0.991	1.640	1.005	1.725	1.663	1.396	0.956
m^2_2G	0.976	1.044	0.980	1.143	1.445	1.449	1.168	1.061	1.162	1.066	0.987	0.991
i6A	0.957	1.061	0.981	1.258	1.339	1.181	1.291	1.091	1.092	1.042	1.172	1.117
yW	1.103	1.002	0.894	0.506	0.977	0.912	0.558	0.512	0.631	0.588	0.829	0.772
m^1A	0.999	1.035	0.967	1.113	1.003	0.995	1.140	1.051	1.217	1.092	0.997	0.950

Set 4												
Nucleosides	Ctrl4_1	Ctrl4_2	Ctrl4_3	EMS_4	γ-rad_4	H_2O_2_4	IMS_4	MMS_4	MNNG_4	NMU_4	ONOO_4	TBHP_4
D	0.976	1.011	1.013	1.092	1.038	1.176	1.230	1.104	1.074	1.095	1.056	1.165
Y	0.973	1.016	1.011	1.117	1.033	1.273	1.259	1.063	1.097	1.084	1.089	1.166
ncm^5U	1.050	0.995	0.954	1.032	1.042	1.440	1.100	0.898	0.939	1.128	1.187	1.198
I	0.995	1.055	0.950	1.176	1.098	1.267	1.197	1.085	1.051	1.187	1.145	1.223
m^5U	0.686	1.362	0.952	0.918	0.732	0.891	1.036	0.976	1.052	1.124	1.474	0.909
Gm	0.993	1.008	0.999	1.237	1.036	1.069	1.519	1.072	1.264	1.121	1.047	1.091
Um	0.960	1.032	1.007	1.190	1.106	0.958	1.290	1.052	1.265	1.275	1.572	1.412
m^5C	0.984	0.998	1.017	1.101	1.169	1.614	1.172	1.031	1.074	1.206	1.360	1.391
m^3C	0.948	1.027	1.025	1.546	0.993	1.002	1.252	1.657	1.188	1.223	0.995	1.071
Cm	0.959	0.982	1.059	1.043	0.954	1.386	1.137	1.028	1.099	1.164	1.082	1.384
mcm^5U	0.914	1.034	1.052	1.204	1.093	1.061	1.224	1.217	1.132	1.200	1.039	1.130
m^1G	0.979	1.006	1.015	1.029	1.085	1.127	1.059	1.006	1.023	1.062	1.058	1.158
m^2G	0.990	1.012	0.998	1.080	1.048	1.141	1.167	1.046	1.086	1.138	1.063	1.114
ac^4C	0.972	1.015	1.013	1.072	1.044	1.351	1.133	0.985	1.026	1.184	1.163	1.166
t^6A	1.395	0.845	0.760	0.803	0.936	1.377	0.819	0.814	0.933	0.819	0.952	0.682
mcm^5s^2U	0.954	1.027	1.020	1.014	0.959	0.822	1.023	0.999	1.085	1.208	0.878	0.825
m^7G	0.896	1.027	1.077	1.454	0.888	1.084	1.189	1.720	1.141	1.635	0.987	1.082
m^1I	0.967	1.003	1.030	0.935	1.022	0.775	0.951	0.955	0.913	0.911	0.982	0.926
Am	1.095	0.979	0.926	0.977	1.017	0.941	1.380	0.992	1.640	1.550	1.612	0.926
m^2_2G	1.143	0.957	0.900	0.977	1.364	1.516	1.019	0.924	1.012	1.009	1.117	0.925
i6A	1.442	0.794	0.765	0.870	1.024	1.601	0.914	0.720	0.784	0.991	1.544	1.205
yW	1.056	1.038	0.906	0.764	1.103	1.268	0.622	0.644	0.604	0.599	1.158	1.088
m^1A	0.968	1.022	1.009	1.119	1.040	1.053	1.174	1.116	1.078	1.156	1.011	1.090

Set 5												
Nucleosides	Ctrl5_1	Ctrl5_2	Ctrl5_3	EMS_5	γ-rad_5	H_2O_2_5	IMS_5	MMS_5	MNNG_5	NMU_5	ONOO_5	TBHP_5
D	1.156	0.948	0.896	0.994	0.946	1.065	1.077	0.945	0.929	0.950	1.008	1.008
Y	1.171	0.939	0.890	1.005	0.993	1.160	1.071	0.938	0.938	0.938	1.084	1.090
ncm^5U	0.992	0.995	1.013	1.018	1.056	1.377	1.109	0.947	1.050	1.138	1.178	1.089
I	1.248	0.885	0.868	0.977	0.979	1.200	1.078	0.897	1.028	1.049	1.159	1.094
m^5U	1.016	0.976	1.008	1.487	0.968	1.148	1.144	1.044	1.044	1.095	0.975	1.056
Gm	1.102	0.953	0.945	1.108	0.960	0.969	1.415	0.968	1.153	0.987	0.952	0.962
Um	0.868	0.998	1.134	1.083	0.945	0.902	1.377	1.020	1.264	1.197	0.682	1.196
m^5C	1.117	0.934	0.948	1.028	1.081	1.474	1.098	0.935	0.997	1.072	1.278	1.229
m^3C	1.115	0.946	0.939	1.358	0.956	1.025	1.118	1.482	1.009	1.046	0.954	0.926
Cm	1.080	0.956	0.964	0.980	0.966	1.230	1.049	0.949	0.969	1.004	0.999	1.248
mcm^5U	0.912	1.011	1.077	1.057	0.927	0.970	1.152	1.130	1.221	1.107	0.857	0.932
m^1G	1.085	0.963	0.952	0.927	0.993	1.044	0.963	0.901	0.881	0.901	0.989	0.999
m^2G	1.089	0.955	0.957	1.017	0.974	1.030	1.079	0.989	1.023	1.036	0.968	0.992
ac^4C	1.092	0.955	0.953	0.912	0.941	0.895	0.985	0.937	0.926	0.922	0.920	0.941
t^6A	1.101	0.944	0.955	0.811	0.982	0.827	0.814	0.823	0.789	0.777	0.944	0.879
mcm^5s^2U	0.526	1.167	1.306	1.234	0.929	0.748	1.245	1.112	1.406	1.309	0.846	1.035
m^7G	1.048	0.991	0.961	1.364	0.991	1.058	1.058	1.479	0.949	1.368	0.987	1.016
m^1I	1.102	0.944	0.954	0.835	0.947	0.696	0.851	0.820	0.806	0.799	0.921	0.803
Am	1.034	0.978	0.989	1.004	0.977	0.961	1.451	1.002	1.638	1.593	1.557	0.959
$m^2{}_2G$	0.985	0.992	1.023	1.058	1.341	1.616	1.105	1.003	1.105	1.136	1.140	1.112
i6A	0.946	1.001	1.053	1.097	1.109	1.695	1.183	0.965	1.112	1.244	1.581	1.207
yW	1.102	0.932	0.965	0.662	1.046	1.121	0.598	0.629	0.590	0.586	1.057	0.995
m^1A	0.894	1.071	1.035	1.005	1.075	1.016	0.986	0.978	0.996	1.035	1.021	0.965

Table 5-2. Fold-change of levels of nucleosides in 5 biological replicates. In the 5 sets of data, each set contains 12 samples, including 3 samples from unexposed cells and 9 samples from cells which each one was exposed to a different toxic agent. Levels of each nucleoside from the three replicates of unexposed cells were averaged; fold-change of the nucleoside in each sample was relative to this mean value.

	Oxidizing agents				Alkylating agents				
Nucleosides	TBHP	γ-rad	H_2O_2	$ONOO^-$	MMS	MNNG	NMU	IMS	EMS
D	1.030	1.021	1.069	0.999	1.035	1.026	1.037	1.149	1.095
Ψ	1.041	1.017	1.096	1.042	1.007	1.029	1.008	1.122	1.066
ncm^5U	1.183	1.162	1.291	1.159	0.947	1.004	1.090	1.062	1.067
I	1.015	1.001	1.081	1.039	0.989	1.005	1.039	1.110	0.996
m^5U	1.018	0.961	1.019	1.107	1.033	1.049	1.057	1.131	1.124
Gm	1.010	1.011	1.021	0.981	1.055	1.252	1.059	1.588	1.120
Um	1.159	1.055	0.905	1.305	0.937	1.122	1.154	1.240	1.008
m^5C	1.273	1.214	1.409	1.289	1.002	1.021	1.063	1.116	1.049
m^3C	1.012	1.010	1.022	0.987	1.582	1.129	1.152	1.247	1.593
Cm	1.263	0.983	1.229	0.989	0.984	0.981	1.014	1.095	0.947
mcm^5U	1.079	1.082	1.101	1.022	1.157	1.176	1.207	1.185	1.224
m^1G	1.031	1.036	1.042	0.987	1.007	0.975	0.994	1.071	0.969
m^2G	1.028	1.027	1.049	0.980	1.081	1.091	1.116	1.191	1.015
ac^4C	1.012	1.020	1.051	1.039	0.981	0.979	1.016	1.082	1.072
t^6A	0.929	1.000	1.374	0.975	1.005	0.992	0.995	1.051	0.971
mcm^5s^2U	1.055	1.029	1.080	1.032	1.173	1.208	1.135	1.283	1.134
m^7G	1.020	0.993	1.038	0.986	1.649	1.036	1.452	1.149	1.395
m^1I	0.860	0.977	0.750	0.945	0.876	0.825	0.860	0.901	0.822
Am	0.977	1.019	0.980	1.543	1.027	1.629	1.604	1.533	1.026
m^2_2G	1.021	1.416	1.556	1.038	1.030	1.074	1.084	1.149	1.000
i6A	1.140	1.133	1.357	1.287	0.988	1.007	1.097	1.172	1.162
yW	0.901	0.979	1.037	1.176	0.555	0.776	0.738	0.766	0.748
m^1A	1.022	1.060	1.040	1.017	1.062	1.060	1.085	1.144	1.085

Table 5-3. Mean values of fold-change data. In the 5 biological replicates of each exposure as shown in Table 5-1, the fold-change of abundance of each modification was averaged and then presented in this table. The changes that are statistically significant ($p < 0.05$) are highlighted.

Patterns of tRNA modifications spectrum in response to toxic agents are class-specific. Relative quantification of modified nucleosides with statistical analysis has illustrated that the spectrum alters in response to a group of alkylating agents and of oxidizing agents. These results provide us the information to test the hypothesis that patterns of changes in tRNA modification spectrum share common features in cells exposed to toxic agents with similar mechanisms of action. Our first step was to use hierarchical clustering to analyze the data in

Table 5-3, which the spectrum from each exposure condition is the average of 5 biological replicates. As shown in Figure 5-2, samples from alkylating agent-exposed cells clustered into one group and those from oxidizing agent-exposed cells clustered into another group, which implies that the patterns of changes in the spectra caused by the same class of toxic agents are more similar than those caused by the other class.

Ribonucleosides responsible for defining the unique patterns can be indicated from the heat map (Figure 5-2). The relative levels of yW and m^1I decreased in all alkylating agent-exposed cells but the changes in oxidizing agent-exposed cells were not significant. Also, all alkylating agents caused an elevation in the levels of Um, m^2G, mcm^5s^2U, mcm^5U, and m^1A, while these modifications responded to oxidizing agents mildly. In contrast, the levels ncm^5U, m^5C, and i^6A did not change in all alkylating agent-exposed cells but they increased significantly in response to all oxidizing agents.

Subclass signatures were also observed among the alkylating agent group. Modifications spectra from cells exposed to MMS and EMS were clustered to form one group while IMS, MNNG, and NMU were clustered to form another group; the formation of subgroups suggests that the responses to different reagents of the same class may be different. Indeed, the relative levels of m^3C and m^7G increased in MMS- and EMS-exposed cells but their responses to IMS, MNNG, and NMU were weaker. Another group of subclass signatures was the rise of Um and Am levels in cells exposed to IMS, MNNG, and NMU while the levels of these modifications in MMS- and EMS-exposed cells did not increase.

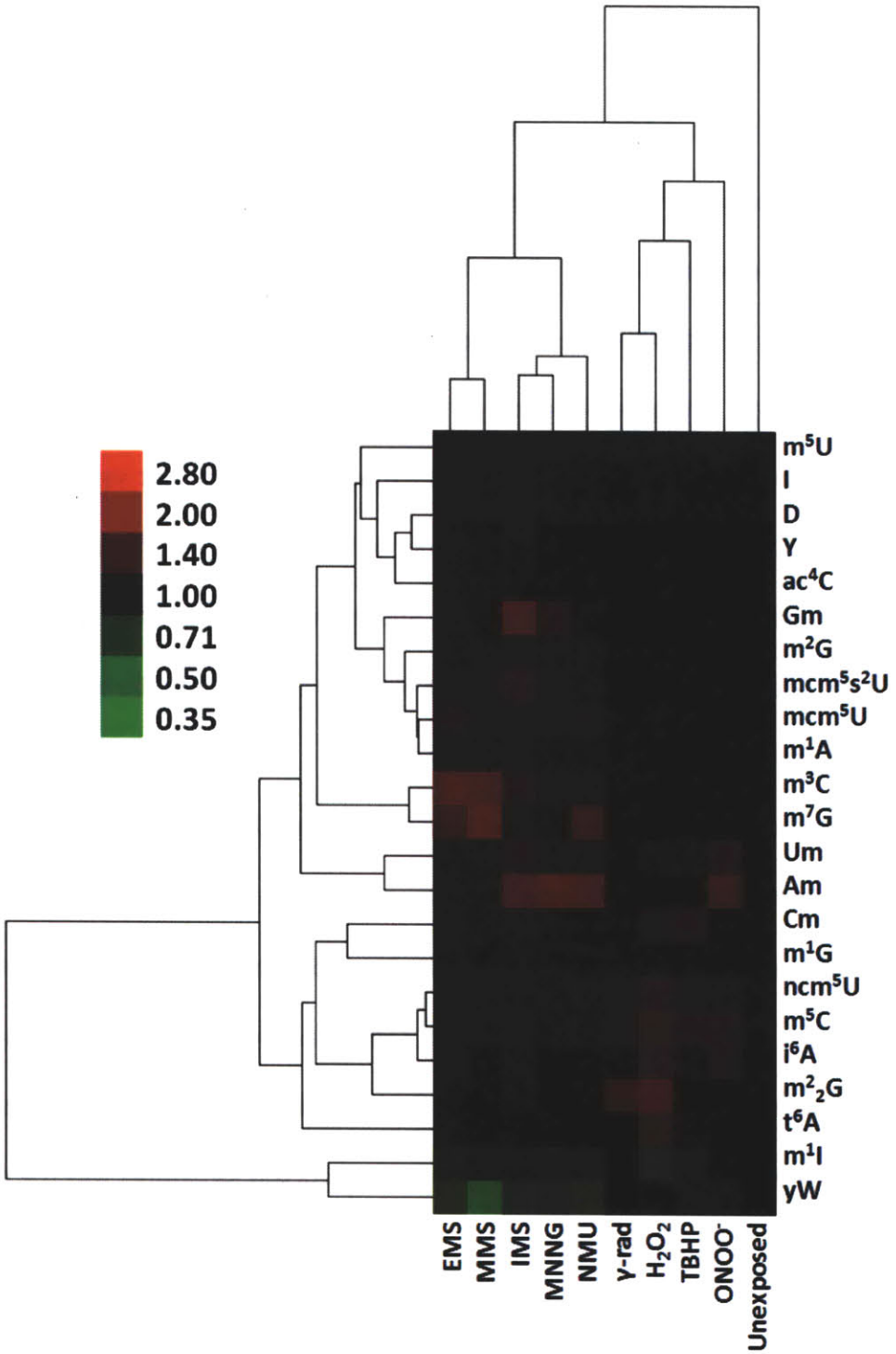
2.80
2.00
1.40
1.00
0.71
0.50
0.35
m5U
I
D
Y
ac4C
Gm
m2G
mcm5s2U
mcm5U
m1A
m3C
m7G
Um
Am
Cm
m1G
ncm5U
m5C
i6A
m22G
t6A
m1I
yW
EMS
MMS
IMS
MNNG
NMU
γ-rad
H2O2
TBHP
ONOO-
Unexposed

Figure 5-2. Hierarchical clustering analysis of averaged tRNA modifications spectra from cells exposed to different alkylating agents and oxidizing agents. The fold-change data was originated from the average of five biological replicates as presented in Table 5-2 and hierarchical clustering analysis was performed in log space (log base 2). Color code of the heat map was shown on the left-top corner.

Hierarchical clustering analysis of the averaged tRNA modification spectra from the five data sets indicates clearly the presence of class-specific patterns of changes in responses to toxic agents. However, when hierarchical clustering analysis was carried out with the data from raw spectra (the five data sets in Table 5-2), signatures for the two groups of toxic agents were less clear (Figure 5-3). In Figure 5-3, most spectra from alkylating agent-exposed cells were grouped together with exceptions of those spectra from EMS-, IMS-, NMU-, and MNNG-exposed cells in data set 1. For the 15 spectra from unexposed cells (3 spectra from each data set), 13 of them were clustered into one subgroup while the other two were mixed with spectra from oxidizing agent-exposed cells. Spectra from cells treated with oxidizing agents were divided into two groups. One group mainly comprised $ONOO^-$- and TBHP-exposed samples, and this group shared more common features with the unexposed samples than with the H_2O_2- and γ-rad-exposed samples in the other cluster group. Further, two spectra from γ-rad-exposed cells were clustered into the unexposed group.

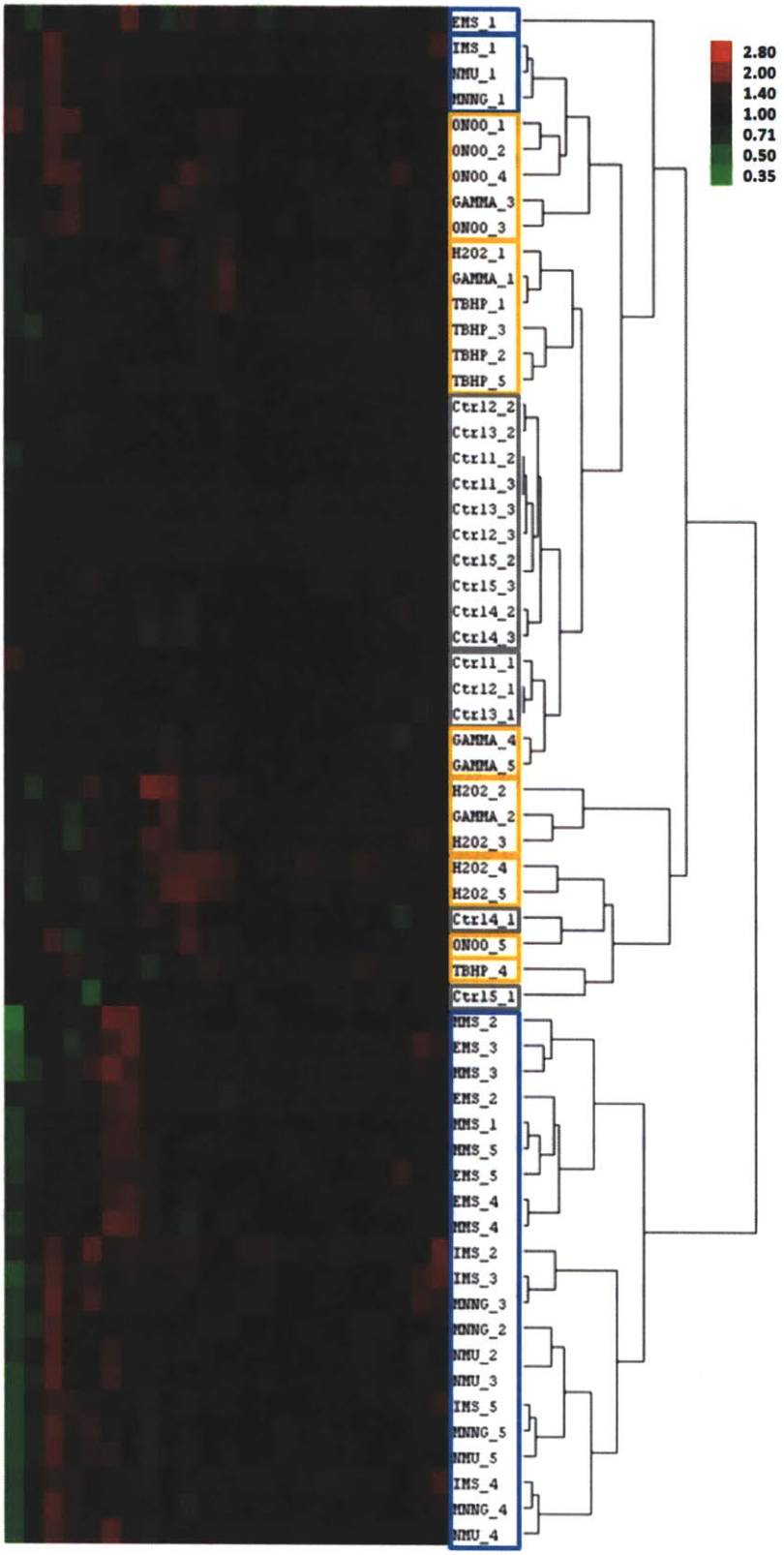
EMS_1
IMS_1
NMU_1
MNNG_1
ON00_1
ON00_2
ON00_4
GAMMA_3
ON00_3
H202_1
GAMMA_1
TBHP_1
TBHP_3
TBHP_2
TBHP_5
Ctrl2_2
Ctrl3_2
Ctrl1_2
Ctrl1_3
Ctrl3_3
Ctrl2_3
Ctrl5_2
Ctrl5_3
Ctrl4_2
Ctrl4_3
Ctrl1_1
Ctrl2_1
Ctrl3_1
GAMMA_4
GAMMA_5
H202_2
GAMMA_2
H202_3
H202_4
H202_5
Ctrl4_1
ON00_5
TBHP_4
Ctrl5_1
MMS_2
EMS_3
MMS_3
EMS_2
MMS_1
MMS_5
EMS_5
EMS_4
MMS_4
IMS_2
IMS_3
MNNG_3
MNNG_2
NMU_2
NMU_3
IMS_5
MNNG_5
NMU_5
IMS_4
MNNG_4
NMU_4
2.80
2.00
1.40
1.00
0.71
0.50
0.35

Figure 5-3. Hierarchical clustering analysis of individual tRNA modifications spectra from unexposed, alkylating agent-exposed, and oxidizing agents-exposed cells. The fold-change data for this analysis was presented in the 5 data sets in Table 5-1. Hierarchical clustering analysis was performed in log space (log base 2) and color code for the heat map was shown on the left-top corner. Clusters of samples that exposed to the same class of reagents are boxed with the following color code; oxidizing agent-exposed: yellow; alkylating agent-exposed: blue; and unexposed: grey.

Data-driven model to describe biomarker signatures for distinguishing alkylating agent-exposed and oxidizing agent-exposed cells. Hierarchical clustering analysis of tRNA modifications levels in cells exposed to alkylating agents and oxidizing agents demonstrates that the patterns of changes in the spectrum are specific to these two classes of reagents (Figure 5-2). These results led us to ask if these changes can be used to identify biological statuses and what changes in the spectrum are important for classifying cells from different exposure groups. To this end, we developed a data-driven model with the K-nearest neighbor method (KNN) to describe differences in changes in tRNA modifications spectrum as responses to the two classes of stimuli (alkylating agents and oxidizing agents). Following 20 training and test cycles of supervised learning by using the programming software R, a stable model has been established. The overall confusion matrix demonstrates prediction sensitivities for the alkylating agent-exposed group (AA) is 95%, for oxidizing agent-exposed group (OX) is 94%, and for unexposed group (CT) is 78%, and prediction specificities for AA is 95%, OX is 76%, and CT is 98% (Figure 5-4). Based upon this model, the modified ribonucleosides that contributed in identifying exposures to alkylating agents include m^3C, m^7G, yW, mcm^5U, Am, Gm, m^1A, m^5C, m^2G, mcm^5s^2U, and m^1I, and those for identifying oxidizing agent-exposures are m^5C, m^3C, m^7G,

Gm, ncm^5U, $m^2{}_2G$, i^6A, yW, and Cm. These features match with those in the hierarchical clustering analysis (Figure 5-2). With high prediction sensitivity and specificity for akylating agents, this class of chemicals is significantly different from the others. The prediction specificity of OX is relatively low (76%) due to high variation of the controls, which causes misclassification of controls into the oxidation agent group.

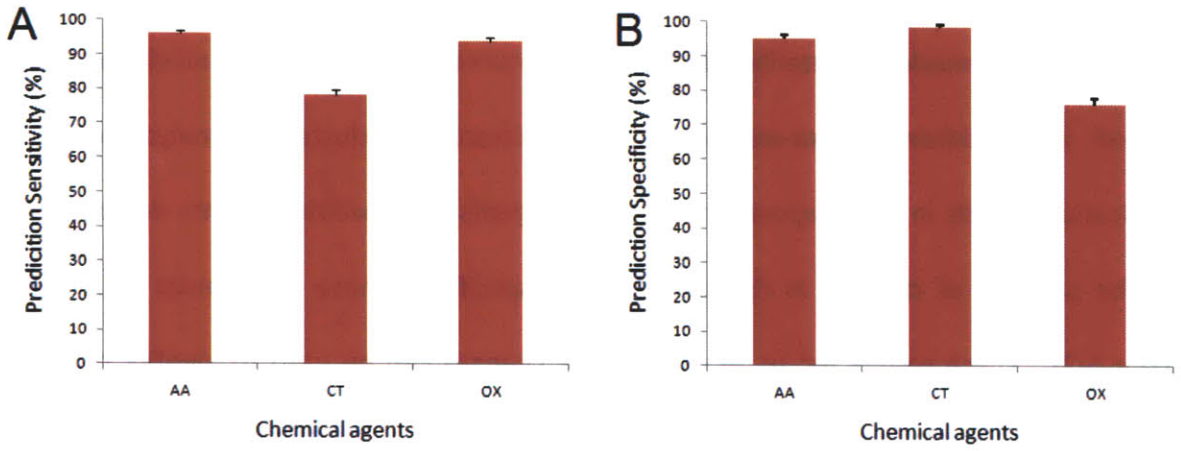

Figure 5-4. Prediction (**A**) sensitivity and (**B**) specificity of the data-driven model. A total of 20 training and test cycles have been performed for the combined data to determine the average prediction sensitivity and specificity. The data driven model is stable due to low standard error with less than 2%.

Discussion

Experimental design for assessing changes in tRNA modifications spectrum. One of our goals of this study is to compare the spectra of tRNA modifications from cells exposed to two classes of toxicants, oxidizing agents and alkylating agents, in which we hypothesized that exposures to reagents of the same class lead to common features of changes. We first isolated tRNA from cell lysates and quantified tRNA in each samples. An isotope-labeled nucleoside was added in proportion to the quantity of tRNA and the samples were hydrolyzed enzymatically to nucleosides. In each sample, the spectrum of modified ribonucleosides was monitored with a LC/MS method. The level of each modified nucleoside was normalized by MS signal intensity of the isotopic standard. In each sample of cells, changes in tRNA modifications spectrum was defined by the fold-change of nucleoside levels relative to that in the unexposed cells. Hierarchical clustering analysis was then used to identify spectra with common features for which we expected spectra from cells exposed to the same class of toxicants to cluster. However, as shown in Figure 5-3, samples from cells with no exposures and with exposures to oxidizing agents and alkylating agents did not distinctly characterized into three groups and these observations suggest that the pattern of changes in each tRNA modifications spectrum contains noises, which can be originated from measurement errors. For instance, spectra from cells exposed to EMS, IMS, NMU, and MNNG in data set 1 were clustered into the oxidizing agent-exposed group while all the other alkylating agent-exposed samples clustered to form another group; these observations strongly suggests that systematic errors occurred in

experiments for data set 1. Besides, fluctuations in levels of modifications can be caused by deviations in environment, such as temperature, aeration, and nutrients supply.

To solve this problem, we reduced the noises in our data by replicating the experiments. As all spectra were compared to the spectrum of unexposed cells, fluctuations in this spectrum would affect the fold-change data of all samples. Thus, we triplicated the quantification of tRNA modifications from unexposed cells and used the average for data analysis. Also, the whole set of experiments was repeated with 5 biological replicates. Mean values of the 5 data sets were analyze with hierarchical clustering to generate Figure 5-2, which have shown class-specific signatures as responses to the two mechanistically different groups of toxic agents.

Correlations between subclass signatures and mechanisms of action among alkylating agents. Results of hierarchical clustering analysis as shown in Figure 5-2 illustrate that patterns of changes induced by the 5 alkylating agents were also classified into two subgroups, where changes induced by MMS and EMS were more similar to each other and so as those by IMS, MNNG, and NMU. For instances, the relative levels of m^7G and m^5C in MMS- and EMS-exposed cells increased more significantly than in IMS-, MNNG-, and NMU-exposed cells. In contrast, the levels of Am and Um did not change in response to MMS and EMS but they were elevated when cells were treated with the other three alkylating agents. These results suggest that depending on chemical properties of the alkylating agents, a unique set of cellular response pathways was activated. It has been shown that alkylating agents can react with various biological molecules, including proteins and DNA (*10-12*), in which DNA adducts caused by these reagents were studied extensively (Table 5-4). As listed in Table 5-3, MMS and EMS can

alkylate DNA via a S_N2 mechanism while IMS, MNNG, and NMU only via S_N1. The difference in reaction mechanisms affects the alkylation reactivity at different sites. For instance, in in vitro reactions, less than 0.5% of DNA adducts are formed at O^6 of guanine when DNA reacts with MMS or EMS but 7.0% to 23.7% of adducts formed by IMS, MNNG or NMU are at this position (Table 5-4). DNA adducts are generally repaired by either direct transfer of the modifying alkyl group to a transferase, or removal of the modified base by a glycosylase, followed by excision of the apurinic or apyrimidinic site (*13*). In cases that the structure of DNA helix was distorted, nucleotide excision repair may be employed (*14*). Each transferase and glycosylase is responsible for repairing a specific set of adducts. For O^6-alkylguanines that mentioned above, these adducts are exclusively repaired by O^6-alkylguanine-DNA alkyltransferase in both rat and *E. coli* (*13, 15-17*) and a homologue of this enzyme was also found in *S. cerevisiae*. Thus, in response to each alkylating agent, the translation machinery may be reprogrammed to favor the expression of enzymes responsible for repairing the specific group of adducts, and these changes may be reflected as subclass signatures in tRNA modifications spectrum for S_N1 and S_N2 alkylating agents.

For the four oxidizing agents, we used one reactive nitrogen species (RNS), $ONOO^-$, one species of strong ionizing radiation, γ-rad, and two reactive oxygen species (ROS), H_2O_2 and TBHP. Potentially, reactive oxygen species and reactive nitrogen species can induce different response pathways as they generate widely different species of adducts (*18-20*). Hierarchical clustering analysis (Figure 5-2) indicates that spectrum of $ONOO^-$ contains unique features from spectra of other oxidizing agents. For instance, Am increased in $ONOO^-$-exposed cells but not in other oxidizing agent samples. Experiments with more species of oxidants are necessary to

define subclass signatures between ROS and RNS. Interestingly, among spectra of the other three oxidizing agent, H_2O_2 is more similar to γ-rad than to TBHP. Both H_2O_2 and γ-rad generate hydroxyl radical that leads to DNA strand breaks, and formations of abasic sites and a broad spectrum of adducts. Thus, the cellular responses for both reagents may be very similar.

Sit of Alkylation	MMS	EMS	IMS	MNNG	NMU
Adenine					
N^1	3.8	1.7	--	1.0	1.3
N^3	11.3	4.9	0.4	12.0	9.0
N^7	1.8	1.9	--	--	2.0
Cytosine					
N^3	<1.0	0.6	--	2.0	0.6
Guanine					
N^3	0.6	0.9	--	--	1.9
O^6	0.3	0.2	23.7	7.0	8.2
N^7	83.0	65.0	47.4	67	70
Thymidine					
O^2	nd	nd	4.3	0.3	--
N^3	0.1	nd	0.4	0.3	--
O^4	nd	nd	4.3	0.7	--
Mechanisms	S_N2	S_N1/S_N2	S_N1	S_N1	S_N1

Table 5-3. In vitro alkylation patterns of DNA by MMS, EMS, IMS, MNNG, and NMU. Adducts formed at different sites are expressed as percent of total adducts. 'nd' indicates the adduct is not detectable and '--' indicates information is not found. The proposed mechanism (S_N1 or S_N2) for each alkylating agent is also listed at the last row of this table. Information was collected from several studies (*21-27*).

tRNA modifications spectrum as a source of biomarkers. Given that the spectra of tRNA modifications formed class-specific patterns, we developed a data-driven model to predict the type of stress that cells were exposed to, based upon the unique features induced by each class of stimuli. The purposes of this exercise are to gain insight in the biological functions of tRNA modifications in stress responses, and also, to explore the utilities of tRNA modifications spectra as biomarkers. Based on our model, 14 tRNA modifications were involved in defining unique patterns and they are listed in Table 5-4. As shown in this table, some modifications are located at more than one position and at multiple species of tRNA, which complicated the scenario as our method cannot assess their quantitative distribution. Interestingly, 10 of these 14 model-defining modifications are found at anticodon region, which suggests that they can be involved in interacting with codons and in recognizing aminoacyl-tRNA synthetases (*28*). For instance, level of m^5C increased in response to oxidizing agent and it is located at the wobble position of the tRNA for coding the codon UUG; in Chapter 3 and 4, we gained evidence to support our hypothesis that m^5C confers resistance to H_2O_2 by regulating translation of H_2O_2-resisting genes that are enriched in TTG. Further studies are necessary to test if other modifications are involved in similar regulatory pathways. In contrast, some model-defining modifications are only located at a single species of tRNA, which allow us to study their biological roles directly by altering their biosynthetic pathways. These modifications include, mcm^5U, mcm^5s^2U, m^3C, Am, yW, and m^1I. The increases in relative level of mcm^5U and mcm^5s^2U are consistent with the results of a study by Begley and coworkers, using trm9-knockout to demonstrate that mcm^5U confers resistance to MMS by promoting the expression of a specific group of DNA damage-response genes (*29*). For Am and m^3C, the same approach

cannot be used to study their functions as genes responsible for the formation of these two modifications are not identified (*30*). Also, gene-knockout experiments cannot be used to study yW and m^1I as formation of both modifications require an essential gene, *trm5*. Niu and coworkers suggested that *trm5* is involved in regulation of cell cycle (*31*) and thus, the decreases in both yW and m^1I levels may be indicating that cells were not ready for differentiation under stress from alkylating agents.

To validate the predictive power of our data-driven model, we used it to distinguish spectra from cells with the three classes of exposures (alkylating agents, oxidizing agents, and no exposure) and results showed that both sensitivity and specificity for predicting the three classes are all above 75%. Previously, numerous studies used transcriptomes, proteomes, and metabolomes to indicate disease-states and toxicant-exposures (*6, 7, 32, 33*). However, to our awareness, this is the first time that spectrum of tRNA modifications was demonstrated to be a potential source of biomarkers. tRNA of each organism comprises 20-30 modifications, which combination of changes can potentially result as a wide range of patterns that can be used for identifying subtly different physiological conditions. This is supported by the presence of subclass signatures for S_N1 and S_N2 alkylating agents.

In conclusion, we employed mass spectrometric-based quantitative techniques and computational statistical tools to demonstrate that the patterns of changes in tRNA modifications spectrum are specific to classes of toxicants. To serve as a proof of principle, we developed a predictive model to show that unique features from the spectra can be used as toxicant class-specific identifier of cellular exposures. We expected that tRNA modifications in other organisms also change dynamically as a function of cellular conditions, and this may

provide a new level of information to develop diagnostic and prognostic biomarkers for various diseases.

tRNA modification	Position of modification	Genes responsible for modification
Increased in alkylating agents		
m^3C	32 of $tRNA^{Thr}$(IGU)	Unknown
m^7G	46 of multiple tRNAs	*TRM8, TRM82*
mcm^5U	34 of $tRNA^{Arg}$(mcm^5UCU)	*TRM9, ELP1-ELP6, KTI11-KTI13*
mcm^5s^2U	34 of $tRNA^{Glu}$(mcm^5s^2UUC)	*TRM9, NFS1, ELP1-EPL6, KTI11-*
Am	4 of $tRNA^{His}$(GUG)	Unknown
Gm	18 of multiple tRNAs	*TRM3*
	34 of $tRNA^{Phe}$(GmAA)	*TRM7*
m^2G	10 of multiple tRNAs	*TRM11*
	26 of $tRNA^{Val}$(CAC)	Unknown
Decreased in alkylating agents		
yW	37 of $tRNA^{Phe}$(GmAA)	*TRM5*
m^1I	37 of $tRNA^{Ala}$(IGC)	*TAD1, TRM5*
Increased in oxidizing agents		
m^5C	34 of $tRNA^{Leu}$(m^5CAA)	*TRM4*
	40 of $tRNA^{Phe}$(GmAA)	*TRM4*
	48 and 49 of multiple tRNAs	*TRM4*
ncm^5U	34 of $tRNA^{Val}$(ncm^5UAC)	*ELP1-EPL6, KTI11-KTI13*
$m^2{}_2G$	26 of multiple tRNAs	*TRM1*
i^6A	37 of multiple tRNAs	*MOD5*
Cm	32 of multiple tRNAs	*TRM7*
	34 of $tRNA^{Trp}$(CmCA)	*TRM7*
	4 of multiple tRNAs	Unknown

Table 5-4. tRNA modifications for defining class-specific patterns of changes in response to alkylating agents and oxidizing agents. The modifications are organized into three groups, depending on whether their levels increased or decreased in response to the two classes of stimuli. The species of tRNA are only mentioned if the modification is only located in that single species of tRNA. For tRNA modifying genes, 'unknown' indicates that no genes were identified

to our awareness. Information was collected from Modomics Database (*9*) and Sacchromyces Genome Database (*34*).

References

1. Blake, G. J., and Ridker, P. M. (2002) Inflammatory bio-markers and cardiovascular risk prediction, *J Intern Med 252*, 283-294.
2. Ridker, P. M., Hennekens, C. H., Buring, J. E., and Rifai, N. (2000) C-reactive protein and other markers of inflammation in the prediction of cardiovascular disease in women, *N Engl J Med 342*, 836-843.
3. Sabatine, M. S., Morrow, D. A., Jablonski, K. A., Rice, M. M., Warnica, J. W., Domanski, M. J., Hsia, J., Gersh, B. J., Rifai, N., Ridker, P. M., Pfeffer, M. A., and Braunwald, E. (2007) Prognostic significance of the Centers for Disease Control/American Heart Association high-sensitivity C-reactive protein cut points for cardiovascular and other outcomes in patients with stable coronary artery disease, *Circulation 115*, 1528-1536.
4. Egner, P. A., Groopman, J. D., Wang, J. S., Kensler, T. W., and Friesen, M. D. (2006) Quantification of aflatoxin-B1-N7-Guanine in human urine by high-performance liquid chromatography and isotope dilution tandem mass spectrometry, *Chem Res Toxicol 19*, 1191-1195.
5. Wogan, G. N., Hecht, S. S., Felton, J. S., Conney, A. H., and Loeb, L. A. (2004) Environmental and chemical carcinogenesis, *Semin Cancer Biol 14*, 473-486.

6. Merrick, B. A., and Bruno, M. E. (2004) Genomic and proteomic profiling for biomarkers and signature profiles of toxicity, *Curr Opin Mol Ther 6*, 600-607.

7. van Doorn, M., Vogels, J., Tas, A., van Hoogdalem, E. J., Burggraaf, J., Cohen, A., and van der Greef, J. (2007) Evaluation of metabolite profiles as biomarkers for the pharmacological effects of thiazolidinediones in Type 2 diabetes mellitus patients and healthy volunteers, *Br J Clin Pharmacol 63*, 562-574.

8. Abe, T., Ikemura, T., Sugahara, J., Kanai, A., Ohara, Y., Uehara, H., Kinouchi, M., Kanaya, S., Yamada, Y., Muto, A., and Inokuchi, H. (2011) tRNADB-CE 2011: tRNA gene database curated manually by experts, *Nucleic Acids Res 39*, D210-213.

9. Czerwoniec, A., Dunin-Horkawicz, S., Purta, E., Kaminska, K. H., Kasprzak, J. M., Bujnicki, J. M., Grosjean, H., and Rother, K. (2009) MODOMICS: a database of RNA modification pathways. 2008 update, *Nucleic Acids Res 37*, D118-121.

10. Osterman-Golkar, S., and Bergmark, E. (1988) Alkylation of haemoglobin, plasma proteins and DNA in the mouse by diethylnitrosamine, *Carcinogenesis 9*, 1915-1917.

11. Segerback, D., Calleman, C. J., Ehrenberg, L., Lofroth, G., and Osterman-Golkar, S. (1978) Evaluation of genetic risks of alkylating agents IV. Quantitative determination of alkylated amino acids in haemoglobin as a measure of the dose after-treatment of mice with methyl methanesulfonate, *Mutat Res 49*, 71-82.

12. Tannenbaum, S. R., and Skipper, P. L. (1984) Biological aspects to the evaluation of risk: dosimetry of carcinogens in man, *Fundam Appl Toxicol 4*, S367-373.

13. Lindahl, T. (1982) DNA repair enzymes, *Annu Rev Biochem 51*, 61-87.

14. Myles, G. M., and Sancar, A. (1989) DNA repair, *Chem Res Toxicol 2*, 197-226.

15. Morimoto, K., Dolan, M. E., Scicchitano, D., and Pegg, A. E. (1985) Repair of O6-propylguanine and O6-butylguanine in DNA by O6-alkylguanine-DNA alkyltransferases from rat liver and E. coli, *Carcinogenesis 6*, 1027-1031.

16. Pegg, A. E., Dolan, M. E., Scicchitano, D., and Morimoto, K. (1985) Studies of the repair of O6-alkylguanine and O4-alkylthymine in DNA by alkyltransferases from mammalian cells and bacteria, *Environ Health Perspect 62*, 109-114.

17. Sedgwick, B., and Lindahl, T. (1982) A common mechanism for repair of O6-methylguanine and O6-ethylguanine in DNA, *J Mol Biol 154*, 169-175.

18. Dedon, P. C., and Tannenbaum, S. R. (2004) Reactive nitrogen species in the chemical biology of inflammation, *Arch Biochem Biophys 423*, 12-22.

19. Dizdaroglu, M. (1992) Oxidative damage to DNA in mammalian chromatin, *Mutat Res 275*, 331-342.

20. Dizdaroglu, M. (1992) Measurement of radiation-induced damage to DNA at the molecular level, *Int J Radiat Biol 61*, 175-183.

21. Singer, B., and Grunberger, D. (1983) *Molecular biology of mutagens and carcinogens*, Plenum Press, New York.

22. Beranek, D. T., Weis, C. C., and Swenson, D. H. (1980) A comprehensive quantitative analysis of methylated and ethylated DNA using high pressure liquid chromatography, *Carcinogenesis 1*, 595-606.

23. Lawley, P. D., and Thatcher, C. J. (1970) Methylation of deoxyribonucleic acid in cultured mammalian cells by N-methyl-N'-nitro-N-nitrosoguanidine. The influence of cellular thiol

concentrations on the extent of methylation and the 6-oxygen atom of guanine as a site of methylation, *Biochem J 116*, 693-707.

24. Newbold, R. F., Warren, W., Medcalf, A. S., and Amos, J. (1980) Mutagenicity of carcinogenic methylating agents is associated with a specific DNA modification, *Nature 283*, 596-599.

25. Den Engelse, L., De Graaf, A., De Brij, R. J., and Menkveld, G. J. (1987) O2- and O4-ethylthymine and the ethylphosphotriester dTp(Et)dT are highly persistent DNA modifications in slowly dividing tissues of the ethylnitrosourea-treated rat, *Carcinogenesis 8*, 751-757.

26. Li, F., Solomon, J. J., Mukai, F., and Segal, A. (1990) In vitro reactions of isopropyl methanesulfonate with DNA and with 2'-deoxyribonucleosides, *Cancer Biochem Biophys 11*, 253-264.

27. Beranek, D. T. (1990) Distribution of methyl and ethyl adducts following alkylation with monofunctional alkylating agents, *Mutat Res 231*, 11-30.

28. Björk, G. R. (1995) Biosynthesis and function of modified nucleosides, in *tRNA : structure, biosynthesis, and function* (Söll, D., and RajBhandary, U., Eds.), pp 65-205, ASM Press, Washington, D.C.

29. Begley, U., Dyavaiah, M., Patil, A., Rooney, J. P., DiRenzo, D., Young, C. M., Conklin, D. S., Zitomer, R. S., and Begley, T. J. (2007) Trm9-catalyzed tRNA modifications link translation to the DNA damage response, *Mol Cell 28*, 860-870.

30. Johansson, M. J. O., and Byström, A. S. (2005) *Transfer RNA modifications and modifying enzymes in Saccaromyces cerevisiae*, Springer-Verlag, Heidelberg, Germany.

31. Niu, W., Li, Z., Zhan, W., Iyer, V. R., and Marcotte, E. M. (2008) Mechanisms of cell cycle control revealed by a systematic and quantitative overexpression screen in S. cerevisiae, *PLoS Genet 4*, e1000120.

32. Auffray, C., Chen, Z., and Hood, L. (2009) Systems medicine: the future of medical genomics and healthcare, *Genome Med 1*, 2.

33. Poste, G. (2011) Bring on the biomarkers, *Nature 469*, 156-157.

34. Dwight, S. S., Balakrishnan, R., Christie, K. R., Costanzo, M. C., Dolinski, K., Engel, S. R., Feierbach, B., Fisk, D. G., Hirschman, J., Hong, E. L., Issel-Tarver, L., Nash, R. S., Sethuraman, A., Starr, B., Theesfeld, C. L., Andrada, R., Binkley, G., Dong, Q., Lane, C., Schroeder, M., Weng, S., Botstein, D., and Cherry, J. M. (2004) Saccharomyces genome database: underlying principles and organisation, *Brief Bioinform 5*, 9-22.

Chapter 6

Conclusions and Future Directions

Goals of this thesis

The purpose of studies described in this thesis is to advance our understanding on the biological functions of tRNA secondary modifications in cellular response to toxic agents. Prior studies have demonstrated the sensitivities of levels of tRNA modifications to metabolic stress conditions and developmental stages and the functional roles of many modifications in conferring resistance to specific stress (*1-3*). These evidences strongly suggest that tRNA modifications are involved in cellular responses. However, the complex nature of tRNA and function redundancy of modification has limited our knowledge on cellular functions of these modifications.

A platform for characterizing and quantifying the spectrum of tRNA modifications.

To achieve our goals, a quantitative systems approach was used to study the spectrum of tRNA modifications in *S. cerevisiae* under different stress. The first step was to characterize the ribonucleosides from enzymatically hydrolyzed tRNAs with the following three approaches. First, liqud chromatography-mass spectrometry (LC-MS) was used to determine the mass and collision-induced dissocation (CID) patterns of ribonucleoside candidates with high mass accuracy. Second, these candidates were compared to synthetic standards in retention time, mass, and fragmentation patterns. Third, changes in abundance of tRNA modifications in mutants lacking tRNA modifying genes were monitored to further confirm the identities of these modified ribonucleosides. Based upon the characterization, we have developed a sensitive and robust LC-MS/MS method to quantify 23 modified ribonucleosides. However, this method cannot provide information on the positions of these modifications while some

modified nucleosides are located at various locations and species of tRNA (*4*). As a future direction, we can use cleavage site-specific endonucleases to generate oligonucleotide fragments and monitor them with mass spectrometry (*5*). Location of modifications can then be derived from the sequence of nucleotides.

Changes in spectrum of tRNA modifications in response to mechanistically distinct toxicants

Quantification of modified ribonucleosides from yeast tRNAs reveals agent-specific and dose-specific patterns in the spectrum of tRNA modifications in response to exposures to mechanistically distinct toxic agents, including hydrogen peroxide, methyl methanesulfonate, hypochlorite, and arsenite. Specifically, the modifications Cm, m^5C, and $m^2{}_2G$ increase following hydrogen peroxide-exposures but decrease or do not change in response to methyl methanesulfonate, arsenite, and hypochlorite. Moreover, sensitivity to hydrogen peroxide increases in cells lacking specific enzymes that catalyze the formation of Cm or m^5C on tRNAs, which demonstrates critical roles of tRNA modifications in cellular stress responses. The results of our study support a general model of dynamic control of tRNA modifications in cellular response pathways. Besides, characterizing changes in the spectrum of tRNA modifications of cells lacking specific tRNA modifying enzymes reveal several potential biosynthetic pathways of tRNA modifications.

Potential roles of tRNA modifications in translational regulation

As observed in quantification of tRNA modifications, m^5C increases after exposure to hydrogen peroxide and loss of tRNA m^5C-methyltransferase Trm4 reduces the survivability of

cells under this stress. It is known that m^5C is found in many species of tRNA but only a leucine tRNA translating the codon UUG comprises this modification at the wobble position. Thus, m^5C may affect the translation of UUG as previous studies have suggested that m^5C at wobble position can be involved in codon-anticodon interactions (*6*). *S. cerevisiae* contains many duplicated genes encoding ribosomal proteins with differences between the UUG usages of these homologues.

These observations led us to hypothesize that *trm4* and m^5C are involved in regulating the expression of ribosomal protein homologues. Through studies of ribosomal protein homologues with a quantitative proteomics approach, we demonstrate that the protein level of a UUG-enriched gene, *rpl22a*, decreases in the absence of Trm4 and increases in H_2O_2-exposed cells relative to its homologue, *rpl22b*. In contrast, exposing H_2O_2 to *trm4Δ* mutant does not lead to changes in relative level of this pair of homologues. These data indicate involvements of Trm4 in modulating expression of ribosomal proteins under stress. Moreover, only the *rpl22aΔ* mutant is sensitive to H_2O_2 but not the *rpl22bΔ* mutant which indicates distinct functional roles of ribosomal homologues in stress responses. Together, these results support a model that tRNA m^5C-methyltransferase Trm4 regulates translation of *rpl22a* to confer resistance to specific stress.

Besides understanding the biological role of m^5C, this study opens up the opportunity to investigate the functions of ribosomal homologues in stress response with a quantitative approach. Within 115 sequence-specific ribosomal proteins, our LC/MS method can only monitor 39 of them. The next step is to optimize this method to cover the full spectrum of ribosomal proteins and use it to assess changes as a function of cell states.

Spectrum of tRNA modifications as a potential source of biomarkers of class-specific exposures

The observations of unique signatures in spectrum of tRNA modifications for exposures to mechanistically distinct toxicants led us to ask whether the patterns of changes are common among stimuli with similar mechanisms of action. We characterized changes in the spectrum from cells exposed to four oxidizing agents, hydrogen peroxide, *tert*-butyl hydroperoxide, peroxynitrite, and gamma-radiation, and five alkylating agents, methyl methanesulfonate, ethyl methanesulfonate, isopropyl methanesulfonate, *N*-methyl-*N'*-nitro-*N*-nitrosoguanidine, and *N*-nitroso-*N*-methylurea. Multivariate statistical analysis on these data indicates class-specific features for both oxidizing agents and alkylating agents, involving 14 modifications, Am, m^2G, mcm^5U, mcm^5s^2U, m^3C, m^7G, yW, Gm, m^5C, ncm^5U, $m^2{}_2G$, i^6A, and Cm. Further, signatures specific to S_N1 and S_N2 alkylating agents were observed, which suggests that the spectrum can potentially serve as an identifier of cellular conditions with subtle differences. These features were used to develop a data-driven model with predictive power on the class of toxic agents, which demonstrates that the spectrum of tRNA modifications is a potential source of biomarkers of exposures. To explore the utilities of profiles of tRNA modifications as index of diseases and pharmaceutical exposures, this study has to be translated to models of human cells and animals.

Overall, we demonstrate that tRNA modifications are involved in cellular response to stress. To investigate a specific response pathway, we have shown that the modification m^5C regulates the expression of a H_2O_2-resistance-conferring gene based on codon usage. On the

application side, the spectrum of tRNA modifications has potential to be used as biomarkers of exposures. Further studies with other classes of stimuli may reveal more biological pathways that tRNA modifications are involved.

References

1. Björk, G. R. (1995) Biosynthesis and function of modified nucleosides, in *tRNA : structure, biosynthesis, and function* (Söll, D., and RajBhandary, U., Eds.), pp 65-205, ASM Press, Washington, D.C.
2. Costanzo, M. C., Skrzypek, M. S., Nash, R., Wong, E., Binkley, G., Engel, S. R., Hitz, B., Hong, E. L., and Cherry, J. M. (2009) New mutant phenotype data curation system in the Saccharomyces Genome Database, *Database (Oxford) 2009,* bap001.
3. Johansson, M. J. O., and Byström, A. S. (2005) *Transfer RNA modifications and modifying enzymes in Saccaromyces cerevisiae*, Springer-Verlag, Heidelberg, Germany.
4. Czerwoniec, A., Dunin-Horkawicz, S., Purta, E., Kaminska, K. H., Kasprzak, J. M., Bujnicki, J. M., Grosjean, H., and Rother, K. (2009) MODOMICS: a database of RNA modification pathways. 2008 update, *Nucleic Acids Res 37*, D118-121.
5. Hossain, M., and Limbach, P. A. (2007) Mass spectrometry-based detection of transfer RNAs by their signature endonuclease digestion products, *RNA 13*, 295-303.
6. Strobel, M. C., and Abelson, J. (1986) Effect of intron mutations on processing and function of Saccharomyces cerevisiae SUP53 tRNA in vitro and in vivo, *Mol Cell Biol 6*, 2663-2673.

Appendix A

Preliminary characterization of tRNA modifications in *M. bovis BCG*

In October 2009 to April 2010, I worked in the Infectious Disease IRG (ID-IRG) of Singapore-MIT Alliance in Research and Technology in Singapore to set up a new research group and to explore the possibilities of new projects. Projects in this recently established center have to be related to infectious diseases, which gave me unique opportunities to experience different fields of sciences. The work I accomplished in ID-IRG is presented in this Appendix because the studies are not directly related to the story of my thesis. However, these experiences are also an important part of my Ph.D. education and training.

Abstract

The observations of specific tRNA modifications conferring resistance to different toxic stimuli suggest that the biosynthetic pathways of this family of molecules are potential targets of antimicrobial agents. To understand the biological roles of tRNA modifications in *Mycobacterium* and to explore the utility of these modifications in drug development, we have characterized the spectrum of tRNA modifications in *Mycobacterium bovis BCG* by various mass spectrometric techniques. With our methods, 26 candidates of nucleoside-like species are observed in tRNA; the structure of 12 of them was identified while one of them, N^6, N^6-dimethyladenosine, was previously only observed in ribosomal RNAs.

Introduction

Tuberculosis (TB) is a disease caused by *Mycobacterium*, such as *M. tuberculosis* and *M. bovis*, with an estimation of about 10 millions new TB patients in 2010 (*1*). The high prevalence of TB is partly due to increases in drug resistance of pathogens and lack of new medications; the last drug with a novel mechanism of action for curing TB was discovered in 1963 (*2*). A major obstacle for development of anti-mycobacterial agents is the lack of understanding on cellular processes of *Mycobacterium*.

tRNA modifications in the *Mycobacterium* family have not been characterized systematically. However, modified nucleosides in tRNA of many organisms have been studied

extensively. About 20 to 30 of these modifications are present in each organism studied with a total of more than 100 distinct structures (*3*). It is clear that these modifications must be of high importance or else this complexity would not have evolved. In recent years, some derivatives of canonical nucleosides have been demonstrated to have anti-mycobacterial properties, including 2-methyladenosine (*4, 5*). It is possible that these ribonucleosides disrupt the formation of essential RNA modifications. To modify these candidates for discoveries of new TB drugs, advances in the understanding on modifications of RNA in *Mycobacterium* are necessary. To this end, we initiate the characterization of spectrum of tRNA modifications in *Mycobacterium Bovis BCG* with mass spectrometric techniques.

M. bovis BCG is used as vaccine for TB and more than 90% of its genome is identical to the infectious *M. tuberculosis* (*6*). Thus *M. bovis* BCG is frequently used as a model organism to understand TB. By using a mass spectrometry-based approach, we identified 26 candidates of tRNA modifications; the identities of 12 of them are determined, including Y, m^5C, m^3C, m^1A, I, m^7G, Cm, m^5U, Gm, m^2G, t^6A, and $m^6{}_2A$, in which $m^6{}_2A$ was previously only observed in rRNA. Besides providing the knowledge on *Mycobacterium*, the strategy we developed can also be used as a tool for characterizing spectra of modified nucleosides in any organisms.

Materials and Methods

Materials. All chemicals and reagents were of the highest purity available and were used without further purification. OADC solution, 7H9 culture media powder, and 7H11 agar powder were purchased from Biomed Diagnostics (White City, OR). TRIZOL reagent and PureLink

miRNA Isolation Kit was purchased from Invitrogen (Carlsbad, CA). 2′-*O*-Methyluridine (Um), pseudouridine (Y), N^1-methyladenosine (m^1A), N^2,N^2-dimethylguanosine (m^2_2G), N^6,N^6-dimethyladensoine (m^6_2A), and 2′-*O*-methylguanosine (Gm) were purchased from Berry and Associates (Dexter, MI). N^6-threonylcarbamoyladenosine (t^6A) was purchased from Biolog (Bremen, Germany). N^6-isopentenyladenosine (i^6A) was purchased from International Laboratory LLC (San Bruno, CA). 2′-*O*-Methyladenosine (Am), N^4-acetylcytidine (ac^4C), 5-methyluridine (m^5U), inosine (I), 2-methylguanosine (m^2G), N^7-methylguanosine (m^7G), 2′-*O*-methylcytidine (Cm), 3-methylcytidine (m^3C), 5-methylcytidine (m^5C), alkaline phosphatase, RNase A, ammonium acetate, geneticine, bovine serum albumin, deferoxamine mesylate, butylated hydroxytoluene, glucose, sodium chloride, nuclease P1, formic acid, and 20% Tween80 solution were purchased from Sigma Chemical Co. (St. Louis, MO). Glycerol was purchased from SinoChem Corp. (Beijing, China). Phosphodiesterase I was purchased from USB (Cleveland, OH). Ambion RNA structure buffer, RNase A, RNase V1 and RNase T1 were purchased from Ambion Inc. (Austin, TX). HPLC-grade water, acetonitrile, and chloroform were purchased from Mallinckrodt Baker (Phillipsburg, NJ). *M. bovis* BCG was purchased from American Type Culture Collections (Manassas, VA).

Culturing *M. bovis BCG*. *M. bovis BCG* cells were grown in 7H9 culture media at 37 °C in an incubator with 5 % CO_2. After the culture reached an optical density of OD600 ~0.6, at which the concentration of cells was ~3 $\times 10^7$ /mL, the cells were harvested by centrifugation at 12000× g for 10 min at 4 °C. Cell pellets were snap-frozen with liquid nitrogen and stored at -80 °C.

For glycerol stocks, the post-centrifugation cell pellet was resuspended in 1 mL of 7H9 culture media with 25% glycerol. The solution was then further diluted to a final concentration with OD_{600}~1 and the stocks stored at -80 °C. To determine the quantity of living cells in a glycerol stock or a culture, the cell culture was serially diluted and 100 μL of each dilution was plated onto a 7H11 agar plate. The plates were incubated at 37 °C with 5% CO_2 and resulting colonies were counted.

The 7H9 media were prepared by mixing 4.9 g of 7H9 powder, 10 mL of 50% glycerol, 2.5 mL of 20% TWEEN 80, 900 mL of double-deionized water, and 100 mL of ADS solution. The ADS solution was prepared by mixing 50 g of BSA, 20 g of glucose, and 8.1 g of sodium chloride in 950 mL of double-deionized water. The 7H11 agar plates were prepared by mixing 4.2 g of 7H11 agar powder, 2 mL of 50% glycerol, 180 mL of double-deionized water, and 20 mL of OADC solution. The solution was then heated in a microwave oven until a clear solution was achieved and the solution was transferred to petri dishes. The agar plates were cooled and solidified at ambient temperature.

Isolation of tRNA. tRNA was isolated from several organisms, including BCG (~10^9 cells), *S. cerevisiae* (5x10^7 cells), human B lymphoblastoid TK6 cells (3x10^7 cells), and rat liver (~150 mg). Cells or tissues were suspended in 1.5 mL of Trizol reagent with 5 mg/mL coformycin, 50 μg/mL tetrahydrouridine, 0.1 mM deferoxamine mesylate, and 0.5 mM butylated hydroxytoluene to prevent ribonucleoside modification artifacts (*7, 8*). *BCG* and *S. cerevisiae* cells were lyzed by 3 cycles of bead beating in a Thermo FP120 Bead Beater set at 6.5 m/s for each 20 s cycle, with 1 min of cooling on ice between cycles. The TK6 cells and rat liver tissues

were lyzed with a Qiagen TissueRuptor. Following cell or tissue disruption, all lysates were warmed to ambient temperature for 5 min and extracted with 0.3 mL volume of chloroform, with subsequent incubation at ambient temperature for 3 min. The solutions were centrifuged at 12000× g for 15 min at 4 °C and the aqueous phase was collected. Absolute ethanol was added to the aqueous phase to reach a final concentration of 35% (v/v) and tRNA was then isolated using the PureLink miRNA Isolation Kit according to manufacturer's instructions. The quality and concentration of the resulting small RNA mixture was assessed by Bioanalyzer analysis, with tRNA comprising >95% of the small RNA species present in the mixture (Figure 2). There was no detectable 5S rRNA present in the samples, as illustrated in Figure 2.

Enzymatic hydrolysis of tRNA. Samples of purified small RNA (6 μg) were lyophilized and redissolved in 100 μL of a solution with 10 ng/μL RNase A, 0.01 units/μL RNase T1, 0.001 units/μL RNase V1, 0.15 units/μL nuclease P1, 2.5 mM deferoxamine mesylate, 10 μg/mL coformycin, 50 μg/mL tetrahydrouridine, 0.5 mM butylated hydroxytoluene, and 1×RNA Structure Buffer from Ambion (provided with RNases T1, V1 and A). The solution was incubated at 37 °C for 3 h, after which alkaline phosphatase was added to a final concentration of 0.1 Units/mL. The sample was incubated at 37 °C overnight, followed by removal of proteins by filtration (YM10 filter). The resulting filtrate was used directly for mass spectrometric analysis.

Identification of ribonucleosides in *BCG* small RNA. The samples of ribonucleosides were resolved with a Thermo Hypersil aQ column (100 × 2.1 mm, 1.9 μ) with acetonitrile in 0.1% (v/v) formic acid in water as mobile phase. The flow rate was 0.3 mL/min. The gradient of

acetonitrile was as follow: 0-12 min, 0%; 12-15.3 min, 0-1%; 15.3-18.7 min, 1-6%; 18.7-20 min, 6%; 20-24 min, 6-100%. The HPLC column was directly connected to a triple quadrupole mass spectrometer (LC-MS/MS) in positive ion, neutral loss mode for loss of *m/z* 132 and 146 in the range of *m/z* 200-700. The voltages and source gas parameters were as follow: gas temperature, 300 °C; gas flow, 6 L/min; nebulizer, 15 psi; and capillary voltage, 4000 V. The ions that were detected in the neutral loss scan were selected for identification with the LC-MS/MS system in MRM mode using the same HPLC method and mass spectrometer parameters. The retention times, *m/z* of the transmitted parent ions, and *m/z* of the monitored product ions for ribonucleoside-like species are listed in Table A-1.

Structural characterization of N^6, N^6-dimethyladenosine in *BCG* small RNA. The ribonucleoside-like species eluting at 20.1 min and possessing an [M+H] ion with *m/z* of 296.13 was subjected to structural characterization by collision-induced dissociation (CID) using both MS^2 and pseudo-MS^3 (*i.e.*, in-source fragmentation) performed on the LC-QTOF system using a Thermo Hypersil aQ column (100 x 1 mm, 3 μm particle size) at a flow rate of 90 μL/min using the same mobile phase described earlier, with a gradient of organic phase as follow: 0-9 min, 0%; 9-18 min, 0-7%; 18-22 min, 7%; and 22-30 min, 7-100%. The mass spectrometer was operated in positive ion mode with the following voltages and source gas parameters: gas temperature, 325 °C; drying gas, 8 L/min; nebulizer, 30 psi; capillary voltage, 3500 V. The *m/z* detection range for parent ions was 100 to 800 and that for product ions was 50 to 800. For MS^2 analysis, the fragmentor voltage was 85 V and the target ion for the unknown was *m/z* 296.1, while the fragmentor voltage was increased to 250 V for MS^3 analysis, which caused an

in-source fragmentation of *m/z* 296.13 to give *m/z* 164.1 for further CID analysis. The *m/z* 164.1 ion was fragmented with collision energies of 0 V, 20 V, 30 V, and 60V.

Absolute quantification of $m^6{}_2A$ in tRNA from BCG and other organisms. For tRNA samples from each organism (BCG, S.cerevisiae, TK6, and Rat liver tissue), 4 pmol of $[^{15}N]_5$-2-deoxyadenosine ($[^{15}N]_5$-dA) internal standard was added to 4 μg of tRNA and the samples were subjected to enzymatic hydrolysis as described above. Following volume adjustment to achieve final concentrations of ~40 nM $[^{15}N]$-dA and ~40 ng/μL ribonucleosides, 10 μL of sample was analyzed by LC-MS/MS. Ribonucleosides were resolved on a Thermo Hypersil aQ column (100 x 2.1 mm, 1.9 μm particle size) with acetonitrile in 0.1% (v/v) formic acid as mobile phase and a flow rate of 0.3 mL/min. The gradient for acetonitrile in 0.1% formic acid was as follow: 0-10 min, 5%; 10-12 min, 30%; 12 min, 95%. The HPLC column was coupled to a triple quadrupole mass spectrometer with electrospray ionization operated in positive ion mode with the following parameters for voltages and source gas: gas temperature, 350°C; gas flow, 10 L/min; nebulizer, 20 psi; and capillary voltage, 3500 V. The mass spectrometer was operated in multiple reaction monitoring mode (MRM) to quantify two ribonucleosides with the following parameters (retention time, *m/z* of the transmitted parent ion, *m/z* of the monitored product ion, fragmentor voltage, collision energy): $[^{15}N]$-dA, 3.0 min, *m/z* 257→141, 90 V, 10 V; and $m^6{}_2A$, 11.1 min, *m/z* 296→164, 90 V, 15 V. The dwell time for each ribonucleoside was 200 ms and these two ions were monitored throughout the whole HPLC run. Linear calibration curves were obtained using a fixed concentration (40 nM) of $[^{15}N]$-dA and varying concentrations of $m^6{}_2A$ (5, 10, 50, 100, 500 nM).

Results

Growth rate of *BCG* and yield of *BCG* tRNA. As the spectrum of modified nucleosides may differ significantly according to the growth conditions, it was essential to standardize the culturing procedures. The OD_{600} of *M. bovis BCG* culture was measured each day in the first eight days after inoculation from a glycerol stock. Results were summarized in Figure A-1. At day 7, OD_{600} of the culture was approximately 0.6. Cells were harvested at this point for all experiments. Based upon the quantification by using bioanalyzer and UV-vis spectrophotometer, approximately 4 μg of tRNA can be isolated from 10^9 BCG cells. Characterization of the tRNA samples by bioanalyzer (Figure A-2) determined that the average size of tRNA in *M. bovis BCG* was about 65 nt.

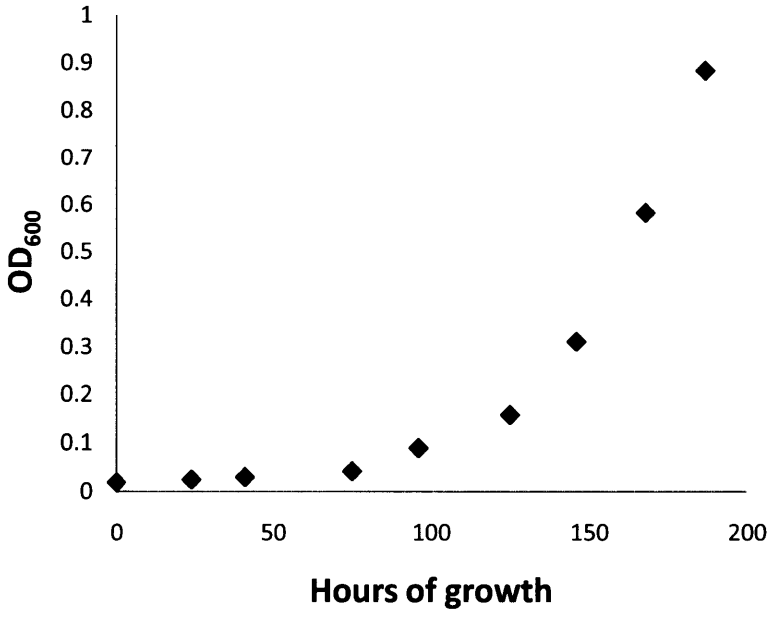

Figure A-1. Growth curve of *M. bovis BCG*. The population of cells was determined by absorbance at 600 nm as described in Materials and Methods. The data points were obtained from a single experiment.

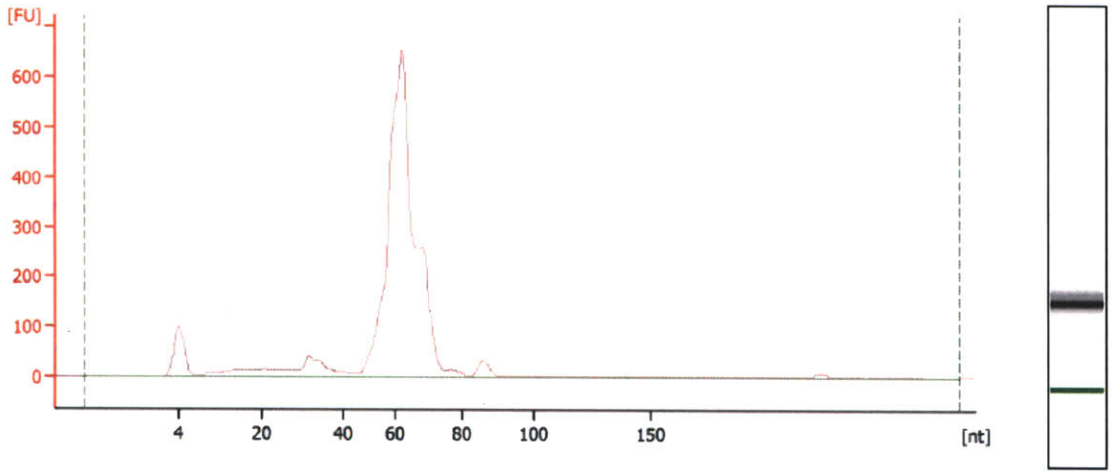

Figure A-2. Bioanalyzer chromatograph of *BCG* tRNA.

Survey of ribonucleosides in *BCG*. Ribonucleosides from enzymatic hydrolysis of *BCG* tRNA were characterized by using reverse phase HPLC-coupled triple quadrupole mass spectrometer (LC/QQQ). Most nucleosides share a characteristic neutral loss of 132 Da during collision-induced dissociation (CID) with low collision energy. This loss corresponds to the dissociation of the ribose from the base. For nucleosides that are methylated at 2'-O or other positions of the ribose, they have a loss of 146 Da instead of 132 Da. Based on this property of nucleosides, we screened for modified nucleosides by searching for molecules with either one

of these two neutral losses. As a control experiment, a sample of double-deionized water was used for tRNA isolation, enzymatic hydrolysis, and neutral loss scan; results of neutral loss screening of the water sample was compared to that of the tRNA samples. After removing the artifacts that were also present in the control, there were 26 candidates of modified nucleosides in the hydrolyzed tRNA. Based upon the retention time and *m/z* value of these candidates, the hydrolyzed tRNA samples were analyzed in MRM mode. By comparing with synthetic chemical standards, we determined that these 26 candidates include Y, m^5C, m^3C, m^1A, m^7G, I, Cm, Gm, m^5U, t^6A and m^2G (Table A-1).

RT	Precursor	Product	Quantity	Identification
1.3	255.1	123.1	11100	?
1.43	245.1	125.1	110	Y
2.15	258.1	126.1	70	m^5C
2.45	258.1	126.1	279	m^3C
2.47	282.1	150.1	500000	m^1A
3.85	298.1	166.1	500000	m^7G
3.97	320	188	3000	?
4.21	280	133.9	7000	?
4.22	258.1	112.1	2500	Cm
4.4	269.1	137.1	80000	I
5.16	352	220	16000	io^6A??
5.16	368	236	17000	?
5.18	285.1	153.1	40000	?
5.27	322	190	24000	imG-14??
8.22	259.1	127.1	30	m^5U
8.6	282.1	150.1	7000	mA??
10.69	298.1	166.1	3500	mG??
10.7	320	188	40000	?
11.4	298.1	152.1	450	Gm
12.9	282.1	150.1	17000	mA??
13.8	320	188	1800	?
13.91	298.1	166.1	600	m^2G
17.6	416.2	270.1	700	?
20.1	296.1	164.1	25000	dimethylA??
21.08	307.4	161.3	1000	?
21.88	413.1	281.1	2500	t^6A

Table A-1. List of candidates of modified ribonucleosides identified by neutral loss scan using LC/QQQ. The quantity of each species is the approximate raw counts obtained by mass spectrometer. In the column of identification, nucleosides with '??' are not certain due to the lack of standards for comparisons; they are assigned based on *m/z* values of the ions. The nucleosides that are not assigned (with a '?') have no known modifications with same mass (*9, 10*).

Structural characterization of unknown with *m/z* 296.13. To gain information of chemical structure of these candidates of modified nucleoside, LC/QTOF was used to obtain

exact mass (error < 10 ppm). An ion with *m/z* value of 296.1350 ± 0.0011 (this value is the average ± SD of all mass spectra of the chromatographic peak) was observed (Figure A-3). Based upon this *m/z* value, this ion was most likely to have a chemical formula of $C_{12}H_{18}N_5O_4^+$ (*m/z* 296.1359). This formula corresponded to an adenosine with 2 methyl group or 1 ethyl group.

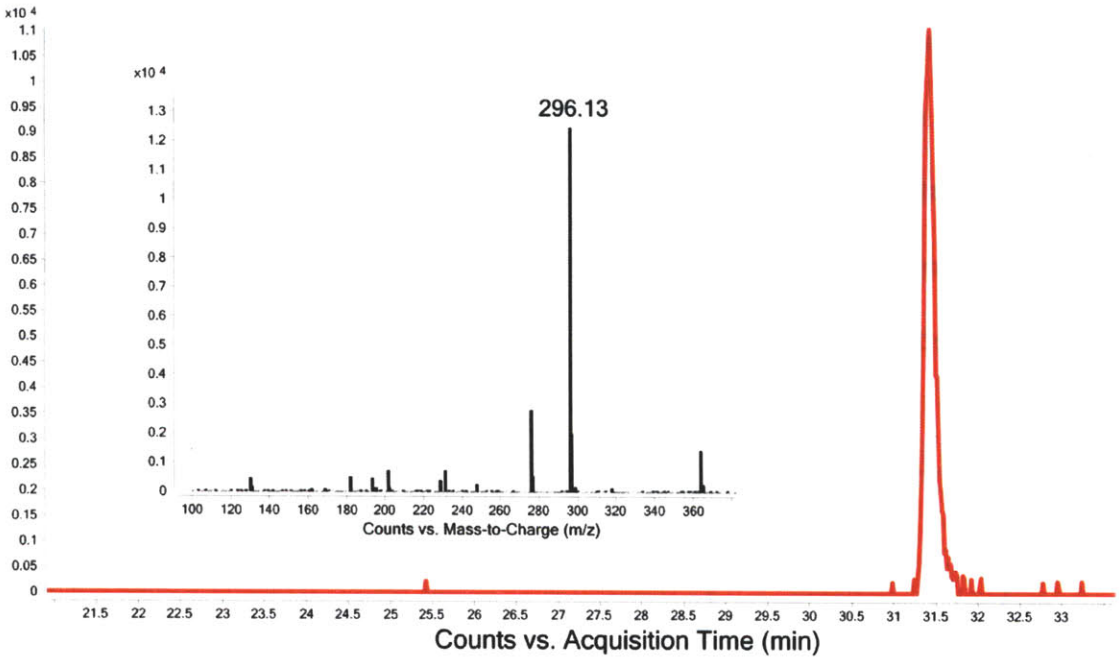

Figure A-3. Extracted ion chromatogram and mass spectrum of $[M+H]^+$ ion of $m^6{}_2A$. The peak in the small graph (black) represents the *m/z* of all ions observed between time = 31 to 31.5 minutes. The large graph (red) represents MS signal intensity of ions with *m/z* 296.1359 (error < 10 ppm) in HPLC eluent.

We carried out MS^2 and pseudo MS^3 analysis on the unknown ion *m/z* 296.13 to gain structural information for identification. In MS^2 analysis, the unknown was fragmentized to form an ion *m/z* 164.09, which the loss of mass was corresponded to a ribose (Figure A-4). The free base was likely to have a chemical formula of an adenine with a C_2H_4 (*m/z* 164.0936). Pseudo MS^3 analysis was used to gain structural information on this adenine derivative. The ribosyl group was detached from the base by in-source fragmentation which produced an ion *m/z* 164.09. This ion was then selected for collision-induced dissociation to generate the mass spectrum on Figure A-5(A). The mechanism of collision-induced dissociation of adenosine was studied previously (*11*); based upon that dissociation model and the fragmentation pattern, we derived that the structure of the m/z 296.13 ion was N^6,N^6-dimethyladenosine ($m^6{}_2A$). This conclusion was confirmed by the retention time and MS^2 and pseudo MS^3 fragmentation patterns of synthetic $m^6{}_2A$ (Figure A-5(B)).

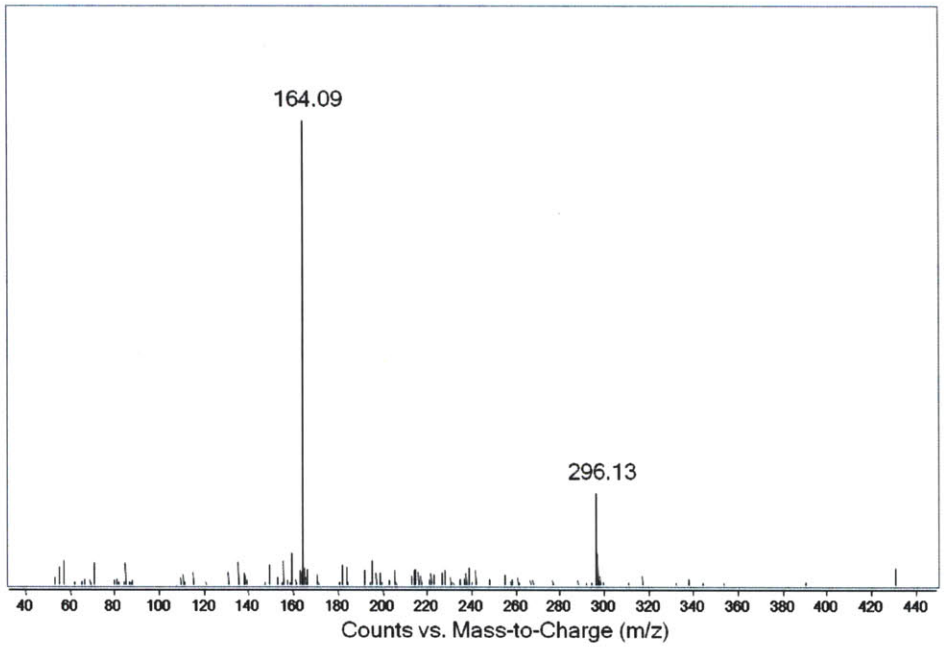

Figure A-4. MS^2 mass spectrum of $m^6{}_2A$. This CID mass spectrum was obtained with by LC/QTOF as described in the Materials and Methods section.

(A)

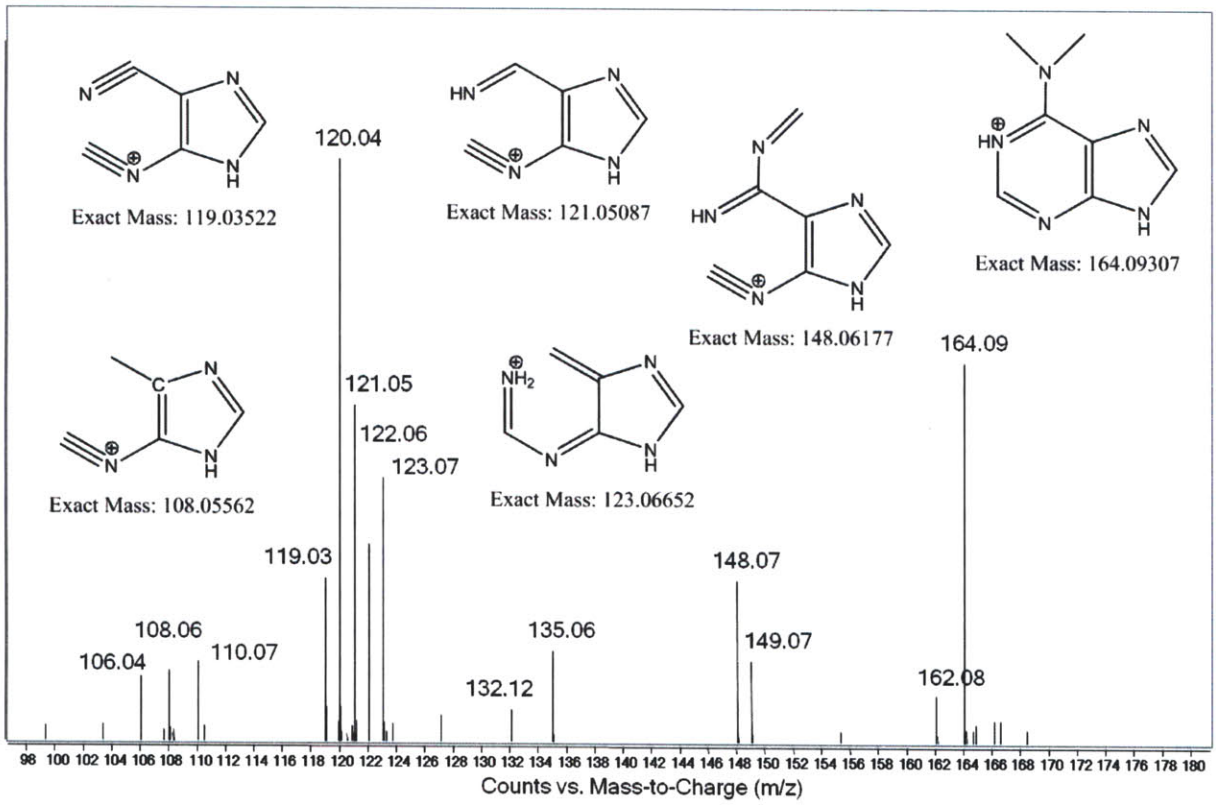

(B)

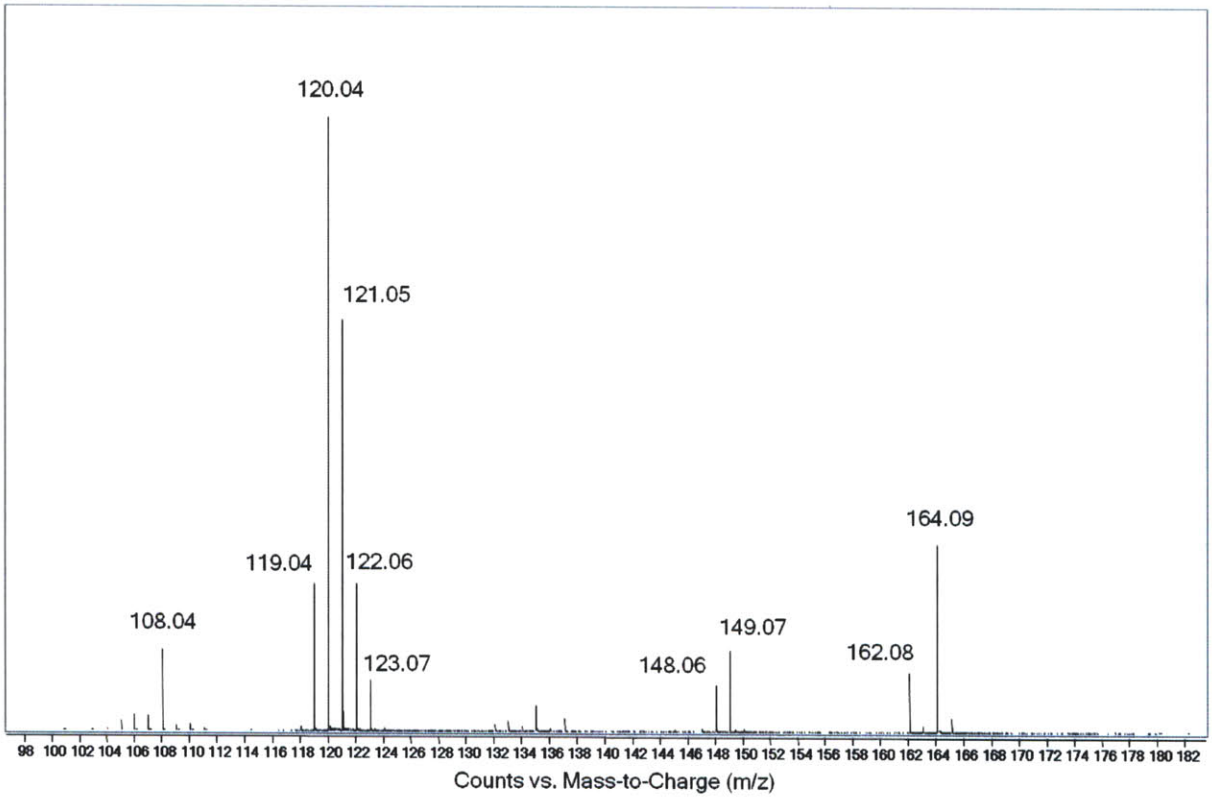

Figure A-5. **(A)** Pseudo-MS^3 spectrum of $m^6{}_2A$ from tRNA hydrolysate. **(B)** Pseudo-MS^3 spectrum of synthetic $m^6{}_2A$. The nucleoside was fragmentized to form the free base by high ionization energy at ion source (fragmentor voltage = 250V). The free base (*m/z* 164.09) was selected to pass through the first quadrupole (Q1) and fragmentized in the second quadrupole (Q2) by collision-induced dissociation with collision energy of 30 V. Proposed structure of fragmented ions with m/z 108.06, 119.04, 121.05, 123.07, 148.06, and 164.09 are presented in (A).

Absolute quantification of $m^6{}_2A$. We quantify m62A in BCG small RNA samples by using external calibration (Figure A-6). In *M. bovis* BCG, the level of $m^6{}_2A$ was 0.88 pmol per 1 μg of

tRNA (Table A-2). Based upon the results from bioanalyzer, the average size of tRNA in *M. bovis* BCG is 65 nt (Figure A-2). Assuming that each nucleotide is 340 Da, there was approximately one molecule of $m^6{}_2A$ in every 51 tRNA molecules. It is known that $m^6{}_2A$ is present in ribosomal RNA of yeast, rat and human (*12*). However, it was not observed in tRNA previously (*13-17*). To illustrate the $m^6{}_2A$ observed in *M. bovis* BCG tRNA samples were not from contaminating rRNA, we employed the same method to isolate tRNA from yeast, rat liver tissues and human TK6 cells and quantify $m^6{}_2A$ in these samples. The amount of $m^6{}_2A$ in these samples is below quantification limit (Table A-2).

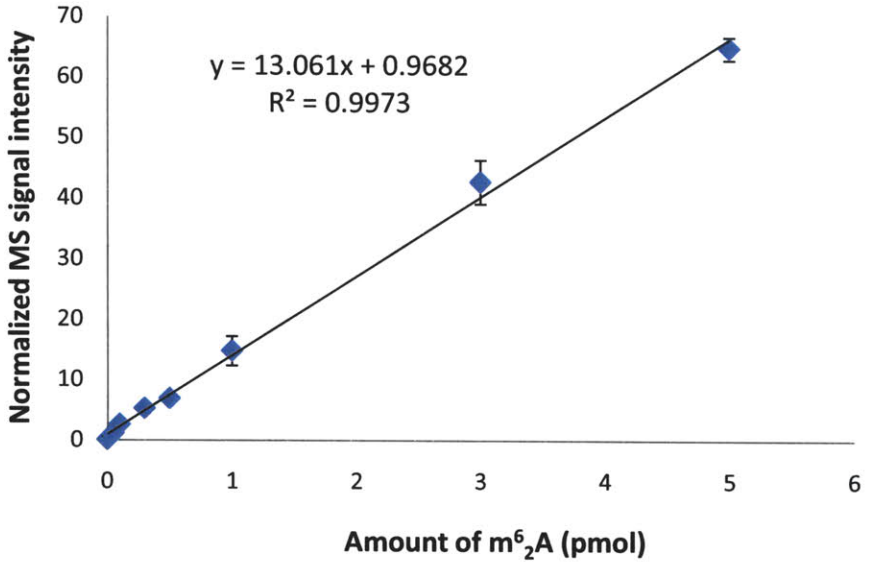

Figure A-6. External calibration curve for quantifying $m^6{}_2A$ as described in Materials and Methods section.

	tRNA samples			
	M. bovis BCG	**Human TK6**	**Rat liver**	**Yeast**
Normalized MS signals (0.4 μg tRNA)	5.8 ± 0.9	0.0054 ± 0.0002	0.0056 ± 0.0002	0.0054 ± 0.0004
Amount of $m^6{}_2A$ (pmol/μg tRNA)	0.88 ± 0.14	< 0	< 0	< 0

Table A-2. Quantification of $m^6{}_2A$ in tRNA from *M. bovis BCG*, human TK6 cells and rat liver tissue. Quantity of MS signals is converted to molarity of $m^6{}_2A$ by fitting into the external calibration curve in Figure A-6.

Discussion

Spectrum of *M. bovis BCG* tRNA modifications. We developed a general approach to characterize spectra of modified ribonucleosides. This method begins with isolation of small RNA species below 200 nucleotides and quantification of the tRNA content with bianalyzer and UV-vis spectrophotometer. Individual ribonucleosides in enzymatic hydrolysates of tRNA were resolved by HPLC and determined by their characteristic fragmentation pattern using mass spectrometry. In samples of *M. bovis BCG* small RNA, we obtained 26 candidates of modified nucleosides and identified 12 of them. They include Y, m^5C, m^3C, m^1A, m^7G, Cm, I, m^5U, Gm, m^2G, t^6A, and $m^6{}_2A$. Besides m^1A, the presence of these modifications in *Mycobacterium* is not reported in the literature to our awareness (*18, 19*). All these modifications are found in tRNA

of other organisms except $m^6{}_2A$ (*9, 10*) and they have important biological functions. Pseudouridine (Y) is the most abundant modifications in tRNA; it is found in at least 15 positions. While most Y on tRNA are non-essential, loss of Y38, Y39, or Y40 leads to a decrease in growth rate in both *E. coli*, *S. typhimurium*, and *S. cerevisiae* (*20-22*). 5-methylcytosine (m^5C) is also located at several locations (position 34, 37, 48, and 49) including wobble position, which is suggested to affect the affinity of codon-anticodon binding (*23*). 3-methylcytosine (m^3C) is located at position 32 and e2 in bacterial and eukaryotic tRNA. 1-methyladenosine (m^1A) is formed at position 58 of tRNA in *Mycobacterium tuberculosis* and many organisms (*19, 24*); mutants with deletion of the gene *trm6* or *trm61*, which is the m^1A-methyltransferase in *S. cerevisiae*, are nonviable. 7-methylguanosine (m^7G) is found at tRNA position 36 and 46 of many organisms, such as *E. coli*, mammalian cells, and plants; this modification promotes tRNA aminoacylation and enhances the stability of tRNA (*25-27*). 2'-*O*-methylcytosine (Cm) is located at position 32, 34, and 56; Cm34 in *E. coli* affects fidelity of codon reading (*28*). Inosine (I) is found at wobble position of tRNA from all three phylogenetic domains; genes that are responsible for the formation of I34 are essential in *S. cerevisiae (29)*. 5-methyluridine (m^5U) is located at position 54; m^5U54 is conserved in all three domains of life (*3*). 2'-*O*-methylguanosine (Gm) can be formed at position 18 and 34; Gm34 promotes the accuracy of mRNA decoding (*30*). 2-methylguanosine (m^2G) forms at position 6, 10, and 26; m^2G10 promotes the efficiency of aminoacylation in some tRNA (*31*). N^6-theonylcarbamoyladenosine (t^6A) is located at position 37; it promotes the codon-anticodon interactions (*32*). As these highly conserved tRNA modifications play important roles in other organisms, they may also be involved in centric biological processes of *Mycobacterium*.

Among these modifications, one of them was previously not observed in tRNA. This modification has a *m/z* value of 296.13. To obtain information of the structure of this ribonucleoside, we used high mass accuracy MS, MS^2 and pseudo-MS^3 analysis to study its fragmentation patterns. The modification is confirmed to be N^6,N^6-dimethyladenosine (m^6_2A) by comparing with the synthetic standard. m^6_2A is only reported to be present in rRNA of several organisms, including yeast, human and rat (*9, 10, 33*). It is possible that this modification may be originated from contaminating rRNA in the tRNA sample. For validation, we quantified m^6_2A in tRNA samples from *M. bovis* BCG, yeast, human TK6 cells, and rat liver tissue that were isolated with the same method. The results show that there was about one m^6_2A per 51 copies of tRNA in *M. bovis* BCG; levels of m^6_2A in samples from human TK6 cells and rat liver tissue were below detection limit. These results suggest that m^6_2A is from tRNA in *M. bovis* BCG.

There are 14 unidentified candidates of ribonucleosides. All of these candidates have a loss of *m/z* 132 or *m/z* 146 in collision-induced dissociation. These fragmentations are common features of ribonucleosides corresponding to the loss of a ribose or a 2'-*O*-methylribose. Molecular transitions of some candidates are the same as that of monomethylated adenosine (*m/z* 282 to *m/z* 150), monomethylated guanosine (*m/z* 298 to *m/z* 166), N^6-(cis-hydroxyisopentenyl)adenosine (*m/z* 352 to *m/z* 220), and 4-demethylwyosine (*m/z* 322 to *m/z* 190). These modifications have been observed in tRNA. Molecular transitions of nine candidates are unique to all known RNA modifications. These candidates can possibly be modifications that have not been discovered yet.

Besides characterizing the spectrum of tRNA modifications in *M. bovis BCG*, here we also present a general strategy to identify modified ribonucleosides. In this strategy, candidates of RNA modifications were identified with LC/QQQ in neutral loss mode based upon the characteristic loss of ribose or 2'-*O*-methylribose during collision-induced dissociation. The highly accurate mass of these candidates were identified with LC/QTOF to predict their chemical formulae. Then, these candidates were analyzed with MS^2 and MS^3 (*i.e.*, in-source fragmentation) by using LC/QTOF to gain structural information. This strategy can potentially be used to characterize the spectrum of modifications of all species of RNA in any kind of organisms.

References

1. Dye, C., and Williams, B. G. The population dynamics and control of tuberculosis, *Science 328*, 856-861.
2. Koul, A., Arnoult, E., Lounis, N., Guillemont, J., and Andries, K. The challenge of new drug discovery for tuberculosis, *Nature 469*, 483-490.
3. Cantara, W. A., Crain, P. F., Rozenski, J., McCloskey, J. A., Harris, K. A., Zhang, X., Vendeix, F. A., Fabris, D., and Agris, P. F. (2011) The RNA Modification Database, RNAMDB: 2011 update, *Nucleic Acids Res 39*, D195-201.
4. Barrow, E. W., Westbrook, L., Bansal, N., Suling, W. J., Maddry, J. A., Parker, W. B., and Barrow, W. W. (2003) Antimycobacterial activity of 2-methyl-adenosine, *J Antimicrob Chemother 52*, 801-808.

5. Parker, W. B., Barrow, E. W., Allan, P. W., Shaddix, S. C., Long, M. C., Barrow, W. W., Bansal, N., and Maddry, J. A. (2004) Metabolism of 2-methyladenosine in Mycobacterium tuberculosis, *Tuberculosis (Edinb) 84*, 327-336.

6. Mahairas, G. G., Sabo, P. J., Hickey, M. J., Singh, D. C., and Stover, C. K. (1996) Molecular analysis of genetic differences between Mycobacterium bovis BCG and virulent M. bovis, *J Bacteriol 178*, 1274-1282.

7. Pang, B., Zhou, X., Yu, H., Dong, M., Taghizadeh, K., Wishnok, J. S., Tannenbaum, S. R., and Dedon, P. C. (2007) Lipid peroxidation dominates the chemistry of DNA adduct formation in a mouse model of inflammation, *Carcinogenesis 28*, 1807-1813.

8. Taghizadeh, K., McFaline, J. L., Pang, B., Sullivan, M., Dong, M., Plummer, E., and Dedon, P. C. (2008) Quantification of DNA damage products resulting from deamination, oxidation and reaction with products of lipid peroxidation by liquid chromatography isotope dilution tandem mass spectrometry, *Nat Protoc 3*, 1287-1298.

9. Cantara, W. A., Crain, P. F., Rozenski, J., McCloskey, J. A., Harris, K. A., Zhang, X., Vendeix, F. A., Fabris, D., and Agris, P. F. The RNA Modification Database, RNAMDB: 2011 update, *Nucleic Acids Res 39*, D195-201.

10. Czerwoniec, A., Dunin-Horkawicz, S., Purta, E., Kaminska, K. H., Kasprzak, J. M., Bujnicki, J. M., Grosjean, H., and Rother, K. (2009) MODOMICS: a database of RNA modification pathways. 2008 update, *Nucleic Acids Res 37*, D118-121.

11. Nelson, C. C. M., J. A. (1992) Collision-Induced Dissociation of Adenine, *J Am Chem Soc 114*, 3661 to 3668.

12. Littlefield, J. W., and Dunn, D. B. (1958) Natural occurrence of thymine and three methylated adenine bases in several ribonucleic acids, *Nature 181*, 254-255.

13. Brown, G. M., and Attardi, G. (1965) Methylation of nucleic acids in HeLa cells, *Biochem Biophys Res Commun 20*, 298-302.

14. Dubin, D. T., and Brown, R. E. (1967) A novel ribosomal RNA in hamster cell mitochondria, *Biochim Biophys Acta 145*, 538-540.

15. Fox, G. E., Magrum, L. J., Balch, W. E., Wolfe, R. S., and Woese, C. R. (1977) Classification of methanogenic bacteria by 16S ribosomal RNA characterization, *Proc Natl Acad Sci U S A 74*, 4537-4541.

16. Lai, C. J., Dahlberg, J. E., and Weisblum, B. (1973) Structure of an inducibly methylatable nucleotide sequence in 23S ribosomal ribonucleic acid from erythromycin-resistant Staphylococcus aureus, *Biochemistry 12*, 457-460.

17. Starr, J. L., and Fefferman, R. (1964) The Occurrence of Methylated Bases in Ribosomal Ribonucleic Acid of Escherichia Coli K12 W-6, *J Biol Chem 239*, 3457-3461.

18. Brahmachari, V., and Ramakrishnan, T. (1984) Studies on 1-methyl adenine transfer RNA methyltransferase of Mycobacterium smegmatis, *Arch Microbiol 140*, 91-95.

19. Varshney, U., Ramesh, V., Madabushi, A., Gaur, R., Subramanya, H. S., and RajBhandary, U. L. (2004) Mycobacterium tuberculosis Rv2118c codes for a single-component homotetrameric m1A58 tRNA methyltransferase, *Nucleic Acids Res 32*, 1018-1027.

20. Bruni, C. B., Colantuoni, V., Sbordone, L., Cortese, R., and Blasi, F. (1977) Biochemical and regulatory properties of Escherichia coli K-12 hisT mutants, *J Bacteriol 130*, 4-10.

21. Carbone, M. L., Solinas, M., Sora, S., and Panzeri, L. (1991) A gene tightly linked to CEN6 is important for growth of Saccharomyces cerevisiae, *Curr Genet 19*, 1-8.

22. Roth, J. R., Anton, D. N., and Hartman, P. E. (1966) Histidine regulatory mutants in Salmonella typhimurium. I. Isolation and general properties, *J Mol Biol 22*, 305-323.

23. Strobel, M. C., and Abelson, J. (1986) Effect of intron mutations on processing and function of Saccharomyces cerevisiae SUP53 tRNA in vitro and in vivo, *Mol Cell Biol 6*, 2663-2673.

24. Bujnicki, J. M. (2001) In silico analysis of the tRNA:m1A58 methyltransferase family: homology-based fold prediction and identification of new members from Eubacteria and Archaea, *FEBS Lett 507*, 123-127.

25. Alexandrov, A., Chernyakov, I., Gu, W., Hiley, S. L., Hughes, T. R., Grayhack, E. J., and Phizicky, E. M. (2006) Rapid tRNA decay can result from lack of nonessential modifications, *Mol Cell 21*, 87-96.

26. Chernyakov, I., Whipple, J. M., Kotelawala, L., Grayhack, E. J., and Phizicky, E. M. (2008) Degradation of several hypomodified mature tRNA species in Saccharomyces cerevisiae is mediated by Met22 and the 5'-3' exonucleases Rat1 and Xrn1, *Genes Dev 22*, 1369-1380.

27. Hoburg, A., Aschhoff, H. J., Kersten, H., Manderschied, U., and Gassen, H. G. (1979) Function of modified nucleosides 7-methylguanosine, ribothymidine, and 2-thiomethyl-N6-(isopentenyl)adenosine in procaryotic transfer ribonucleic acid, *J Bacteriol 140*, 408-414.

28. Satoh, A., Takai, K., Ouchi, R., Yokoyama, S., and Takaku, H. (2000) Effects of anticodon 2'-O-methylations on tRNA codon recognition in an Escherichia coli cell-free translation, *RNA 6*, 680-686.

29. Gerber, A. P., and Keller, W. (1999) An adenosine deaminase that generates inosine at the wobble position of tRNAs, *Science 286*, 1146-1149.

30. Yokoyama, S., and Nishimura, S. (1995) Modified nucleosides and codon recognition, in *tRNA : structure, biosynthesis, and function* (Söll, D., and RajBhandary, U., Eds.), pp p 207-223, ASM Press, Washington, D.C.

31. Roe, B., Michael, M., and Dudock, B. (1973) Function of N2 methylguanine in phenylalanine transfer RNA, *Nat New Biol 246*, 135-138.

32. Weissenbach, J., and Grosjean, H. (1981) Effect of threonylcarbamoyl modification (t6A) in yeast tRNA Arg III on codon-anticodon and anticodon-anticodon interactions. A thermodynamic and kinetic evaluation, *Eur J Biochem 116*, 207-213.

33. Szymanski, M., Barciszewska, M. Z., Erdmann, V. A., and Barciszewski, J. (2002) 5S Ribosomal RNA Database, *Nucleic Acids Res 30*, 176-178.

Curriculum Vitae
Clement T. Y. Chan

Education

2005-2011	Ph.D. in Chemistry, Massachusetts Institute of Technology
2001-2005	B.S. in Chemistry and Biochemistry, University of Wisconsin-Madison

Research Experience

2005-2011	Research Assistant, Massachusetts Institute of Technology
2009-2010	Visiting scholar, Infectious Disease IRG, SMART, Singapore
2002-2005	Research Assistant, University of Wisconsin-Madison

Publications and Patents

Chan C.T.Y., Dyavaiah M., DeMott M.S., Taghizadeh K., Dedon P.C., and Begley T.J. (2010). A quantitative systems approach reveals dynamic control of tRNA modifications during cellular stress. PLoS Genetics. 6(12):e1001247. Doi:10.1371/journal.pgen.1001247.

Fu, D., Brophy J.A., **Chan, C.T.Y.**, Atmore, K.A., Begley, U., Paules, R.S., Dedon, P.C., Begley, T.J., and Samson, L.D. (2010). Human AlkB homolog ABH8 is a tRNA methyltransferase required for wobble uridine modification and DNA damage survival. Molecular and Cellular Biology. 30(10):2449-2459.

Seyedsayamdost, M.R., Xie, J., **Chan, C.T.Y.**, Alfonta, L., Schultz, P.G., and Stubbe, J. (2009). The site-specific incorporation of redox-active and chemically-reactive amino acid in proteins in *E. coli*. US patent publication number: US 2009/0208994 A1.

Seyedsayamdost, M.R., **Chan, C.T.Y.**, Mugnaini, V., Stubbe, J. and Bennati, M. (2007). PELDOR spectroscopy with DOPA– 2 and NH_2Y– 2: distance measurements between residues involved in the radical propagation pathway of *E. coli* ribonucleotide reductase. Journal of American Chemical Society. 129:15748-15749.

Seyedsayamdost, M.R., Xie, J., **Chan, C.T.Y.**, Schultz, P.G., and Stubbe, J. (2007). Site-specific insertion of 3-aminotyrosine into subunit 2 of *E. coli* ribonucleotide reductase: direct evidence for involvement of Y_{730} and Y_{731} in radical propagation. Journal of American Chemical Society. 129:15060-15071.

Honors and Awards

2009-2011	Merck-MIT Fellowship Award
2009	AACR-Aflac, Inc. Scholar-in-Traning Award
2008	CEHS Award
2004-2005	Hilldale Undergraduate/Faculty Research Fellowship
2003	Ingersol Award

Selected Presentations

2011	Research talk, MIT's Boston DNA Repair and Mutagenesis Group, MIT, Cambridge, MA
2010	Research talk, Microbial Systems (and Beyond) Seminar, MIT, Cambridge, MA
2010	Poster, American Chemical Society National Meeting, Boston, MA
2009	Research talk, Annual Meeting of Society of Toxicology, Baltimore, ML
2008	Poster, Annual Meeting of American Association for Cancer Research, San Diego, CA